NASA CR-156819

CHARGE COUPLED DEVICES

James W. Walker
Larry J. Hornbeck
Dan P. Stubbs

Texas Instruments Incorporated
Central Research Laboratories
13500 North Central Expressway
Dallas, Texas 75222

[redacted] CHARGE COUPLED DEVICES X78-10144
Final Technical Report, Jan. 1976 - Jul. 1977 (Texas Instruments, Inc.) 283 p LIMIT
GOVT.+CONTR. Unclas
E3/33 33477

September 1977
Final Technical Report for Period January 1976 through July 1977

Prepared for

GODDARD SPACE FLIGHT CENTER

Greenbelt, Maryland 20771

NASA
National Aeronautics and Space Administration

1. Report No.	2. Government Accession No.	3. Recipient's Catalog No.
4. Title and Subtitle CHARGE COUPLED DEVICES		5. Report Date September 1977 6. Performing Organization Code
7. Author(s) James W. Walker, Larry J. Hornbeck, Dan P. Stubbs		8. Performing Organization Report No. 08-77-40
9. Performing Organization Name and Address Texas Instruments Incorporated Central Research Laboratories 13500 North Central Expressway Dallas, Texas 75222		10. Work Unit No. 11. Contract or Grant No. NAS5-22924
12. Sponsoring Agency Name and Address Goddard Space Flight Center Greenbelt, Maryland 20771 Attention: Mr. Jack Williams, Code 673		13. Type of Report and Period Covered Final Technical Report January 1976 - July 1977 14. Sponsoring Agency Code
15. Supplementary Notes		

16. Abstract

This report presents the results of a program to design, fabricate, and test CCD arrays suitable for operation in an electron-bombarded mode. These intensified charge coupled devices (ICCD) have potential application to astronomy as photon-counting arrays.

The objectives of this program were to deliver arrays of 250 lines of 400 pixels each and some associated electronics. Some arrays were delivered on tube-compatible headers and some were delivered after incorporation in vacuum tubes.

Delivery of these devices required considerable improvements to be made in the processing associated with intensified operation. These improvements resulted in a high yield in the thinning process, reproducible results in the accumulation process, elimination of a dark current source in the accumulation process, solution of a number of header related problems, and the identification of a remaining major source of dark current. Two systematic failure modes were identified and protective measures established.

A total of twenty-two 250 x 400 arrays were delivered, together with characterization data. This characterization data is repeated and summarized in this report. The effects of tube processing on the arrays in the delivered ICCDs were determined and are reported here.

17. Key Words	18. Distribution Statement
CCD, Intensified CCD, Photon Counting, Low Light Level Imaging	

19. Security Classif. (of this report)	20. Security Classif. (of this page)	21. No. of Pages	22. Price
UNCLASSIFIED	UNCLASSIFIED	276	

PRECEDING PAGE BLANK NOT FILMED

PREFACE

This report was prepared by Texas Instruments Incorporated, Dallas, Texas under Contract No. NAS5-22924. The work under this contract was administered and funded by National Aeronautics and Space Administration, Goddard Space Flight Center, Greenbelt, Maryland. Mr. Jack Williams was the Technical Officer.

At Texas Instruments the work was performed in the CCD Technology Laboratory, a part of Central Research Laboratories. Dr. James W. Walker was Principal Investigator.

This is the Final Technical Report for the contract. It covers work done from January 1976 through July 1977.

PRECEDING PAGE BLANK NOT FILMED

TABLE OF CONTENTS

SECTION		PAGE
I	INTRODUCTION	1
II	250 x 400 DEVICE CHARACTERISTICS	3
	A. Device Design	3
	B. On-Chip Amplifier	6
	C. Device Fabrication	11
	D. Header Redesign	11
III	IMPROVEMENTS IN THINNED CCD IMAGER PROCESSING	16
	A. Outline of Thinned CCD Imager Processing	16
	B. Characterization of Critical Processing Steps	17
	1. Thinning Process	17
	2. Accumulation Process	18
	a. Characterization Requirements	18
	b. Measurement Techniques	21
	c. Measurement Results	21
	d. Conclusions	27
	3. Alloy and Bond Process	27
	a. Mechanical Buckling	27
	b. Dark Current Changes	29
	4. Header Manufacture	36
	C. Conclusions	41
IV	DEVICE TESTING AND CHARACTERIZATION	43
	A. Multiprobe Evaluation	43
	B. Optical and Electrical Characterization	47
	1. Dark Current Density and Uniformity	47
	2. Spectral Response and Uniformity	48
	3. Full Well Capacity	51
	4. Noise and Dynamic Range	52
	5. Charge Transfer Efficiency	55
	C. Summary of Delivered Device Characterization	55

TABLE OF CONTENTS

(Continued)

SECTION		PAGE
V	CCD IMAGER FAILURE ANALYSES	64
	A. Failure Modes	64
	B. Static Electric Discharge Damage	64
	C. Bond Degradation	69
	D. Unidentified Failure Modes	69
	E. Summary	72
VI	INTENSIFIED CHARGE COUPLED DEVICE FABRICATION	74
	A. Tube Processing Steps	74
	B. Tube Processing Results	74
	1. Varo Results	74
	2. ITT Results	76
VII	SIGNAL CONDITIONING ELECTRONICS	83
VIII	CONCLUSIONS AND RECOMMENDATIONS	85
	APPENDIX A - Characterization Reports for 22 Delivered Devices	87
	APPENDIX B - Bond Pad Protection Developments	261
	REFERENCES	276

LIST OF ILLUSTRATIONS

FIGURE		PAGE
1	Schematic of Backside-Illuminated, 3ϕ, Double-Level Aluminum CCD Imager	4
2	Organization of the 250 x 400 Imager	5
3	Photomicrograph of the 250 x 400 Imager	7
4	On-Chip Balanced Sample-And-Hold Amplifier of 250 x 400 Imager	8
5	Modified On-Chip Amplifier Output for 250 x 400 Imager	9
6	Schematic of Precharge Amplifier	10
7	Cutaway Drawing of Tube Header	12

LIST OF ILLUSTRATIONS

(Continued)

FIGURE		PAGE
8	Variations of Basic Tube Headers with Array Size and Outside Flanges	13
9	Pin Connections for 250 x 400 Tube Header	15
10	Improperly Etched Membrane	19
11	Uniformly Thinned 250 x 400 Membrane	20
12	Summary of Spectral Response Data for Twenty 100 x 160 Devices	22
13	Effects of TI Accumulation Process on Photoresponse and Dark Current	23
14	Response Reproducibility of the TI Accumulation Process	25
15	Optimization Data for the TI Accumulation Process	26
16	Spectral Response of Six Recent 100 x 160 Devices	28
17	Effects of Isochronal Anneals on CCD Dark Current	32
18	Gated Diode Bias Conditions	34
19	I-V Characteristics of an Isochronally Annealed Implanted Gated Diode	35
20	Gated Diode Leakage Current, Type I Behavior	37
21	Gated Diode Leakage Current, Type II Behavior	38
22	Modifications of Original Tube Header Design	40
23	Header Welds by (a) Heliarc Welding and (b) Laser Welding	42
24	Examples of On-Slice CTE Measurement Results	44
25	Examples of On-Slice Dark Current Signature Photographs	45
26	Observation of Open Parallel Clock Lines During On-Slice Device Operation	46
27	Schematic of Basic Clamp Sample-and-Hold Circuit	54
28	Waveform Observed at Nodes 1, 2, and 3 of Figure 27	54
29	Distribution of Dark Current for Delivered Devices	56
30	Summary of Spectral Response Characteristics of the Delivered Devices	58
31	Image Quality Achieved	59
32	Background Dark Current Uniformity Achieved	60
33	Blue Response Uniformity Achieved	61
34	High Voltage Damage to Amplifier Gates	65

LIST OF ILLUSTRATIONS

(Continued)

FIGURE		PAGE
35	SEM Comparison of (a) Damage to Returned Devices and (b) Tesla Coil Damage	67
36	Distribution of Oxide Breakdown Voltage	68
37	Diode Protection on a Tube Header	70
38	High Current Damage to CCD Amplifiers	71
39	Unusual Failure Mechanism	73
40	Electrostatically Focused Intensified Charge Coupled Device	75
41	EBS Gain for Delivered ICCDs	78
42	Spot Scan of Tube #287 Photocathode	79
43	Spot Scan of Tube #299 Photocathode	80
44	Imaging Capability of Tube #243	81
45	Signal Conditioning Board	84

LIST OF TABLES

TABLE		PAGE
1	Alloy Effects on Dark Current	30
2	Imager Performance Goals	62
3	Varo ICCD Processing Results	77

SECTION I
INTRODUCTION

This report presents the results of a program to design, fabricate, and test CCD imager arrays suitable for operation in an electron-bombarded mode. These devices have potential as photon-counting arrays.[1] The imager chosen for this development was a modification of an existing 250 line by 400 column imager. The modifications required elimination of a portion of the on-chip amplifiers and redesign of electronic drive circuitry to allow the option of simultaneous readout of two halves of the parallel array. In the performance of this development and device delivery, significant improvements were made in the processing of large area thinned CCD imagers.

The program included the processing and delivery of intensified charge coupled devices (ICCDs). Characterized imagers were delivered directly to tube manufacturers for incorporation in vacuum intensifier tubes. The resulting tubes were characterized for CCD degradation and intensified operation.

Twenty-three imagers were delivered under this contract. Eighteen of these were 250 x 400 CCD arrays mounted on tube headers compatible with ITT image intensifier tubes. Four of the imagers were 250 x 400 ICCDs, two of which were based on Varo electrostatically focused triode intensifiers and two on ITT magnetically focused intensifiers. One device was a 100 x 160 ICCD based on the Varo intensifier (the CCD was furnished to NASA-Goddard under a separate contract). Two signal conditioning boards for use with existing electronics were also supplied.

Section II of this report describes the 250 x 400 array employed in this development. Section III describes the processing of these devices and the problems encountered, along with improvements achieved in yield and device characteristics. The testing and characterization of the delivered CCDs are discussed in Section IV. Device failures occurred early in the development work, and devices were returned to Texas Instruments by Goddard for failure analysis. Section V presents the results of these analyses. The tube processing results are discussed in Section VI. Section VII describes the signal conditioning electronics. Conclusions resulting from this work and recommendations for further development

effort are presented in Section VIII. Appendix A contains the characterization reports for the 22 delivered devices. Appendix B is a discussion of bond pad protection developments.

SECTION II
250 x 400 DEVICE CHARACTERISTICS

A. Device Design

At the beginning of this program the CCD imager technology of Texas Instruments was based on three-phase, two-level aluminum architecture[2] with backside illumination,[3] operated in a buried-channel mode.[4] A schematic representation of this technology is presented in Figure 1. As shown in the figure, an array of metallic transfer electrodes is formed over a SiO_2 gate oxide on a silicon substrate to allow charge to be transferred along the array. Charge packets (electrons) are held in depletion regions of each MOS capacitor as it is pulsed into depletion. Signal charge can be injected into the array by an n^+ diode or by optical or electron radiation falling on the backside of the array. After a period of time sufficient for the collection of signal charge (the integration time), the packets are transferred by appropriate clocking pulses to the depletion region of a reverse-biased (n^+) output diode. The diode is connected to an on-chip amplifier. The silicon itself must be thinned over the CCD electrode region as shown in Figure 1 for high resolution, since an excessive thickness of silicon will allow image electrons to diffuse in a lateral direction before collection in the potential wells of the CCD. Charge transport occurs at the junction of a shallow n layer and the p substrate to avoid surface state transfer loss (buried channel mode).

Three sizes of arrays were available for implementation of this program, a 100 x 160, a 250 x 400, and a 400 x 400. The 250 x 400 array was chosen because the size of the 400 x 400 made it difficult to build and led to problems in data handling. The 100 x 160 array was too small.

The 250 x 400 array consists of 250 lines with 400 pixels per line. Each pixel is 27.4 μm (1.08 mils) by 22.9 μm (0.9 mil). The maximum spatial frequency expected to be resolved by this sampled imaging system is 18.2 line pairs per millimeter parallel to each line and 21.9 line pairs per millimeter perpendicular to each line. The array is organized as indicated in Figure 2. The 250 lines comprise the parallel array. Serial registers are provided at the top and bottom

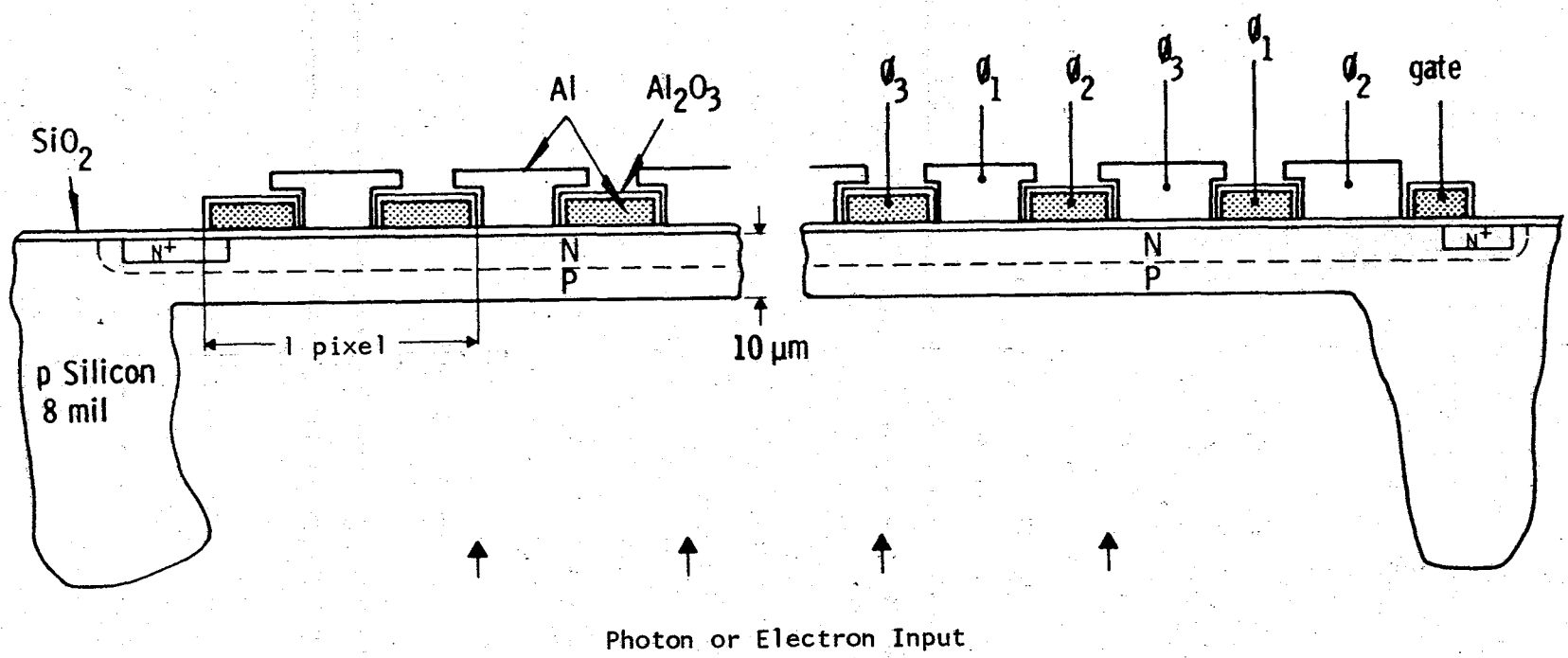

Figure 1 Schematic of Backside-Illuminated, 3ø, Double-Level Aluminum CCD Imager

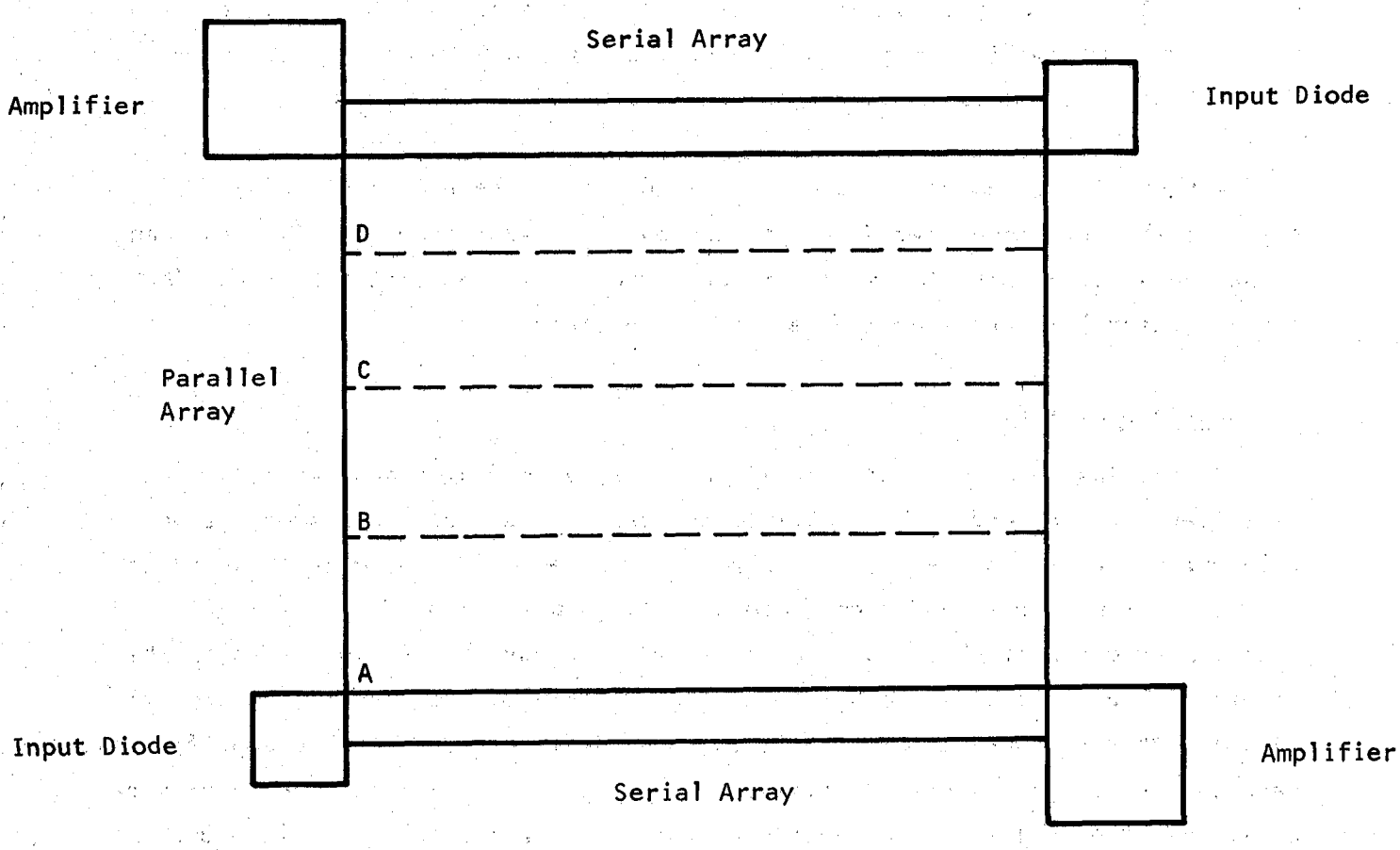

Figure 2 Organization of the 250 x 400 Imager

of the parallel array. Each serial register has an output amplifier and provision for electrical input. The amplifiers are placed at diagonal corners, providing 180° rotational symmetry. The parallel section is divided into four segments, each with separate connections to the three phases. This feature allows operation of 1/4, 1/2, 3/4, or the complete parallel array and allows simultaneous readout through the two amplifiers by clocking sections A and B toward the lower amplifier and sections C and D toward the upper amplifier.

A photomicrograph of the 250 x 400 imager is presented in Figure 3. To complete the rotational symmetry provided by the diagonal amplifiers, redundant connections to the parallel array are provided. A set of test structures (MOSFETs and capacitors) is provided at the top of the array.

B. On-Chip Amplifier

As originally configured, the 250 x 400 array had balanced sample-and-hold amplifiers[4] at the end of both serial registers. The load transistors associated with these amplifiers were located away from the edge of the array to avoid heating effects that were observed when these amplifiers were located over thin silicon. A photomicrograph of this amplifier is shown in Figure 4. As indicated in this figure, an option existed to delete the sample-and-hold portion of the amplifier, allowing this critical processing to be done off-chip. The on-chip amplifier then becomes a balanced precharge amplifier. This option was implemented to provide additional flexibility. The on-chip amplifier as fabricated for this program is shown in Figure 5.

A schematic of the precharge output is shown in Figure 6. The output diode of the CCD is connected directly to the gate of a source-follower MOSFET. Video output is taken directly from the source, and an external load resistor (typically 4.7 kΩ) is connected between source and ground. The output node is precharged to a voltage close to V_{Ref} by turning on Q1 with a precharge pulse of ϕ_{PC}. When ϕ_{PC} is removed, the voltage at the gate of Q2 falls to a new level, $V_{Ref} - V_C = V$

ORIGINAL PAGE IS
OF POOR QUALITY

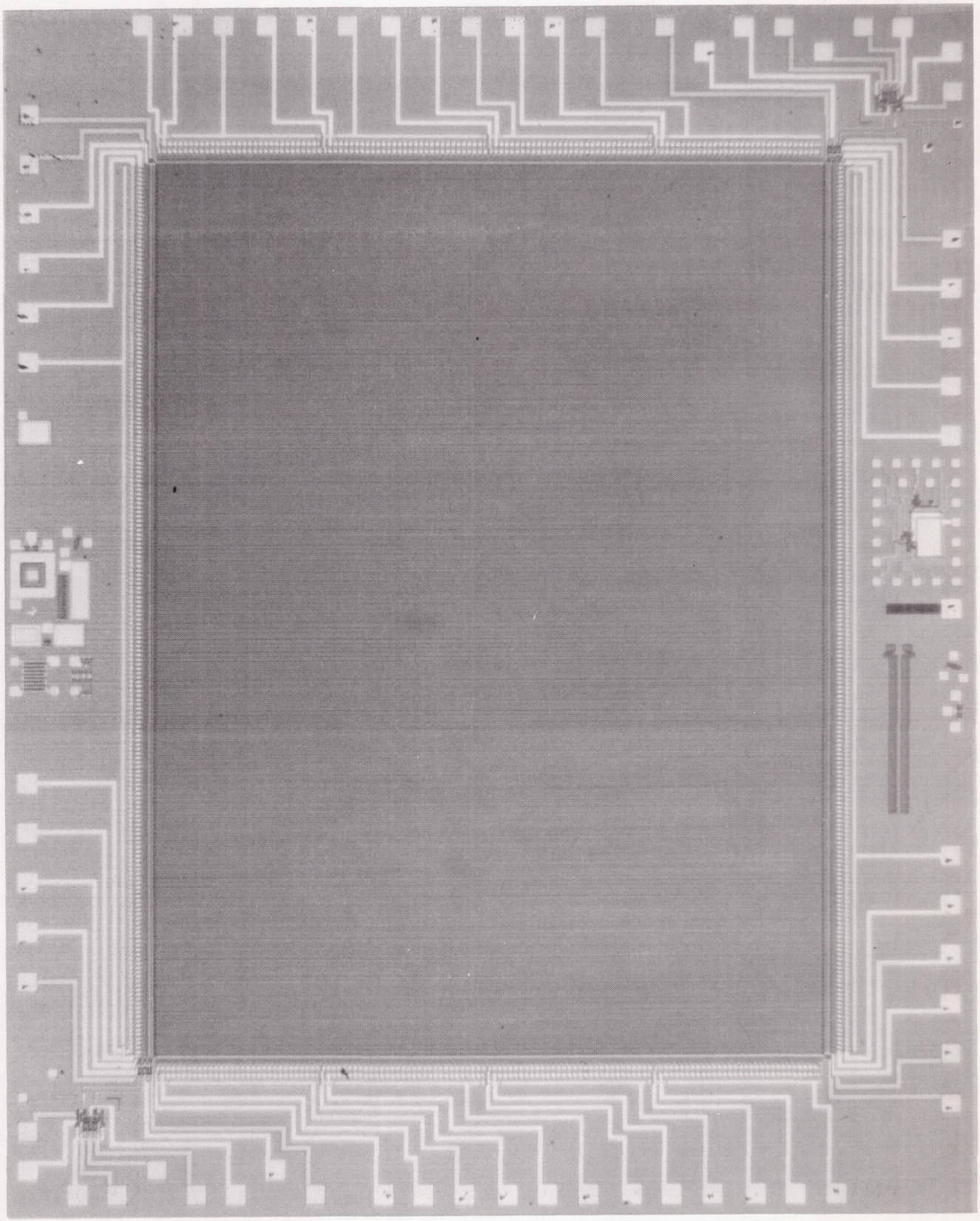

Figure 3 Photomicrograph of the 250 x 400 Imager

ORIGINAL PAGE IS
OF POOR QUALITY

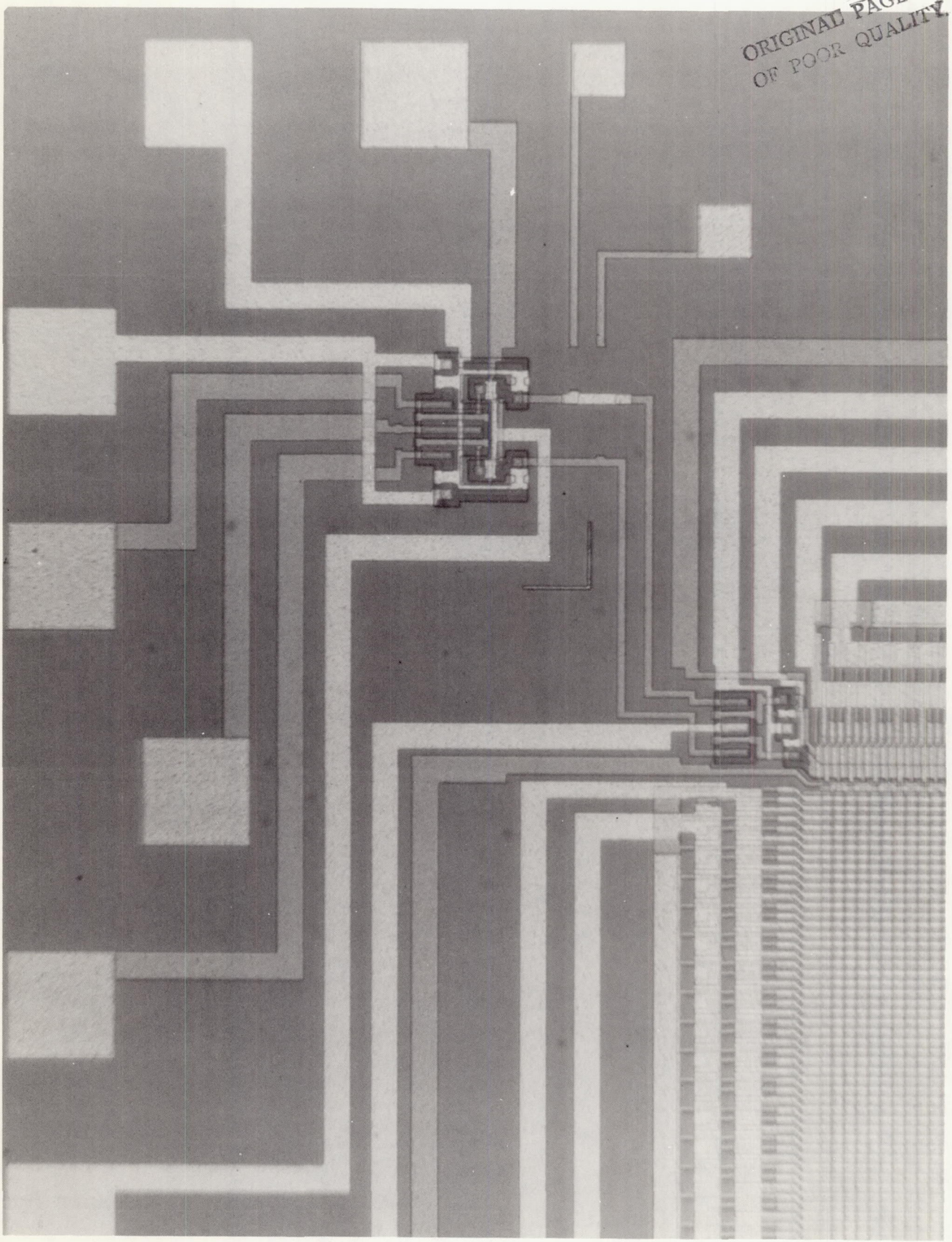

Figure 4 On-Chip Balanced Sample-And-Hold Amplifier of 250 x 400 Imager

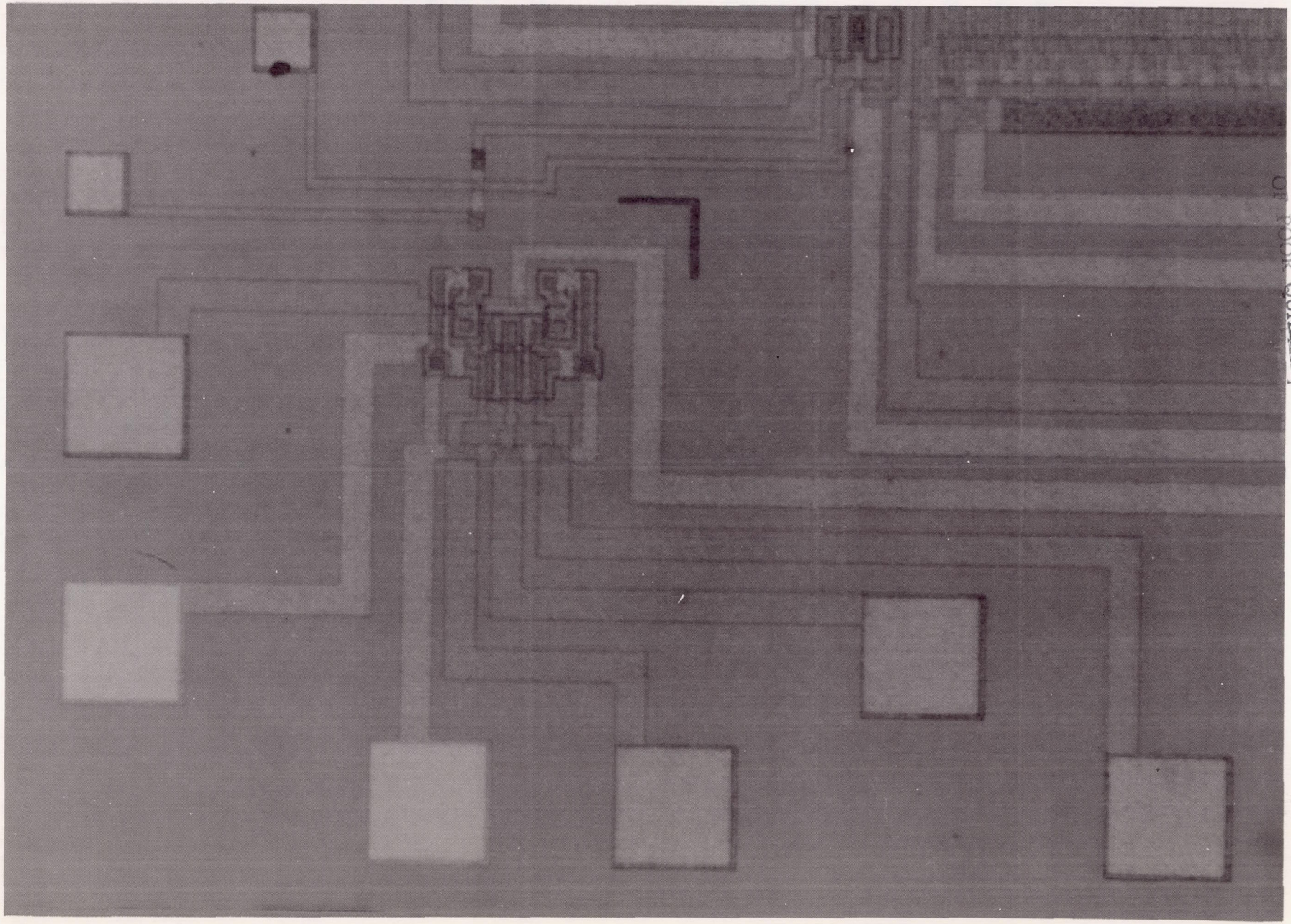

ORIGINAL PAGE IS
OF POOR QUALITY

Figure 5 Modified On-Chip Amplifier Output for 250 x 400 Imager

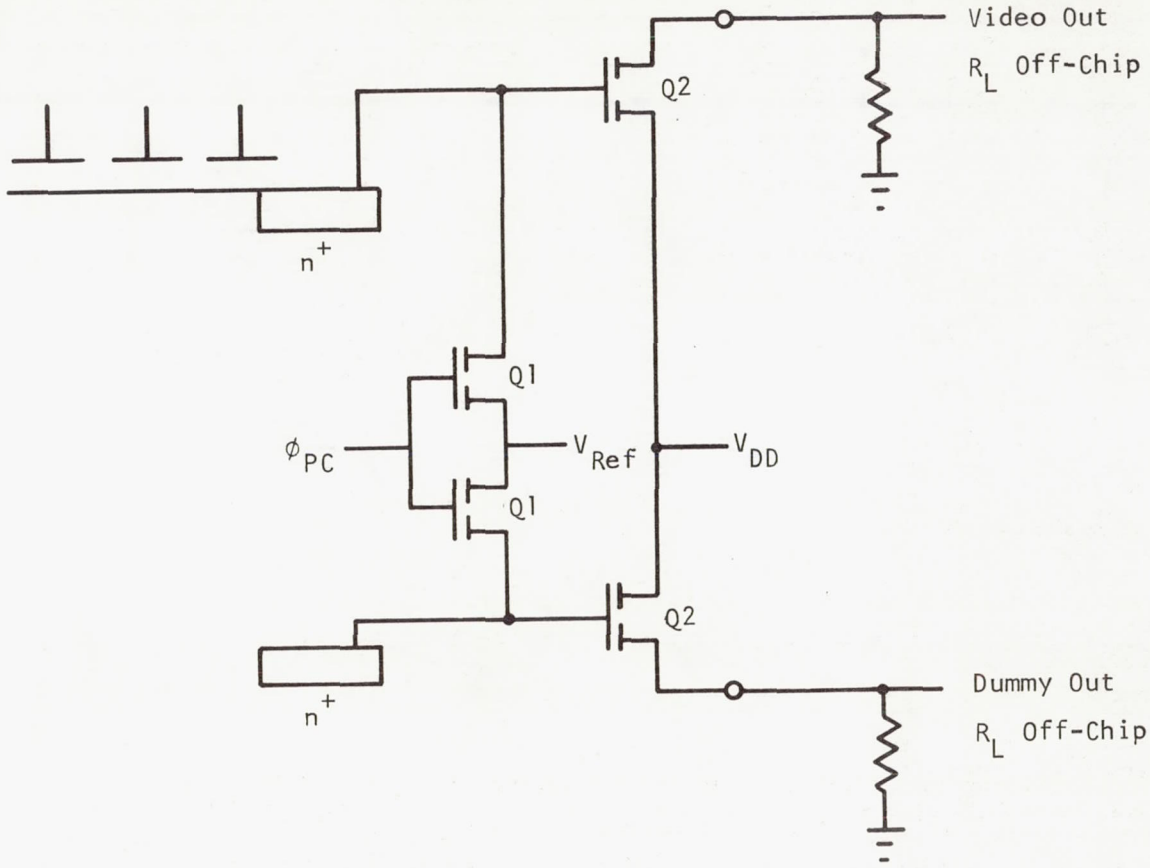

Figure 6 Schematic of Precharge Amplifier

due to the gate-source capacitance of Q2. Charge appears at the fall of the ϕ_2 pulse on the CCD register and appears as a further decrease in the voltage level V at the follower gate. The dummy output is used to allow off-chip reduction in common mode noise. The sensitivity of this precharge amplifier is about 0.50 μV/electron.

C. Device Fabrication

The imagers employed in this program were fabricated using processes described in detail elsewhere.[4] No significant changes were required in this processing as it relates to slice processing. However, a number of problems were encountered in chip processing related to thinning, accumulation, and alloying to headers. These problems and their solutions are described in Section III.

D. Header Redesign

This program called for the first delivery of large area imagers on tube-compatible headers. Previous electron-bombarded silicon studies had employed the smaller 100 x 160 array. A tube header had been designed to accommodate this device. Figure 7 is a schematic of this header. To accommodate the larger 250 x 400 array, it was necessary to enlarge the hole in the molybdenum alloy stage and in the ceramic substrate. However, it was desired to keep the diameter of the ceramic substrate constant so that it would be compatible with the existing tube flanges.

With this constraint a new tube header was designed. The basic design was that of Figure 7 with the pin circle diameter increased, the seal flange diameter increased, and the holes in the ceramic substrate and molybdenum alloy stage made rectangular and large enough for the 250 x 400 chip. In addition, the surface area of bare ceramic on the vacuum side of the header was minimized. Figure 8 shows the resulting tube header compared to the original design. Also illustrated is an example of the difference in tube flanges required for different tube manufacturers.

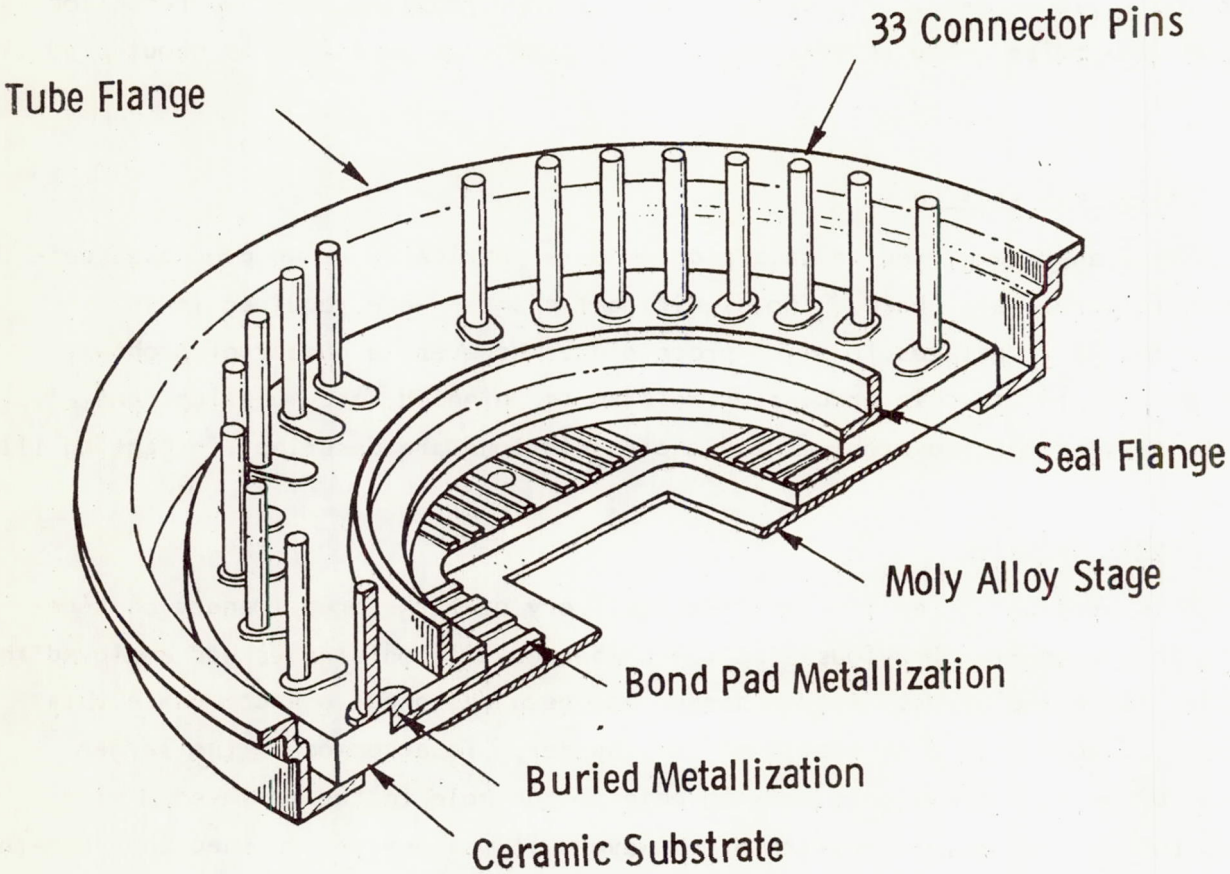

Figure 7 Cutaway Drawing of Tube Header

ORIGINAL PAGE IS
OE POOR QUALITY

Figure 8 Variations of Basic Tube Headers with Array Size and Outside Flanges

This straightforward extension of the basic design led to header fabrication problems due to the reduced ceramic thickness between the hole and the outer edge. These problems are discussed in Section III.

The pin connections for the 250 x 400 tube header are shown in Figure 9.

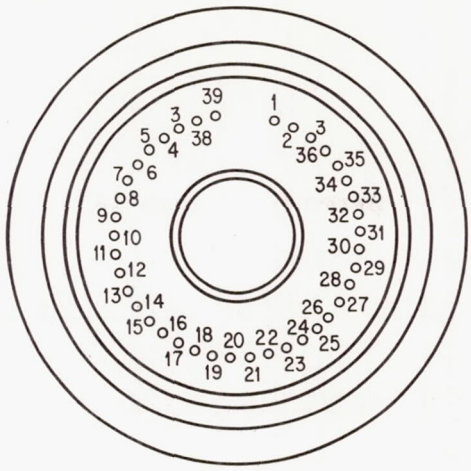

ORIGINAL PAGE IS
OF POOR QUALITY

Tube Pin Number	Symbol	Function	Tube Pin Number	Symbol	Function
1	$\phi_T{}^U$	Upper Transfer Phase	21	ϕ_{1B}	Parallel Phase 1 Section B
2	$V_{DD}{}^U$	Upper Drain Voltage	22	ϕ_{3A}	Parallel Phase 3 Section A
3		Open	23	ϕ_{1A}	Parallel Phase 1 Section A
4*	SUB	Substrate	24	$V_{DD}{}^L$	Lower Drain Voltage
5	$OUT^U{}_{(DUM)}$	Upper Dummy Output	25	$OUT^L{}_{(DUM)}$	Lower Dummy Output
6	$OUT^U{}_{(SIG)}$	Upper Signal Output	26	$OUT^L{}_{(SIG)}$	Lower Signal Output
7	OG^U	Upper Output Gate	27	OG^L	Lower Output Gate
8	$V_{REF}{}^U$	Upper Reference Voltage	28	$V_{REF}{}^L$	Lower Reference Voltage
9	$\phi_{PC}{}^U$	Upper Precharge Gate	29	$\phi_{PC}{}^L$	Lower Precharge Voltage
10	$\phi_{3S}{}^U$	Upper Serial Phase 3	30	$\phi_{3S}{}^L$	Lower Serial Phase 3
11		Open	31	SUB	Substrate
12	$\phi_{1S}{}^U$	Upper Serial Phase 1	32	$\phi_{1S}{}^L$	Lower Serial Phase 1
13	$\phi_{2S}{}^U$	Upper Serial Phase 2	33	$\phi_{2S}{}^L$	Lower Serial Phase 2
14	ID^U	Upper Input Diode	34	ID^L	Lower Input Diode
15	ϕ_{3D}	Parallel Phase 3 Section D	35	$\phi_T{}^L$	Lower Transfer Phase
16	ϕ_{1D}	Parallel Phase 1 Section D	36	ϕ_{2A}	Parallel Phase 2 Section A
17	ϕ_{3C}	Parallel Phase 3 Section C	37	ϕ_{2B}	Parallel Phase 2 Section B
18	ϕ_{1C}	Parallel Phase 1 Section C	38	ϕ_{2C}	Parallel Phase 2 Section C
19	ϕ_{3B}	Parallel Phase 3 Section B	39	ϕ_{2D}	Parallel Phase 2 Section D
20	SUB	Alloy Stage			

*Open if the device is not diode protected.

Figure 9 Pin Connections for 250 x 400 Tube Header

SECTION III
IMPROVEMENTS IN THINNED CCD IMAGER PROCESSING

A. Outline of Thinned CCD Imager Processing

The fabrication of thinned CCD imagers begins with slices of silicon and progresses through a standard set of processing steps involving photolithography, oxidations, diffusions, metallizations, and etches.[4] The fabrication of a slice of CCD imagers varies little in fundamental detail from the fabrication of other MOS semiconductor devices. However, the remaining processing required to produce the final device is nonstandard and requires development specifically for backside-illuminated CCD arrays. The remaining processing steps are (1) thinning, (2) accumulation, and (3) alloy and bond to a tube-compatible header. Discussion of these processes follows.

(1) Thinning. CCD imagers are backside-illuminated to improve spectral response and to allow electron-bombarded operation. These backside-illuminated imagers must be thinned to provide adequate resolution. Resolution is degraded when charge carriers diffuse laterally while diffusing toward the CCD storage wells. The degradation is maximum for blue light and for electron input, since these radiations are absorbed near the silicon surface. Thinning brings this surface near the CCD wells and minimizes lateral diffusion.

(2) Accumulation. An unoxidized silicon surface is a region of rapid electron recombination. Signal electrons that recombine at the back surface are not detected by the CCD. Since most signal electrons generated by blue light and by energetic electrons are created near the back surface, this recombination must be inhibited to achieve adequate CCD response. This is accomplished by building into the CCD an electric field that forces signal electrons away from the back surface. The electric field is generated by enhancing the boron doping density of the silicon at the surface compared to the bulk doping density. Since boron atoms in silicon are negatively charged, this accumulation of boron introduces a fixed space charge that repels signal electrons from the silicon surface.

(3) Alloy and Bond. Intensified charge coupled imaging requires the incorporation of the CCD in a vacuum bottle with a photocathode and provision for electron focus. Tube processing requires high vacuum, high temperature ($\sim 350°C$) bakes, and photocathode processing. The CCD header must be compatible with this tube processing and must allow frontside bonding with backside imaging. The high temperature bakes and vacuum requirements prohibit the use of epoxies to attach the chip to the header. Alloying of the chip to the header is therefore required. The chip and header are then interconnected by the thermocompression bonding of gold wire between the gold pads on the header and the aluminum pads on the CCD.

Basic procedures for these processes existed at the beginning of the program. Early experiences with these procedures during the course of the program indicated the need for improved device yield and performance. The next section presents a discussion of (1) problems encountered with yield loss experienced during the thinning of large arrays, (2) a study of the accumulation process that indicated problems of unpredictable photoresponse and increases in dark current, (3) problems in the alloy and bond that led to yield loss and dark current increase, and (4) problems in header manufacture and reliability.

B. Characterization of Critical Processing Steps

1. Thinning Process

The thinning process developed at Texas Instruments[3] had been applied primarily to the 100 x 160 devices prior to the beginning of the program. Thinning of 400 x 400 imagers had been accomplished, but because of the low number of these devices, little had been learned about the problems of extending this progress to larger imagers. The results of the thinning process were described as "variable"[4] immediately prior to the start of this contract.

When the thinning process was applied to the 250 x 400 array, excessive yield loss resulted. The mechanism of this yield loss was that the membranes

thinned nonuniformly, the edges of the membrane etching much more rapidly than the central portion. This could be tolerated on the 100 x 160 membrane, but not on the larger membranes. Device loss occurred when holes were etched completely through the membrane. When the imager was removed prior to this etch-through, the central portion of the device was still too thick to allow adequate imaging performance. These problems are illustrated in Figure 10, a photograph of a back-lighted membrane (without CCD) improperly etched so that holes were produced. The dark area is thick silicon. Circular regions in the membrane are bubbles in the underlying wax.

This accelerated etching near the edges of the membrane is caused by flow effects in the rotating beaker used in this process. Analysis of these effects allowed modifications of the process to be chosen that have eliminated yield loss due to etching through the membrane. Figure 11 illustrates the improvements achieved. No indication of etch-through is observed in this photograph. Through these modifications the thinning process has been developed so that it is now a geometry-independent, high yield process. Equally good results are obtained if the chips are individually thinned or whole-slice thinned.

2. Accumulation Process*

a. Characterization Requirements

As discussed earlier, the thinned surface of a backside-illuminated imager must have an accumulation layer of boron atoms to minimize signal loss at this surface. This can usually be accomplished by diffusion of boron atoms at high temperature (1000°C) after thinning.[5] However, this process cannot be used with the CCDs employed in this work due to the aluminum metallization. Texas Instruments had developed a process that allows this accumulation to be accomplished without the use of high temperatures after metallization. This process

* This work also supported by NASA-Goddard Contract No. NAS5-23578 and NVL Contract No. DAAG53-75-C-0191.

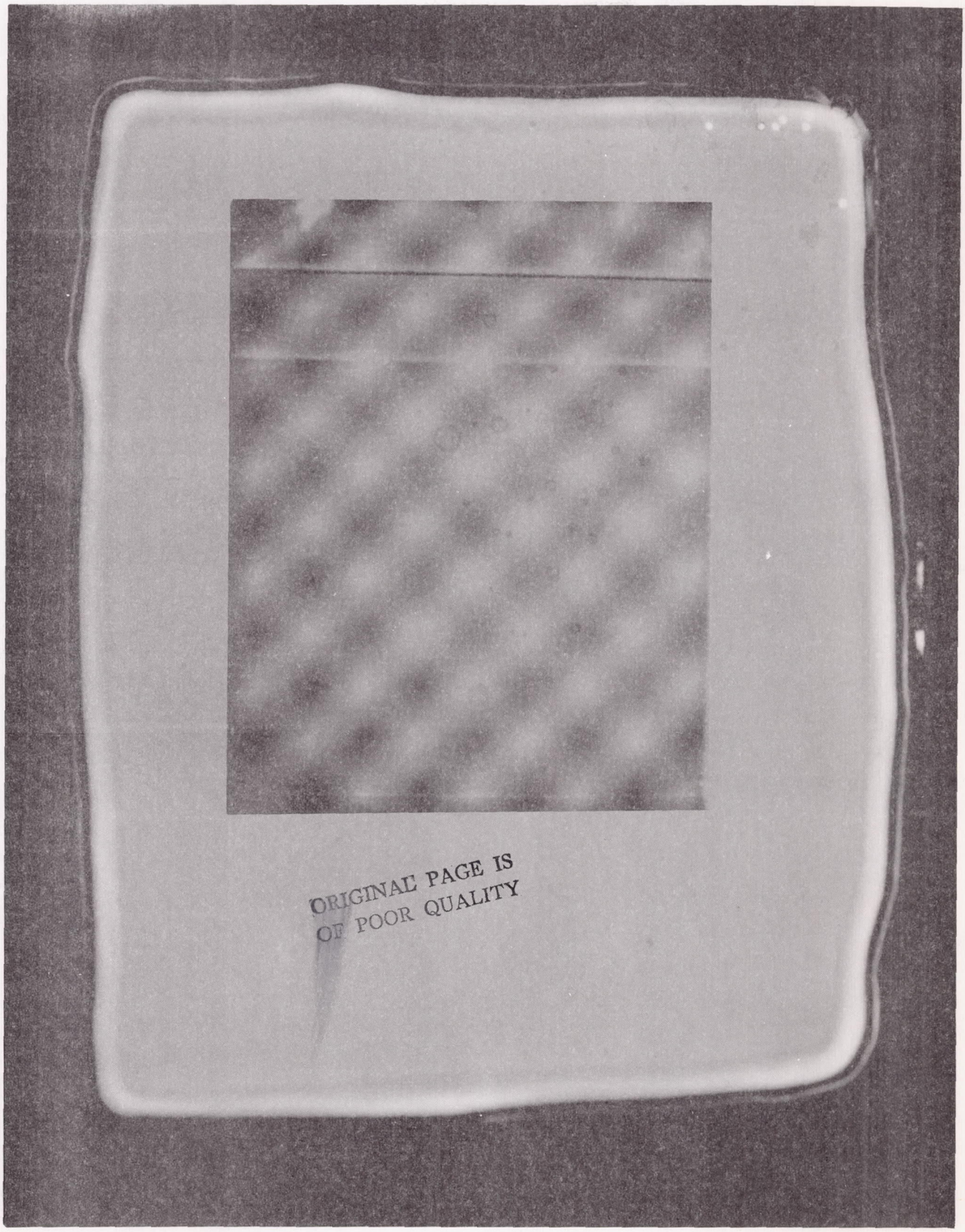

ORIGINAL PAGE IS
OF POOR QUALITY

Figure 10 Improperly Etched Membrane

ORIGINAL PAGE IS
OF POOR QUALITY

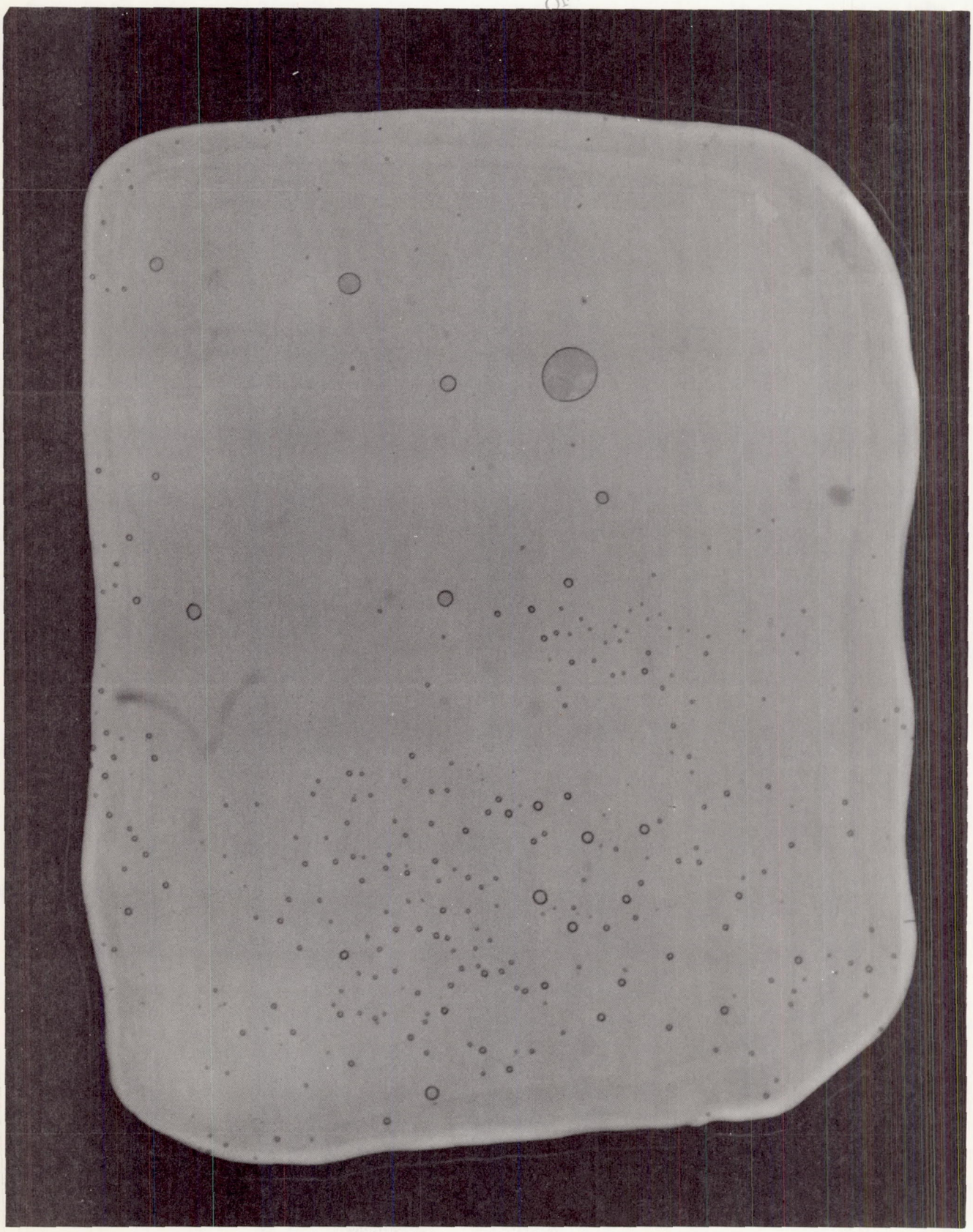

Figure 11 Uniformly Thinned 250 x 400 Membrane

has been shown to be capable of producing spectral responses that are apparently not degraded by losses at the back surface, except for optical reflection. However, results have varied from device to device as shown in Figure 12. Measurements were made, as described below, to characterize this process, with the goals of reproducibility of spectral response and determination of the effects of the process on dark currents.

b. Measurement Techniques

The accumulation process was characterized with respect to its most critical variable "α," a controllable variable. The process was characterized by processing a device with sequential, monotonic changes in α, monitoring the device dark current and photoresponse before and after each step. To facilitate this sequential processing, all measurements were made on unmounted chips using a functional multiprobe. This multiprobe consists of a chuck with imbedded light sources for backside illumination and a probe card with individual probes for each bond pad. Electrical signals are supplied to the probes as required to operate the chip.

c. Measurement Results

The first sets of measurements were made using a green 5600 Å light-emitting diode for photoresponse measurements. Typical results are shown in Figure 13 where dark circles represent the normalized photoresponse at 5600 Å and the Δ's represent the dark current density for sequential values of the variable α.

These data indicate the effectiveness of TI's accumulation process. The photoresponse at 5600 Å is increased by a factor of 550 as a result of this processing. The maximum response observed corresponds approximately to the reflection limit. The data also indicate, however, that the process can have a serious effect on the dark current level. For values of the variable α above an optimum value, the dark current density increases rapidly, and the photoresponse

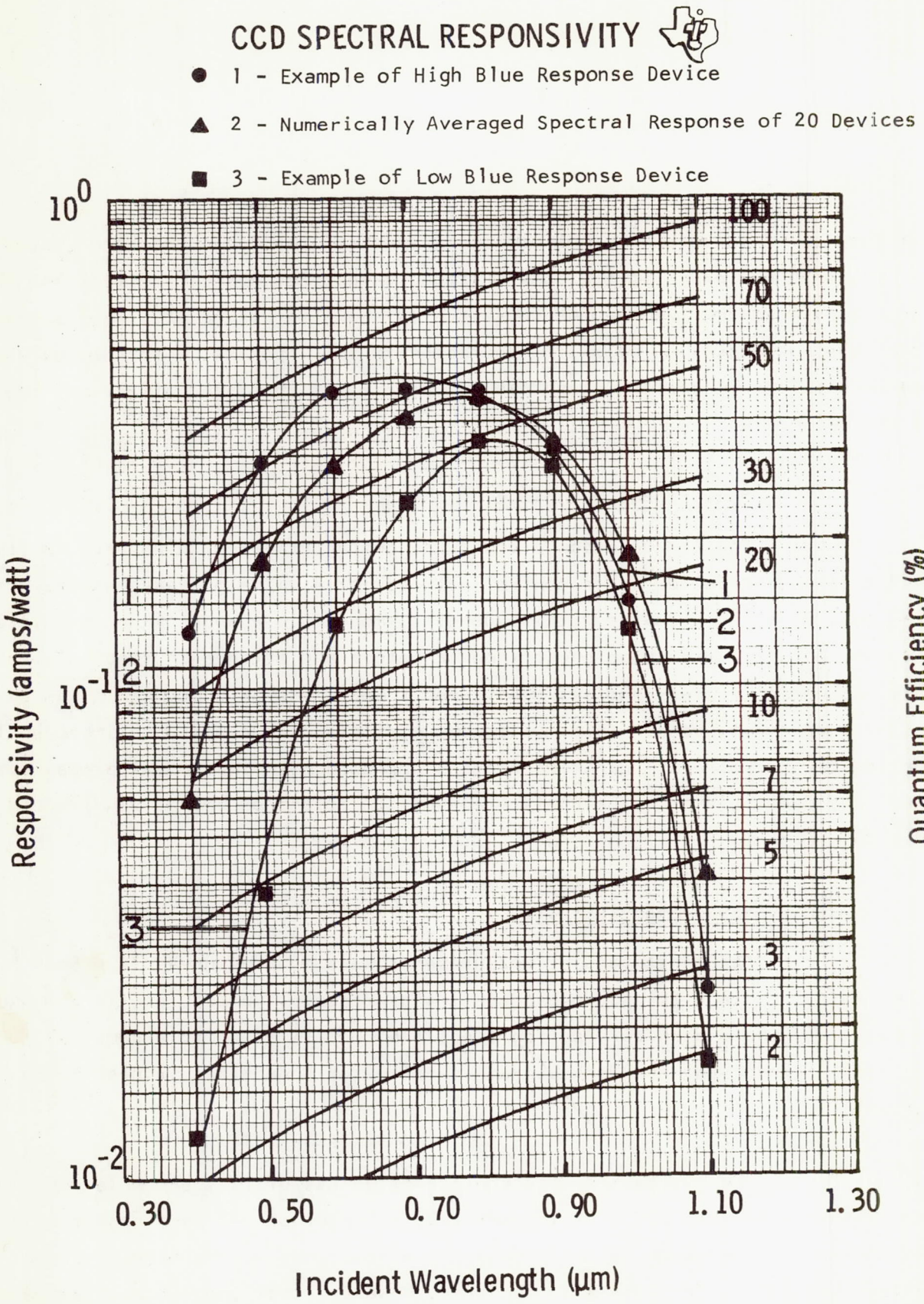

Figure 12 Summary of Spectral Response Data for Twenty 100 x 160 Devices

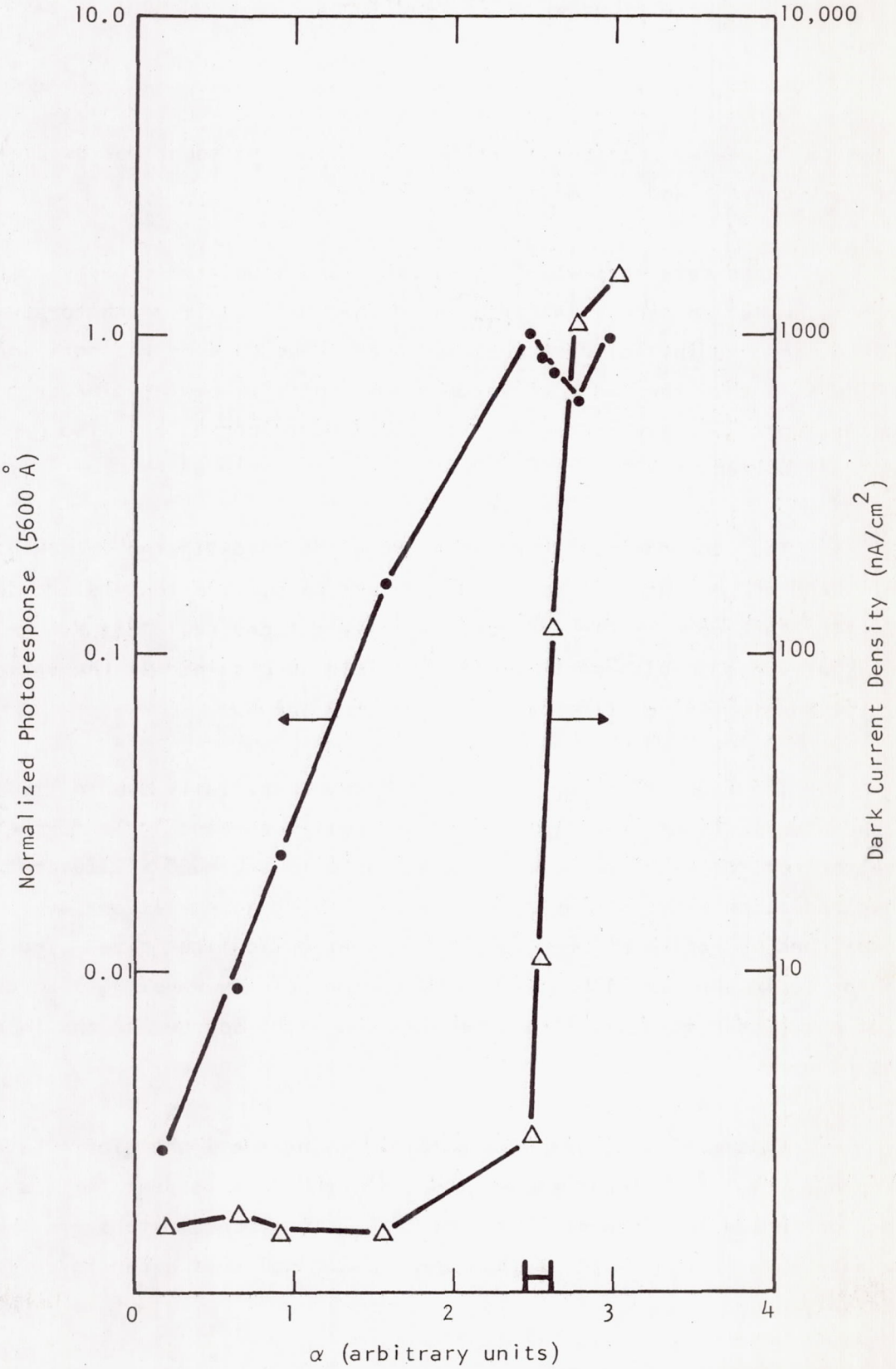

Figure 13 Effects of TI Accumulation Process on Photoresponse and Dark Current

is observed to decrease. Devices processed to this point sometimes display time-dependent dark current and photoresponse.

These data indicate that the variable α must be closely controlled during the accumulation processing at a value that will maximize photoresponse while maintaining the initial dark current level. The bars on the horizontal axis of Figure 13 show the range of values of α typically employed prior to these measurements. These values lead to high photoresponse, but also produce increased dark current.

The reproducibility of these data was investigated by taking other chips and processing them to various values of α. The results are shown in Figure 14. Each open circle indicates a different device. This figure indicates that reproducible spectral responses can be obtained if the variable α is maintained at a value at or below its optimum value.

The light emitting diode was employed initially due to its availability and simplicity of installation in the multiprobe chuck. To further investigate the optimum value of α, it was desirable to use 4000 Å illumination, since this radiation is more sensitive to the backside accumulation layer. This was accomplished by replacing the LED with a fiber optic light pipe. The backside of the chips could then be illuminated with photons of any wavelength through the use of narrowband optical filters between the light source and the input to the light pipe.

Figure 15 shows results obtained using the light pipe. Data on green response (5461 Å), blue response (4000 Å), and dark current for a single device are presented for sequential values of α. Incremental steps are smaller in these data than in Figure 13 so that the optimum value of α can be defined more precisely.

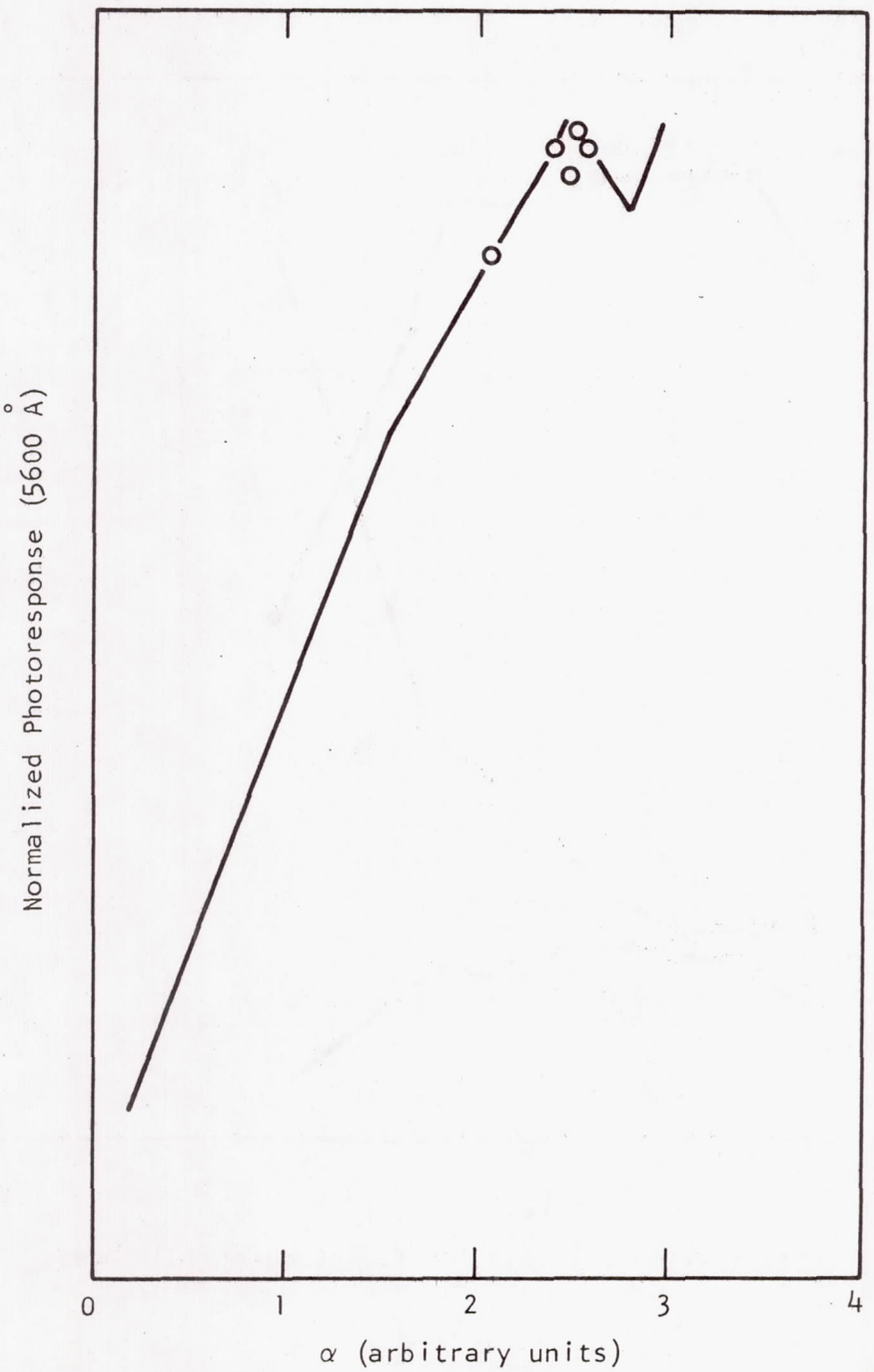

Figure 14 Response Reproducibility of the TI Accumulation Process

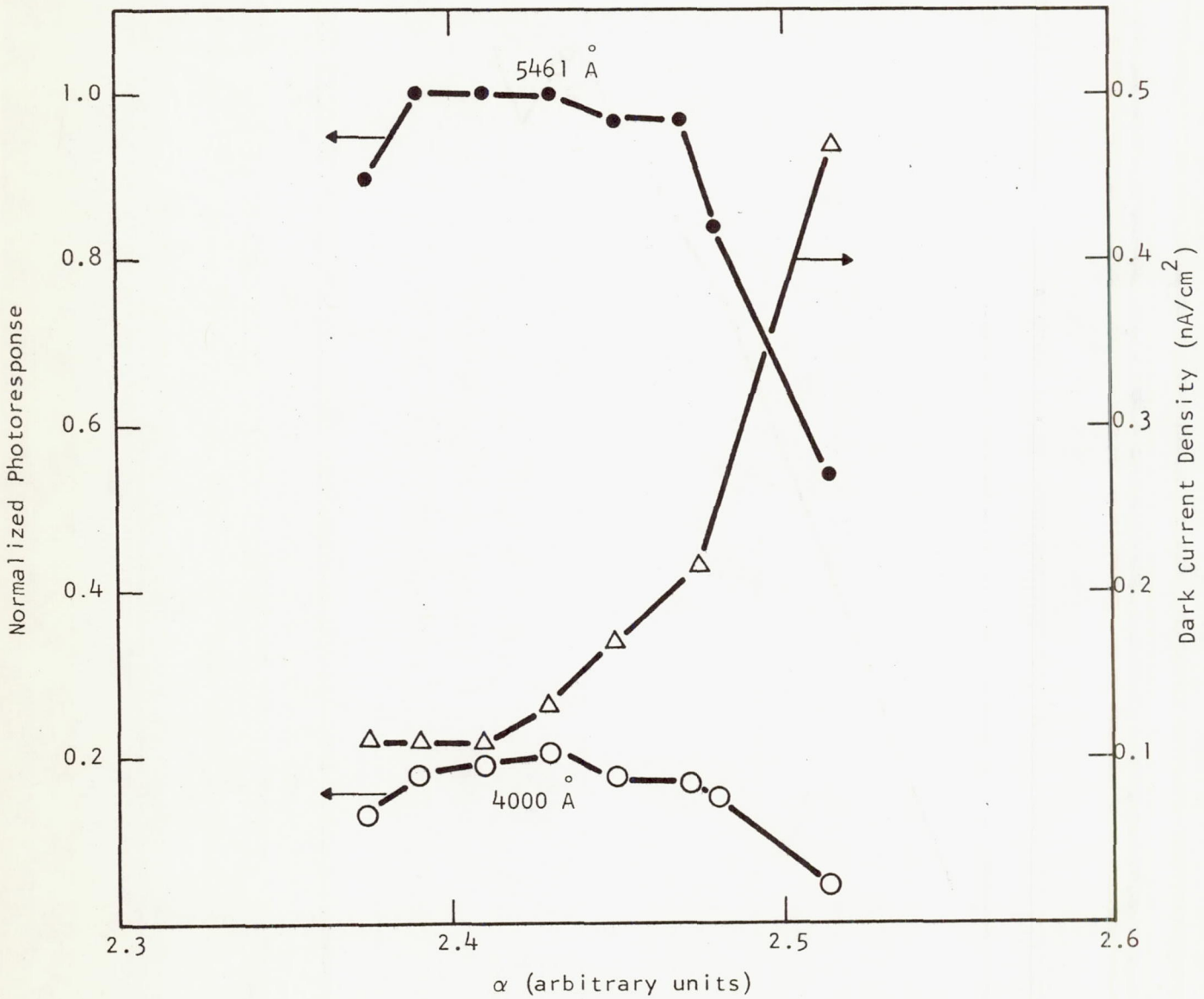

Figure 15 Optimization Data for the TI Accumulation Process

Two important results are indicated in Figure 15: (1) Although the blue response and the green response show similar behavior, the blue response peaks at a lower quantum efficiency ($\sim$ 20%) than the green response ($\sim$ 70%); and (2) the maximum blue response occurs at the onset of dark current increase. The magnitude of the blue response peak is a function of other variables in the process that are normally held constant. Internal investigations are being made to determine the causes of this blue response limit. The increase in dark current can be avoided by choosing a value of α somewhat below the value for peak blue response.

These results were immediately applied to device processing. Reproducible spectral response curves have been obtained, and dark current increases during the accumulation process have been eliminated. Typical data are presented in Figure 16 showing spectral data for six recently processed devices.

d. Conclusions

The accumulation process has been characterized with respect to its most critical variable. The results indicate that reflection-limited response can be reproducibly obtained above 6000 Å. Dark current increases during the accumulation process have been discovered and eliminated. The blue response is limited to about 15% to insure low dark current and stability.

3. Alloy and Bond Process

a. Mechanical Buckling

Thinned CCDs are attached to the header using a gold-silicon eutectic alloy. The eutectic temperature is 370°C. In the alloy process the header is heated to about 390°C and a gold preform is placed on the molybdenum alloy stage (see Figure 7). The device is scrubbed against the preform until the melted eutectic results. The header is then cooled to room temperature. As this cooling takes place, both the silicon and the molybdenum contract, the molybdenum more than the silicon because of its larger thermal coefficient of expansion. This results in compressive stress on the silicon after the eutectic

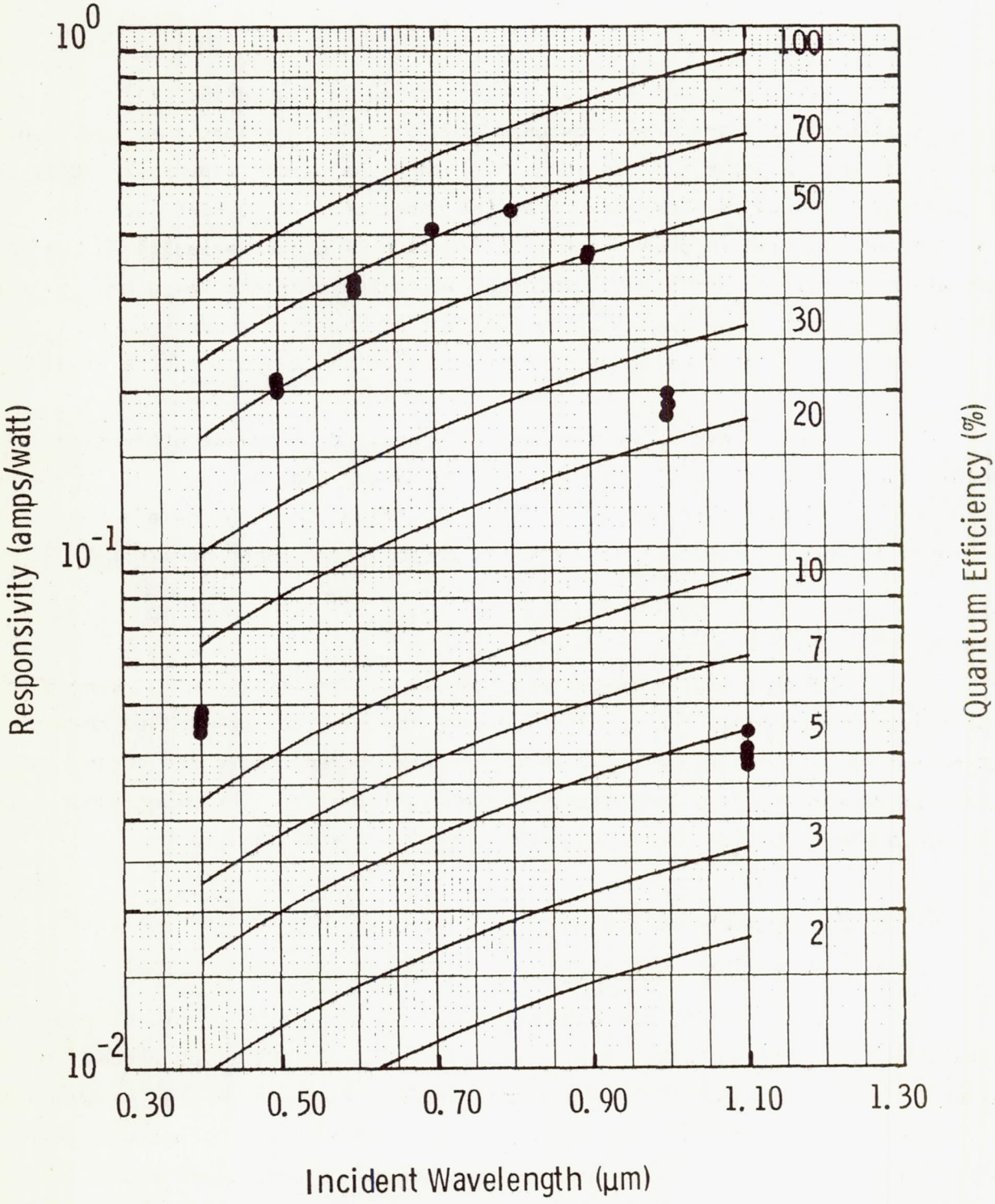

Figure 16 Spectral Response of Six Recent 100 x 160 Devices

solidifies, and the membrane buckles to accommodate this stress. This effect is evident, but not critical, on 100 x 160 arrays; however, on 250 x 400 arrays the stress can be large enough to cause membrane fracture.

Several variations in the alloy procedure and in the device configuration were investigated in an effort to diminish the buckling of the membrane. Variations in the cooling rate were ineffective. A wider or thicker supporting rim around the membrane reduces the buckling on the 100 x 160 arrays, but is not effective for the 250 x 400 arrays. These investigations indicated that a permanent solution to the problem would require implementation of an alternative attachment method (beam lead) or redesign of the header to compensate for temperature-induced stresses.

To continue progress in other areas, a temporary solution to the buckling problem was sought. It was found that when the device was alloyed only at one corner, the membrane did not buckle. This was implemented to avoid device loss at the alloy step. This attachment method is adequate only for laboratory evaluation of the ICCDs. Under moderate shock the device will separate from the header. Effort has begun at TI under other contracts to develop a reliable attachment method that does not result in membrane buckling.

b. Dark Current Changes

During the characterization of the accumulation process, the dark current of the arrays was monitored after each step. It was found that the processing could be performed so that no significant dark current change occurred from that observed on-slice to that observed after accumulation. However, it was found that the dark current increased during the alloy and bond process. Table 1 illustrates this effect. It can be seen that this increase in dark current at alloy is the dominant source of dark current in ICCDs. It can also be seen that the increase is reversible to some extent, as indicated by device 7. This device

Table 1

Alloy Effects on Dark Current

Device	Dark Current (nA/cm^2) Pre-Alloy	Dark Current (nA/cm^2) Post-Alloy	Change (%)
1	1.8	7.9	+340
2	2.5	18.9	+660
3	2.2	8.7	+300
4	1.3	12.0	+820
5	1.3	11.4	+780
6	1.2	5.5	+360
7	2.0	16.6	+730
7*	16.6	7.5	-550
8	2.8	22.4	+700

*Re-alloy

was alloyed to one header, then removed and alloyed to a second header. During the first cycle, the dark current increased by 730%. During the second cycle, it decreased by 550%.

Experiments were immediately begun to determine the cause of this dark current increase. Stress effects versus heating effects were investigated by heating imagers to 390°C without alloying. It was found that heating without alloying produced the same dark current increase indicated in Table 1. The dark current is therefore not stress induced. Thinning and accumulation effects were investigated by heating unthinned devices. The results were again similar to those in Table 1. Ambient effects were investigated by heating chips in air, nitrogen, and forming gas. No differences in results were observed. Temperature effects were investigated by heating unthinned devices in nitrogen for ten minutes at various temperatures. The results are shown in Figure 17. Little change is observed for temperatures below 300°C.

These initial results indicated that the dark current increase was not a problem unique to thinned CCD imagers and that minor modifications of the alloy procedure would not be effective in eliminating this increase. More detailed studies of the effects of heat treatments on the properties of silicon would be required to understand and eliminate the dark current increase.

Gated diode test structures are very useful for studying dark currents in silicon devices[6] and were applied to this problem. These structures are included on each CCD imager. On the 100 x 160 imager, two gated diodes exist, one with buried channel under the gate and one without the buried channel. After the imager chips were subjected to isochronal anneals, the I-V characteristics of the gated diodes were determined.

Measurement of the gated diode I-V characteristics allows the dark current contributions from various regions of the silicon to be determined. These regions are the bulk region near the metallurgical junction, the $Si-SiO_2$ interface region, and the bulk region below the gate, either implanted or unimplanted.

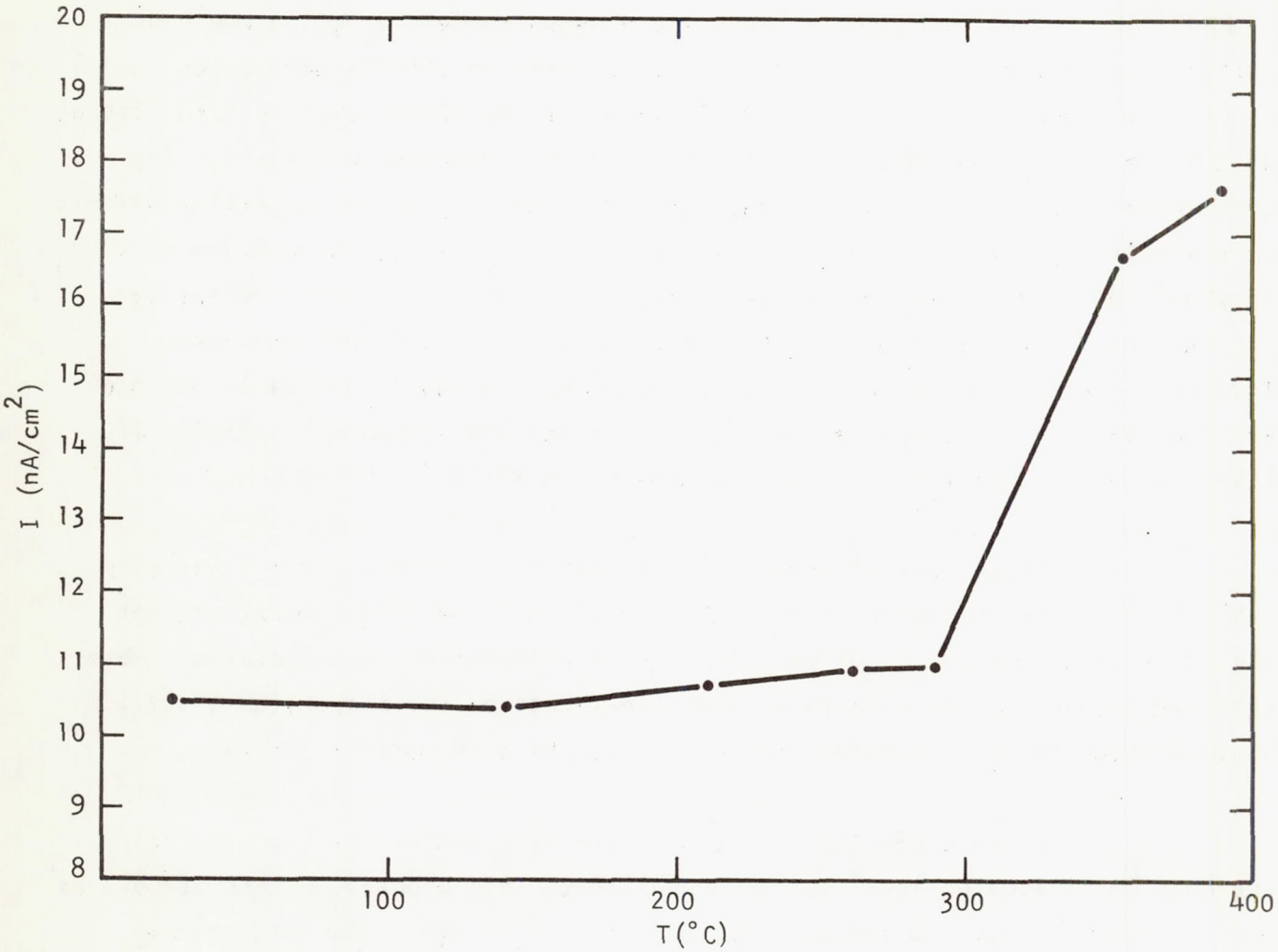

Figure 17 Effects of Isochronal Anneals on CCD Dark Current (Ten Minute Anneals)

Figure 18 shows an implanted gated diode under three different gate bias conditions. A constant reverse bias is applied between the n^+ diffusion and the substrate; leakage current is also monitored in this circuit. For large, positive gate potential, V_G, the surface under the gate is accumulated [Figure 18(a)]. Dark current is generated through the depletion regions of the metallurgical junction. The metallurgical junction now includes the implanted n region as well as the n^+ diffused region. As V_G is swept less than zero, the buried channel region under the gate starts to deplete. As soon as the surface is depleted, the surface generation contributes to the leakage current through the diode [Figure 18(b)]. Further decreases in gate voltage increase the depleted volume in the buried channel, and the leakage current increases correspondingly. When V_G becomes less than the voltage necessary to invert the surface, V^*, the surface inverts and the surface generation is eliminated [Figure 18(c)]. Typical I-V curves for implanted gated diodes are shown in Figure 19. The steps in these curves can be used to determine the dark current contributions from the unimplanted bulk region, from the $Si-SiO_2$ interface region, and from the implanted bulk region.

A similar analysis can be made for the case of unimplanted diodes.[6] Annealing experiments on these devices, however, revealed no significant change in dark current. This indicates that the dark current changes are related to the implanted region of the devices. The remaining data reported here deal with results from implanted diodes.

Figure 19 presents the results of I-V measurements made on an implanted diode after various anneals. Two types of behavior have been observed. Type I behavior is illustrated in Figure 19. Important points to note from Figure 19 are that (1) relatively little change occurs between 25°C and 300°C, (2) a large change is observed between 300°C and 350°C, (3) most of the 350°C change occurs in the portion of the curve related to the implanted region, (4) the 400°C anneal reduces the dark current, and (5) the 400°C reduction in dark current results from decreased dark current under the gate and increased dark current from the remainder of the diode.

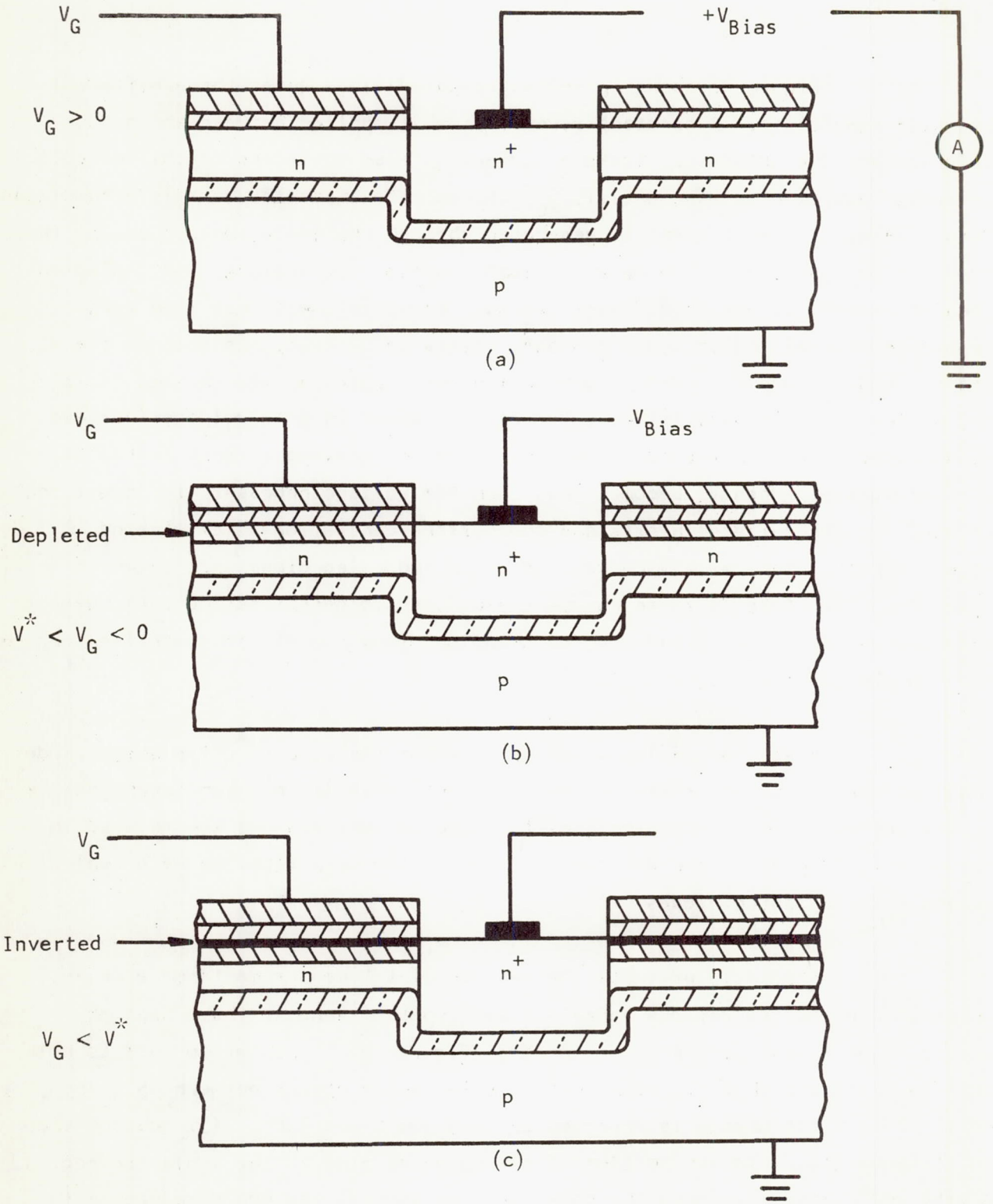

Figure 18 Gated Diode Bias Conditions

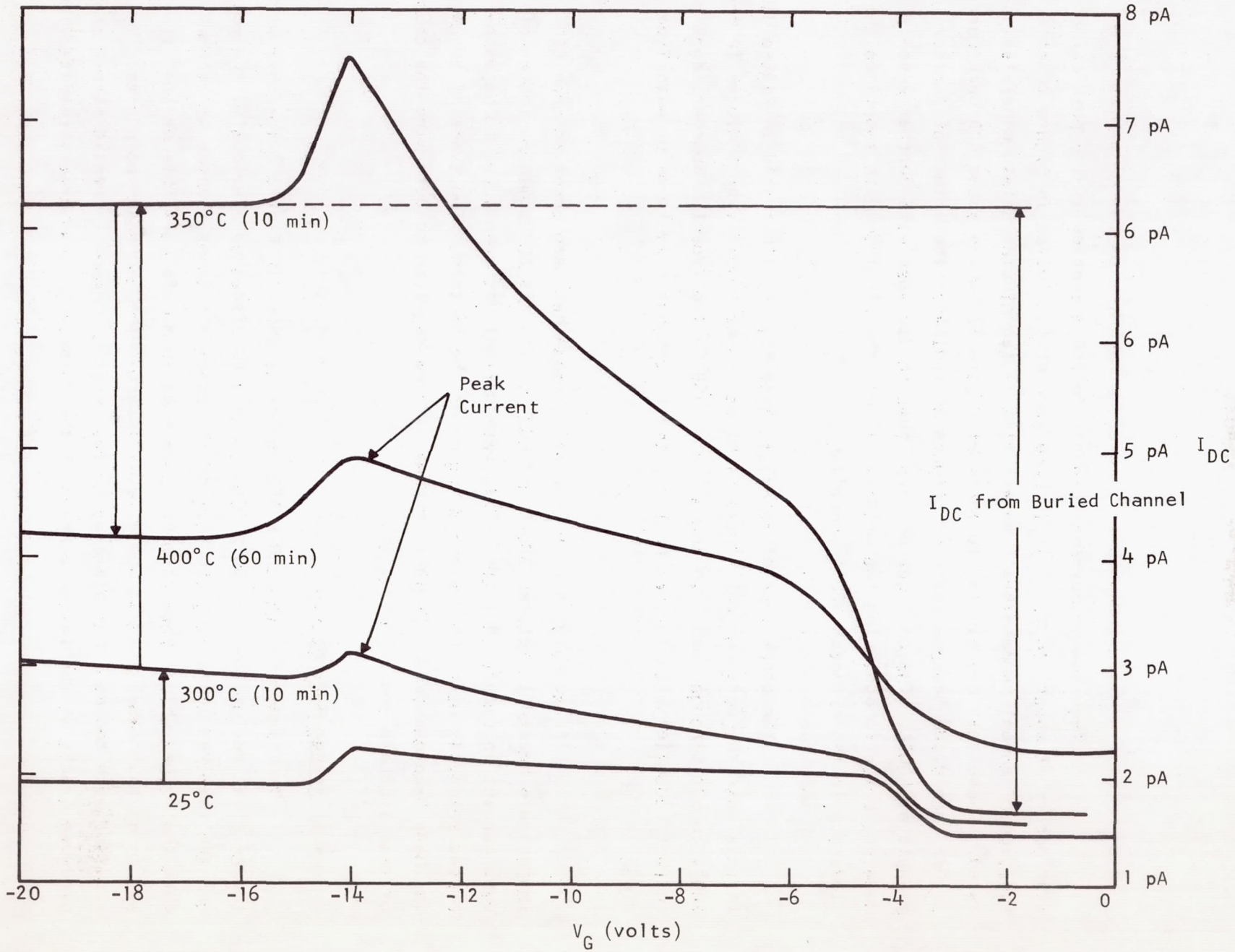

Figure 19 I-V Characteristics of an Isochronally Annealed Implanted Gated Diode

The leakage current relevant to CCD operation is the peak current that occurs at about -14 V. This leakage current is plotted in Figure 20 as a function of anneal temperature. Anneal time is ten minutes unless otherwise noted. These data are similar to those of Figure 17, which shows CCD dark current rather than diode leakage current. Figure 20 indicates the effect of further anneals at 400°C. The dark current continues to decrease with further anneals. However, prior to achieving the original level, the aluminum gate shorts to the diode due to the extended 400°C annealing.

The other type of behavior, Type II, is illustrated in Figure 21. In this case the dark current starts high, decreases toward Type I diodes in the 200°C to 300°C range, and then increases at 350°C like Type I. However, dark current reduction with further heat treatment does not seem to occur with Type II diodes.

In summary, a dark current increase has been observed when CCD imagers are heated to between 300°C and 400°C. This is the dominant source of dark current in completed ICCDs. This dark current has been found to be associated primarily with the implanted region of the devices. Two types of behavior have been observed. Further studies will be required to determine the cause of this increase and eliminate it.

4. Header Manufacture

The header for the 250 x 400 device is shown in Figure 8 together with the original design for the 100 x 160 device. As discussed previously, the primary changes involved increasing the size of the holes and inner flanges to accommodate the larger chip. When attempts were made to manufacture this device, it was found that other changes would be necessary. The increased hole size, together with the constant diameter of the ceramic, caused increased stress that produced cracks at the inside corners of the ceramic. These cracks resulted in

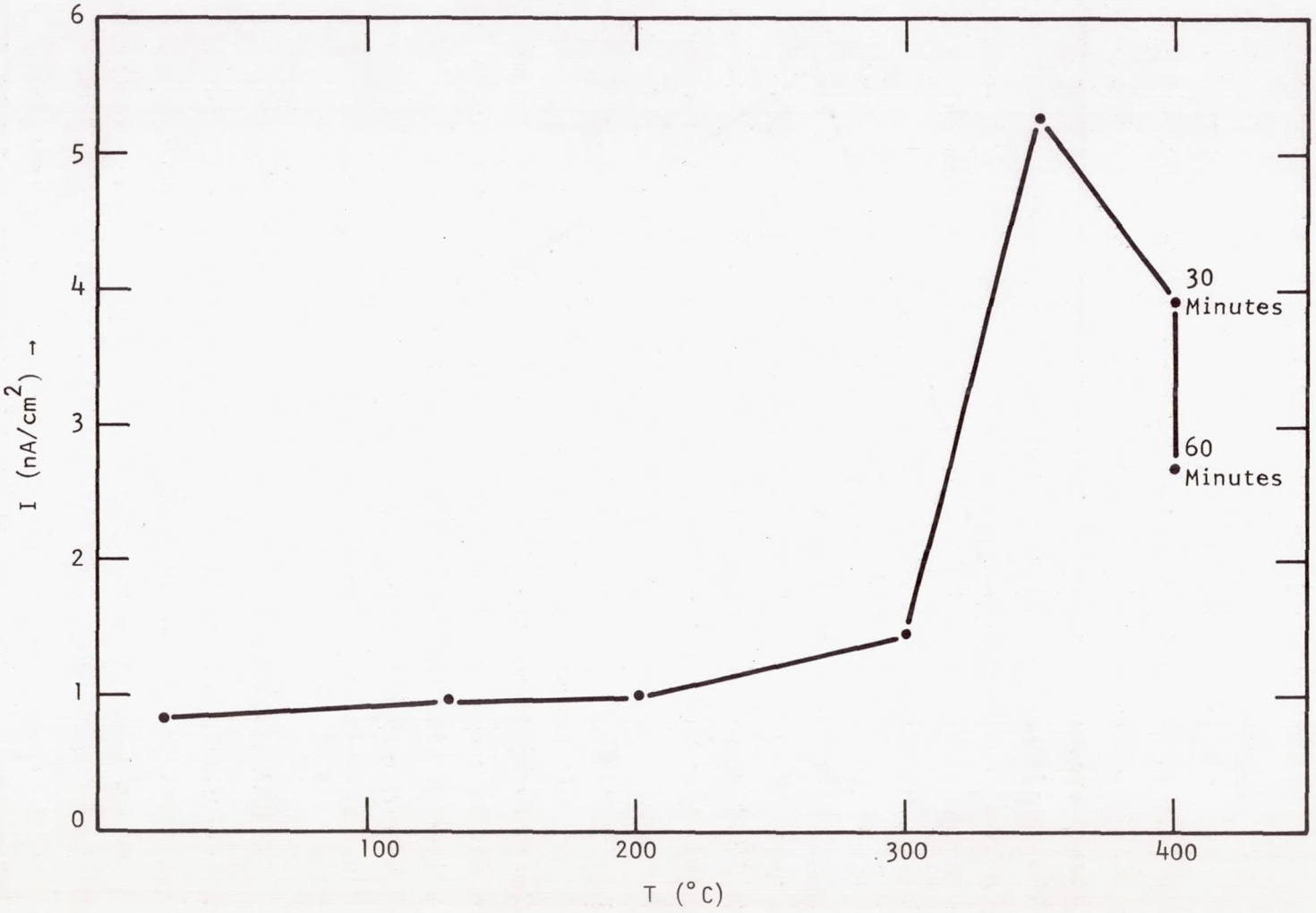

Figure 20 Gated Diode Leakage Current, Type I Behavior

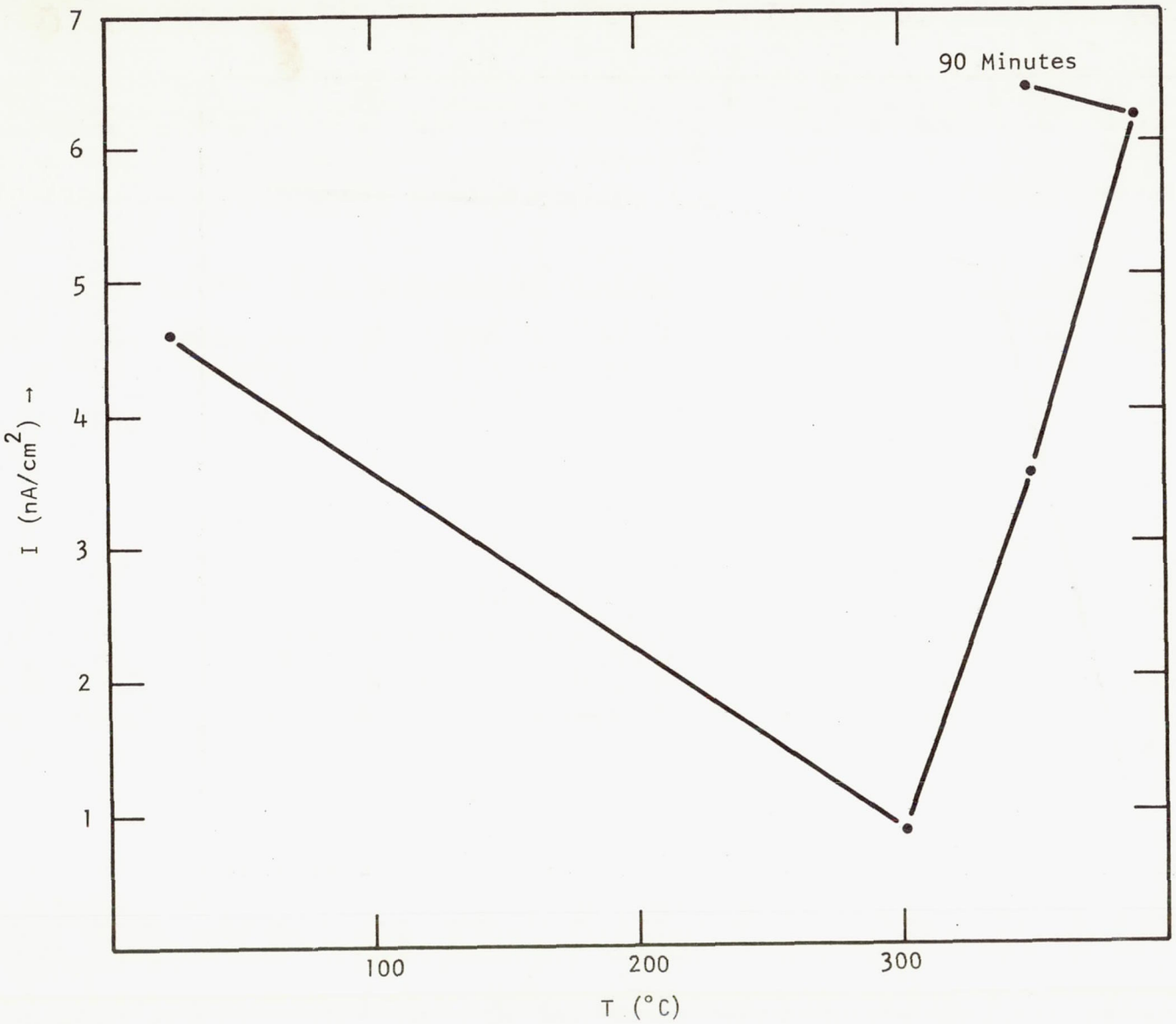

Figure 21 Gated Diode Leakage Current, Type II Behavior

vacuum leaks. Three structural changes were required to relieve these stresses: (1) The ceramic thickness was doubled. (2) The corners of the hole were rounded. (3) The back molybdenum plate was decreased in area. The original redesign is compared to the final header configuration in Figure 22. With these modifications crack-free headers could be produced.

The first attempts at tube processing using these headers revealed a reliability problem. The thermal processing caused cracks to develop in some headers, resulting in the loss of good imagers. The remaining stock of headers was subjected to simulated tube processing and rechecked for vacuum leaks. All leaking headers were returned to the manufacturer for replacement. The header manufacturer instituted a postprocessing temperature bake to screen for these unreliable headers. Since this screening has been in effect, no additional device losses have been caused by header failures.

Another problem was encountered in the implementation of these redesigned headers. The preparations for tube processing require the chip to be alloyed and bonded to a header and then a Kovar cap welded to the inner flange to provide vacuum compatibility. This had previously been accomplished using heliarc welding. Device losses occur during this step unless the pins are carefully wired together and grounded and adequate heat sinking is provided. These precautions had been developed during earlier 100 x 160 imager processing. Initially, the same procedures were applied to the welding of the larger Kovar cap on the 250 x 400 header. It was found, however, that vacuum-tight welds were sometimes not obtained. Bubbles formed in the melt that resulted in holes in the weld. The problem was thought to be related either to the increased power required for the larger cap or to impurities left on the inner flange during tube processing.

As a result of this problem, alternative welding techniques were considered. A laser welder had recently been installed at Texas Instruments. This

ORIGINAL PAGE IS
OF POOR QUALITY

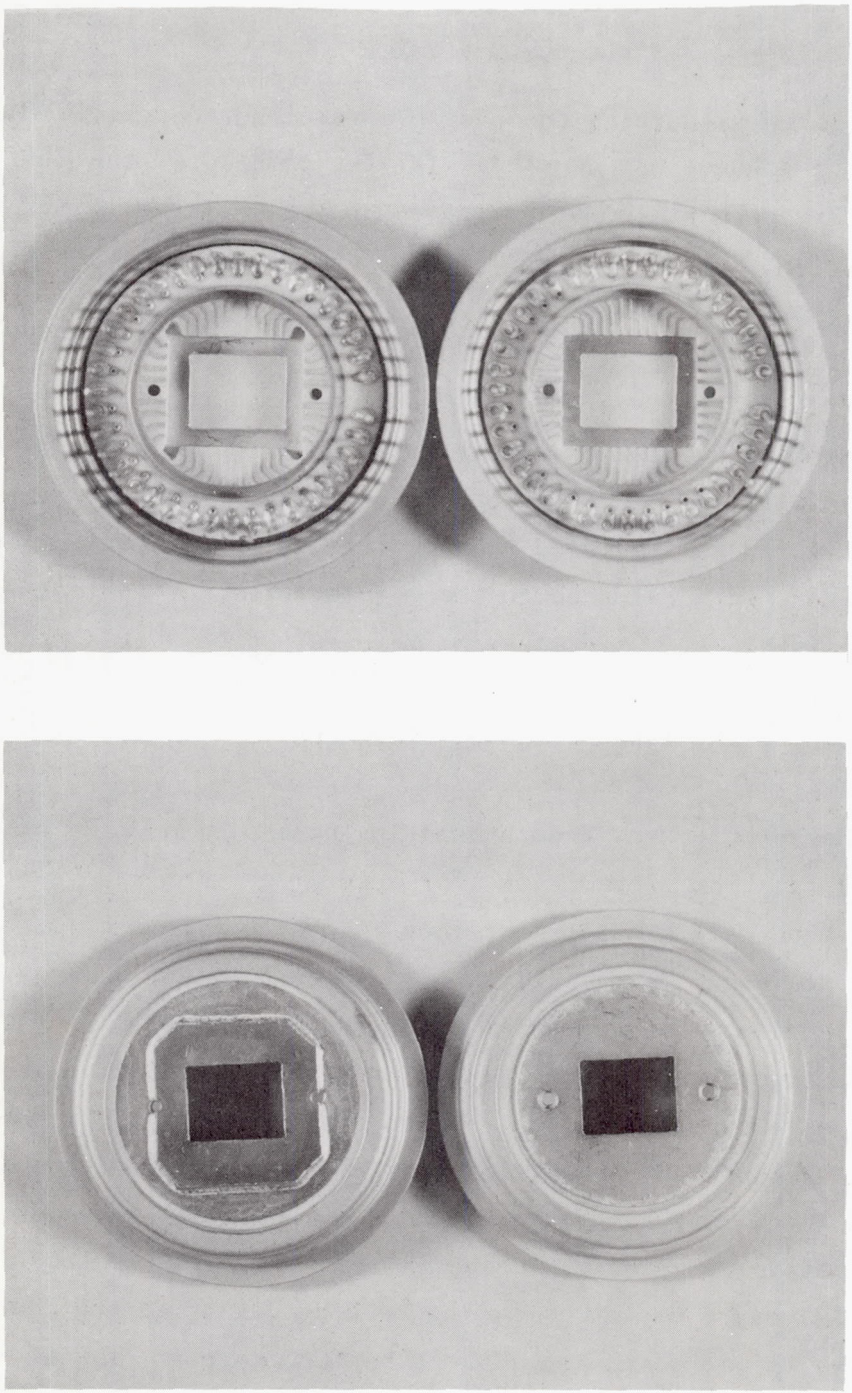

Figure 22 Modifications of Original Tube Header Design

technique was investigated and found to be superior to heliarc welding in several respects. Reliable welds were obtained in all cases. Significantly less heat is generated so that no oxidation of the Kovar is noticeable. In addition, the high voltages associated with heliarc welding are absent, greatly reducing the likelihood of CCD damage. Laser welding has been implemented at Texas Instruments, eliminating the vacuum leaks and CCD risks associated with heliarc welding. Heliarc welds and laser welds are compared in Figure 23.

C. Conclusions

At the beginning of this contract, processing procedures existed for small area (100 x 160), thinned CCD imagers, but experience with these procedures was not sufficient to allow evaluation of their effectiveness for larger area devices. As this experience was developed during this program, severe yield problems were observed. Thinning yields were about 50%. The accumulation process produced variable results. Yields at the alloy step were about 30%. Losses due to header welding and reliability amounted to about 50%. As various problems were encountered, solutions were generated as previously described. As a result, the overall yield of the chip processing has been increased by over an order of magnitude. Systematic yield losses associated with thinning, accumulation, alloy, and headers have been eliminated. The accumulation process has been characterized and now results in reproducible spectral response without dark current increase. A header has been produced that will allow laboratory evaluation of ICCDs. Preliminary work has begun to develop an alternative bonding technique (beam leads) that has the potential to eliminate the remaining buckling problems while providing a reliable chip attachment method. The major source of dark current in completed imagers has been identified, allowing detailed studies to be made to reduce the dark current magnitude. These developments allow large area intensified charge coupled devices to be fabricated reproducibly and with good yield.

ORIGINAL PAGE IS
OF POOR QUALITY

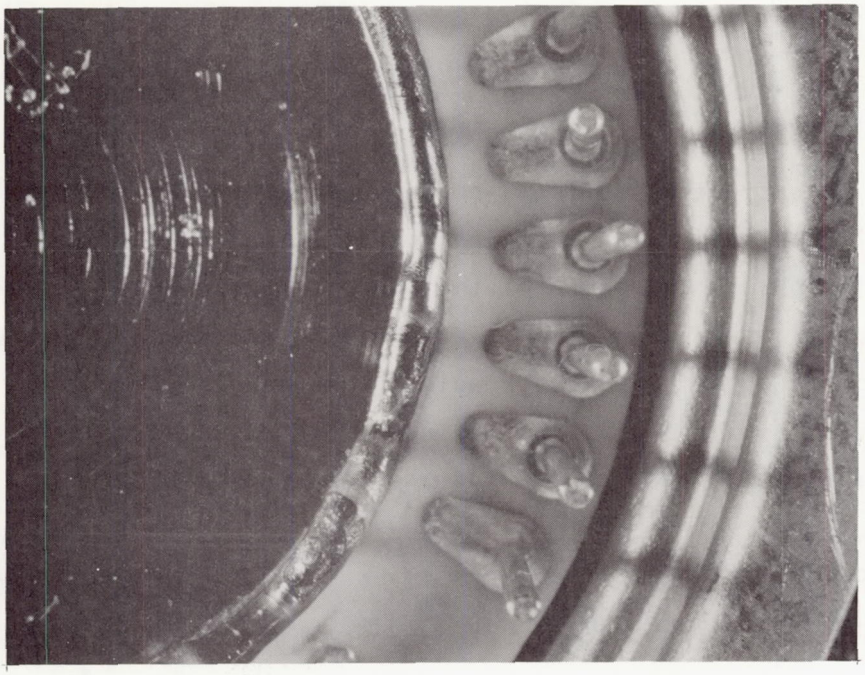

(a)

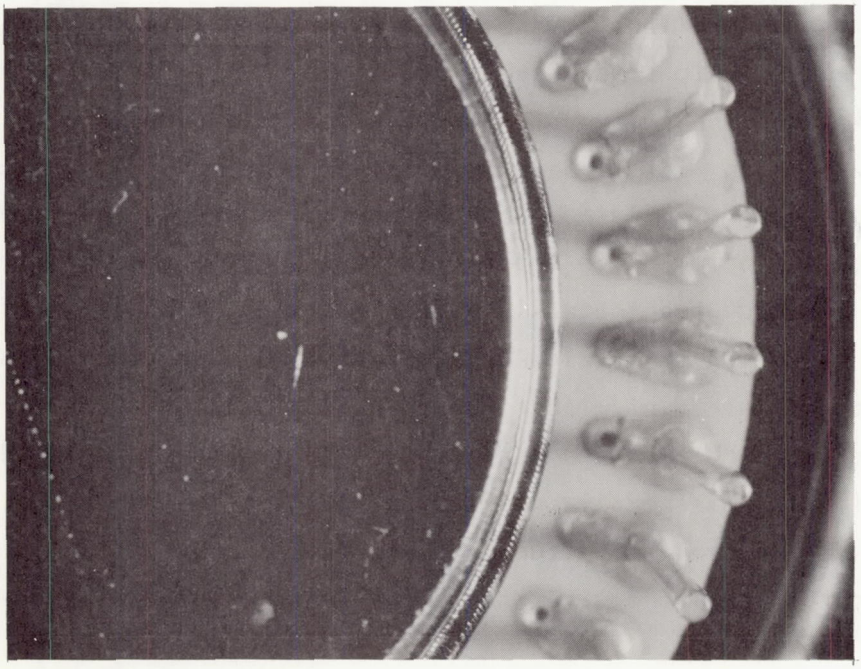

(b)

Figure 23 Header Welds by (a) Heliarc Welding and (b) Laser Welding

SECTION IV
DEVICE TESTING AND CHARACTERIZATION

A. Multiprobe Evaluation

The evaluation of completely processed slices begins with a high speed multiprobe test for shorted metallization and oxide pinholes. Devices without catastrophic physical defects are then subjected to functional multiprobe analysis.

The functional multiprobe can be used to determine CTE, dark current signatures, and potential imaging performance. The electrical properties are determined by contacting each bond pad with a probe. The required electrical signals are then supplied to these probes. This allows operation of the device to determine CTE and dark current signatures.

Examples of CTE measurements made on-slice on 250 x 400 arrays are shown in Figure 24. In one case, the CTE is too large for accurate measurement on this equipment. In the second case, the CTE indicated is 0.9996.

The dark current signatures of all devices with CTE > 0.999 were observed by operating the devices at a 2-to-1 integrate-to-readout frame time. Examples of these dark current signatures are given in Figure 25. (The horizontal lines are electronic artifacts.) In one case, only a small number of dim spots are observed. In the other example, many spots and lines are observed. Devices with excessive dark current magnitude or blemish counts were not processed further.

The device dark current nonuniformity can be used to evaluate the eventual imaging performance with the functional multiprobe. This is accomplished by integrating the dark current until the nonuniformity can be observed on the monitor. Discontinuities in the CTE caused by open metal lines in the serial or parallel array can be detected by observing this monitor display. Figure 26 is an example in which a discontinuity in the CTE of the parallel section is revealed. The dark current pattern is sharp on the output side of this discontinuity, blurred above. This effect would be observed in the imaging performance at any frame time.

ORIGINAL PAGE IS
OF POOR QUALITY

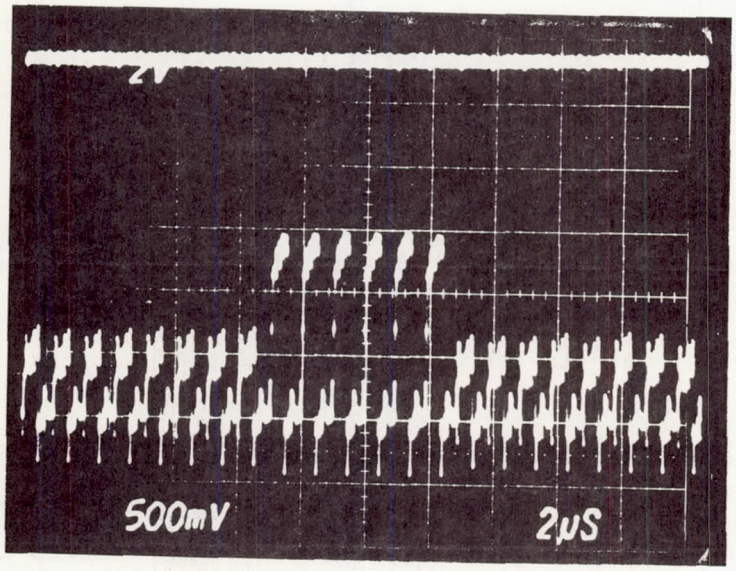

(a) CTE > 0.9999

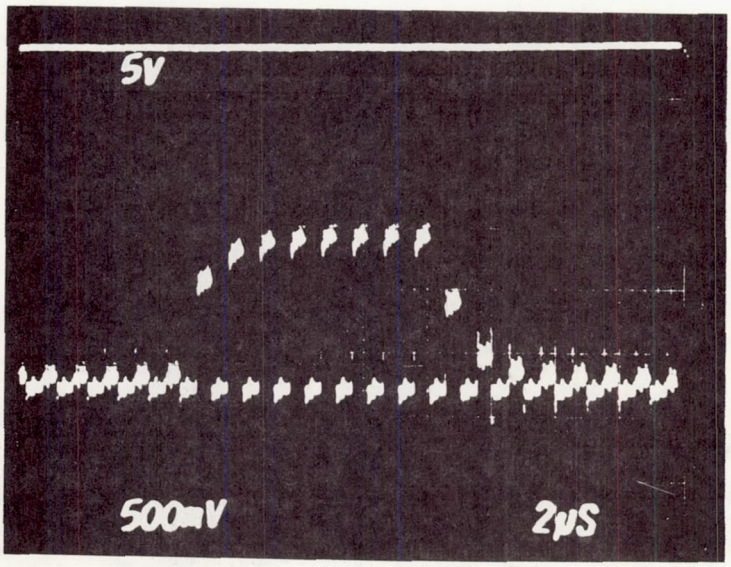

(b) CTE = 0.9996

Figure 24 Examples of On-Slice CTE Measurement Results

ORIGINAL PAGE IS
OF POOR QUALITY

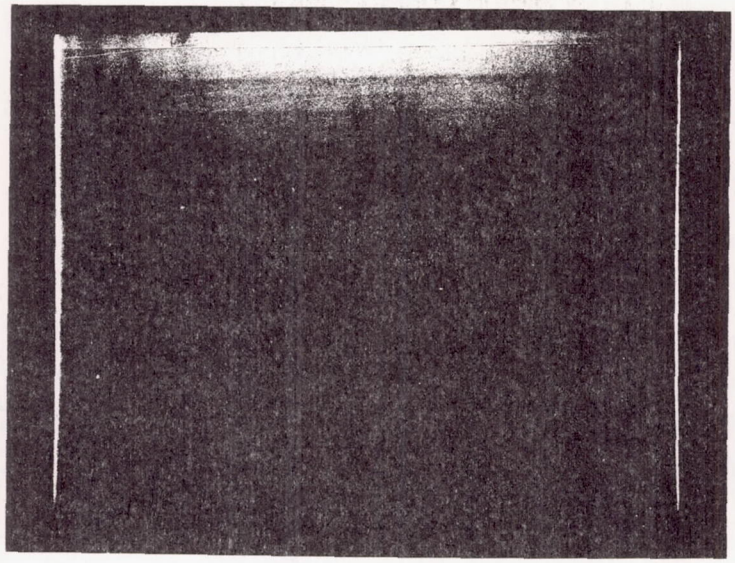

(a) Low Blemish Count

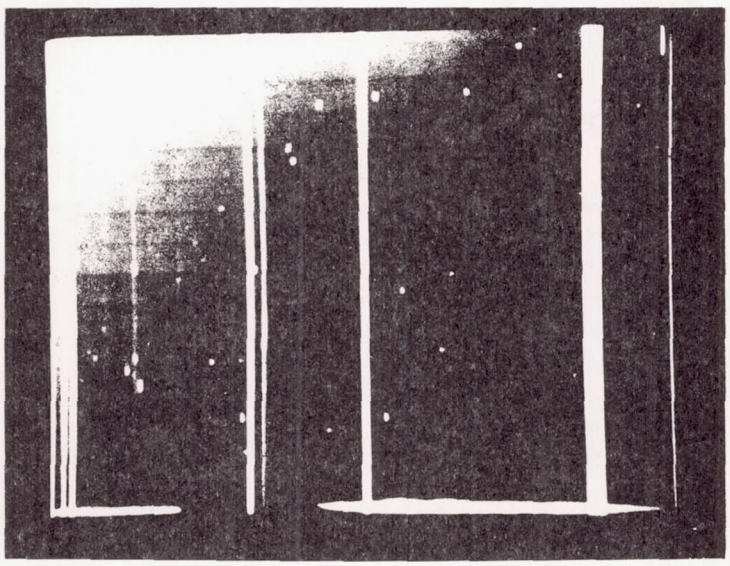

(b) High Blemish Count

Figure 25 Examples of On-Slice Dark Current Signature Photographs

ORIGINAL PAGE IS
OF POOR QUALITY

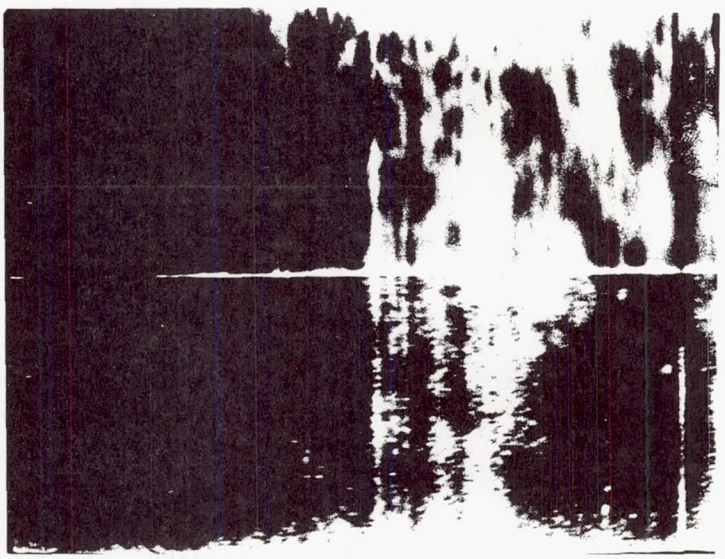

Figure 26 Observation of Open Parallel Clock Lines During On-Slice Device Operation

The results of the functional multiprobe analysis were used to select imagers from each lot that were suitable for further processing. After thinning, accumulation, alloy, and bond, the devices were characterized as discussed in the following section.

B. Optical and Electrical Characterization

1. Dark Current Density and Uniformity

At room temperature, dark current can be reliably measured by precharge current measurements. The precharge current method is accomplished by measuring the precharge current I_{pc} (1) of the CCD under normal operating conditions and subtracting the precharge current I_{pc} (2), measured with the serial register operating in reverse so that array dark current is shifted to the input diode. I_{pc} (2) is amplifier and header leakage. The dark current density is

$$J_D(PC) = I_D(PC)/A = \left[I_{pc}(1) - I_{pc}(2)\right]/A \quad , \qquad (1)$$

where A is the active array area:

$$A = Nd_x d_y + N'd'_x d'_y$$

N = number of pixels in the parallel section; d_x, d_y are the pixel dimensions in parallel section; N′ = number of pixels in the serial register; and d'_x, d'_y are the pixel dimensions in the serial register.

It has been assumed that the serial register and parallel array generate the same average dark current density. For three-phase arrays, reverse operation of the parallel section is possible with dark current being removed via the upper serial register. In that case, the dark current contribution of the serial register can be isolated and measured.

The dark current uniformity is indicated in the device characterization reports through monitor photographs produced with the imager in complete darkness

and through oscilloscope photographs of a single line and a complete frame of video signal producing this monitor display.

2. Spectral Response and Uniformity

The responsivity K can be measured in the following manner. The imager is uniformly illuminated, and the precharge current I is measured as a function of incident photon power P. Under the assumption

$$I = K P^{\gamma} + I_D \quad , \tag{2}$$

a plot of ln $(I - I_D)$ versus lnP should result in a straight line of slope γ. (K is called the responsivity and I_D is the dark current, including all leakage contributions.)

For current levels below nominal saturation it is expected that γ is a constant having a value $\cong 1.0$. The constant K is termed wideband responsivity (K) or spectral responsivity (K_λ), depending on whether the light source is wideband, or narrowband centered about λ. The responsivities obtained at a given well population (i.e., given $I - I_D$ and frame time τ_F) by the prescription $(I - I_D)/P$ are defined as wideband sensitivity (S) or spectral sensitivity (S_λ).

It should be pointed out that if γ is not unity, then $S = (I - I_D)/P$ depends on P. If K is measured in units of amperes/watt$^{\gamma}$, then if γ is slightly different from unity, K can be significantly different from S at the 1 μW level. For example, suppose $\gamma = 0.95$ and K = 0.100 ampere/watt$^{0.95}$. At the 1 W level $S = 0.100 \times (1.00)^{0.95}/1.00 = 0.100$ A/W, but at the 1 μW level, $S = 0.100 \times (10^{-6})^{0.95}/10^{-6} = 0.200$ A/W. Thus, to make K more representative of S at the incident power levels of interest, the units of K are chosen as nanoamperes/microwatt$^{\gamma}$. In this case, at the 1 μW level, S and K are identical. However, $\gamma \neq 1$ should be regarded as an experimental problem. Recent data on many arrays at Texas Instruments show $\gamma = 1$ within better than 1% for a large number of arrays tested.

Once K_λ has been obtained at each wavelength, it can be plotted as a function of λ. However, to avoid this tedious bit of data taking, we plot, instead, spectral sensitivity, S_λ, measured at a fixed well population, i.e., fixed precharge current level, where

$$S_\lambda \equiv (I - I_D)/P_\lambda \quad . \tag{3}$$

The quantum efficiency (QE) of the device is defined as the number of charge carriers accumulated in the depletion wells per incident photon, at a given photon wavelength. From this definition we have

$$QE = (hc/e)S_\lambda/\lambda = 1.24\ S_\lambda/\lambda \quad , \tag{4}$$

where S_λ is in amperes/watt and λ is in micrometers.

For purposes of rapid comparison, the spectral sensitivity of the imager is plotted together with curves of constant quantum efficiency. Note that from the above definition of QE, reflection losses lower the QE, and these losses are not corrected for in the data that are presented.

The experimental setup for spectral sensitivity is the following. A 3400 K source is provided by a tungsten halogen lamp. The light beam passes through a set of neutral-density filters mounted in slides at 45 degrees to the beam in a light-tight box. Light reflected from the filters is trapped by a parallel array of thin, blackened plates. This prevents light from bypassing the filters and makes the filters additive to a good approximation. The filters have densities of 0.1, 0.3, 0.5, 1, 2, 3, and 4, so that light can be attenuated up to a factor of $10^{10.9}$, ignoring light leakage and multiple reflections. A spectral filter wheel is interposed between the neutral density filter box and the environmental camera. The spectral filters are thin-film interference filters. The lens is removed from the camera for all nonimaging tests.

The light level is varied by the neutral density filters to keep the CCD well population roughly the same for each wavelength selected by the filter wheel. The total filter density used is recorded for each wavelength, and the CCD precharge current is measured by a Keithley 616A autoranging digital picoammeter. The integration time must be reduced to a near-zero value in all tests involving precharge current measurements so that the device is continuously clocking out charge into the picoammeter. Otherwise, the picoammeter does not provide an accurate time-average current measurement. When these measurements are complete, the CCD is removed from the light beam, and a silicon detector probe is placed in exactly the same position for light intensity measurements. A Tektronix J16 radiometer and J6502 silicon detector probe are currently being used.

The wideband sensitivity, S, can be computed from the measured spectral sensitivity, S_λ, by numerical integration of the relation

$$\left[\int_0^\infty S_\lambda (dP_\lambda/d\lambda)\, d\lambda\right] \Big/ \int_0^\infty (dP_\lambda/d\lambda)\, d\lambda \equiv S\ (itg) \quad , \tag{5}$$

where $dP_\lambda/d\lambda$ is the blackbody spectral power distribution for the source temperature T desired:

$$dP_\lambda/d\lambda \propto \lambda^{-5}\ [\exp(hc/\lambda kT) - 1]^{-1} \quad . \tag{6}$$

The integrated wideband sensitivity S(itg) can be compared to the directly measured wideband sensitivity S. S(itg) and S usually agree within 10%, giving confidence in predicting the response to radiation sources not easily adapted to the laboratory, but for which the numerical values of dP_λ/d_λ versus λ have been tabulated.

Response uniformity is indicated through monitor and oscilloscope photographs.

3. Full Well Capacity

Various definitions of full well capacity in a CCD have been proposed by different workers. One relatively common definition is based on the measurement of wideband signal transfer of the imager. In this measurement, the imager is uniformly illuminated with a wideband light source and precharge current I is measured as a function of incident photon power P. If $I - I_D$ is then plotted on log-log paper, the resulting curve will be a straight line over a certain part of the range, with slope approximately unity. If the relation

$$I = K P^{\gamma} + I_D \tag{7}$$

is assumed, the slope on log-log paper is γ. Thus, γ is constant and approximately unity over part of the range. For higher values of P, γ will begin to decrease as the CCD becomes so saturated with charge that carrier recombination (or removal at some point other than the precharge terminal) increases faster than carrier photogeneration. Full well capacity is then defined as the power, charge, or current level at which γ reaches some arbitrarily selected value, for example, 0.8.

The definition of full well should reflect the upper limit of the useful operating range of a sensor. The definition in terms of γ does not always meet this criterion. For example, in many CCD imagers, blooming of charge from one pixel to the next will occur before γ begins to decrease appreciably. In such a case, full well should be defined as the level at which the onset of blooming occurs. Unless certain special design and operational steps are taken to control blooming, the useful range of virtually all CCDs will be limited by blooming rather than by γ decrease. For this reason the maximum well population at the onset of blooming has been adopted as the definition of full well capacity for the measurements made under this program.

The procedure by which this level is determined is as follows. A Nyquist frequency bar pattern, oriented so the bars are perpendicular to the preferential blooming direction, is focused on the device, and the resulting video is observed on an oscilloscope. The intensity of the light is increased until the output level of illuminated pixels suddenly stops increasing, and the output level of unilluminated pixels begins to increase. At that point the output voltage corresponding to the peak of the bright bars is measured on an oscilloscope. From this voltage is subtracted the output voltage obtained in the absence of an optical input. The resulting signal voltage, V_{Sig}, is then converted to the equivalent well population using an amplifier conversion factor k. This factor k is determined by inputting a spatially uniform optical or electrical signal and measuring the resultant precharge current (I) and output video voltage (V). This, together with the frame time τ_F, determines k (N = number of pixels in a frame, e = electronic charge)

$$k = \left(\frac{V}{I}\right) \frac{Ne}{\tau_F} \quad . \tag{8}$$

4. Noise and Dynamic Range

Measurements of temporal noise are made by feeding the signal output into an off-chip double-sampling circuit. This circuit removes noise resulting from presetting the output node, which would be the dominant temporal noise source on these devices. Only one pixel is sampled per frame, so that fixed pattern (spatial) noise sources will not affect the measurement. The rms noise level on this single pixel is determined by amplifying the noise level with a low-noise preamplifier (gain = 100) and after further amplification, storing this level in a multichannel analyzer. After repeated samples have accumulated in the MCA, the variation of this level is analyzed using an HP 9820 calculator to determine the standard deviation of the resulting Gaussian amplitude distribution. Usually, the video channel is low-pass filtered prior to the double-sampling circuit, to a bandwidth of about twice the clock frequency, or about four times the Nyquist frequency. This reduces the amount of wideband amplifier noise aliased into the measurement by the sampling circuit, which is not an intrinsic noise source in the CCD. The resulting rms voltage determined from

the MCA data is then converted to an equivalent rms number of noise electrons per charge packet using the total measured video gain, and the relation between signal voltage (at the CCD output node) and well population.

Operation of a clamp-sample-and-hold circuit (CSH) is shown schematically in Figure 27. The circuit is composed of three MOSFET switches, S_1, S_2, and S_3; three buffer amplifiers, A_1, A_2, and A_3; and two intentionally introduced capacitors, C_C and C_{SH}. Also shown in the figure is a low-pass filter following amplifier A_1, which, for simplicity in analysis, is a simple single-pole, low-pass filter characterized by R_1, C_1.

Operation of the circuit begins at time t_o by the switch S_1 closing (Figure 28 shows a typical waveform) and charging the stray capacitance C_o to the voltage level V_{Ref}. The "on" channel resistance of switch S_1 introduces a thermal noise voltage component on the final value of voltage attained at node 1. The equivalent number of noise electrons resulting from this operation is $(kTC_o)^{\frac{1}{2}}q^{-1}$. In terms of the waveforms shown in Figure 28 this is manifested as an instantaneous uncertainty in the voltage of the waveform from time t_1 to t_3, which is given by $(kT/C_o)^{\frac{1}{2}}$. This uncertainty which appears at nodes 2 and 3 of Figure 27 is eliminated by closure of switch S_2 at time t_2. This sets node 3 to a known reference, V_{Clamp}. The uncertainty in initial preset voltage at node 1 is stored on C_C and is, therefore, effectively removed from node 3. Signal charge is then sensed as a shift in the voltage at time t_3. For further signal-to-noise improvement, the signal level is sampled and held at node 4 at time t_4.

For a number of devices, the noise was estimated from the dark current magnitude and an average readout noise of 30 electrons. The shot noise on the dark current was calculated by taking the square root of the average number of dark current-generated electrons in a pixel. This dark current shot noise was added in quadrature to the 30 electrons readout noise to provide an approximate noise value. A significant reduction in characterization time resulted from using this procedure.

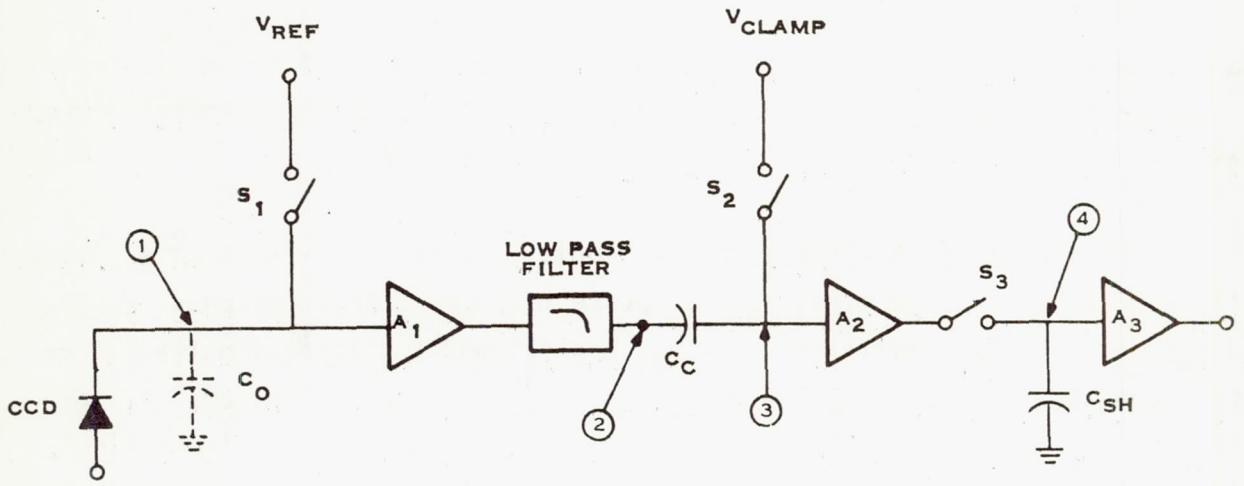

Figure 27 Schematic of Basic Clamp Sample-and-Hold Circuit

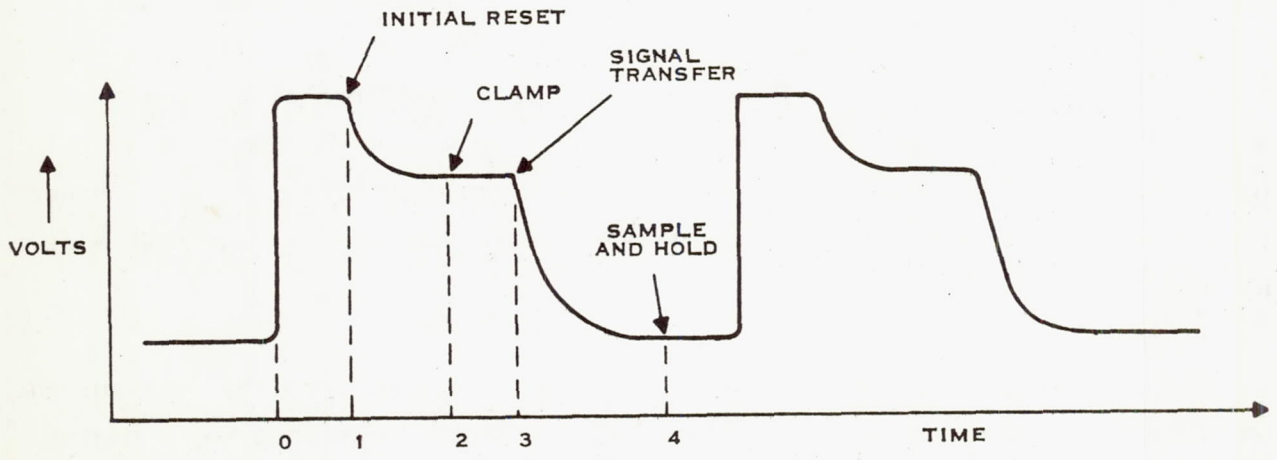

Figure 28 Waveform Observed at Nodes 1, 2, and 3 of Figure 27

Dynamic range is defined as the ratio of full well capacity to rms number of noise electrons.

5. Charge Transfer Efficiency

Charge transfer efficiency (CTE) measurements for the serial register are made by electrical input of a square pulse at the serial input diode. It can be shown that the charge transfer efficiency is given by

$$CTE = 1 - \varepsilon \quad , \tag{9}$$

where ε is the transfer inefficiency given by

$$\varepsilon = \left(\frac{1}{NV_T}\right) \sum_i V_i \quad . \tag{10}$$

N = number of transfers, V_T is the steady-state signal voltage, and V_i (i = 1, 2, 3, . . .) is the voltage decrement in the ith pulse of the output signal packet.

C. Summary of Delivered Device Characterization

Twenty-two 250 x 400 imagers, mounted on tube headers, were delivered under this contract. (Four of these devices were committed to tube processing.) Each device was characterized as described in the preceding section. A copy of each characterization report is presented in Appendix A. These reports are summarized in the following.

Charge transfer efficiency ranged from 0.9995 to > 0.99996, improving as the program progressed. Sixteen of the eighteen delivered devices had CTE > 0.9999.

Dark current densities at room temperature varied from 4.4 nA/cm^2 to 90 nA/cm^2. Figure 29 shows the distribution of dark currents, the percentage of devices

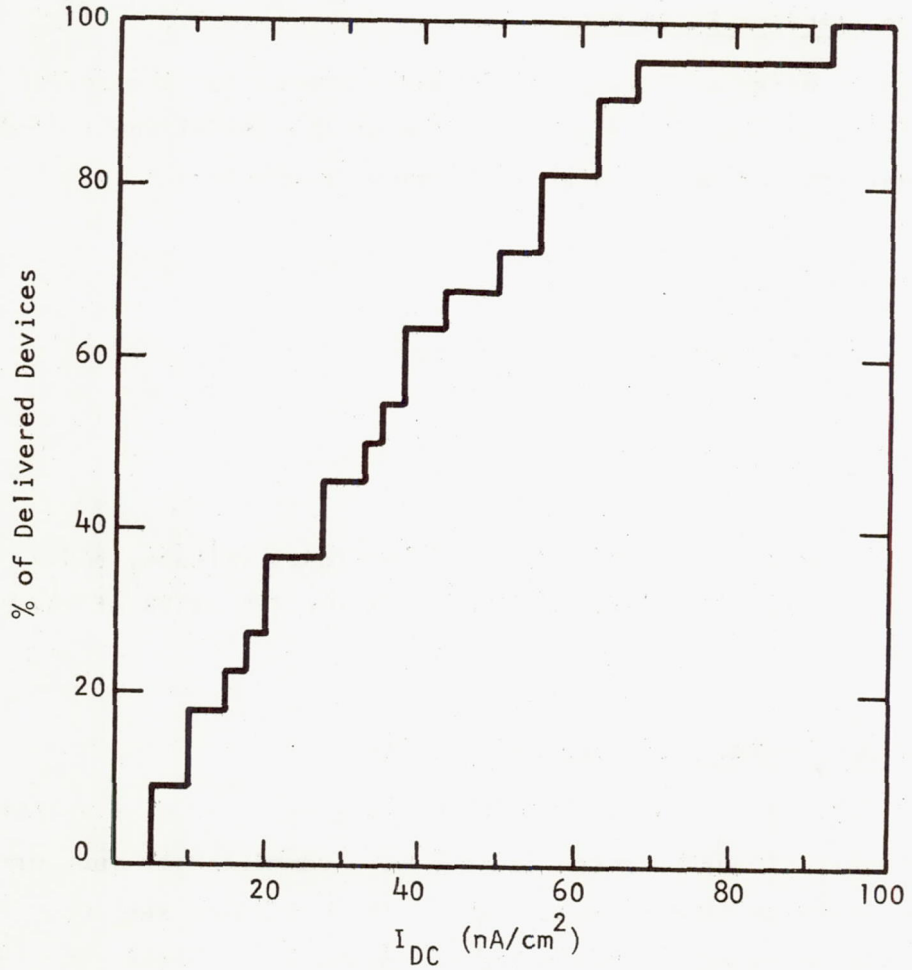

Figure 29 Distribution of Dark Current for Delivered Devices

with dark current below a given value being plotted against the given dark current. Some of the higher dark current devices were processed before the improvements discussed in Section III were developed. All the devices experienced a dark current increase at alloy and bond.

Full well charge capacity ranged from 6.0×10^5 to 2.0×10^6. Dynamic range was determined from these values and the dark current noise assuming a 100 ns frame time. Dynamic range values of 480 to 11900 resulted. Twelve devices had a dynamic range exceeding 3000, nine exceeding 4000, and five exceeding 5000.

The spectral response characteristics of the delivered devices are summarized in Figure 30. The open circles represent the numerical average of the eighteen devices with the rms deviation indicated by the bars. The dark circles represent the highest and lowest values at each wavelength. Figure 30 shows greater deviation than Figure 16 because seven of the eighteen devices were not processed optimally.

The image quality achieved is illustrated in Figure 31, using strobed illumination. This is device 395-10-5 with a CTE of 0.99995 and no bright blemish. The uniformity achieved is illustrated by device 367-10-2 in the next two figures. Figure 32 represents the background dark current uniformity. The device was integrated in the dark for 1.6 seconds to achieve an average 50% full well population, excluding the line blemishes. Figure 33 represents the 4000 Å photoresponse, again at 50% full well. The frame time required was 0.34 seconds.

There were three classifications for the performance goals for these devices. Four devices were to be A type, fourteen B type, and four C type. The goals for each classification are given in Table 2, together with the results of this program. In this table inactive area is defined to include regions of degraded

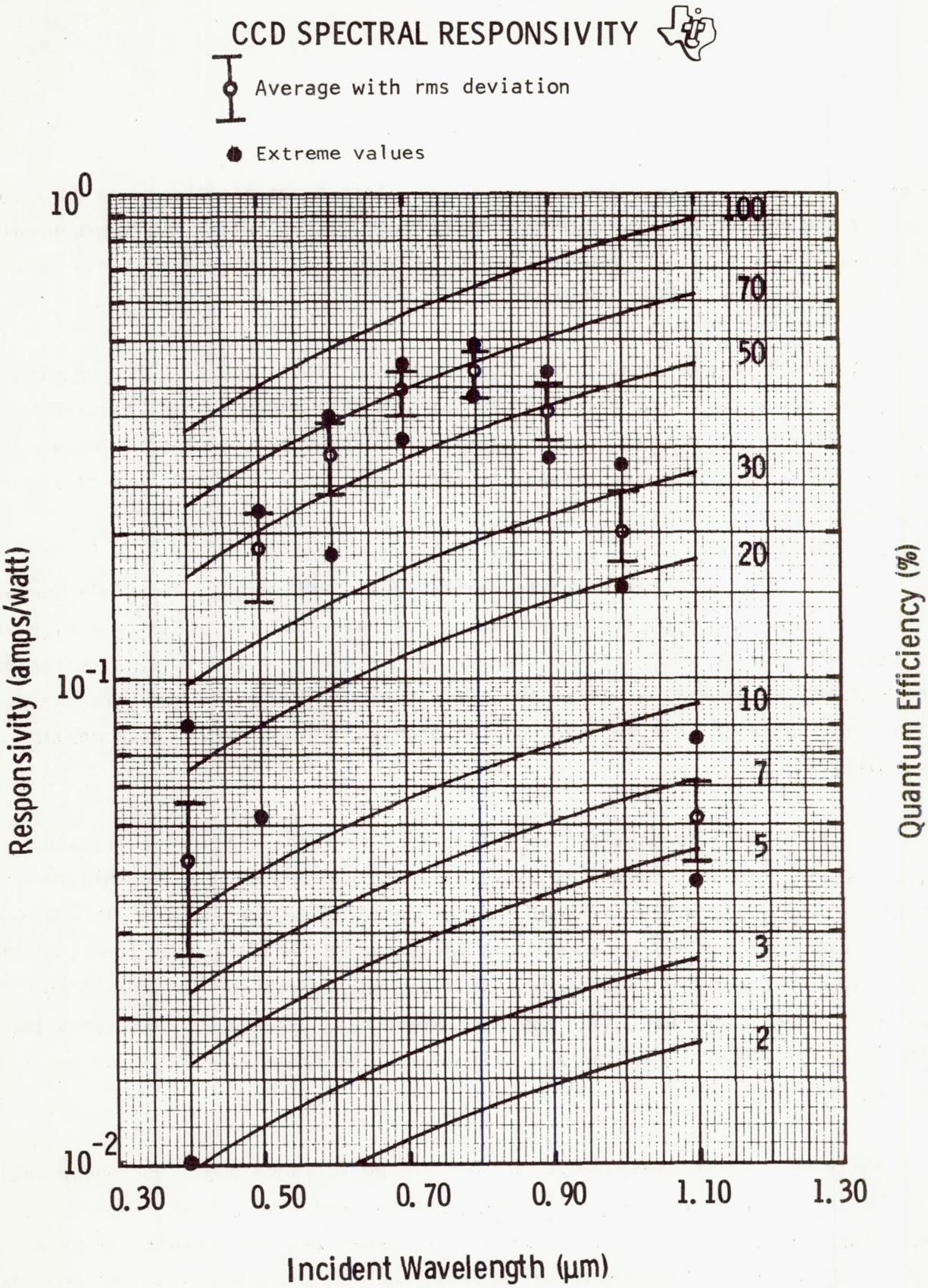

Figure 30 Summary of Spectral Response Characteristics of the Delivered Devices

ORIGINAL PAGE IS
OF POOR QUALITY

Figure 31 Image Quality Achieved

ORIGINAL PAGE IS
OF POOR QUALITY

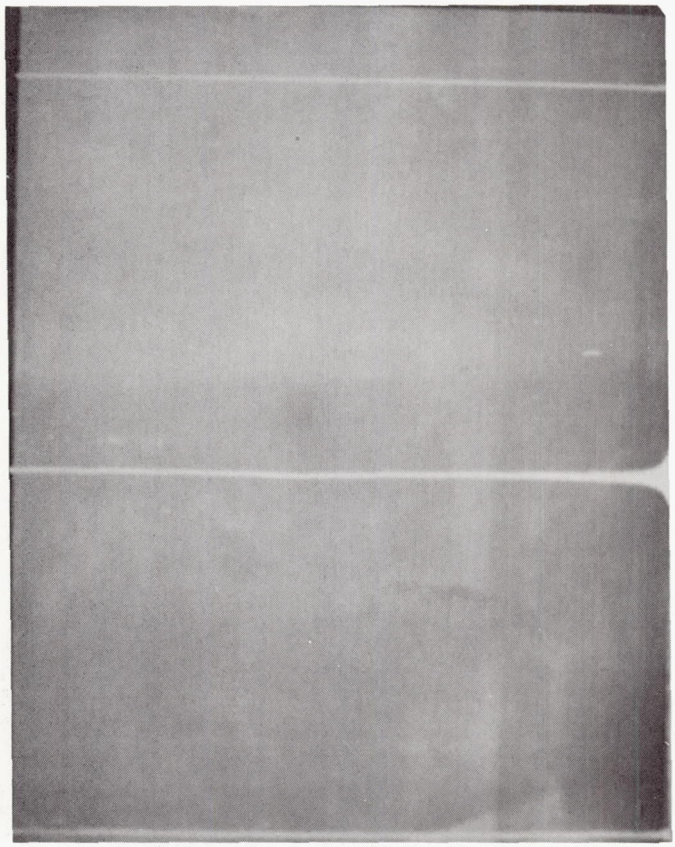

Figure 32 Background Dark Current Uniformity Achieved

ORIGINAL PAGE IS
OF POOR QUALITY

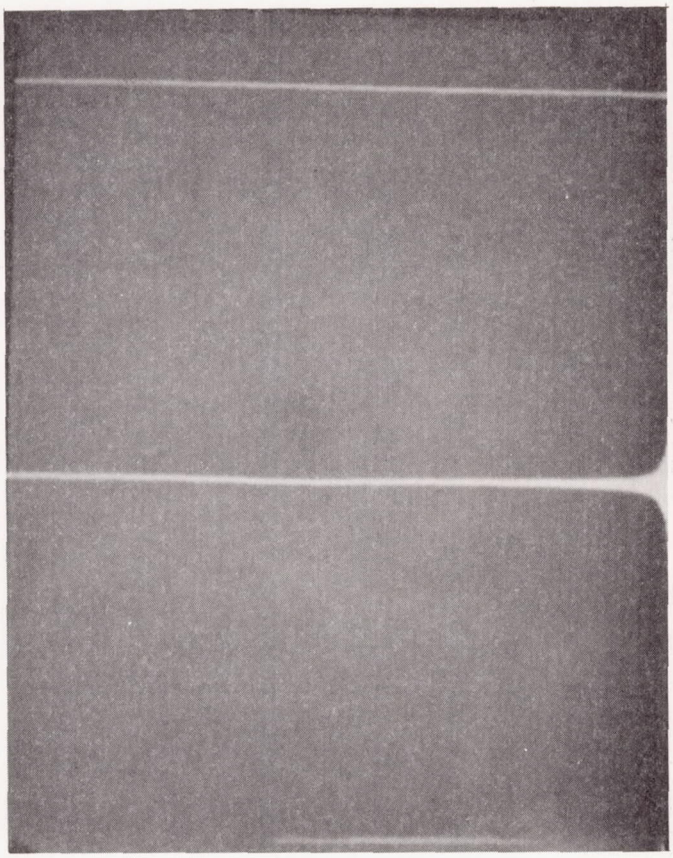

Figure 33 Blue Response Uniformity Achieved

Table 2

Imager Performance Goals

Parameter	Type A		Type B		Type C
	Goal	Times Achieved	Goal	Times Achieved	Devices Not A or B
Active Area	95%	18	85%	20	2
Noise (electrons/pixel)	300	8	600	17	1
Dynamic Range	1500	21	1000	21	1
Q. E. (0.4 μm)	40%	0	10%	17	5
Operable Channels	2	13	1	22	0

CTE due to open parallel electrodes. Inoperable channels include serial registers with open electrodes and those near an open parallel electrode.

The only performance goal not achieved was 40% quantum efficiency at 0.4 μm. As indicated in Section III, this value cannot be achieved reproducibly with the existing technology.

SECTION V
CCD IMAGER FAILURE ANALYSES

A. Failure Modes

Prior to the beginning of this contract, NASA-Goddard had received 100 x 160 imagers for evaluation. In the course of these evaluations a number of device failures were observed. Failure occurred as a cessation of operation, an overwhelming increase in dark current, or intermittent operation. Failures occurred during periods of operation and during inactive periods. These failures were a source of major concern both to NASA and to Texas Instruments. The devices were returned to TI for determination of the cause of failure. The returned devices were tested electrically and subjected to optical and SEM evaluation. Two systematic failure mechanisms were observed, static electric discharge damage and bond pad degradation. These failure mechanisms were eliminated by providing appropriate protection as discussed below.

B. Static Electric Discharge Damage

Electrical evaluation of the returned devices indicated that most had experienced damage to the gate oxide. This damage usually occurred under a small gate connected directly to a header pin (such as the precharge gate). Optical examination revealed small dark spots near the periphery of these gates. Figure 34 illustrates these results. Figure 34(a) shows a curve trace of the gate-to-substrate characteristics, illustrating the flow of current from the gate through the gate oxide into the substrate. For an undamaged device no such current should flow. Figure 34(b) is an optical microphotograph of this gate. The small circular spots near the periphery of the precharge gate indicate oxide breakdown.

This oxide breakdown can be caused by high voltages impressed between the gate and the substrate. Small currents are indicated by the limited physical size of the damage site. A common source of high voltage, low current pulses is static electric discharge.

ORIGINAL PAGE IS
OF POOR QUALITY

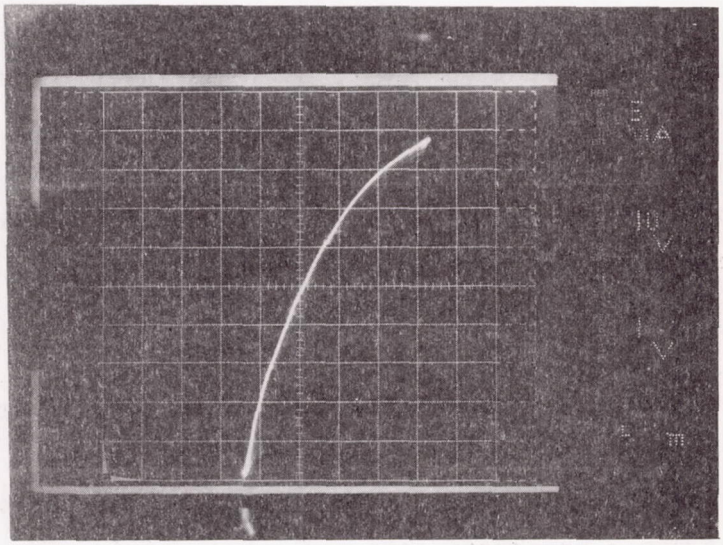

(a)

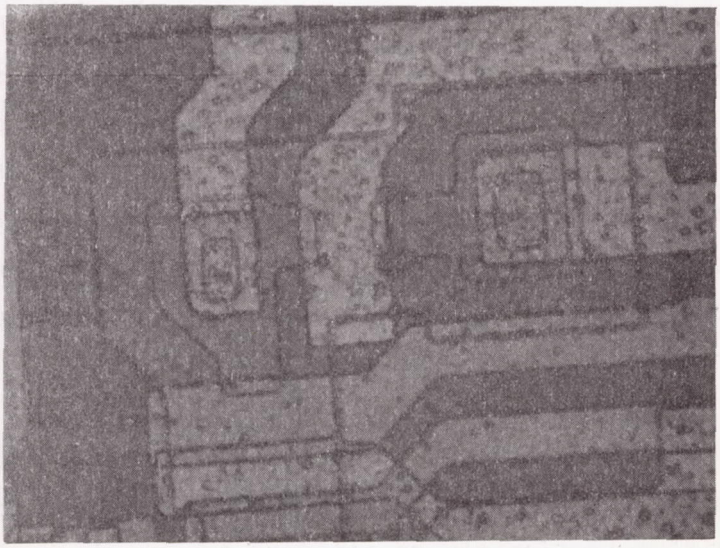

(b)

Figure 34 High Voltage Damage to Amplifier Gates

High voltage, low current damage to CCDs was investigated by discharging a Tesla coil through a CCD. The damage incurred by the test CCD was compared to that observed on the devices returned for failure analysis. SEM photographs of the two devices are shown in Figure 35. Figure 35(a) indicates the damage to a returned device and Figure 35(b) the damage generated by the Tesla coil. The physical damage is remarkably similar.

The voltage required to cause this damage was investigated. It was assumed that the source of this voltage was human body capacitance. This capacitance was simulated by a 10 pF capacitor. The 10 pF was charged to various voltages and connected between a precharge gate and substrate for a number of devices. The voltage was increased until oxide breakdown occurred. The results of this test are indicated in Figure 36. Damage begins to occur at capacitor voltages of 600 V. Static voltages of this magnitude are difficult to avoid. (Note that damage to gates can occur at dc power supply voltages as low as 50 V.)

Since high voltages are required in ICCD operation, high static charges must be assumed to exist. Therefore, the vulnerable gates must be protected against damage. The vulnerable gates are those with small capacitances, such as output gates and precharge gates, which are connected to external pins. Serial gates and parallel gates are ganged together and present relatively large capacitance to the external pins. Static voltages impressed on these pins are divided down by the ratio of capacitances on and off chip. No systematic damage to these clocks has been observed.

The problem of protecting against static discharge damage is therefore reduced to protecting the two output gates and two precharge gates on the 250 x 400 device. This protection can be achieved by shunting the pins to substrate using external Zener diodes. High voltages can then be discharged by forward conduction or reverse breakdown of this diode. The reverse breakdown must be small enough to prevent damage to the oxide, but large enough to sustain normal

ORIGINAL PAGE IS
OF POOR QUALITY

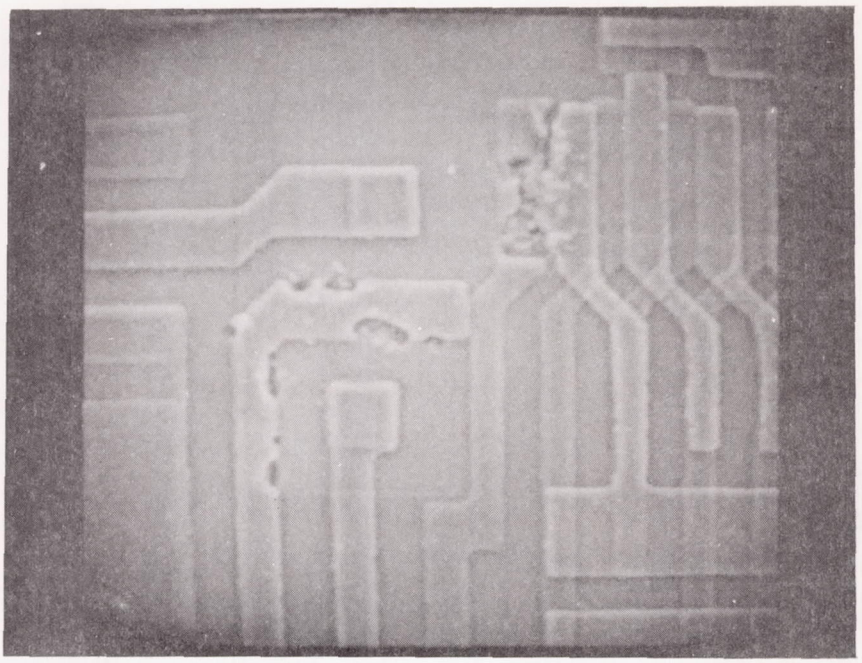

(a)

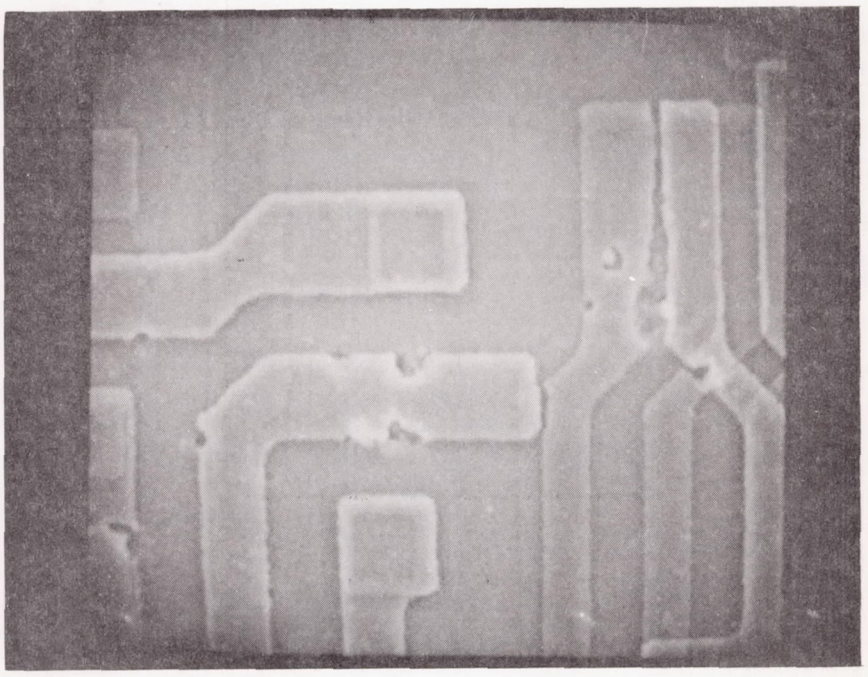

(b)

Figure 35 SEM Comparison of (a) Damage to Returned Devices and (b) Tesla Coil Damage

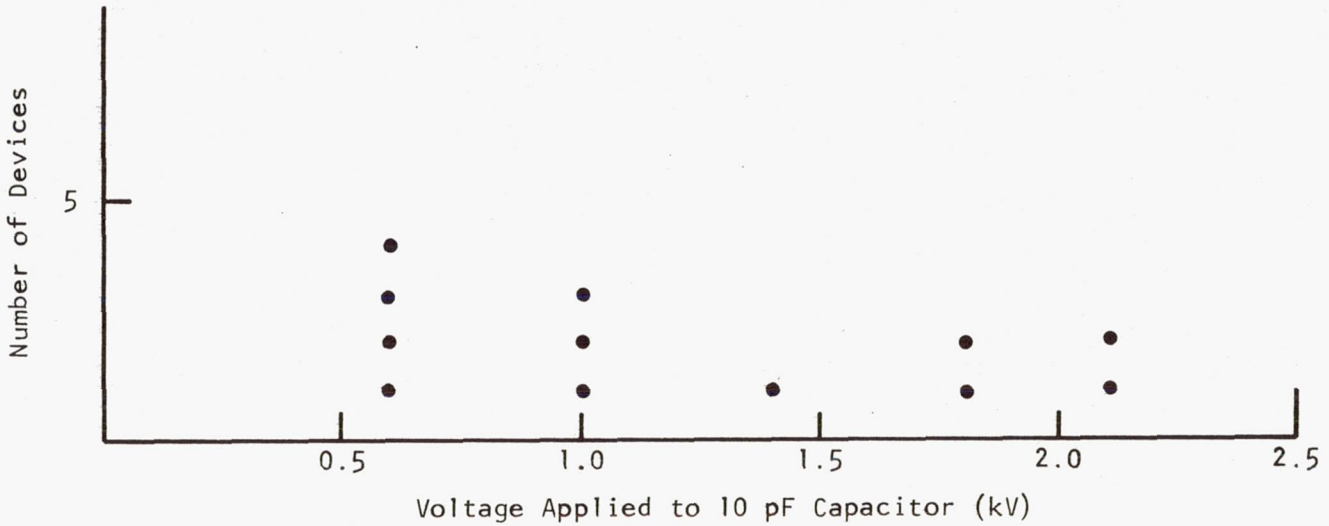

Figure 36 Distribution of Oxide Breakdown Voltage

CCD operating voltages. In addition, the diodes must survive the tube processing cycle, including the 350°C bake. The Zener diode chosen was a JANTX 1N973B because of its glass packaging and 33 V reverse breakdown. These diodes are connected externally using a wire-wrap technique to allow for replacement if diode failure occurs. Experience indicates that static damage is eliminated if these diodes are connected between the precharge pin and the V_{Ref} pin and between the output gate pin and the substrate pin. Figure 37 shows the implementation of the protective diode on a 250 x 400 header.

C. Bond Degradation

A few of the devices returned for examination showed indications of open connections between the chip and the header. Optical examination revealed that the gold wire had separated from the aluminum bond pad. Under Contract No. NAS5-23578 this problem was investigated and eliminated. A discussion of bond pad protection development was given in the final report for that contract and is included as Appendix B of this report.

D. Unidentified Failure Modes

Most of the devices returned failed due to static discharge damage and/or bond failure. No systematic cause was identified for the remaining failures. These failures are thought to have been caused by isolated incidents detrimental to CCDs.

One occasional failure mode without a systematic cause is the opening of V_{DD} or V_{Ref} lines on-chip due to excessive current flow. Figure 38 shows such an open aluminum line. Causes could be excessive dc voltage or inadvertent forward biasing. The problem can be eliminated by putting current limiters in all dc voltage supplies.

ORIGINAL PAGE IS
OF POOR QUALITY

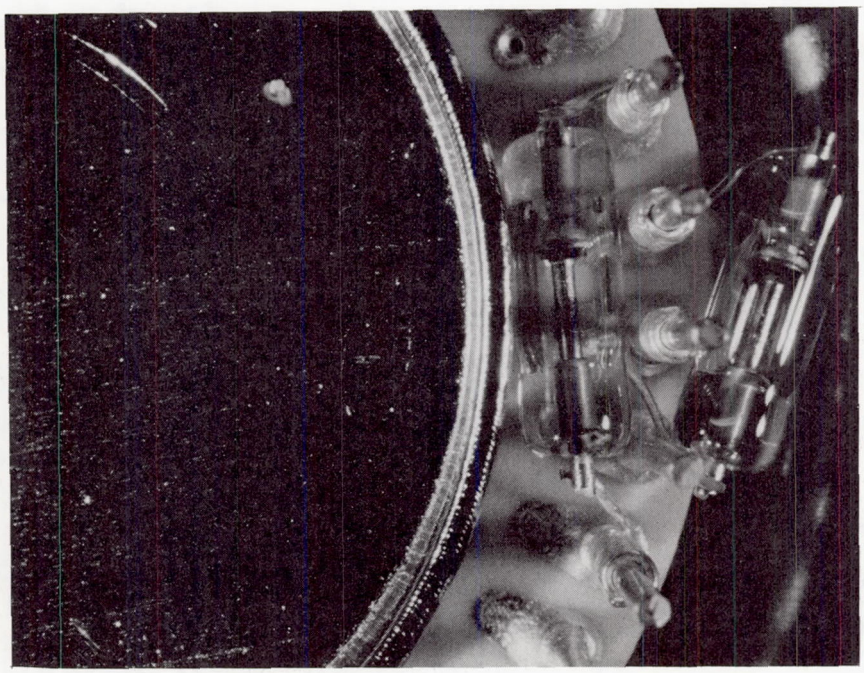

Figure 37 Diode Protection on a Tube Header

ORIGINAL PAGE IS
OF POOR QUALITY

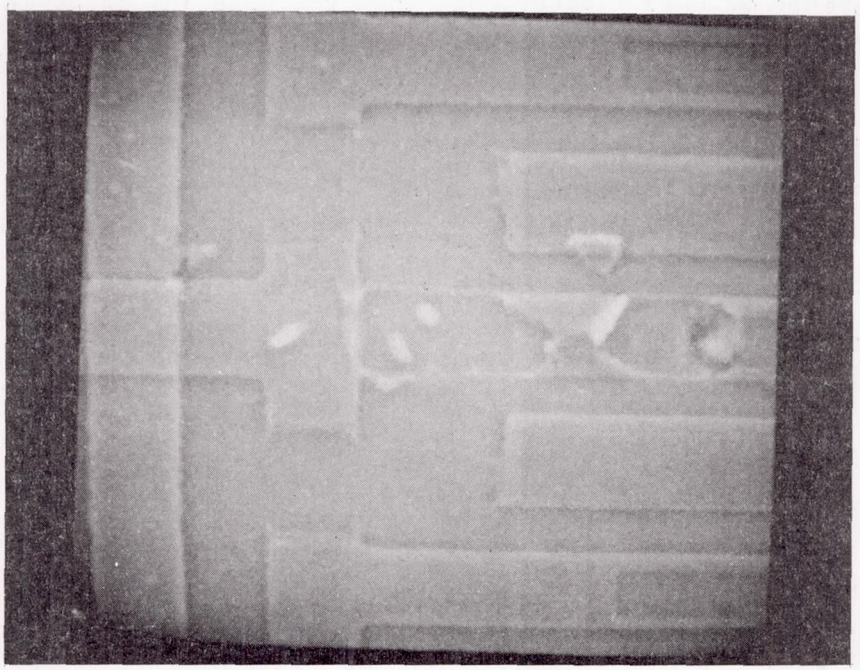

Figure 38 High Current Damage to CCD Amplifiers

One device failed in an apparently unique manner. It ceased to operate after being cooled to below 0°C. Electrical evaluation indicated no problems with the precharge or output gates, but that the parallel gates were shorted to substrate. The results of optical and SEM evaluation are presented in Figure 39. Figure 39(a) shows an optical microphotograph of the device indicating extended regions of degradation. The SEM photograph reveals that the parallel metallization has been separated from the bar. The cause for this damage could not be ascertained. Chips from the same slice as this bar were cooled without being damaged. This effect has not occurred again. Apparently this damage was caused by some particular, unusual event in the device's history prior to cooling.

E. Summary

Two systematic causes of CCD failure have been identified and protective measures developed. The implementation of these measures has all but eliminated the catastrophic loss of imagers.

ORIGINAL PAGE IS
OF POOR QUALITY

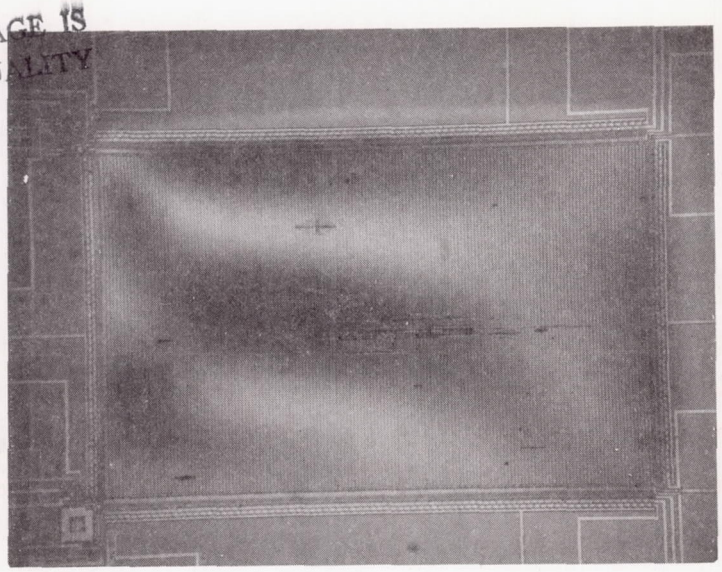

(a)

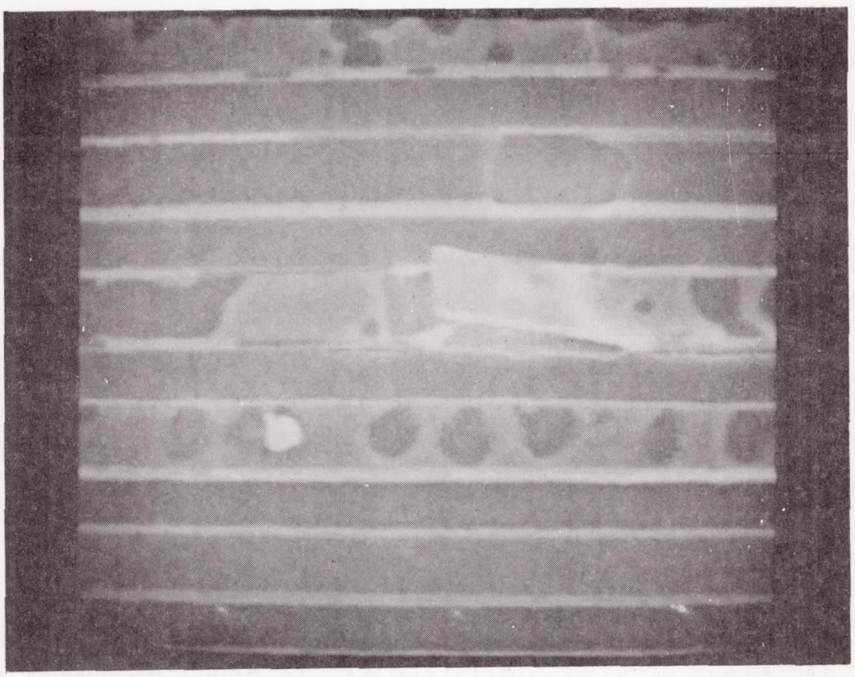

(b)

Figure 39 Unusual Failure Mechanism

SECTION VI
INTENSIFIED CHARGE COUPLED DEVICE FABRICATION

A. Tube Processing Steps

Five CCD imagers were committed to tube processing under this contract. One was a 100 x 160 imager originally delivered to NASA-Goddard under Contract No. NAS5-22403; the remaining four were 250 x 400 imagers. Vacuum tubes were fabricated by two manufacturers, Varo Electron Devices, Inc. and ITT, Electro Optical Products Division.

The main steps in the tube processing are as follows: (1) heliarc-weld the header to the tube body, (2) evacuate the tube body in a tube processing station, (3) vacuum bake, (4) form the photocathode, (5) electron scrub, and (6) seal the tube. These processes are similar to those used to manufacture intensifier tubes with phosphor outputs, but modifications are required due to the properties of the CCD. The temperature of the vacuum bake is limited to about 350°C by the gold-silicon alloy used to attach the chip to the header. Heliarc welding must be done carefully to avoid damage to the CCD. (Laser welding would be preferable, but is not readily available to the tube manufacturers.) The electron scrub must be reduced or eliminated to protect the CCD.

These process modifications have been incorporated by the tube manufacturers with varying degrees of success. In the best case the CCD is not degraded and the properties of the photocathode seem unaffected. In the worst case the photocathode response is degraded and/or the CCD is inoperative.

B. Tube Processing Results

1. Varo Results

Three ICCDs were fabricated at Varo Electron Devices, one 100 x 160 device and two 250 x 400 devices. All tube starts produced operating ICCDs. The tube was based on the Varo Model 2561 electrostatically focused triode intensifier with an S-20 photocathode. A photograph of this tube is given in Figure 40, together with front and back views of the 100 x 160 header. All tubes were potted prior to delivery.

ORIGINAL PAGE IS
OF POOR QUALITY

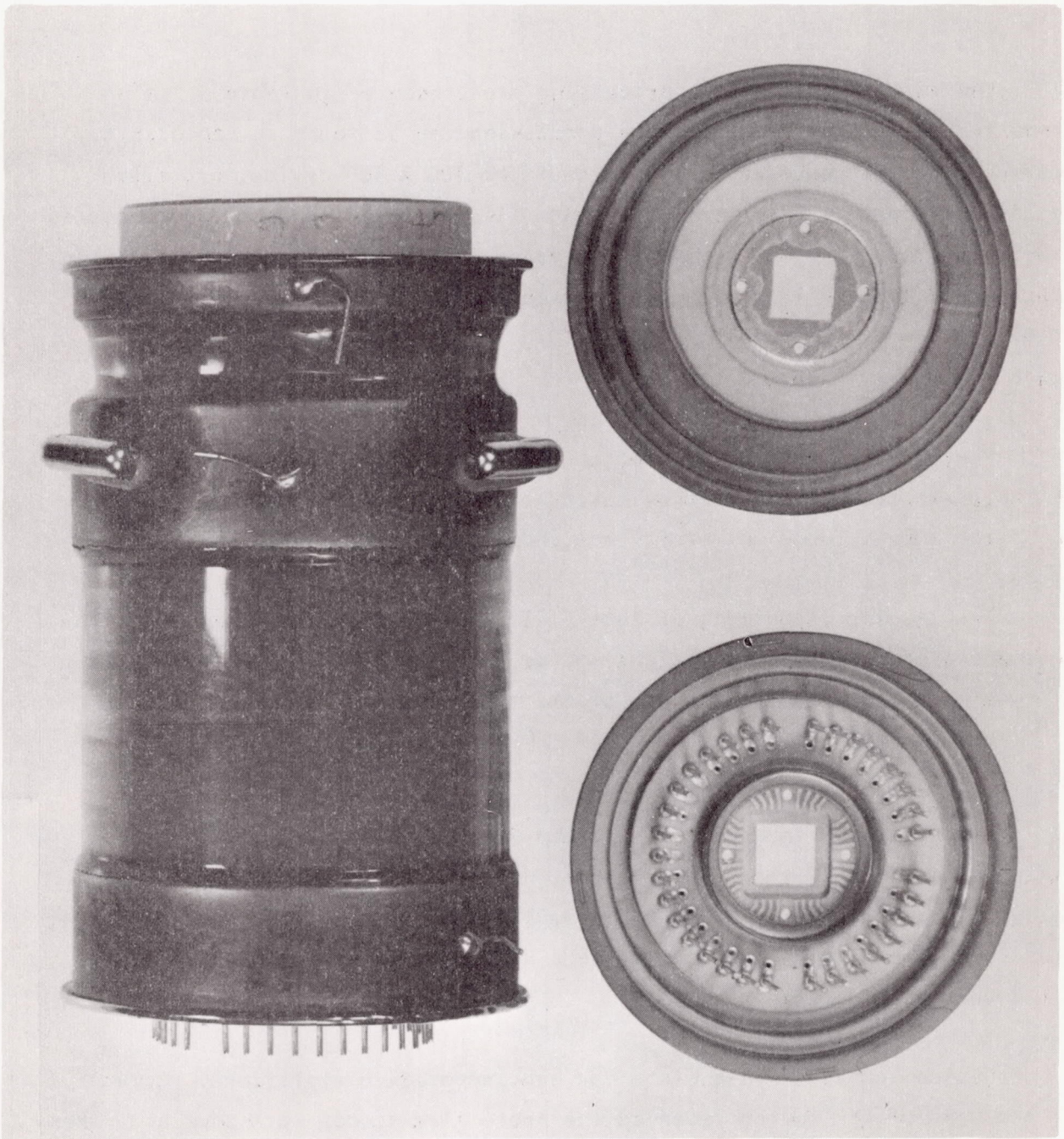

Figure 40 Electrostatically Focused Intensified Charge Coupled Device

The results of the tube processing are presented in Table 3. (The test reports on the CCDs prior to tube processing can be found in Appendix A.) Dark current changes occurred in all cases. The 100 x 160 device, processed before the improvements discussed in Section III, experienced an 83% increase in dark current. The 250 x 400 devices, processed later, experienced decreases in dark current of 30% and 18%. The dark current of tube #299, 9 nA/cm^2, is the lowest dark current achieved in a NASA ICCD. The gain curves for the three devices are given in Figure 41.

Photocathode response varied as indicated in the table. The uniformity of the photocathodes was examined by making a spot scan across the diameter of two of the tubes. Good uniformity was indicated as shown in Figures 42 and 43.

The imaging capability of tube #243 is illustrated in Figure 44. The tube was operated at 15 kV. The light source was a 2854 K tungsten lamp. Intensity was measured at the faceplate of the tube.

2. ITT Results

Two 250 x 400 imagers (321-4-8 and 321-3-7) were committed to tube processing at ITT. Test reports are given in Appendix A. The tube was a magnetically focused intensifier with a bialkali photocathode. The tube processing resulted in severe physical damage to the CCDs. One CCD was inoperable, the other had very high dark current.

Device number 321-4-8, tube #8, had inoperative amplifiers. Curve tracer analysis of the device revealed the protective diodes were shorted. When these were removed, it was found that the precharge gate was also shorted to the V_{Ref} diffusion. The device was removed from the tube and examined under an optical microscope. Damage characteristics of high voltage, low current discharge similar to that shown in Figure 34 was observed. Apparently, both the protective

Table 3

Varo ICCD Processing Results

Tube Number	Device Number	Device Type	Dark Current (nA/cm^2) Before	Dark Current (nA/cm^2) After	Gain 15 kV	Photocathode Response 2854 K Wideband
243	166-3-2	100 x 160	18	33	2400	200
287	367-2-6	250 x 400	35	27	2550	260
299	367-4-4	250 x 400	11	9	2500	250

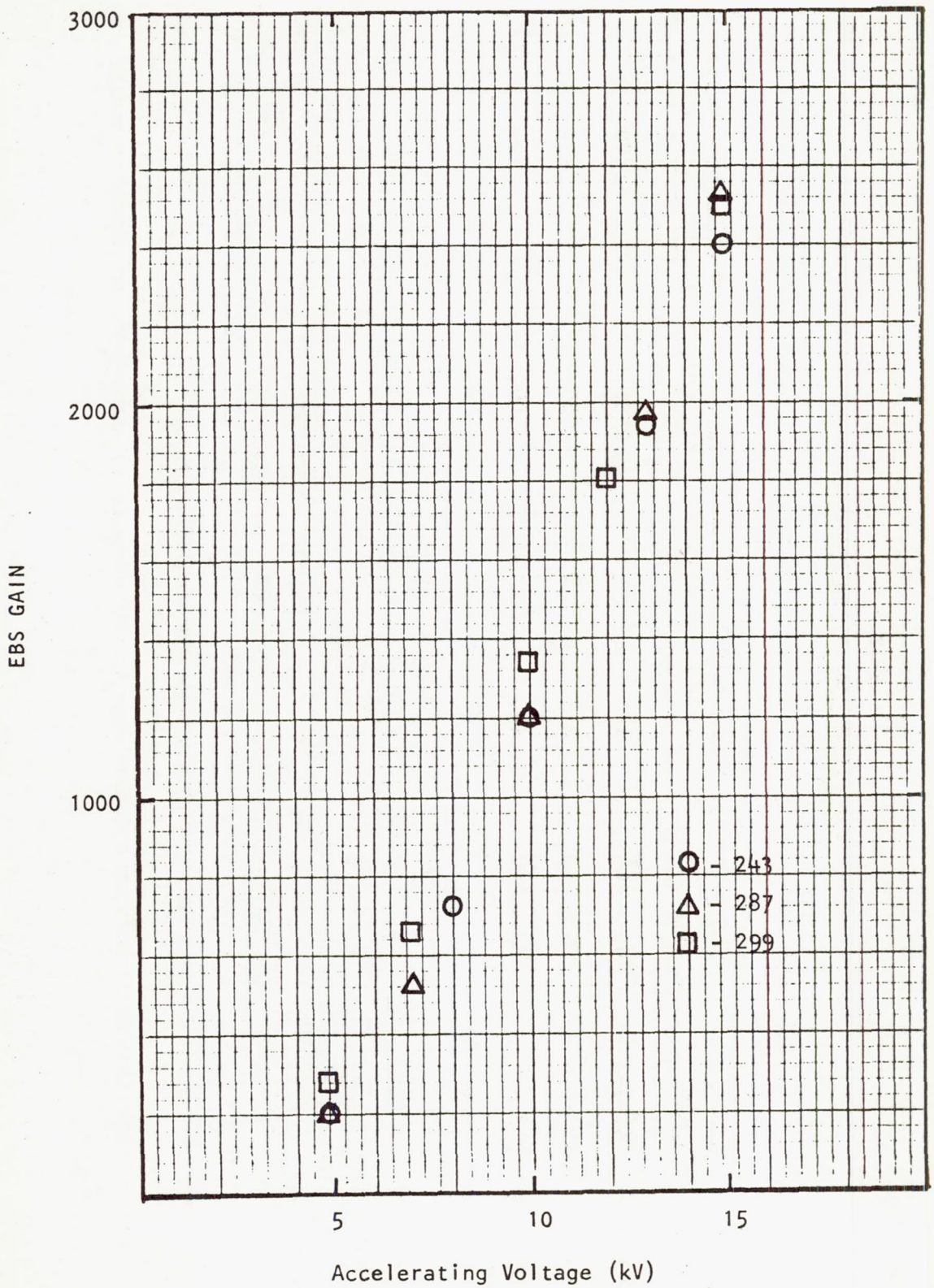

Figure 41 EBS Gain for Delivered ICCDs

ORIGINAL PAGE IS
OF POOR QUALITY

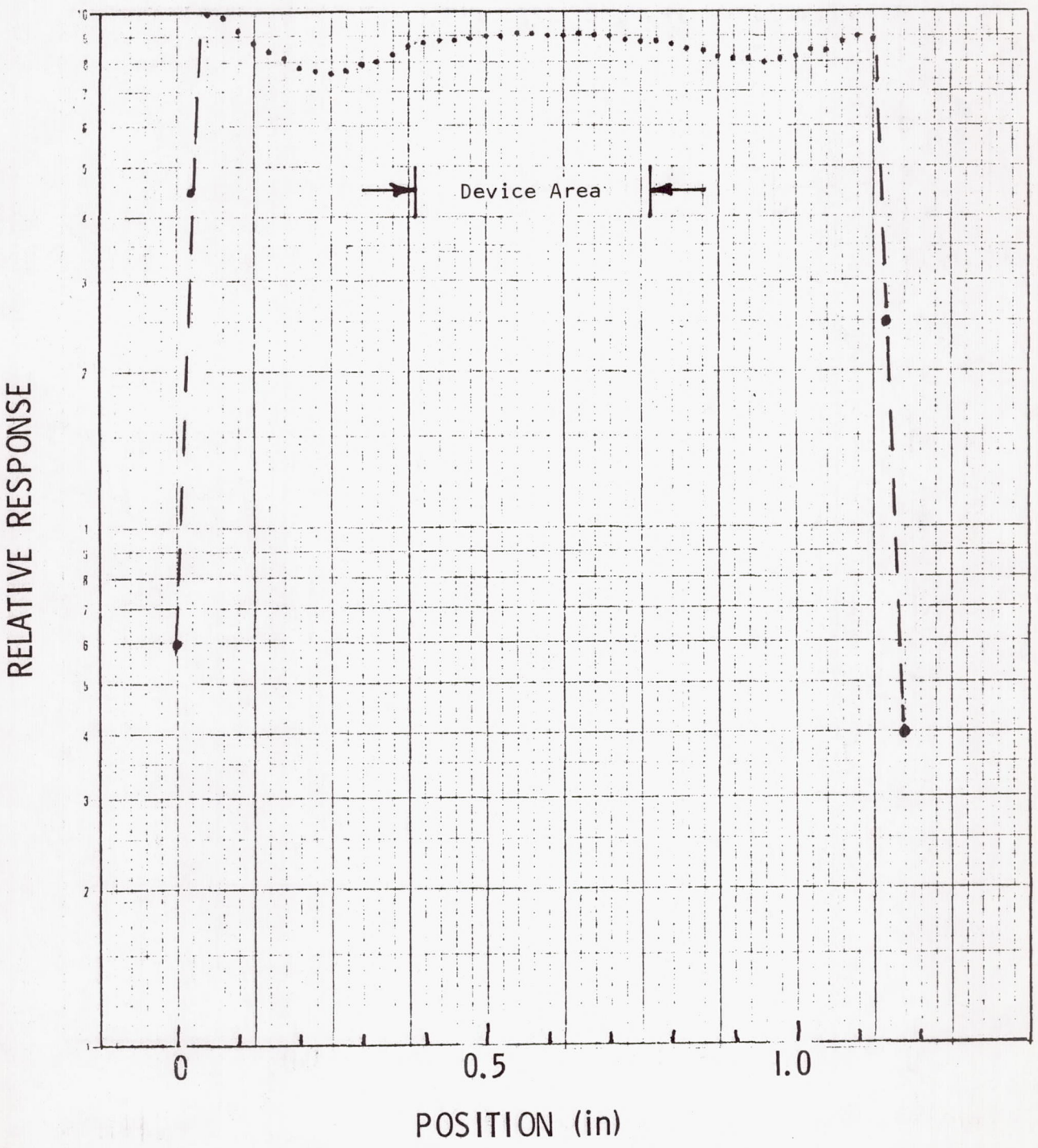

Figure 42 Spot Scan of Tube #287 Photocathode

PHOTOCATHODE SPOT SCAN

TUBE 299

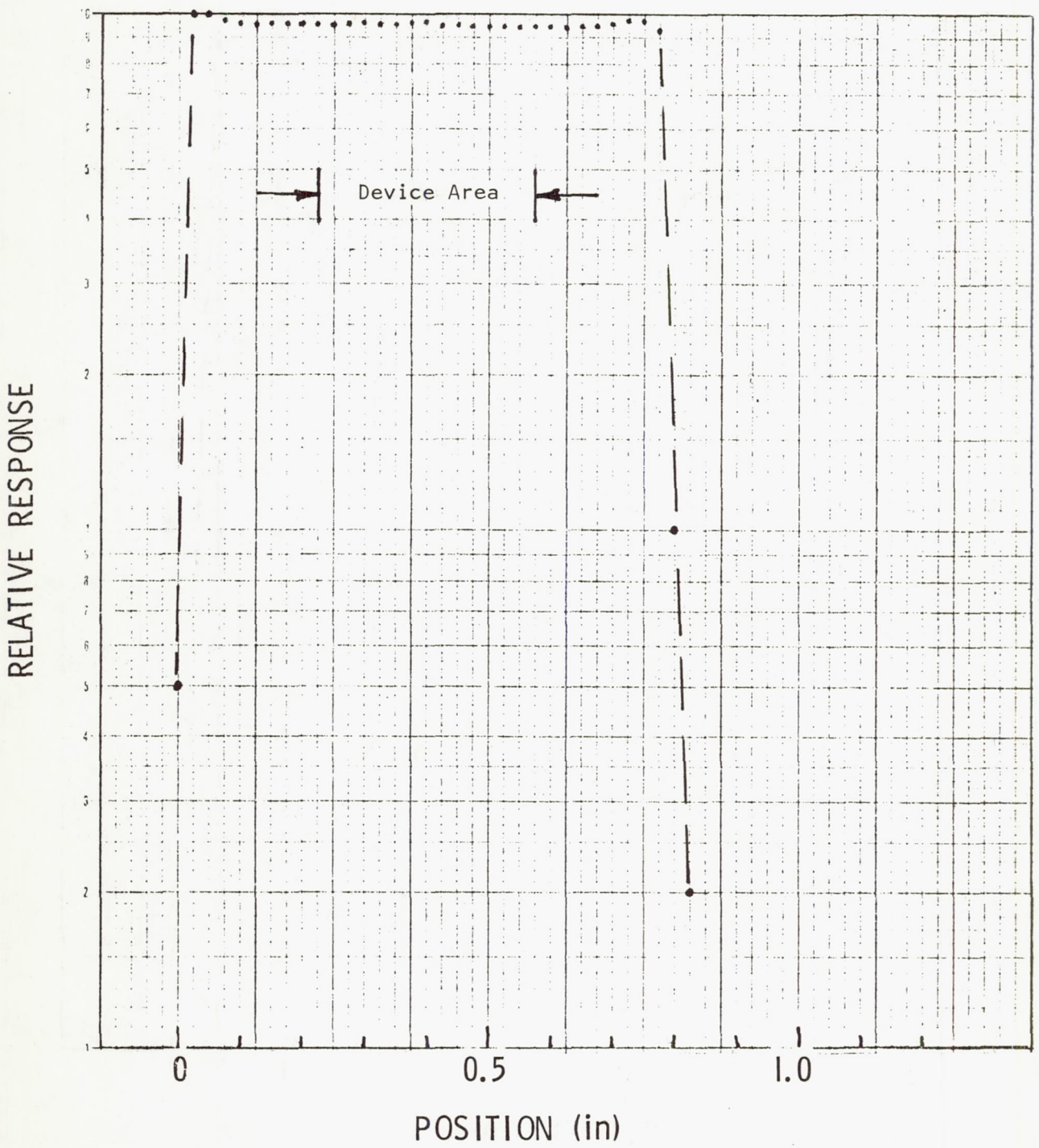

Figure 43 Spot Scan of Tube #299 Photocathode

ORIGINAL PAGE IS
OF POOR QUALITY

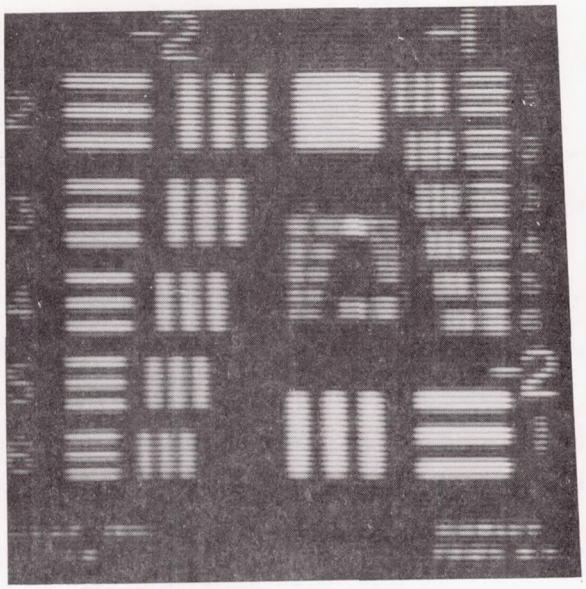

(a)
3.2×10^{-4} fc

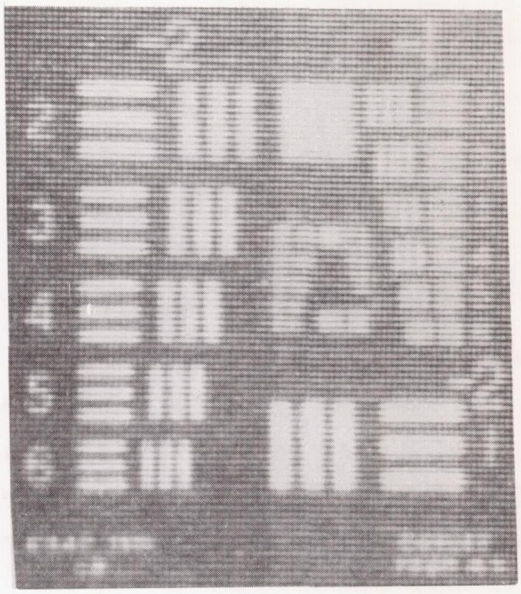

(b)
3.7×10^{-5} fc

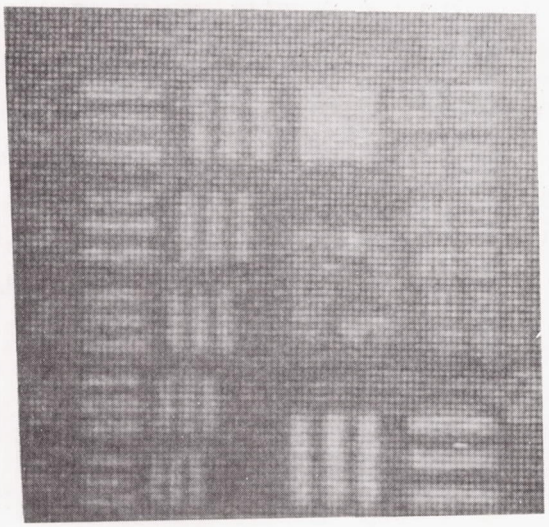

(c)
7.6×10^{-6} fc

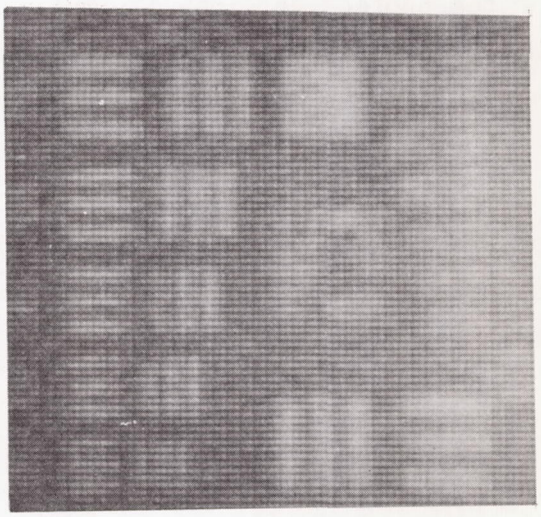

(d)
7.0×10^{-7} fc

Figure 44 Imaging Capability of Tube #243

diode and the precharge gate were damaged simultaneously. Otherwise, the shorted protective diode would have prevented damage to the precharge gate.

Device 321-3-7, tube #7, did not experience amplifier damage. However, very large dark currents existed after tube processing. The original dark current of 4.4 nA/cm^2 increased to 122 nA/cm^2. Curve tracer analysis of this device revealed that three parallel phases were conductive to substrate, ϕ_{1B}, ϕ_{2D}, and ϕ_{3D}. This is likely to be the source of the increased dark current. Since the CCD was operable, it was delivered to NASA without further analysis.

The damage incurred seems to have been caused by an unusual type of high voltage pulse. Normally, the precharge gate is protected against such spikes by the protective diodes; the parallel phases are protected by the large capacitance. Since damage to the protective diodes and to the precharge gate must be simultaneous, a fast rise time of the pulse compared to the turn-on time of the protective diode is implied. Damage to the parallel gates implies sufficient charge to raise the parallel phase voltage above about 20 V. This type of pulse is not ordinarily observed during processing at TI or Varo.

The origin of the damaging pulse cannot be determined. It most likely occurs during the heliarc welding of the header to the tube body or during the electron scrub. Monitoring of the CCD during tube processing should be done to locate the source of this high voltage.

SECTION VII
SIGNAL CONDITIONING ELECTRONICS

Basic drive electronics for CCD imagers had been supplied to NASA-Goddard under Contract No. NAS5-22403. The original electronics were capable of driving the 100 x 160 imagers only, but had provision for expansion to other imager sizes. To operate the 250 x 400 imagers, a new signal conditioning board was required. This board was designed and delivered under this contract. The board provided the options of running the parallel register toward the upper amplifier, toward the lower amplifier, or in a split mode with half the parallel register running up and the other half running down. This board replaces the signal conditioning board required for the 100 x 160 in the original electronics. A photograph of the completed board is shown in Figure 45. A schematic of the board was supplied when the boards were delivered.

ORIGINAL PAGE IS
OF POOR QUALITY

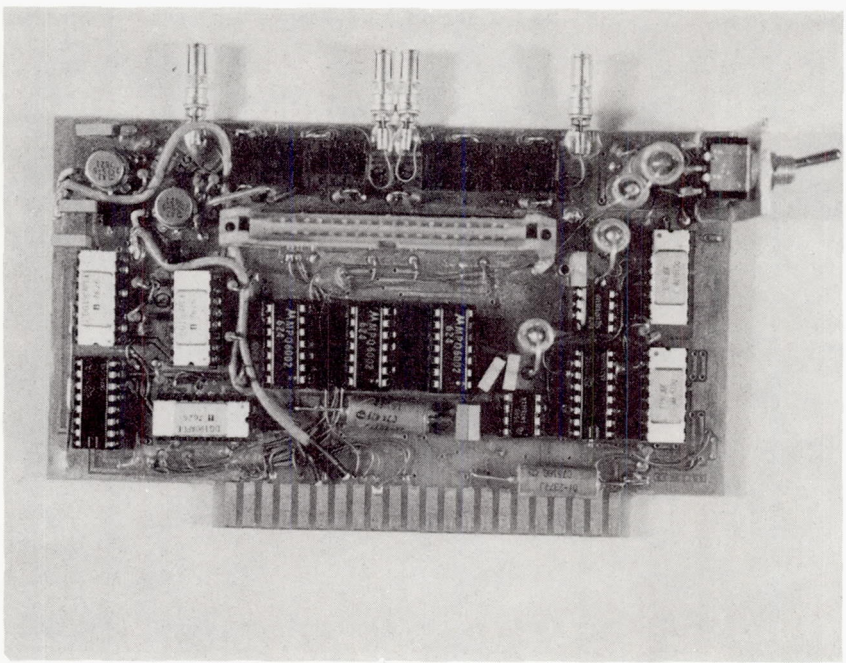

Figure 45 Signal Conditioning Board

SECTION VIII
CONCLUSIONS AND RECOMMENDATIONS

Under this contract significant progress has been made in the processing of thinned CCD imagers for intensified operation. The processing yield from on-slice to to on-header has been improved by more than an order of magnitude. Reproducible spectral response characteristics have been achieved. Major dark current sources have been identified; one has been eliminated and another subjected to study. A header suitable for laboratory investigations has been designed and implemented. Bond reliability problems have been eliminated. Development of beam leads for attachment of the chip to the header has begun to eliminate buckling problems and simplify header manufacture. CCD failure due to static electric discharge has been eliminated through the implementation of protective Zener diodes.

Twenty-two 250 x 400 imagers have been delivered: eighteen directly to NASA-Goddard and four to tube manufacturers. Three ICCDs have been successfully fabricated at Varo Electron Devices. Damage to CCDs processed at ITT has been related to high voltage, low current discharge. All performance goals have been met individually with the exception of 40% quantum efficiency at 0.4 μm.

A signal conditioning board has been designed and fabricated to operate the 250 x 400 devices, providing the option of operating in a forward mode, a reverse mode, or a split mode through both amplifiers simultaneously.

Further development of large area CCDs for intensified operation is recommended. The development of beam leads should be completed. Beam leads should be evaluated for effects on the buckling problem and for effects on the cooled operation of CCD imagers. A new header employing beam leads should be developed. The source of the dark current induced in the implanted buried channel region during heat treatments should be investigated. Elimination of this effect is the most important problem limiting the ultimate capability of ICCDs. Finally, application results of ICCDs should be pursued.

APPENDIX A
CHARACTERIZATION REPORTS FOR 22 DELIVERED DEVICES

CENTRAL RESEARCH LABORATORIES
CCD Optical and Electrical
Characterization Test Report

for

Customer NASA/Goddard

Contract No. NAS5-22924

Device No. 238-6-5

Device Type 250 x 400

CCD OPTICAL AND ELECTRICAL CHARACTERIZATION
TEST REPORT

1. CCD DEVICE NUMBER 238-6-5 DATE 8/19/76

2. DEVICE TYPE 250 x 400

Header type circular tube

Active area 0.63 cm^2, pixel dimensions 0.9 milsX 1.08 mils

3. OPERATING LEVELS in volts

SUB (substrate)	-0.2	SOG (serial output gate)	2
P CLK (parallel clocks)	12.5	Vpc (precharge pulse)	19
S CLK (serial clocks)	12.5	Vref (reference voltage)	17
SID (serial input diodes)	30	V_{dd} (drain voltage)	28

4. AMPLIFIER CONFIGURATION used for the tests in this report simple precharge with off chip load

5. QUANTUM EFFICIENCY at 0.4 microns is 7.7 %, uncorrected for reflection.

Uniformity of response is represented by the accompanying photographs.

6. DYNAMIC RANGE

Full well charge capability, determined from the saturation exposure level, is 1.2×10^6 electrons.

R.M.S. noise electrons/pixel, measured with an output bandwidth of 7.5 MHz, at a 1.0 MHz data rate, and a 120 ms frame time is

- for the lower amplifier, and
210 for the upper amplifier.

The dynamic range is thus computed to be

- : 1 for the lower amplifier, and
5700 : 1 for the upper amplifier.

7. DARK CURRENT

The array dark current at room temperature is 15 nA/cm^2.

8. CHARGE TRANSFER EFFICIENCY at 1MHz data rate is 0.9995.

9. COMMENTS (1) vacuum leak in the tube header, (2) lower transfer gate shorted to ϕ_{3A}; forward operation possible, however.

CCD IMAGING PERFORMANCE

Device Number 238-6-5 Device Type 400 x 250

Light Source STROBE °K Spectral filter N/A microns

Temperature 25 °C Data rate 3.0 MHz

Frame time 35 ms

ORIGINAL PAGE IS
OF POOR QUALITY

CCD DARK CURRENT UNIFORMITY

Device Number 238-6-5 Device Type 400 x 250

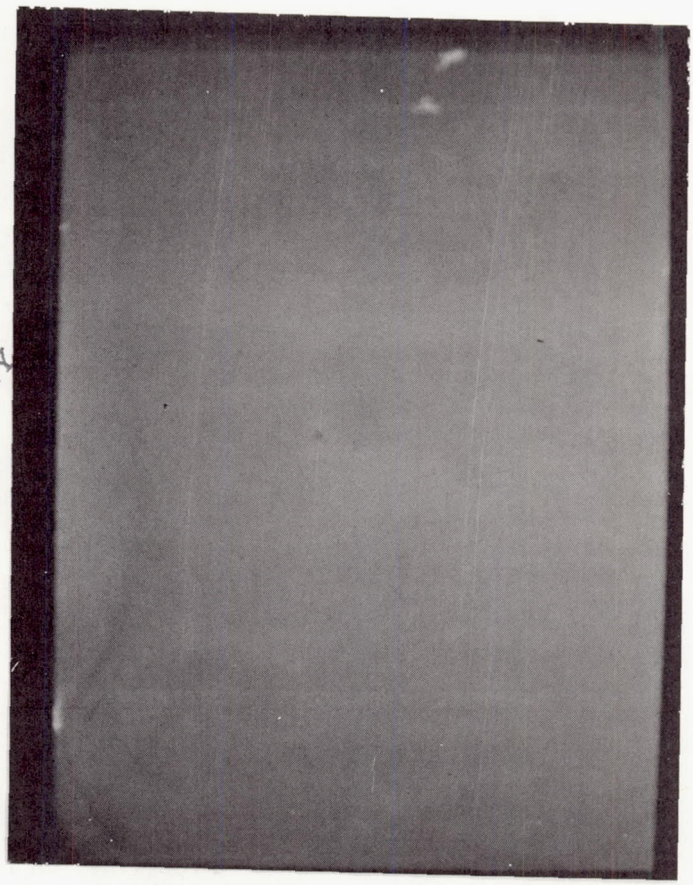

ORIGINAL PAGE IS
OF POOR QUALITY

VIDEO MONITOR DISPLAY

Temperature 25 °C

Data rate 3.0 MHz

Frame time 110 ms

CCD UNIFORMITY OF RESPONSE

Device Number 238-6-5 Device Type 400 x 250

Light source 3400 °K Spectral filter .4000 microns

Average well population 50 % Temperature 25 °C

Data rate 3.0 MHz Frame time 110 ms

ORIGINAL PAGE IS
OF POOR QUALITY

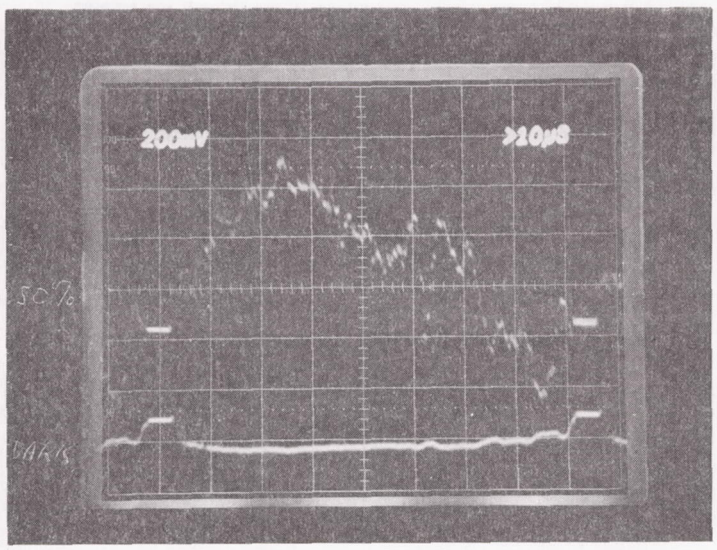

Oscilloscope presentation
Video line number 50

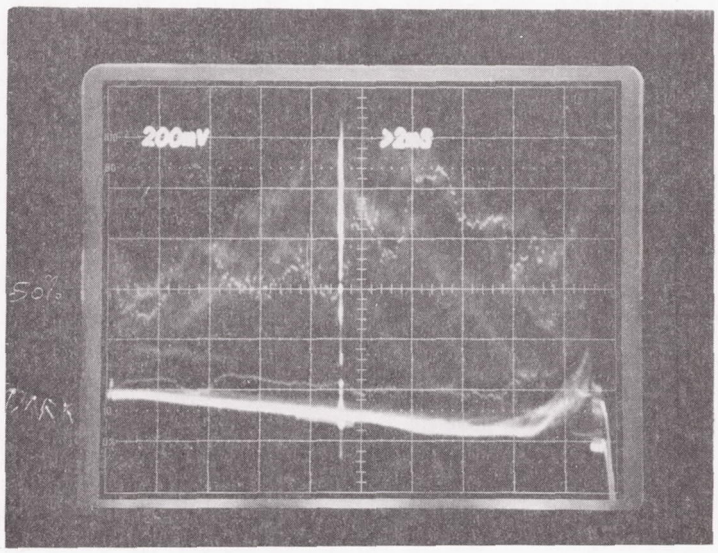

Oscilloscope presentation
Complete video frame

CCD UNIFORMITY OF RESPONSE

Device Number 238-6-5 Device Type 400 x 250

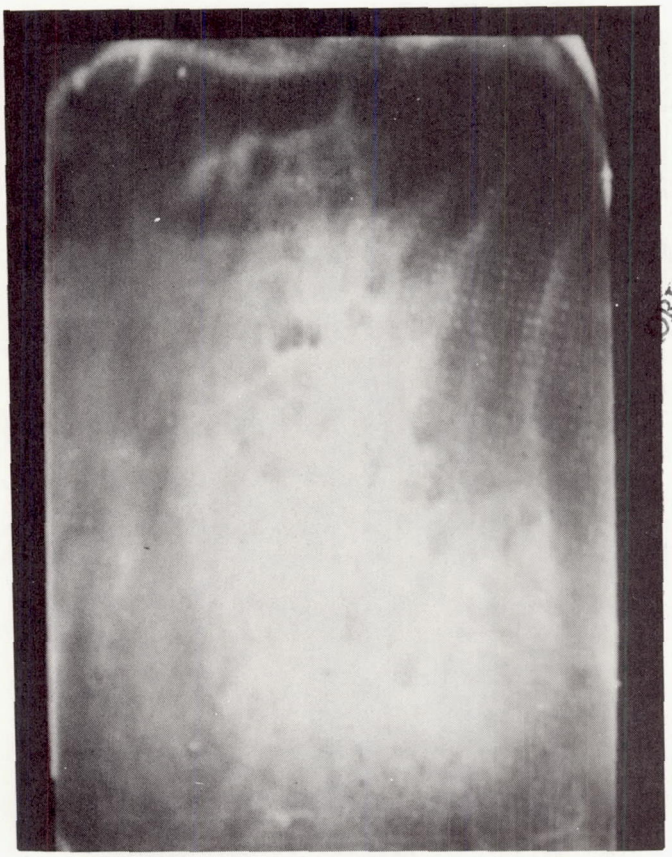

ORIGINAL PAGE IS
OF POOR QUALITY

VIDEO MONITOR DISPLAY

Light source	3400	°K
Spectral filter	.4000	microns
Average well population	50	%
Temperature	25	°C
Data rate	3.0	MHz
Frame time	110	ms

CENTRAL RESEARCH LABORATORIES
CCD Optical and Electrical
Characterization Test Report

for

Customer NASA/ Goddard

Contract No. NAS5-22924

Device No. 278-2-2

Device Type 250 x 400

CCD OPTICAL AND ELECTRICAL CHARACTERIZATION
TEST REPORT

1. CCD DEVICE NUMBER 278-2-2 DATE 12/28/76

2. DEVICE TYPE 250 x 400

Header type Circular tube header with Varo flange; tab alloyed

Active area 0.63 cm^2, pixel dimensions 1.08 milsX 0.9 mils

3. OPERATING LEVELS in volts

SUB (substrate)	-.5	SOG (serial output gate)	2
P CLK (parallel clocks)	9	Vpc (precharge pulse)	19
S CLK (serial clocks)	12	Vref (reference voltage)	20
SID (serial input diodes)	32	V_{dd} (drain voltage)	30

4. AMPLIFIER CONFIGURATION used for the tests in this report simple precharge with offchip load

5. QUANTUM EFFICIENCY at 0.4 microns is 3 %, uncorrected for reflection.

Uniformity of response is represented by the accompanying photographs.

6. DYNAMIC RANGE

Full well charge capability, determined from the saturation exposure level, is 3.15×10^5 electrons.

R.M.S. noise electrons/pixel, measured with an output bandwidth of 7.5 MHz, at a 1.0 MHz data rate, and a 120 ms frame times is

650 (estimated) for the lower amplifier, and

650 (estimated) for the upper amplifier.

The dynamic range is thus computed to be

480 : 1 for the lower amplifier, and

480 : 1 for the upper amplifier.

7. DARK CURRENT

The array dark current at room temperature is 90 nA/cm^2.

8. CHARGE TRANSFER EFFICIENCY at 1MHz data rate is 0.9993.

9. COMMENTS

CCD IMAGING PERFORMANCE

Device Number 278-2-2 Device Type 250 x 400

Light Source strobe °K Spectral filter none microns

Temperature 25 °C Data rate 3.0 MHz

Frame time 40 ms

ORIGINAL PAGE IS
OF POOR QUALITY

CCD DARK CURRENT UNIFORMITY

Device Number 278-2-2 Device Type 250 x 400

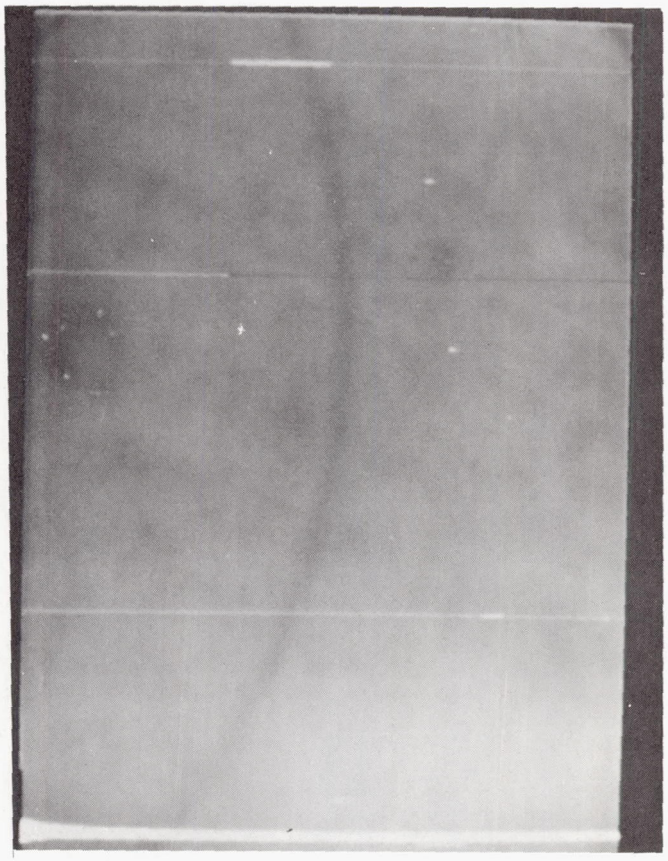

ORIGINAL PAGE IS
OF POOR QUALITY

VIDEO MONITOR DISPLAY

Temperature 25 °C

Data rate 3.0 MHz

Frame time 80 ms

CCD UNIFORMITY OF RESPONSE

Device Number 278-2-2 Device Type 250 x 400

ORIGINAL PAGE IS
OF POOR QUALITY

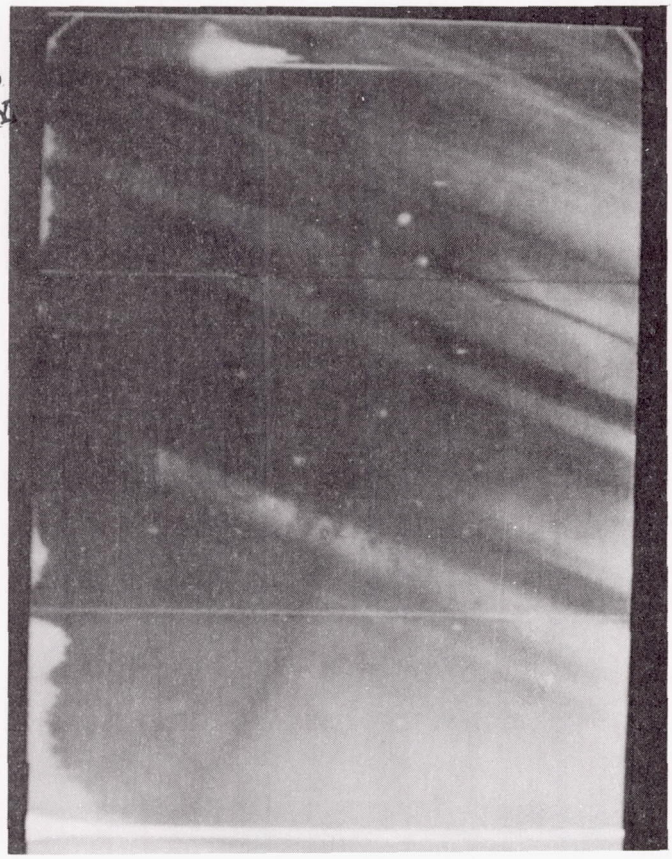

VIDEO MONITOR DISPLAY

Light source	3400	°K
Spectral filter	0.4	microns
Average well population	50	%
Temperature	25	°C
Data rate	3.0	MHz
Frame time	80	ms

CCD UNIFORMITY OF RESPONSE

Device Number 278-2-2 Device Type 250 x 400

Light source 3400 °K Spectral filter 0.4 microns

Average well population 50 % Temperature 25 °C

Data rate 3.0 MHz Frame time 80 ms

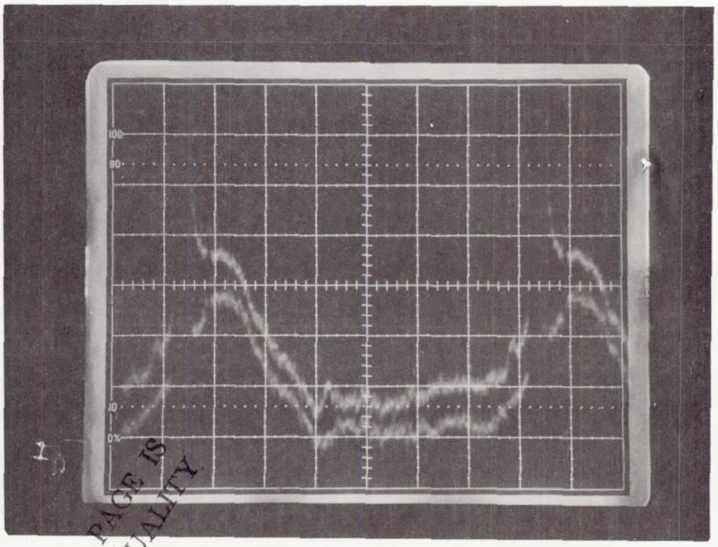

ORIGINAL PAGE IS
OF POOR QUALITY

Oscilloscope presentation
Video line number 50

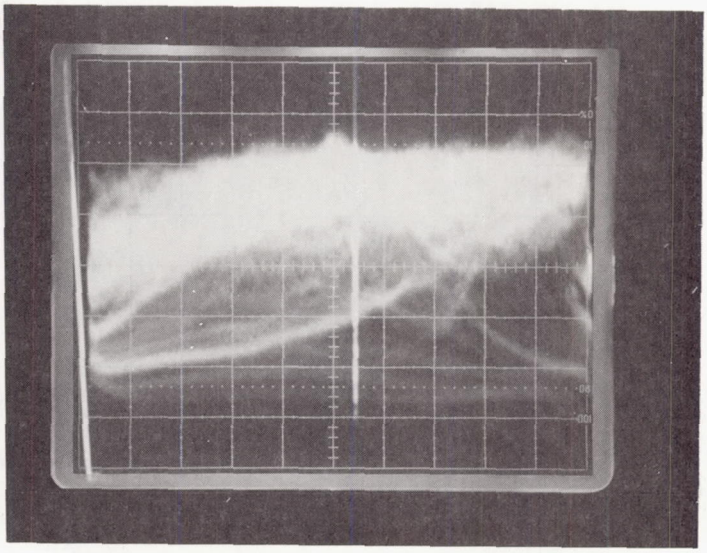

Oscilloscope presentation
Complete video frame

CENTRAL RESEARCH LABORATORIES
CCD Optical and Electrical
Characterization Test Report

for

Customer NASA/GODDARD SPACE FLIGHT CENTER

Contract No. NAS5-22924

Device No. 321-3-7

Device Type 400 x 250

ITT Tube Start

CCD OPTICAL AND ELECTRICAL CHARACTERIZATION TEST REPORT

1. CCD DEVICE NUMBER 321-3-7

2. DEVICE TYPE 400 x 250

   HEADER TYPE tube header with ITT flange

   Active area 0.63 cm^2 , pixel dimensions 0.9 mils X 1.08 mils

3. OPERATING LEVELS in volts

Substrate	-.5	Lower reference	20
Parallel clocks	11	Upper reference	20
Serial clocks	15	Lower drain	28
Input diode	32	Upper drain	28
Output gate	2	Precharge	15

4. AMPLIFIER CONFIGURATION used for the tests in this report:

   simple precharge with external load

5. SPECTRAL RESPONSE (see accompanying graph)

   Quantum efficiency is 14.8 % at 0.4 microns

   73.9 % at 0.7 microns

   23.7 % at 1.0 microns

6. DARK CURRENT measured by the precharge method

   4.4 nanoamps/cm^2 or 1.5×10^5 electrons/pixel/sec

   T = 25 C, data rate 3.0 MHz, frame time 40 ms

7. EBS GAIN (SEM measured) (not Measured)

   Average EBS gain is _____ at ____KV; _____ at ____KV

8. AMPLIFIER RESPONSE: _____ external load, _____MHz data rate
   (not measured)
   lower amplifier _____mV/nA

   upper amplifier _____mV/nA

9. CHARGE TRANSFER EFFICIENCY at 3.0 MHz is 0.99998 .

CCD IMAGING PERFORMANCE

Device Number 321-3-7 Device Type 400 x 250

Light Source 3400 °K Spectral filter none microns

Temperature 25 °C Data rate 3.0 MHz

Frame time 150 ms

ORIGINAL PAGE IS
OF POOR QUALITY

CCD IMAGING PERFORMANCE

Device Number 321-3-7 Device Type 400 x 250

Light Source 3400 °K Spectral filter 0.4000 microns

Temperature 25 °C Data rate 3.0 MHz

Frame time 675 ms

ORIGINAL PAGE IS
OF POOR QUALITY

CCD DARK CURRENT UNIFORMITY

Device Number 321-3-7 Device Type 400 x 250

ORIGINAL PAGE IS
OF POOR QUALITY

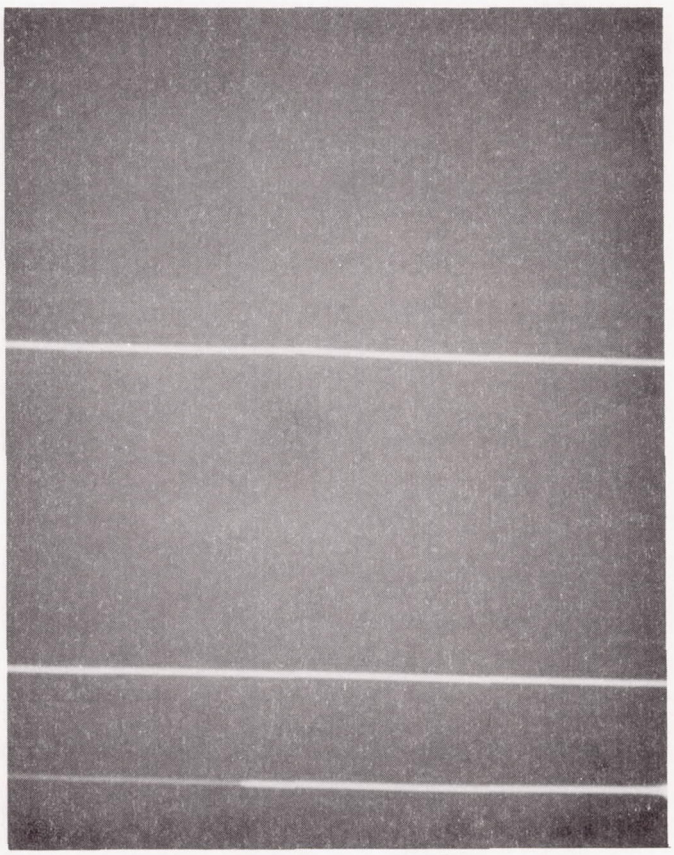

VIDEO MONITOR DISPLAY

Temperature 25 °C

Data rate 4.0 MHz

Frame time 115 ms

CCD DARK CURRENT UNIFORMITY

Device Number 321-3-7 Device Type 400 x 250

Temperature 25 °C Data rate 4.0 MHz

Frame time 115 ms

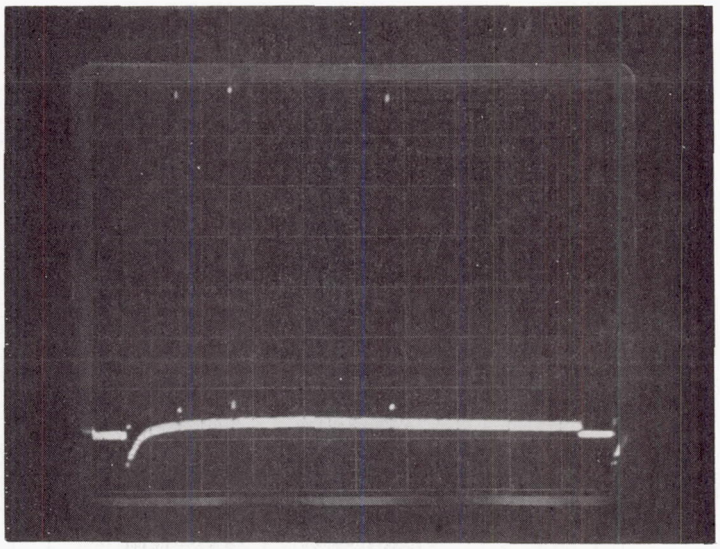

ORIGINAL PAGE IS
OF POOR QUALITY

Oscilloscope presentation

Video line number 50

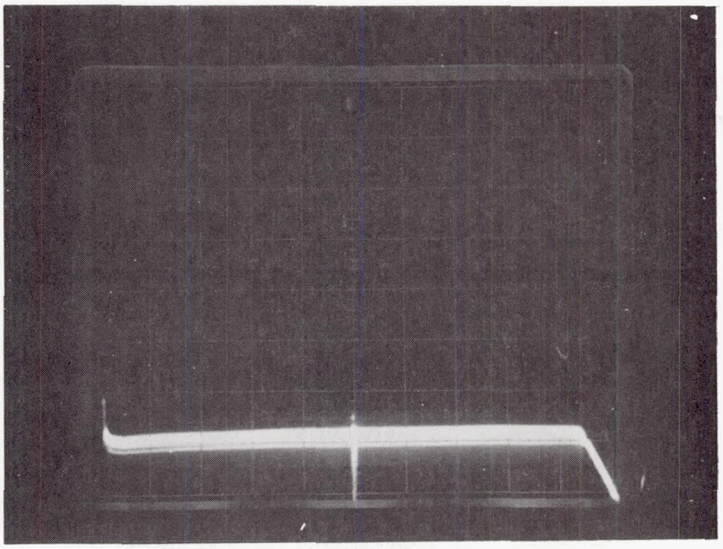

Oscilloscope presentation

Complete video frame

CCD UNIFORMITY OF RESPONSE

Device Number 321-3-7 Device Type 400 x 250

ORIGINAL PAGE IS
OF POOR QUALITY

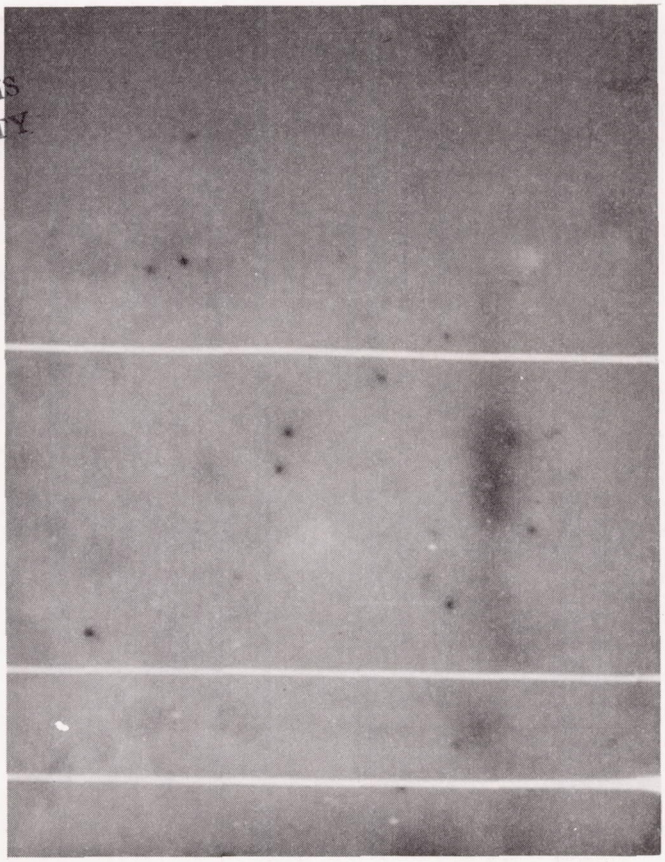

VIDEO MONITOR DISPLAY

Light source	3400	°K
Spectral filter	0.4000	microns
Average well population	50	%
Temperature	25	°C
Data rate	3.0	MHz
Frame time	250	ms

CCD UNIFORMITY OF RESPONSE

Device Number 321-3-7 Device Type 400 x 250

Light source 3400 °K Spectral filter 0.4000 microns

Average well population 50 % Temperature 25 °C

Data rate 3.0 MHz Frame time 250 ms

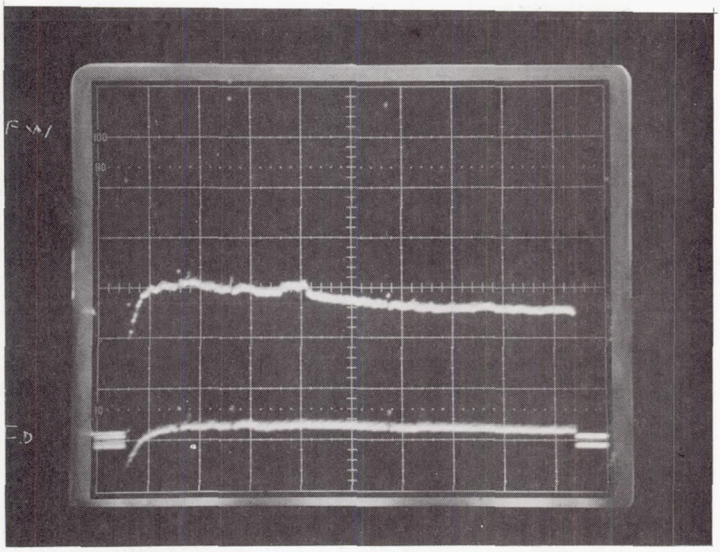

ORIGINAL PAGE IS
OF POOR QUALITY

Oscilloscope presentation
Video line number 50

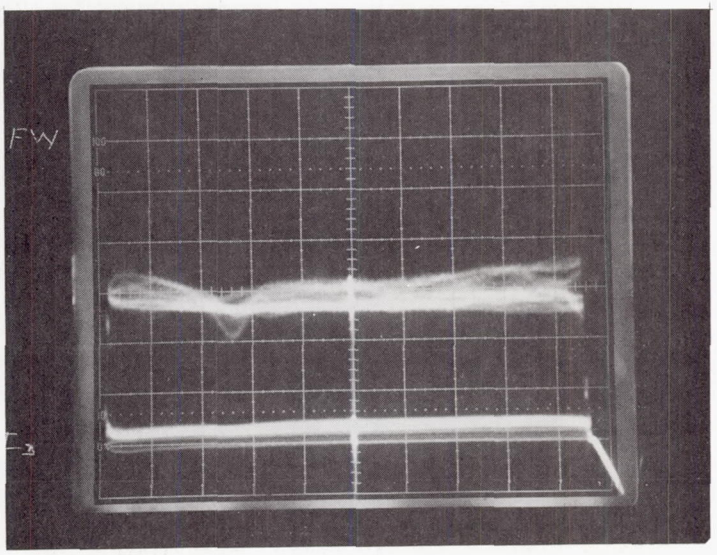

Oscilloscope presentation
Complete video frame

CCD SPECTRAL RESPONSIVITY

Device 321-3-7

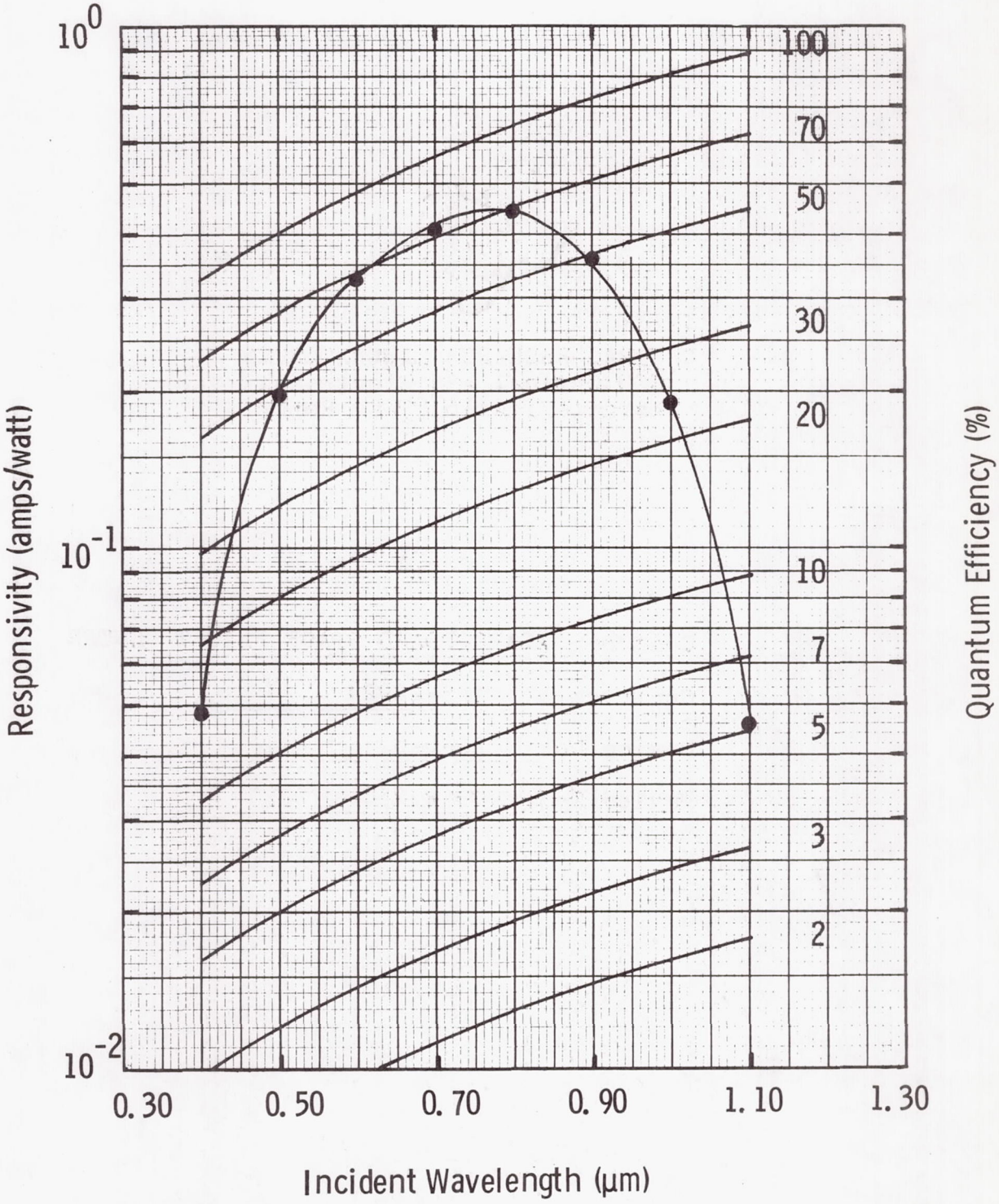

DATA RATE 4.0 MHz

FRAME TIME 64 MS

TEMPERATURE 25 °C

CENTRAL RESEARCH LABORATORIES
CCD Optical and Electrical
Characterization Test Report

for

Customer NASA/GODDARD SPACE FLIGHT CENTER

Contract No. NAS5-22924

Device No. 321-6-6

Device Type 400 x 250

CCD OPTICAL AND ELECTRICAL CHARACTERIZATION
TEST REPORT

1. CCD DEVICE NUMBER 321-6-6

2. DEVICE TYPE 400 x 250

HEADER TYPE tube header with ITT flange

Active area 0.63 cm^2 , pixel dimensions 0.9 mils X 1.08 mils

3. OPERATING LEVELS in volts

Substrate	-.5	Lower reference	20
Parallel clocks	11	Upper reference	20
Serial clocks	15	Lower drain	28
Input diode	30	Upper drain	28
Output gate	2	Precharge	15

4. AMPLIFIER CONFIGURATION used for the tests in this report:

simple precharge with external load

5. SPECTRAL RESPONSE (see accompanying graph)

Quantum efficiency is 12.2 % at 0.4 microns

75.9 % at 0.7 microns

25.4 % at 1.0 microns

6. DARK CURRENT measured by the precharge method

46 nanoamps/cm^2 or 1.5×10^6 electrons/pixel/sec

T = 25 C, data rate 3.0 MHz, frame time 49 ms

7. EBS GAIN (SEM measured) (not measured)

Average EBS gain is _____ at ____KV; _____ at ____KV

8. AMPLIFIER RESPONSE: _____ external load, _____MHz data rate
(not measured)
lower amplifier _____mV/nA

upper amplifier _____mV/nA

9. CHARGE TRANSFER EFFICIENCY at 3.0 MHz is 0.99996 .

CCD IMAGING PERFORMANCE

Device Number 321-6-6 Device Type 400 x 250

Light Source strobe °K Spectral filter none microns

Temperature 25 °C Data rate 3.0 MHz

Frame time 40 ms

ORIGINAL PAGE IS
OF POOR QUALITY

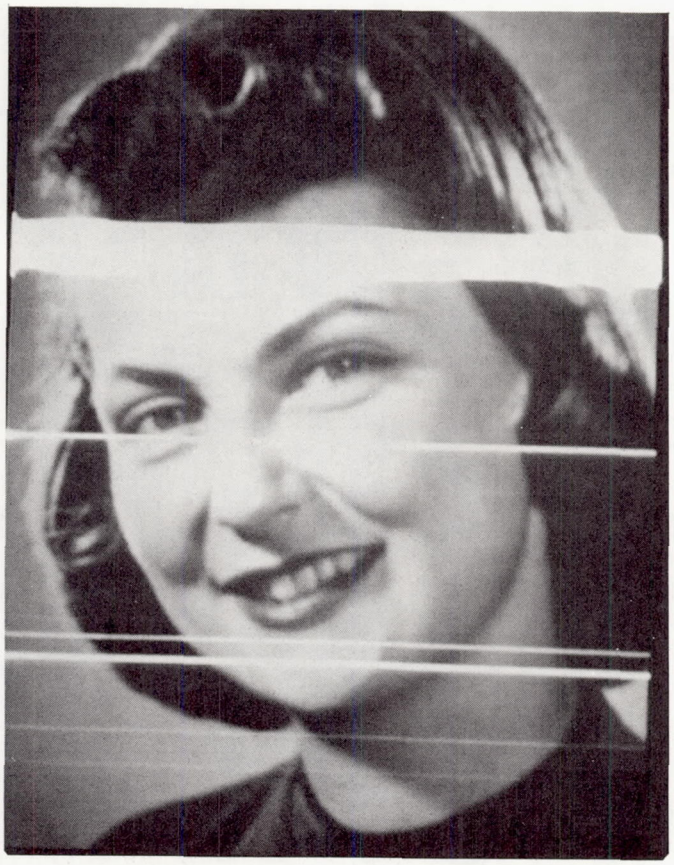

CCD DARK CURRENT UNIFORMITY

Device Number 321-6-6 Device Type 400 x 250

ORIGINAL PAGE IS
OF POOR QUALITY

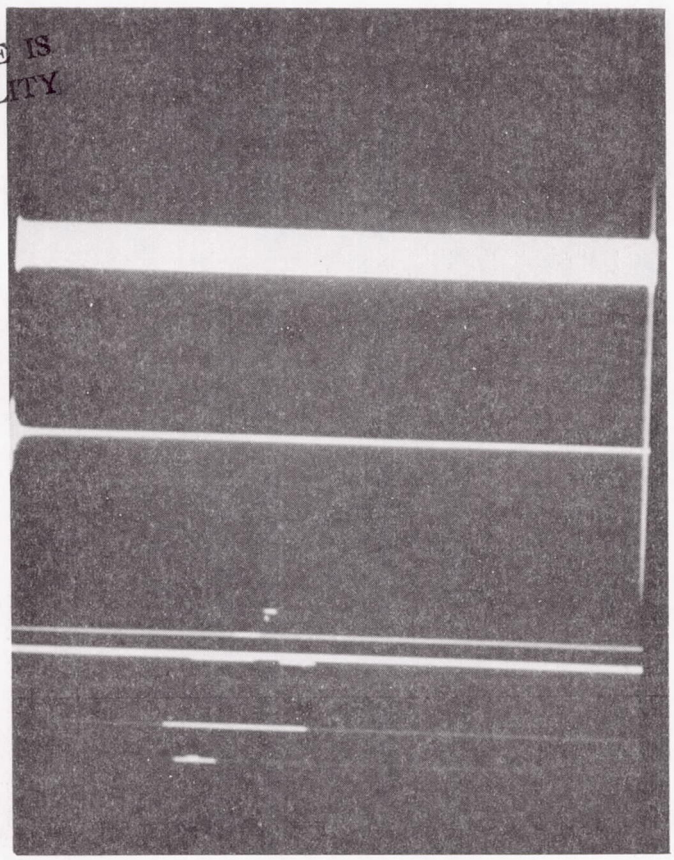

VIDEO MONITOR DISPLAY

Temperature 25 °C

Data rate 3.0 MHz

Frame time 70 ms

CCD DARK CURRENT UNIFORMITY

Device Number 321-6-6 Device Type 400 x 250

Temperature 25 °C Data rate 3.0 MHz

Frame time 70 ms

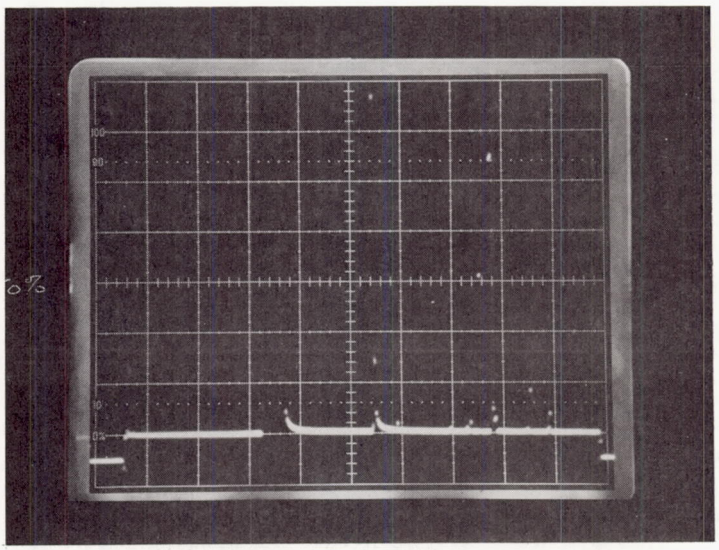

ORIGINAL PAGE IS
OF POOR QUALITY

Oscilloscope presentation

Video line number 50

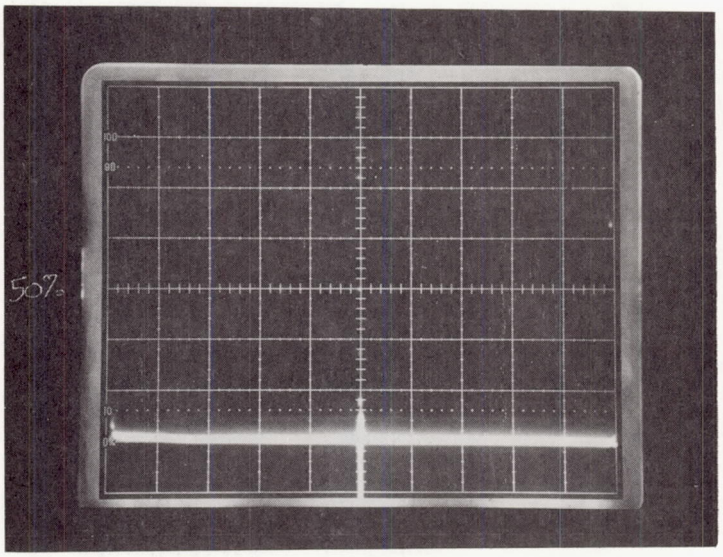

Oscilloscope presentation

Complete video frame

CCD UNIFORMITY OF RESPONSE

Device Number 321-6-6 Device Type 400 x 250

ORIGINAL PAGE IS
OF POOR QUALITY

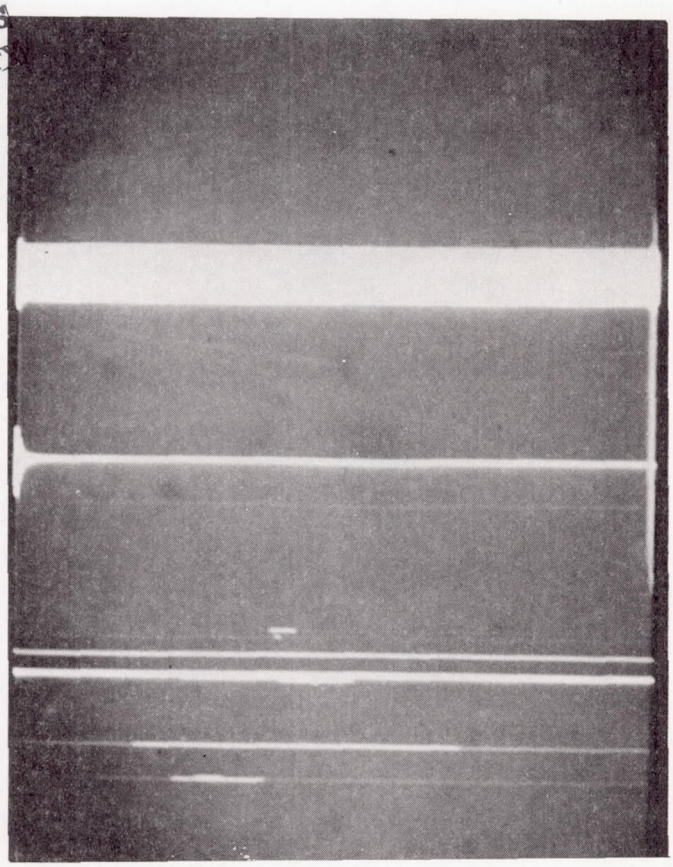

VIDEO MONITOR DISPLAY

Light source	3400	°K
Spectral filter	0.4000	microns
Average well population	50	%
Temperature	25	°C
Data rate	3.0	MHz
Frame time	72	ms

CCD UNIFORMITY OF RESPONSE

Device Number 321-6-6 Device Type 400 x 250

Light source 3400 °K Spectral filter 0.4000 microns

Average well population 50 % Temperature 25 °C

Data rate 3.0 MHz Frame time 72 ms

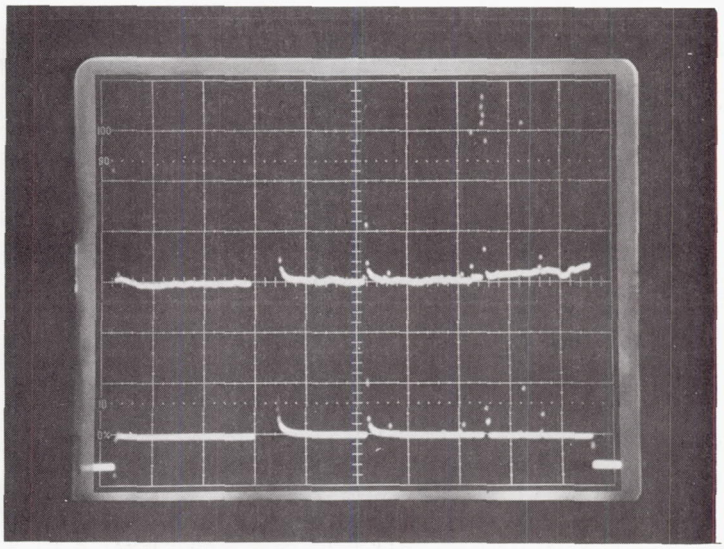

ORIGINAL PAGE IS
OF POOR QUALITY

Oscilloscope presentation
Video line number 50

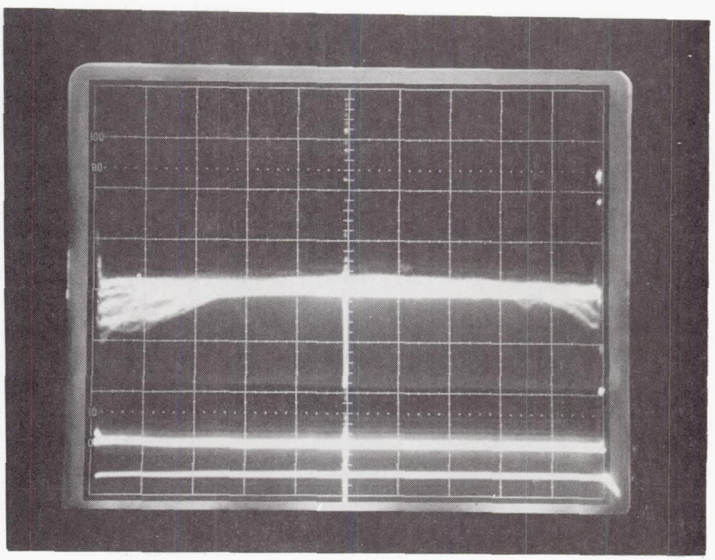

Oscilloscope presentation
Complete video frame

CCD SPECTRAL RESPONSIVITY

Device 321-6-6

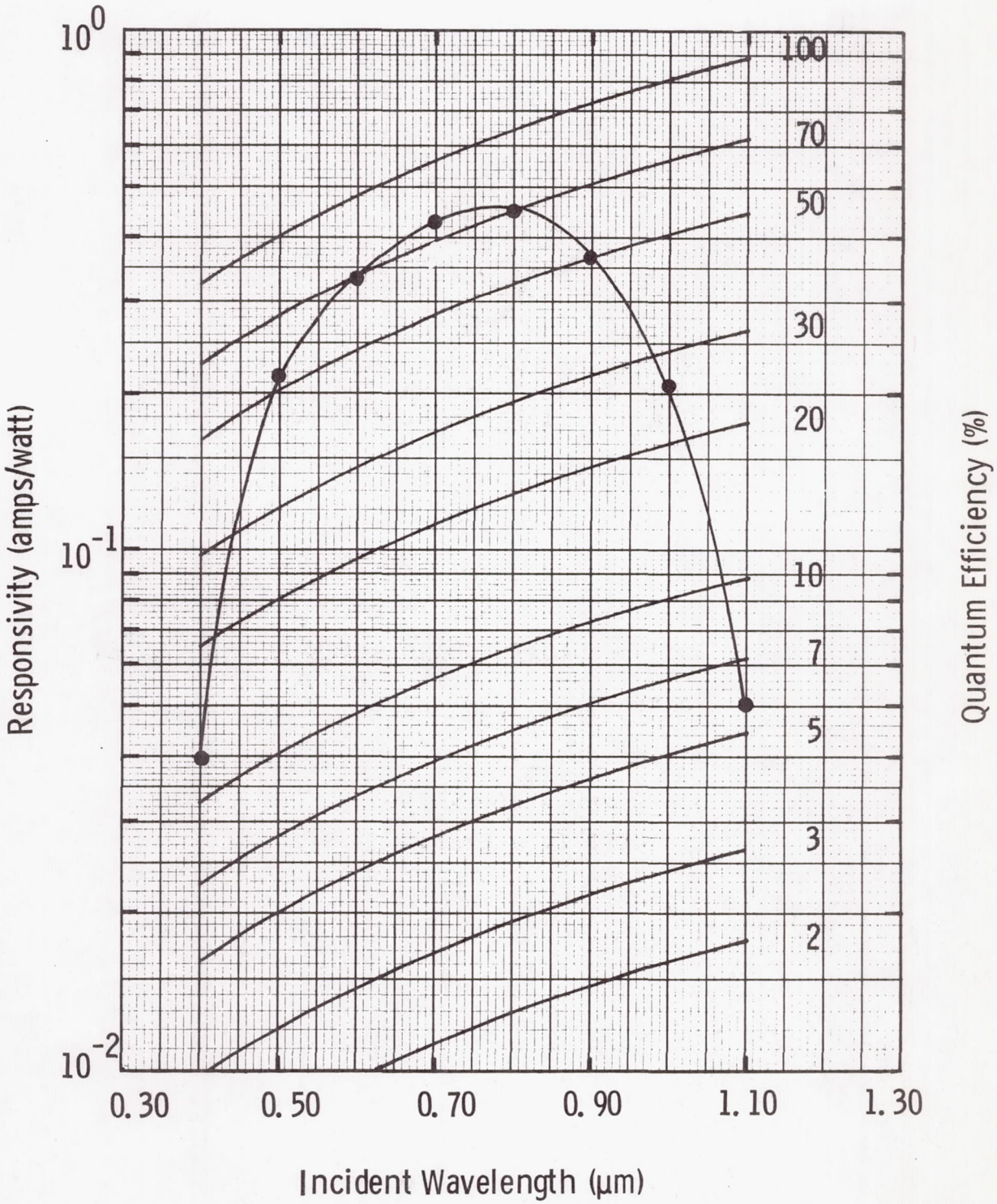

DATA RATE 3.0 MHz

FRAME TIME 40 MS

TEMPERATURE 25 °C

CENTRAL RESEARCH LABORATORIES
CCD Optical and Electrical
Characterization Test Report

for

Customer NASA/GODDARD SPACE FLIGHT CENTER

Contract No. NAS5-22924

Device No. 321-4-8

Device Type 400 x 250
ITT Tube Start

CCD OPTICAL AND ELECTRICAL CHARACTERIZATION
TEST REPORT

1. CCD DEVICE NUMBER 321-4-8

2. DEVICE TYPE 400 x 250

HEADER TYPE tube header with ITT flange

Active area 0.63 cm^2 , pixel dimensions 0.9 mils X 1.08 mils

3. OPERATING LEVELS in volts

Substrate	-.5	Lower reference	20
Parallel clocks	10	Upper reference	20
Serial clocks	10	Lower drain	28
Input diode	30	Upper drain	28
Output gate	2	Precharge	15

4. AMPLIFIER CONFIGURATION used for the tests in this report:

simple precharge with external load

5. SPECTRAL RESPONSE (see accompanying graph)

Quantum efficiency is 20.0 % at 0.4 microns

73.2 % at 0.7 microns

25.9 % at 1.0 microns

6. DARK CURRENT measured by the precharge method

9.2 nanoamps/cm^2 or 3.0×10^5 electrons/pixel/sec

T = 25 °C, data rate 3.0 MHz, frame time 40 ms

7. EBS GAIN (SEM measured) (not measured)

Average EBS gain is _____ at ____KV; _____ at ____KV

8. AMPLIFIER RESPONSE: _____ external load, _____MHz data rate

(not measured)
lower amplifier _____mV/nA

upper amplifier _____mV/nA

9. CHARGE TRANSFER EFFICIENCY at 3.0 MHz is 0.9995 (lower serial)
>0.9999 (upper serial)

CCD IMAGING PERFORMANCE

Device Number 321-4-8 Device Type 400 x250

Light Source strobe °K Spectral filter none microns

Temperature 25 °C Data rate 3.0 MHz

Frame time 40 ms

ORIGINAL PAGE IS OF POOR QUALITY

CCD DARK CURRENT UNIFORMITY

Device Number 321-4-8 Device Type 400 x 250

ORIGINAL PAGE IS
OF POOR QUALITY

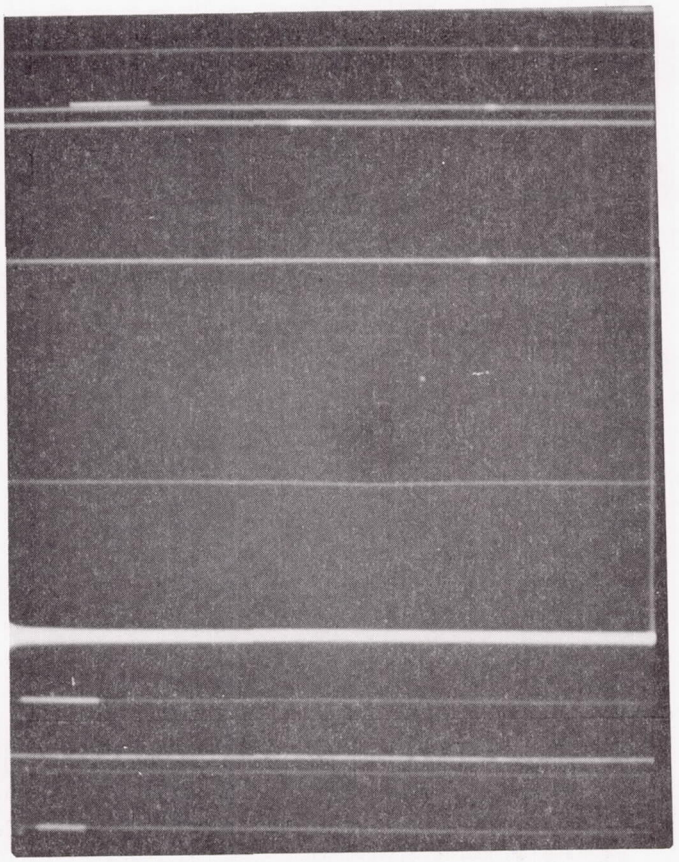

VIDEO MONITOR DISPLAY

Temperature 25 °C

Data rate 3.0 MHz

Frame time 79 ms

CCD DARK CURRENT UNIFORMITY

Device Number 321-4-8 Device Type 400 x 250

Temperature 25 °C Data rate 3.0 MHz

Frame time 79 ms

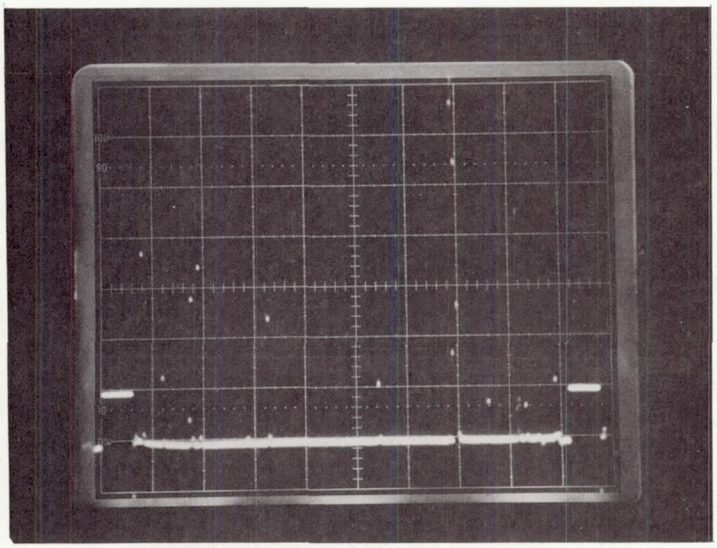

Oscilloscope presentation

Video line number 50

ORIGINAL PAGE IS
OF POOR QUALITY

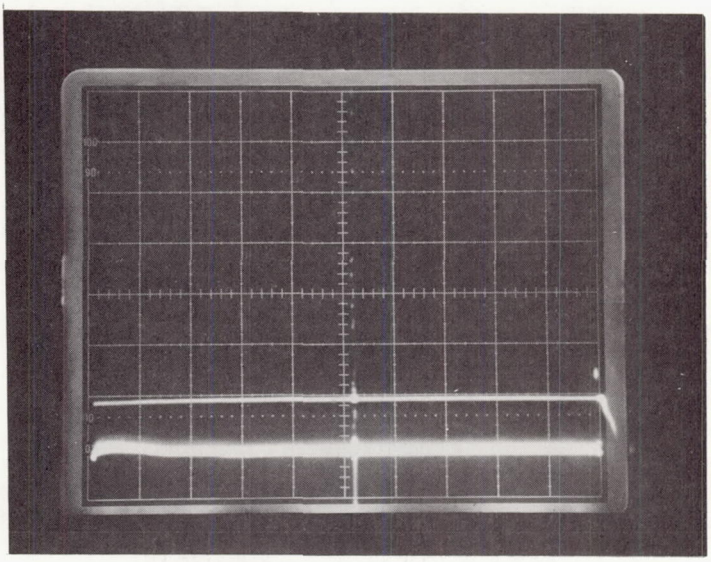

Oscilloscope presentation

Complete video frame

CCD UNIFORMITY OF RESPONSE

Device Number 321-4-8 Device Type 400 x 250

ORIGINAL PAGE IS
OF POOR QUALITY

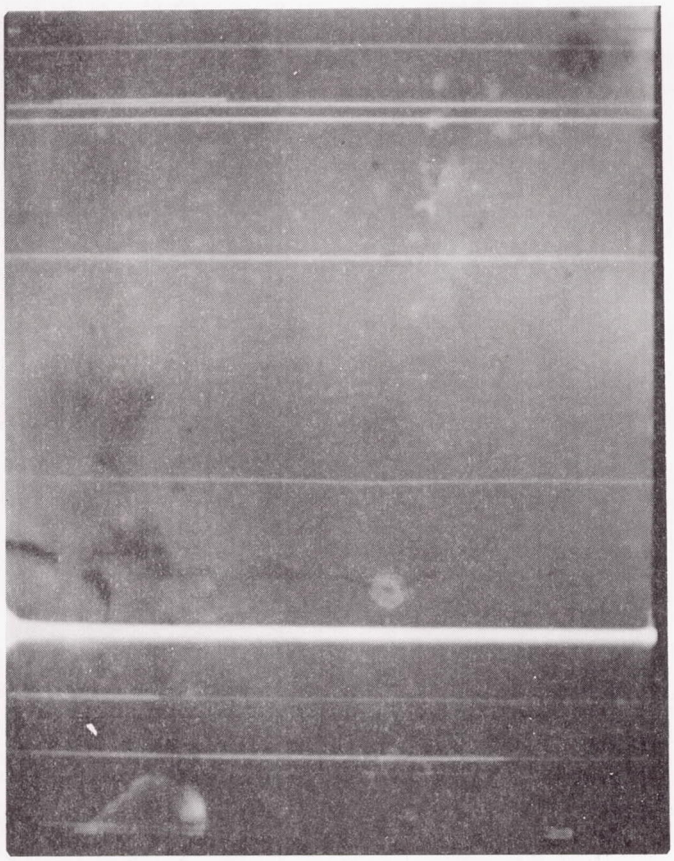

VIDEO MONITOR DISPLAY

Light source	3400	°K
Spectral filter	0.4000	microns
Average well population	50	%
Temperature	25	°C
Data rate	3.0	MHz
Frame time	79	ms

CCD UNIFORMITY OF RESPONSE

Device Number 321-4-8 Device Type 400 x 250

Light source 3400 °K Spectral filter 0.4000 microns

Average well population 50 % Temperature 25 °C

Data rate 3.0 MHz Frame time 79 ms

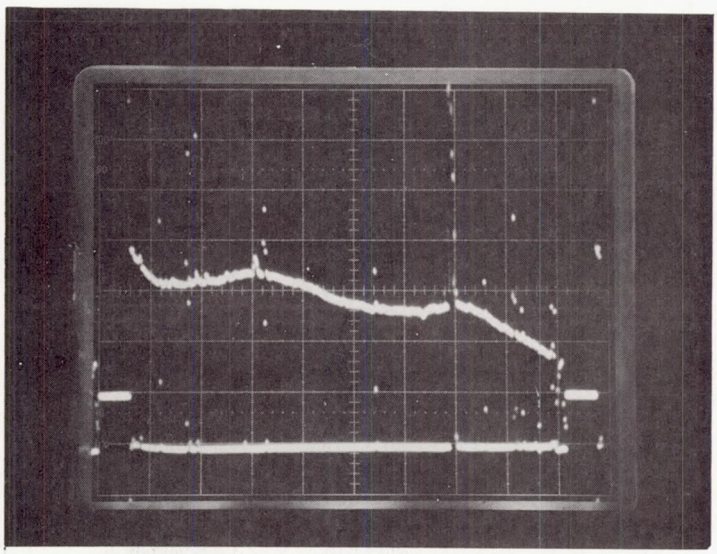

ORIGINAL PAGE IS
OF POOR QUALITY

Oscilloscope presentation
Video line number 50

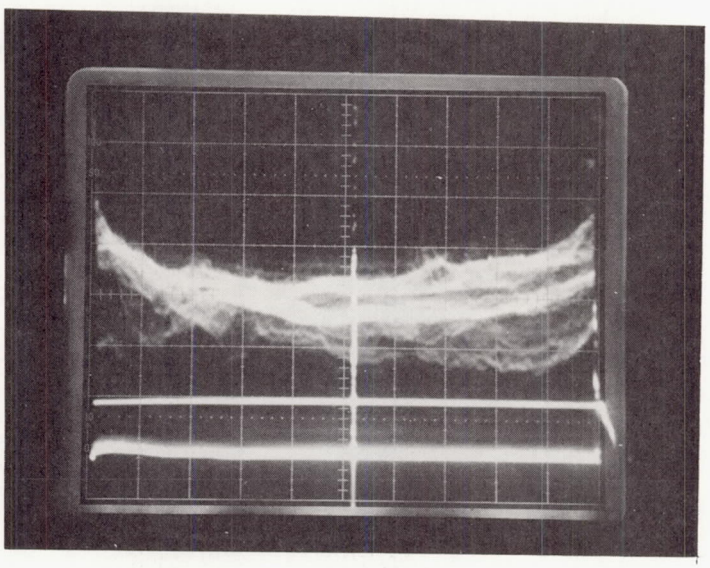

Oscilloscope presentation
Complete video frame

CCD SPECTRAL RESPONSIVITY

Device 321-4-8

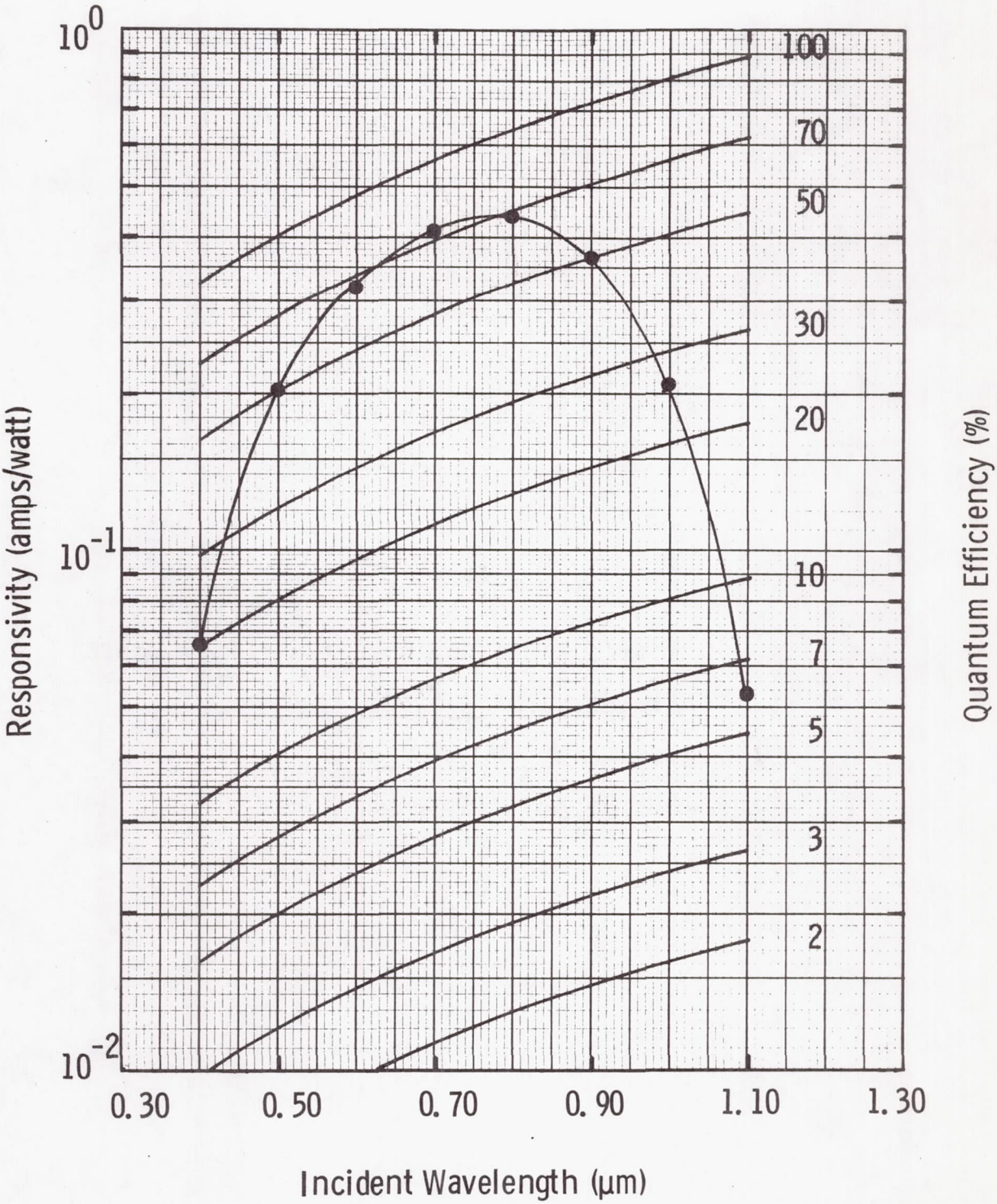

DATA RATE 3.0 MHz

FRAME TIME 40 MS

TEMPERATURE 25 °C

CENTRAL RESEARCH LABORATORIES
CCD Optical and Electrical
Characterization Test Report

for

Customer NASA/GODDARD SPACE FLIGHT CENTER

Contract No. NAS5-22924

Device No. 361-6-6

Device Type 250 x 400

CCD OPTICAL AND ELECTRICAL CHARACTERIZATION
TEST REPORT

1. CCD DEVICE NUMBER 361-6-6

2. DEVICE TYPE 250 x 400 HEADER TYPE ITT tube header

Active area 0.636 cm^2 , pixel dimensions 1.08 mils x 0.9 mils

3. OPERATING LEVELS in volts

Substrate	-.5	Lower reference	20
Parallel clocks	14	Upper reference	20
Serial clocks	15	Lower drain	28
Input diode	32	Upper drain	28
Output gate	2	Precharge pulse	9

4. AMPLIFIER CONFIGURATION used for the tests in this report:
precharge amplifier with off-chip load

5. SPECTRAL RESPONSE (see accompanying graph)

Quantum efficiency is 13.5 % at 0.4 microns

81.4 % at 0.7 microns

26.0 % at 1.0 microns

6. DARK CURRENT measured by the precharge method

30.5 nanoamps/cm^2 or 1.2×10^6 electrons/pixel/sec

T = 25 C, data rate 4.0 MHz, frame time 100 ms

7. R.M.S. NOISE ELECTRONS/PIXEL
Dark current shot noise 350 (100ms) electrons added in quadrature to a readout noise of 30 electrons gives a calculated R.M.S. noise of 350 electrons/pixel

8. FULL WELL CHARGE CAPABILITY, determined from the saturation exposure level, is 6.0×10^5 electrons.

9. DYNAMIC RANGE is computed to be 1700 :1.

10. CHARGE TRANSFER EFFICIENCY at 4.0 MHz is _____.

11. COMMENTS vacuum leak in header due to ceramic crack

CCD IMAGING PERFORMANCE

Device Number 361-6-6 Device Type 250 x 400

Light Source strobe °K Spectral filter none microns

Temperature 25 °C Data rate 4.0 MHz

Frame time 33 ms

ORIGINAL PAGE IS OF POOR QUALITY

CCD DARK CURRENT UNIFORMITY

Device Number 361-6-6 Device Type 250 x 400

ORIGINAL PAGE IS
OF POOR QUALITY

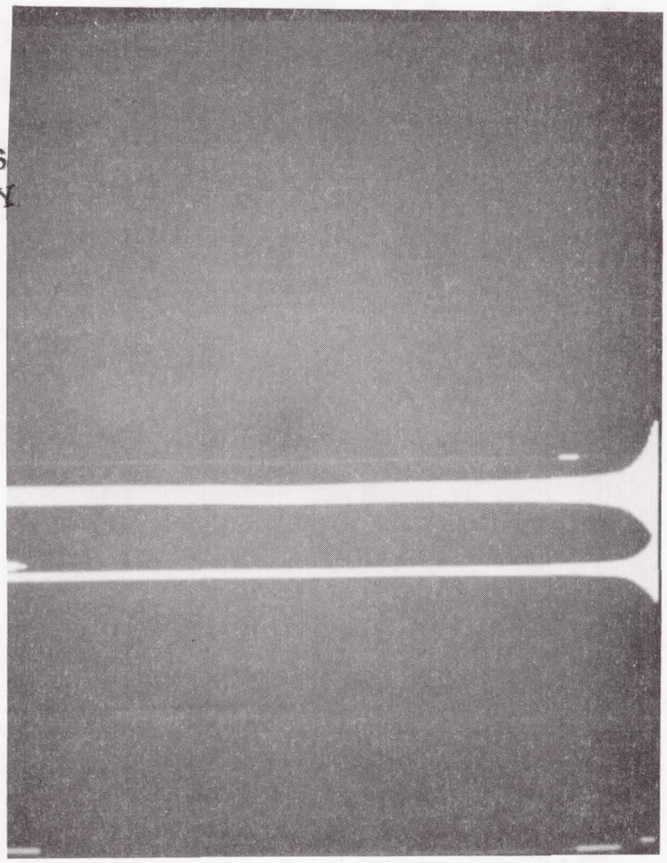

VIDEO MONITOR DISPLAY

Temperature 25 °C

Data rate 4.0 MHz

Frame time 100 ms

CCD DARK CURRENT UNIFORMITY

Device Number 361-6-6 Device Type 250 x 400

Temperature 25 °C Data rate 4.0 MHz

Frame time 100 ms

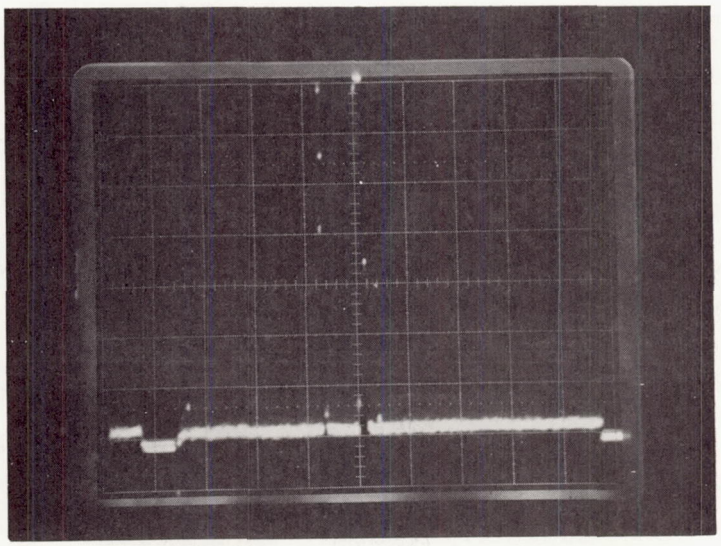

ORIGINAL PAGE IS
OF POOR QUALITY

Oscilloscope presentation

Video line number 50

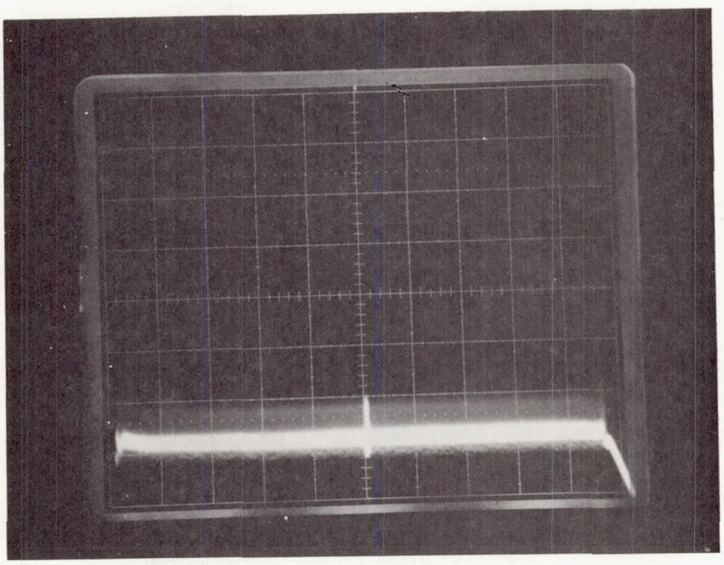

Oscilloscope presentation

Complete video frame

CCD UNIFORMITY OF RESPONSE

Device Number 361-6-6 Device Type 250 x 400

ORIGINAL PAGE IS
OF POOR QUALITY

VIDEO MONITOR DISPLAY

Light source	3400	°K
Spectral filter	0.4000	microns
Average well population	50	%
Temperature	25	°C
Data rate	4.0	MHz
Frame time	135	ms

CCD UNIFORMITY OF RESPONSE

Device Number 361-6-6 Device Type 250 x 400

Light source 3400 °K Spectral filter 0.4000 microns

Average well population 50 % Temperature 25 °C

Data rate 4.0 MHz Frame time 135 ms

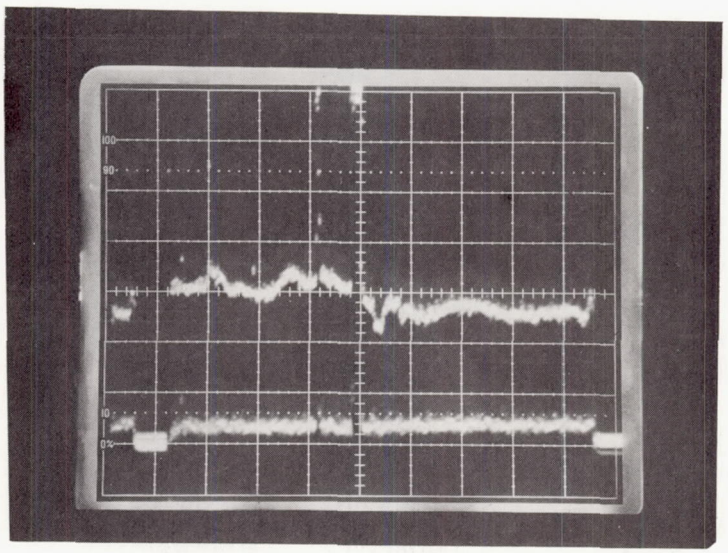

ORIGINAL PAGE IS
OF POOR QUALITY

Oscilloscope presentation
Video line number 50

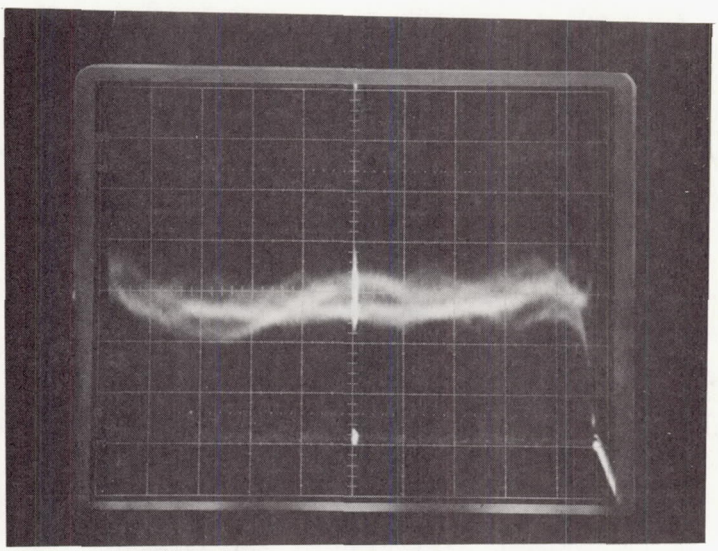

Oscilloscope presentation
Complete video frame

CCD SPECTRAL RESPONSIVITY

Device 361-6-6

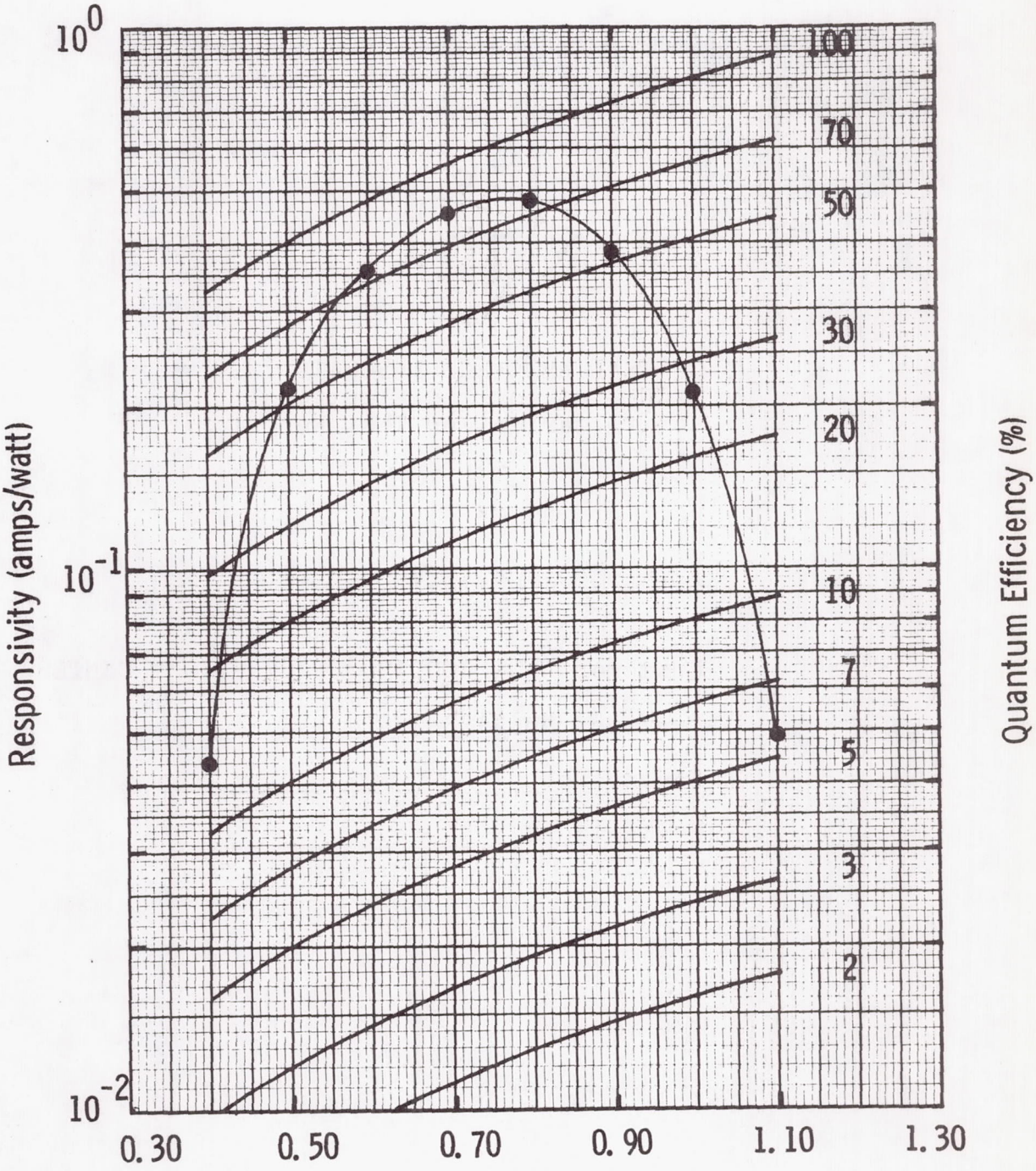

DATA RATE 3.0 MHz

FRAME TIME 50 MS

TEMPERATURE 25 °C

CENTRAL RESEARCH LABORATORIES
CCD Optical and Electrical
Characterization Test Report

for

Customer NASA/GODDARD SPACE FLIGHT CENTER

Contract No. NAS5-22924

Device No. 361-6-8

Device Type 250 x 400

CCD OPTICAL AND ELECTRICAL CHARACTERIZATION
TEST REPORT

1. CCD DEVICE NUMBER 361-6-8

2. DEVICE TYPE 250 x 400 HEADER TYPE Varo tube header

Active area 0.636 cm^2 , pixel dimensions 1.08 mils x 0.9 mils

3. OPERATING LEVELS in volts

Substrate	-.5	Lower reference	20
Parallel clocks	10	Upper reference	20
Serial clocks	15	Lower drain	28
Input diode	32	Upper drain	28
Output gate	2	Precharge pulse	9

4. AMPLIFIER CONFIGURATION used for the tests in this report:
precharge amplifier with off-chip load

5. SPECTRAL RESPONSE (see accompanying graph)

Quantum efficiency is 14 % at 0.4 microns

75 % at 0.7 microns

25 % at 1.0 microns

6. DARK CURRENT measured by the precharge method

21.1 nanoamps/cm^2 or 8.5 x10^5 electrons/pixel/sec

T = 25 C, data rate 4.0 MHz, frame time 100 ms

7. R.M.S. NOISE ELECTRONS/PIXEL

Dark current shot noise 292 (100ms) electrons added in quadrature to a readout noise of 30 electrons gives a calculated R.M.S. noise of 294 electrons/pixel

8. FULL WELL CHARGE CAPABILITY, determined from the saturation exposure level, is _____ electrons.

9. DYNAMIC RANGE is computed to be _____:1_____.

10. CHARGE TRANSFER EFFICIENCY at 4.0 MHz is 0.99993.

11. COMMENTS _____

CCD IMAGING PERFORMANCE

Device Number 361-6-8 Device Type 250 x 400

Light Source strobe °K Spectral filter none microns

Temperature 25 °C Data rate 4.0 MHz

Frame time 33 ms

ORIGINAL PAGE IS OF POOR QUALITY

CCD DARK CURRENT UNIFORMITY

Device Number 361-6-8 Device Type 250 x 400

ORIGINAL PAGE IS
OF POOR QUALITY

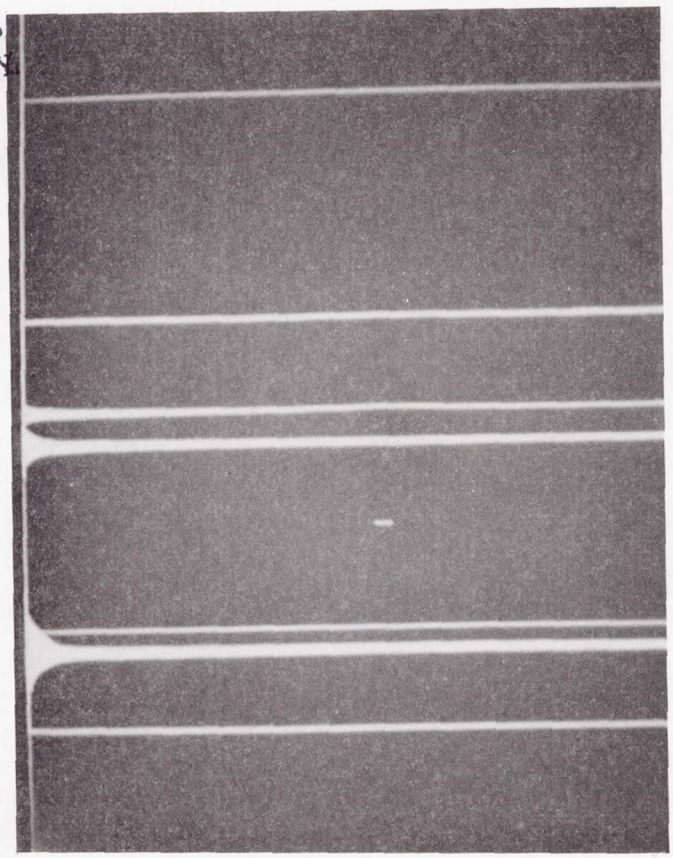

VIDEO MONITOR DISPLAY

Temperature 25 °C

Data rate 4.0 MHz

Frame time 100 ms

CCD DARK CURRENT UNIFORMITY

Device Number 361-6-8 Device Type 250 x 400

Temperature 25 °C Data rate 4.0 MHz

Frame time 100 ms

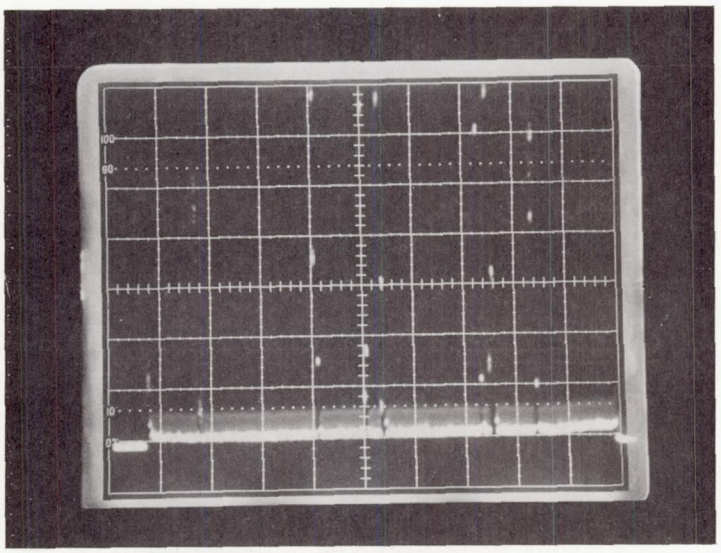

ORIGINAL PAGE IS
OF POOR QUALITY

Oscilloscope presentation

Video line number 50

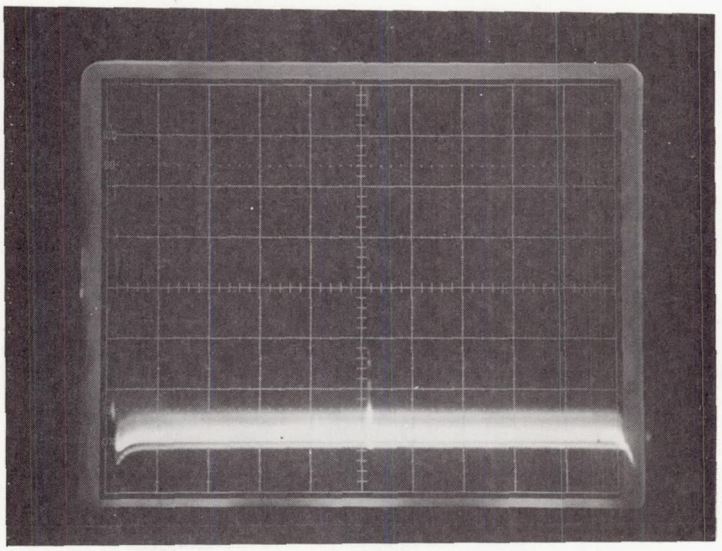

Oscilloscope presentation

Complete video frame

CCD UNIFORMITY OF RESPONSE

Device Number 361-6-8 Device Type 250 x 400

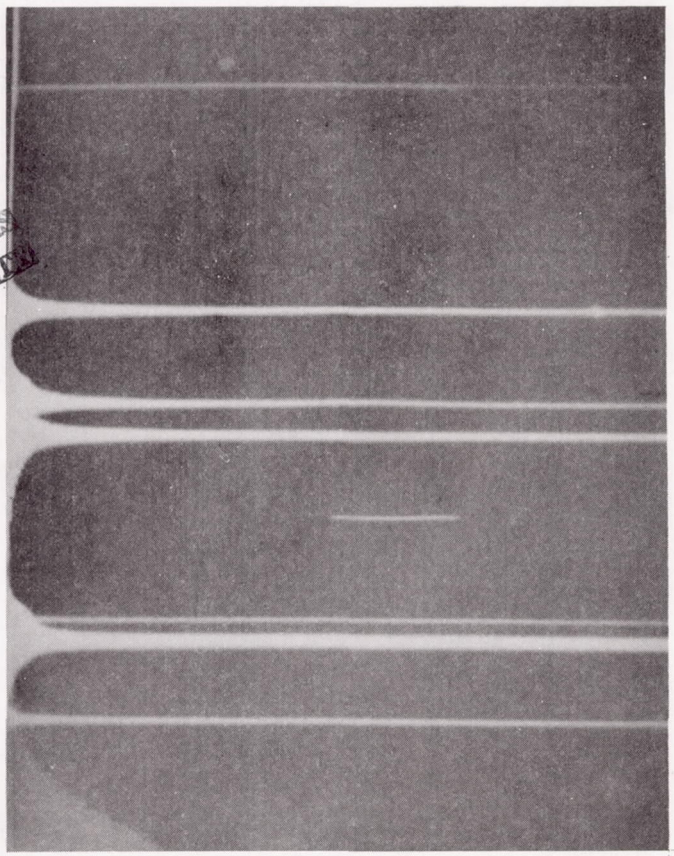

ORIGINAL PAGE IS
OF POOR QUALITY

VIDEO MONITOR DISPLAY

Light source	3400	°K
Spectral filter	0.4000	microns
Average well population	50	%
Temperature	25	°C
Data rate	4.0	MHz
Frame time	239	ms

CCD UNIFORMITY OF RESPONSE

Device Number 361-6-8 Device Type 250 x 400

Light source 3400 °K Spectral filter 0.4000 microns

Average well population 50 % Temperature 25 °C

Data rate 4.0 MHz Frame time 239 ms

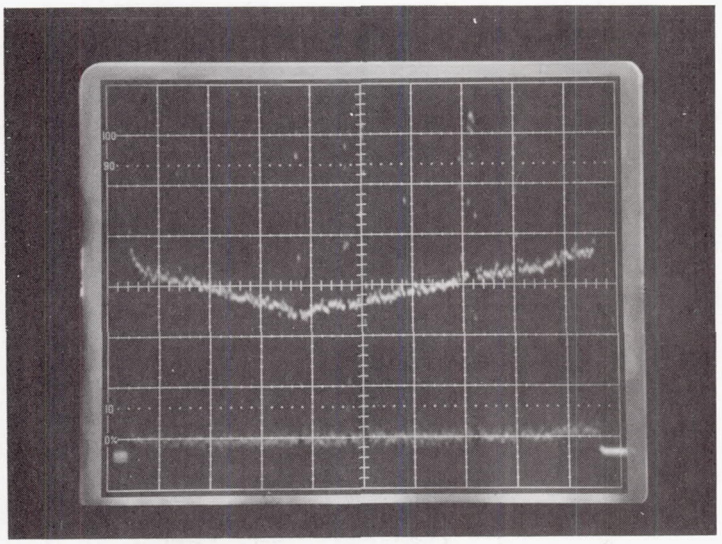

ORIGINAL PAGE IS OF POOR QUALITY

Oscilloscope presentation
Video line number 50

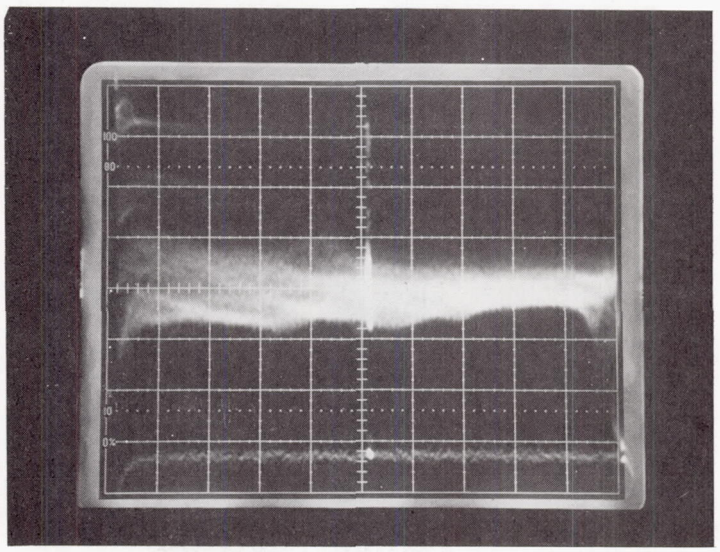

Oscilloscope presentation
Complete video frame

CCD SPECTRAL RESPONSIVITY

Device 361-6-8

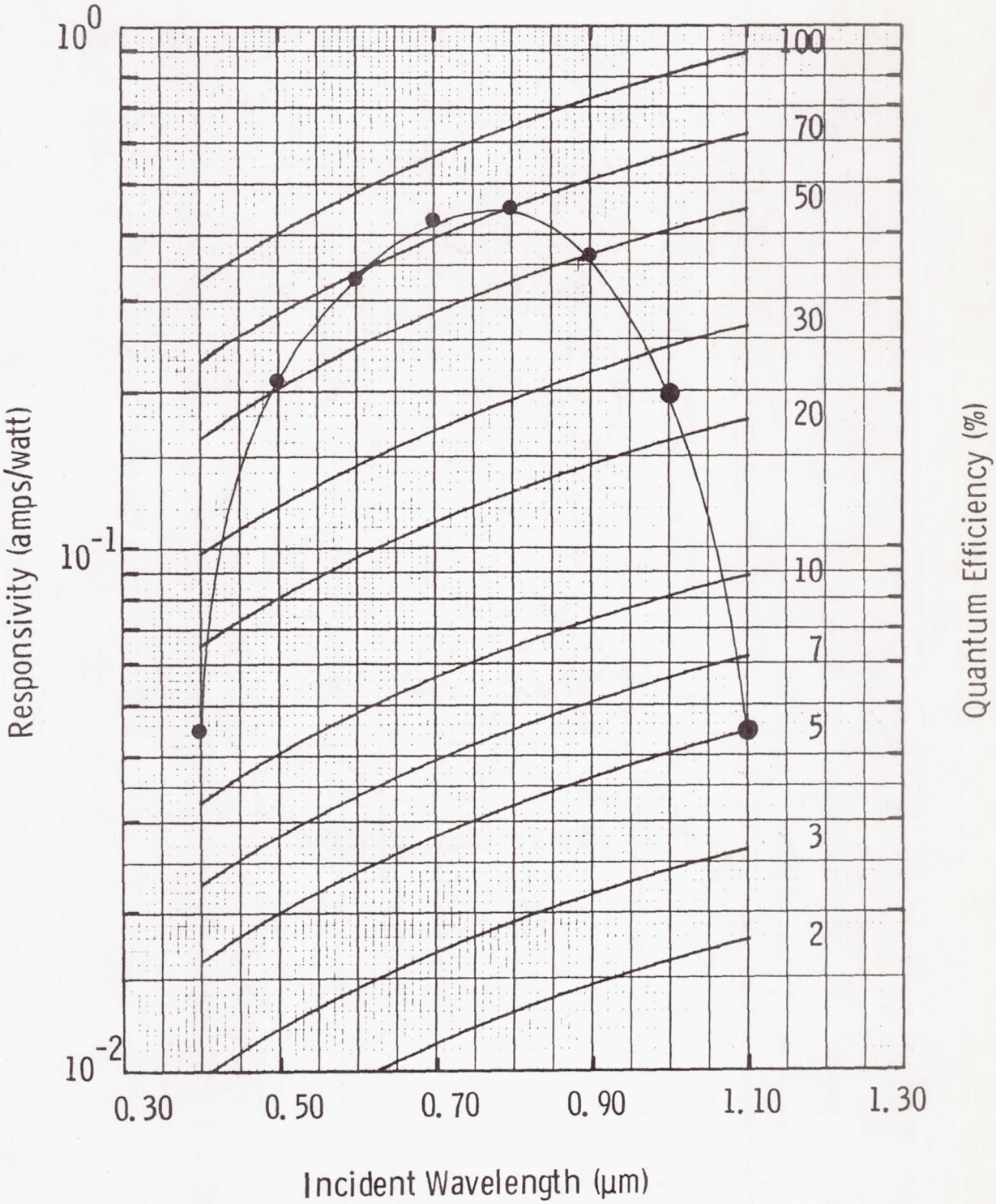

DATA RATE 3.0 MHz

FRAME TIME 50 MS

TEMPERATURE 25 °C

CENTRAL RESEARCH LABORATORIES
CCD Optical and Electrical
Characterization Test Report

for

Customer NASA/GODDARD SPACE FLIGHT CENTER

Contract No. NAS5-22924

Device No. 361-8-4

Device Type 250 x 400

CCD OPTICAL AND ELECTRICAL CHARACTERIZATION
TEST REPORT

1. CCD DEVICE NUMBER 361-8-4

2. DEVICE TYPE 250 x 400 HEADER TYPE Varo tube header

Active area 0.636 cm^2 , pixel dimensions 1.08 mils x 0.9 mils

3. OPERATING LEVELS in volts

Substrate	-.5	Lower reference	20
Parallel clocks	10	Upper reference	20
Serial clocks	10	Lower drain	28
Input diode	32	Upper drain	28
Output gate	2	Precharge pulse	9

4. AMPLIFIER CONFIGURATION used for the tests in this report:
precharge amplifier with off-chip load

5. SPECTRAL RESPONSE (see accompanying graph)

Quantum efficiency is 12.3 % at 0.4 microns

75.9 % at 0.7 microns

27.2 % at 1.0 microns

6. DARK CURRENT measured by the precharge method

26.4 nanoamps/cm^2 or 1.1×10^6 electrons/pixel/sec

T = 25 C, data rate 4.0 MHz, frame time 100 ms

7. R.M.S. NOISE ELECTRONS/PIXEL
Dark current shot noise 320 (100ms) electrons added in quadrature to a readout noise of 30 electrons gives a calculated R.M.S. noise of 320 electrons/pixel

8. FULL WELL CHARGE CAPABILITY, determined from the saturation exposure level, is 8.8×10^5 electrons.

9. DYNAMIC RANGE is computed to be 2740 :1.

10. CHARGE TRANSFER EFFICIENCY at 4.0 MHz is 0.99993.

11. COMMENTS open parallel electrode

CCD IMAGING PERFORMANCE

Device Number 361-8-4 Device Type 250 x 400

Light Source strobe °K Spectral filter none microns

Temperature 25 °C Data rate 4.0 MHz

Frame time 33 ms

ORIGINAL PAGE IS
OF POOR QUALITY

CCD DARK CURRENT UNIFORMITY

Device Number 361-8-4 Device Type 250 x 400

ORIGINAL PAGE IS
OF POOR QUALITY

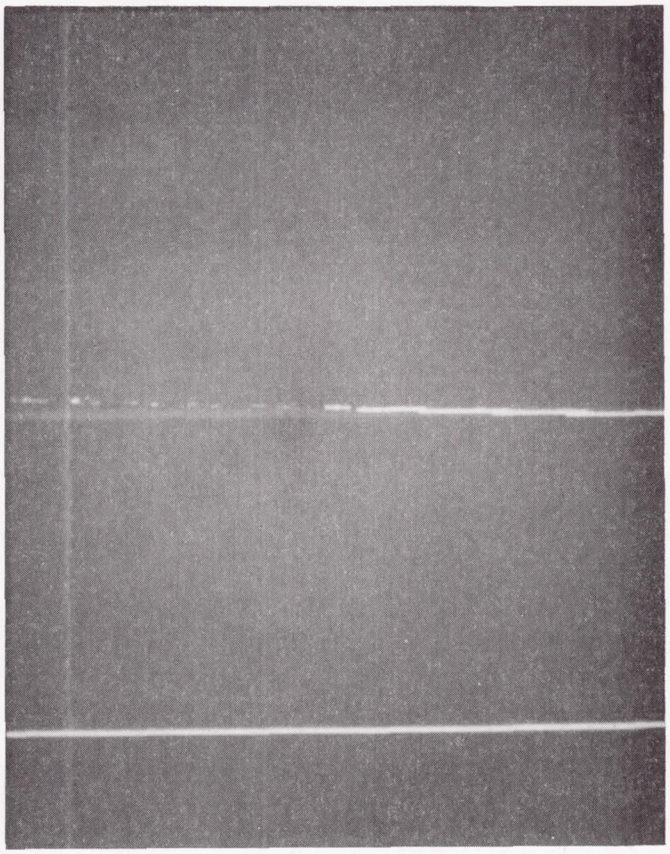

VIDEO MONITOR DISPLAY

Temperature 25 °C

Data rate 4.0 MHz

Frame time 100 ms

CCD DARK CURRENT UNIFORMITY

Device Number 361-8-4 Device Type 250 x 400

Temperature 25 °C Data rate 4.0 MHz

Frame time 100 ms

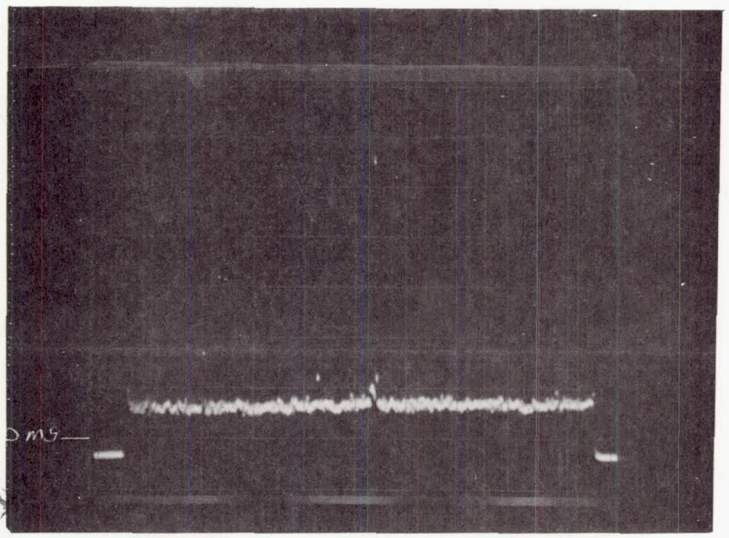

ORIGINAL PAGE IS
OF POOR QUALITY

Oscilloscope presentation

Video line number 50

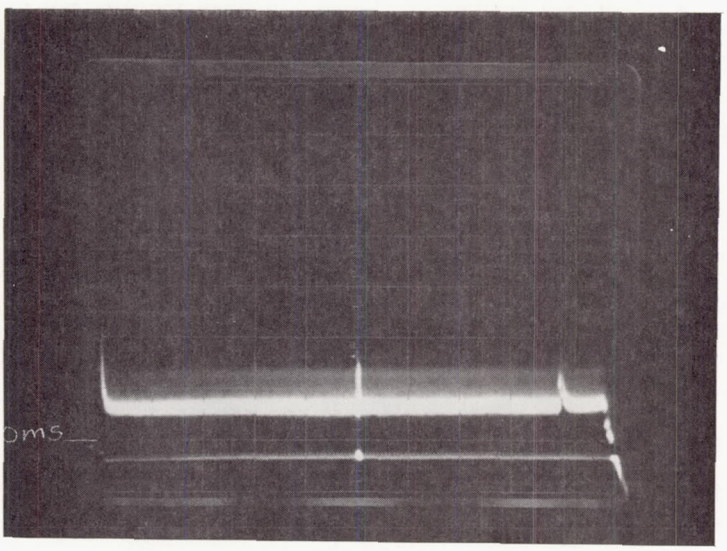

Oscilloscope presentation

Complete video frame

CCD UNIFORMITY OF RESPONSE

Device Number 361-8-4 Device Type 250 x 400

ORIGINAL PAGE IS
OF POOR QUALITY

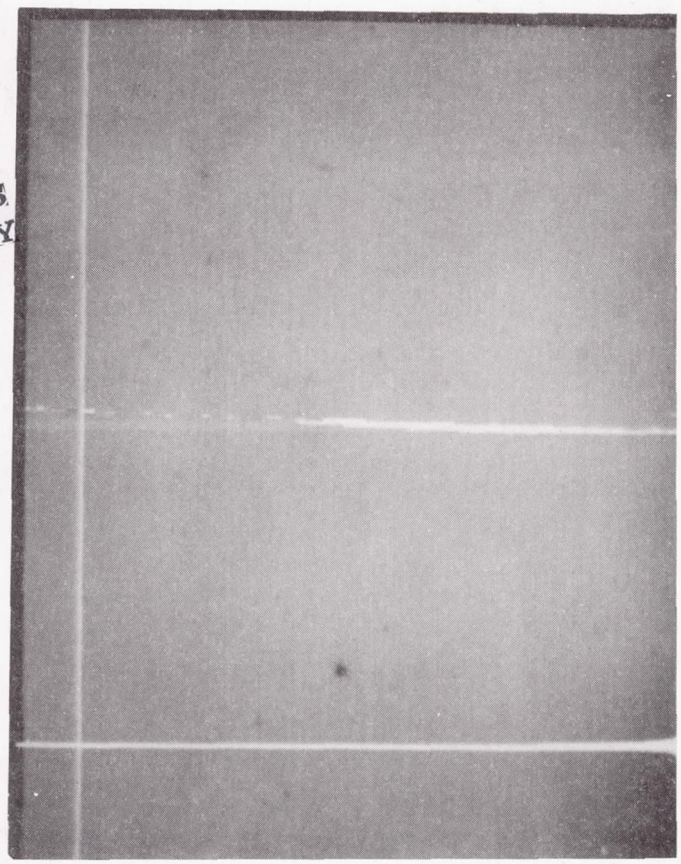

VIDEO MONITOR DISPLAY

Light source	3400	°K
Spectral filter	0.4000	microns
Average well population	50	%
Temperature	25	°C
Data rate	4.0	MHz
Frame time	135	ms

CCD UNIFORMITY OF RESPONSE

Device Number 361-8-4 Device Type 250 x 400

Light source 3400 °K Spectral filter 0.4000 microns

Average well population 50 % Temperature 25 °C

Data rate 4.0 MHz Frame time 135 ms

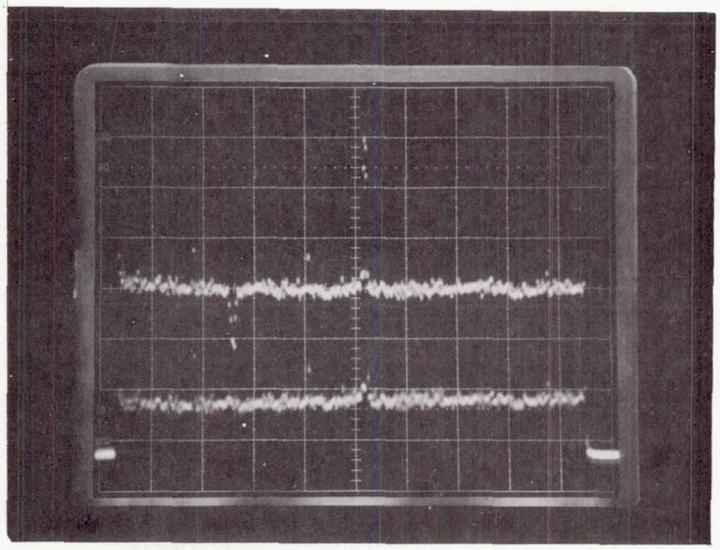

Oscilloscope presentation
Video line number 50

ORIGINAL PAGE IS
OF POOR QUALITY

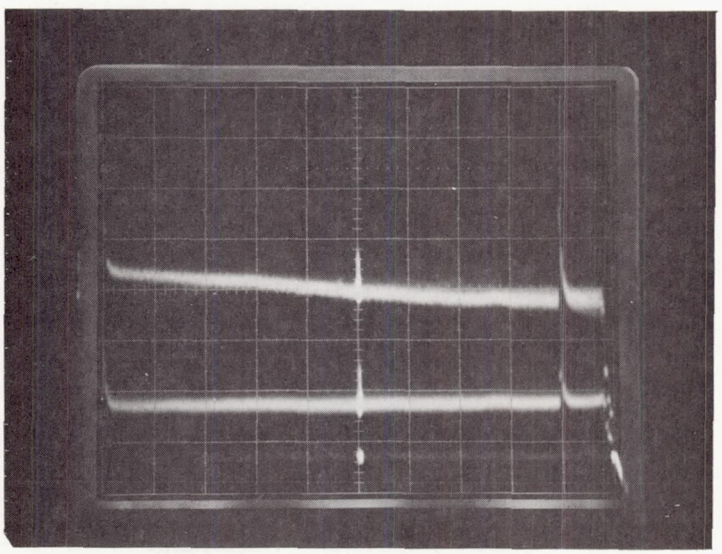

Oscilloscope presentation
Complete video frame

CCD SPECTRAL RESPONSIVITY

Device 361-8-4

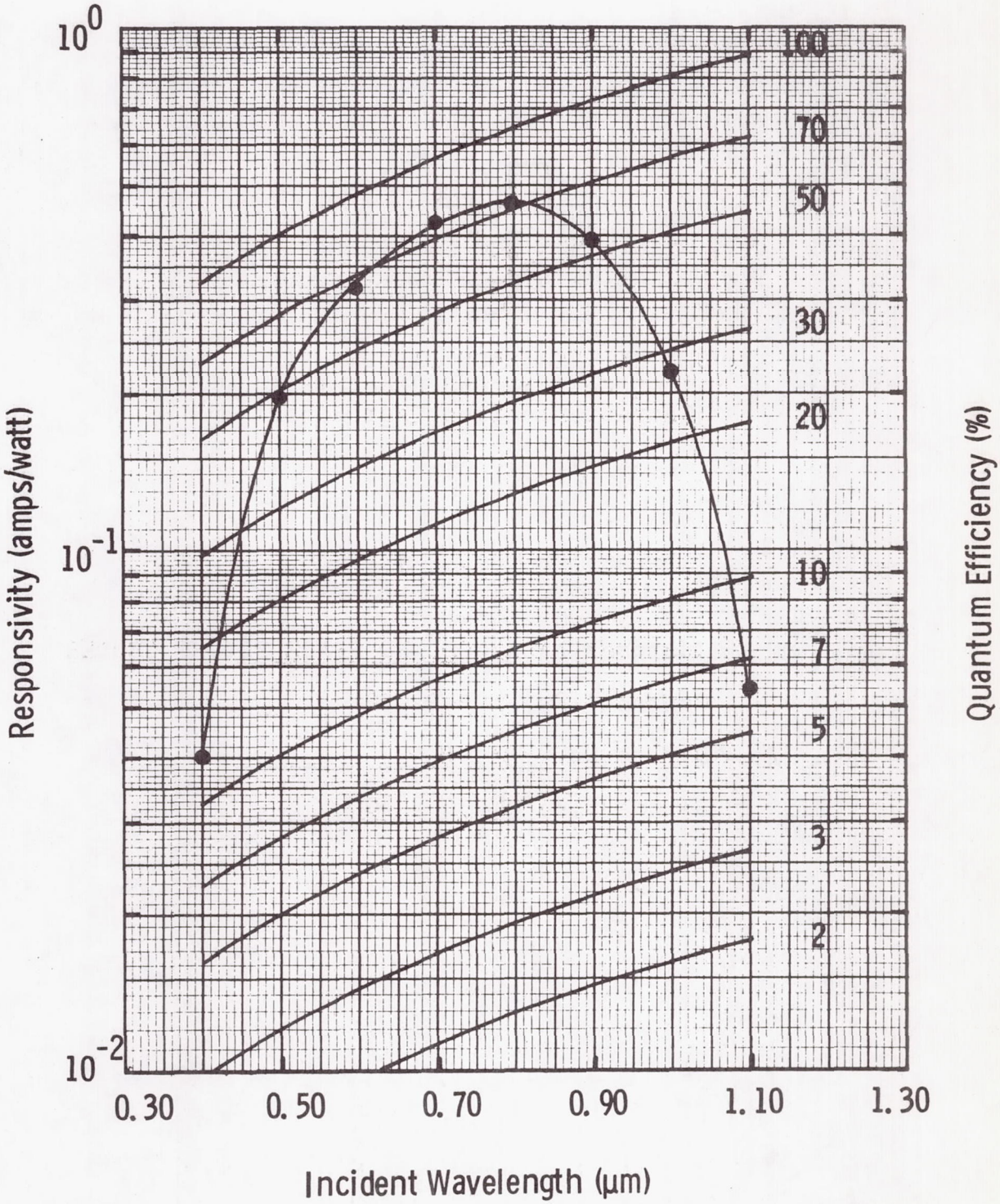

DATA RATE 3.0 MHz

FRAME TIME 50 MS

TEMPERATURE 25 °C

CENTRAL RESEARCH LABORATORIES
CCD Optical and Electrical
Characterization Test Report

for

Customer NASA/GODDARD SPACE FLIGHT CENTER

Contract No. NAS5-22924

Device No. 361-8-7

Device Type 250 x 400

CCD OPTICAL AND ELECTRICAL CHARACTERIZATION
TEST REPORT

1. CCD DEVICE NUMBER 361-8-7

2. DEVICE TYPE 250 x 400 HEADER TYPE ITT tube header

Active area 0.636 cm^2 , pixel dimensions 1.08 mils x 0.9 mils

3. OPERATING LEVELS in volts

Substrate	-.5	Lower reference	20
Parallel clocks	14	Upper reference	20
Serial clocks	15	Lower drain	28
Input diode	32	Upper drain	28
Output gate	2	Precharge pulse	9

4. AMPLIFIER CONFIGURATION used for the tests in this report:
precharge amplifier with off-chip load

5. SPECTRAL RESPONSE (see accompanying graph)

Quantum efficiency is 12.6 % at 0.4 microns

73.9 % at 0.7 microns

26.7 % at 1.0 microns

6. DARK CURRENT measured by the precharge method

36.0 nanoamps/cm^2 or 1.4×10^6 electrons/pixel/sec

T = 25 C, data rate 4.0 MHz, frame time 100 ms

7. R.M.S. NOISE ELECTRONS/PIXEL

Dark current shot noise 380 (100ms) electrons added in quadrature to a readout noise of 30 electrons gives a calculated R.M.S. noise of 380 electrons/pixel

8. FULL WELL CHARGE CAPABILITY, determined from the saturation exposure level, is 1.7×10^6 electrons.

9. DYNAMIC RANGE is computed to be 4500 :1.

10. CHARGE TRANSFER EFFICIENCY at 4.0 MHz is 0.99993.

11. COMMENTS open electrode in the lower serial register, reverse operation best

CCD IMAGING PERFORMANCE

Device Number 361-8-7 Device Type 250 x 400

Light Source strobe °K Spectral filter none microns

Temperature 25 °C Data rate 4.0 MHz

Frame time 33 ms

ORIGINAL PAGE IS OF POOR QUALITY

CCD DARK CURRENT UNIFORMITY

Device Number 361-8-7 Device Type 250 x 400

ORIGINAL PAGE IS
OF POOR QUALITY

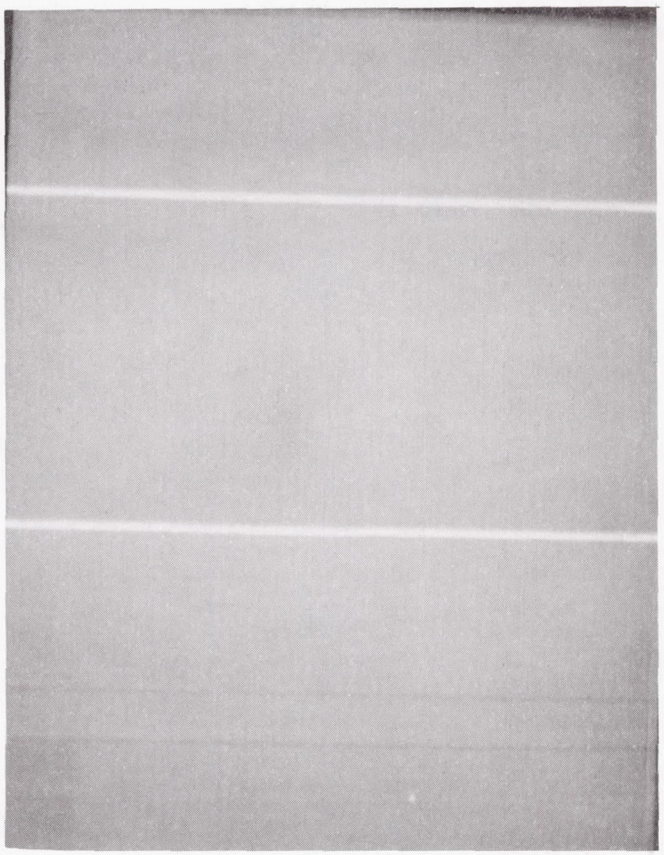

VIDEO MONITOR DISPLAY

Temperature 25 °C

Data rate 4.0 MHz

Frame time 100 ms

CCD DARK CURRENT UNIFORMITY

Device Number 361-8-7 Device Type 250 x 400

Temperature 25 °C Data rate 4.0 MHz

Frame time 100 ms

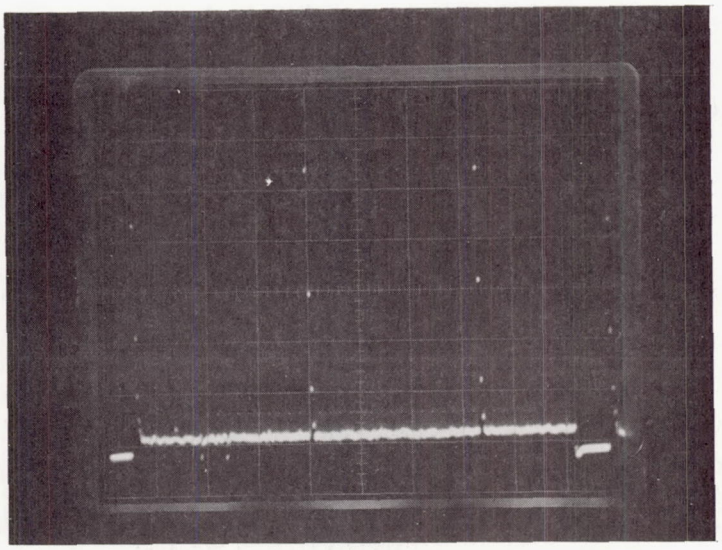

ORIGINAL PAGE IS
OF POOR QUALITY

Oscilloscope presentation

Video line number 50

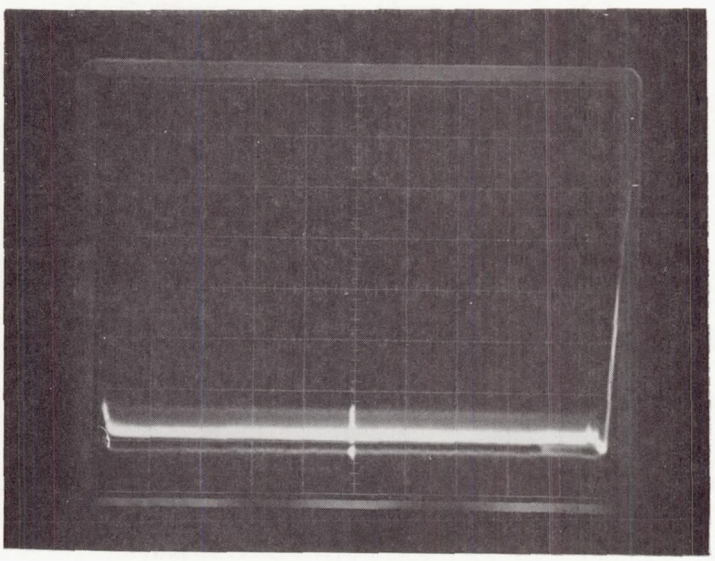

Oscilloscope presentation

Complete video frame

CCD UNIFORMITY OF RESPONSE

Device Number 361-8-7 Device Type 250 x 400

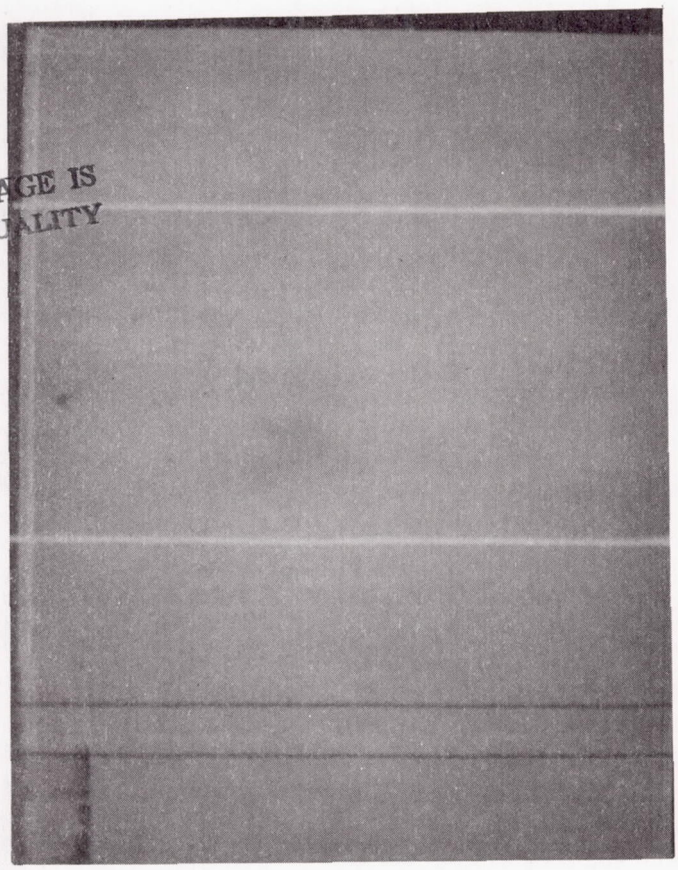

ORIGINAL PAGE IS
OF POOR QUALITY

VIDEO MONITOR DISPLAY

Light source	3400	°K
Spectral filter	0.4000	microns
Average well population	50	%
Temperature	25	°C
Data rate	4.0	MHz
Frame time	250	ms

CCD UNIFORMITY OF RESPONSE

Device Number 361-8-7 Device Type 250 x 400

Light source 3400 °K Spectral filter 0.4000 microns

Average well population 50 % Temperature 25 °C

Data rate 4.0 MHz Frame time 250 ms

ORIGINAL PAGE IS
OF POOR QUALITY

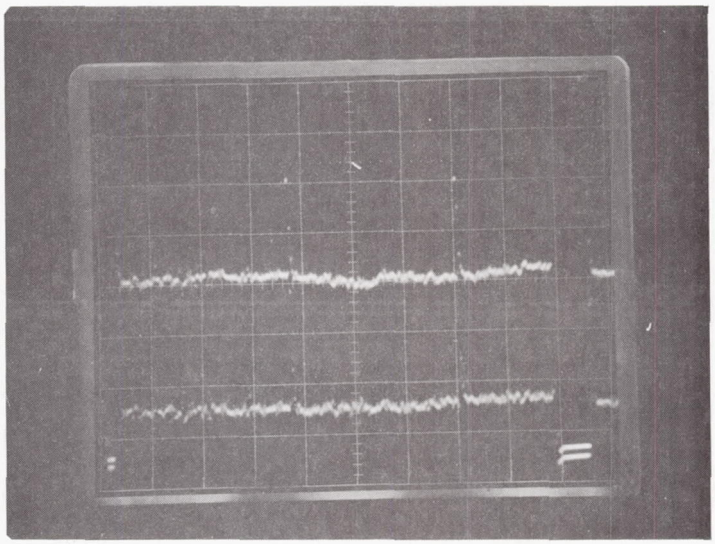

Oscilloscope presentation
Video line number 50

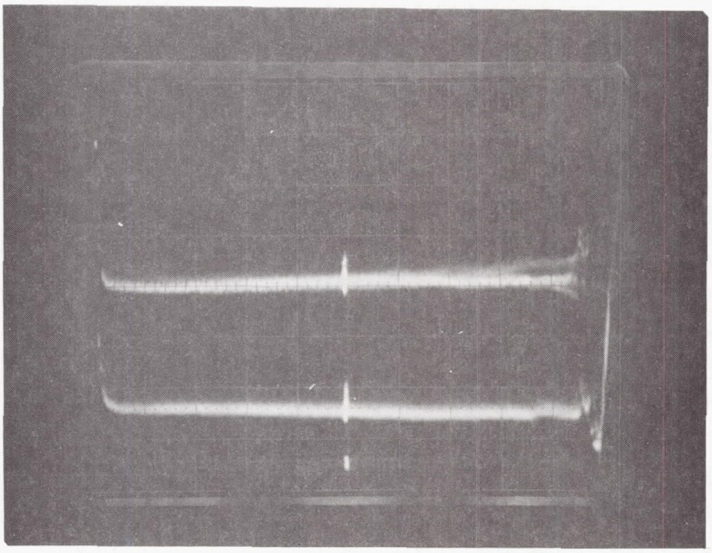

Oscilloscope presentation
Complete video frame

CCD SPECTRAL RESPONSIVITY

Device 361-8-7

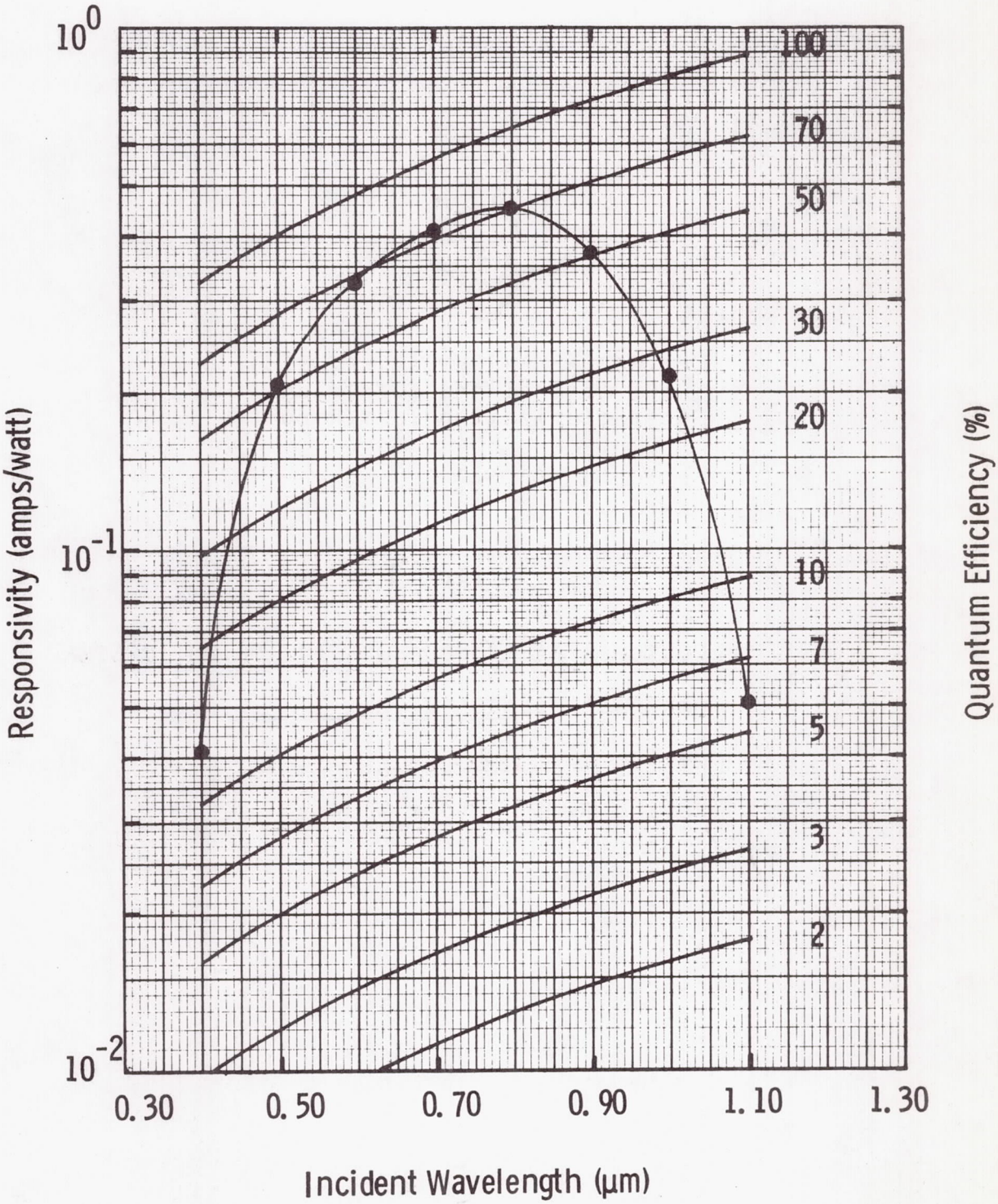

DATA RATE 3.0 MHz

FRAME TIME 50 MS

TEMPERATURE 25 °C

CENTRAL RESEARCH LABORATORIES
CCD Optical and Electrical
Characterization Test Report

for

Customer NASA/GODDARD SPACE FLIGHT CENTER

Contract No. NAS5-22924

Device No. 367-1-5

Device Type 250 x 400

CCD OPTICAL AND ELECTRICAL CHARACTERIZATION
TEST REPORT

1. CCD DEVICE NUMBER 367-1-5

2. DEVICE TYPE 250 x 400 HEADER TYPE ITT tube header

Active area 0.636 cm^2 , pixel dimensions 1.08 mils x 0.9 mils

3. OPERATING LEVELS in volts

Substrate	-.5	Lower reference	20
Parallel clocks	10	Upper reference	20
Serial clocks	10	Lower drain	28
Input diode	32	Upper drain	28
Output gate	2	Precharge pulse	9

4. AMPLIFIER CONFIGURATION used for the tests in this report:
precharge amplifier with off-chip load

5. SPECTRAL RESPONSE (see accompanying graph)

Quantum efficiency is 11.4 % at 0.4 microns

77.7 % at 0.7 microns

31.5 % at 1.0 microns

6. DARK CURRENT measured by the precharge method

50 nanoamps/cm^2 or 2.0×10^6 electrons/pixel/sec

T = 25 C, data rate 4.0 MHz, frame time 100 ms

7. R.M.S. NOISE ELECTRONS/PIXEL
Dark current shot noise 450 (100ms) electrons added in quadrature to a readout noise of 30 electrons gives a calculated R.M.S. noise of 450 electrons/pixel

8. FULL WELL CHARGE CAPABILITY, determined from the saturation exposure level, is 1.0×10^6 electrons.

9. DYNAMIC RANGE is computed to be 2200 :1.

10. CHARGE TRANSFER EFFICIENCY at 4.0 MHz is >0.99996.

11. COMMENTS

CCD IMAGING PERFORMANCE

Device Number 367-1-5 Device Type 250 x 400

Light Source strobe °K Spectral filter none microns

Temperature 25 °C Data rate 4.0 MHz

Frame time 54 ms

ORIGINAL PAGE IS OF POOR QUALITY

CCD DARK CURRENT UNIFORMITY

Device Number 367-1-5 Device Type 250 x 400

ORIGINAL PAGE IS
OF POOR QUALITY

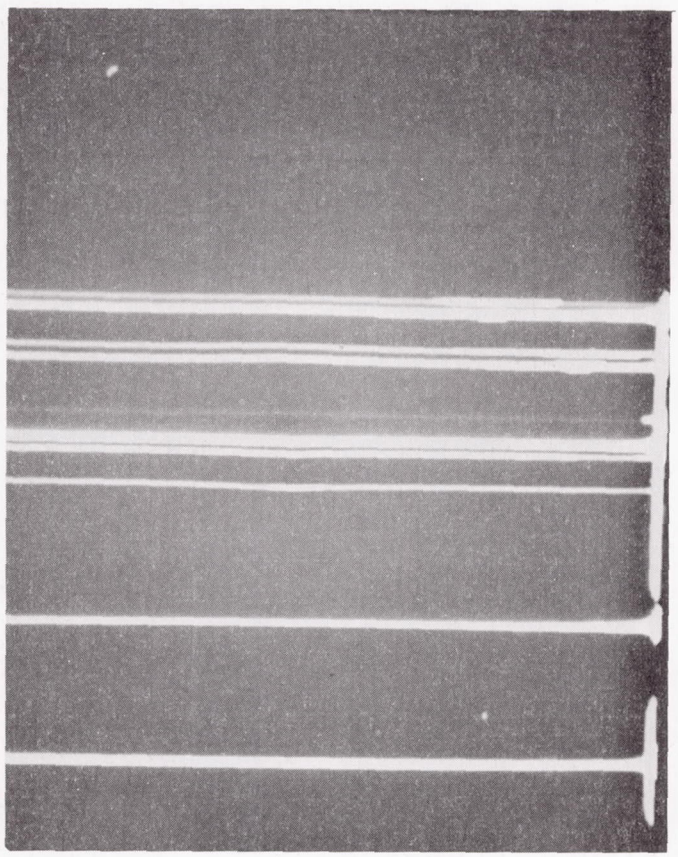

VIDEO MONITOR DISPLAY

Temperature 25 °C

Data rate 4.0 MHz

Frame time 87 ms

CCD DARK CURRENT UNIFORMITY

Device Number 367-1-5 Device Type 250 x 400

Temperature 25 °C Data rate 4.0 MHz

Frame time 87 ms

ORIGINAL PAGE IS
OF POOR QUALITY

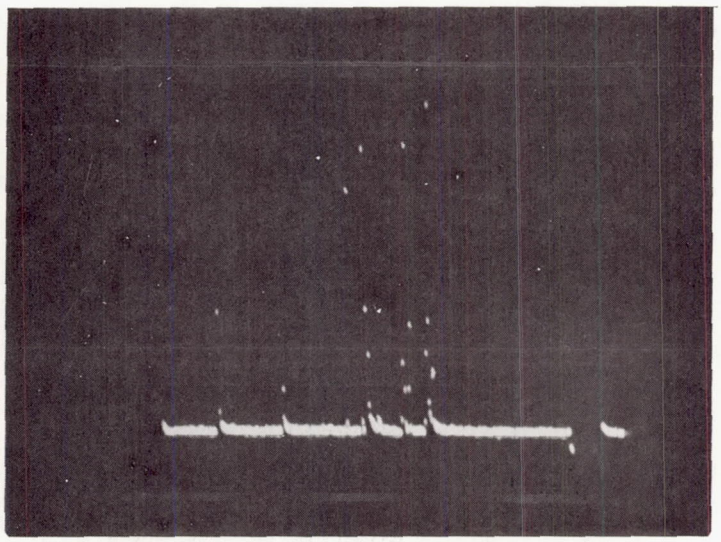

Oscilloscope presentation

Video line number 50

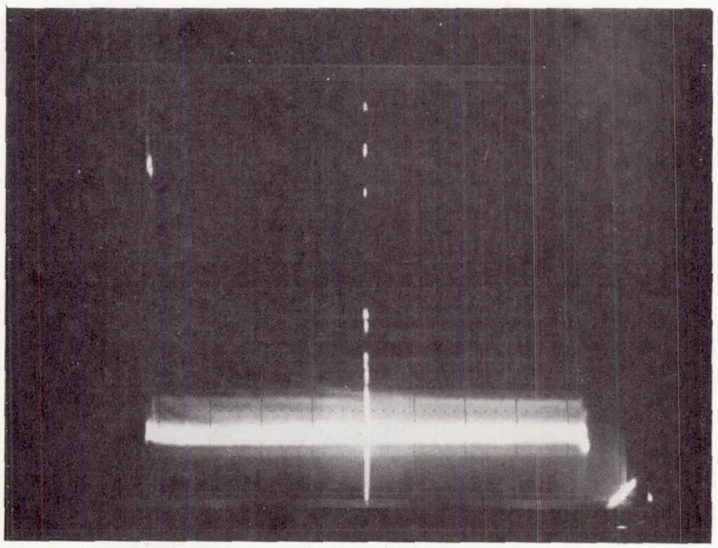

Oscilloscope presentation

Complete video frame

CCD UNIFORMITY OF RESPONSE

Device Number 367-1-5 Device Type 250 x 400

ORIGINAL PAGE IS
OF POOR QUALITY

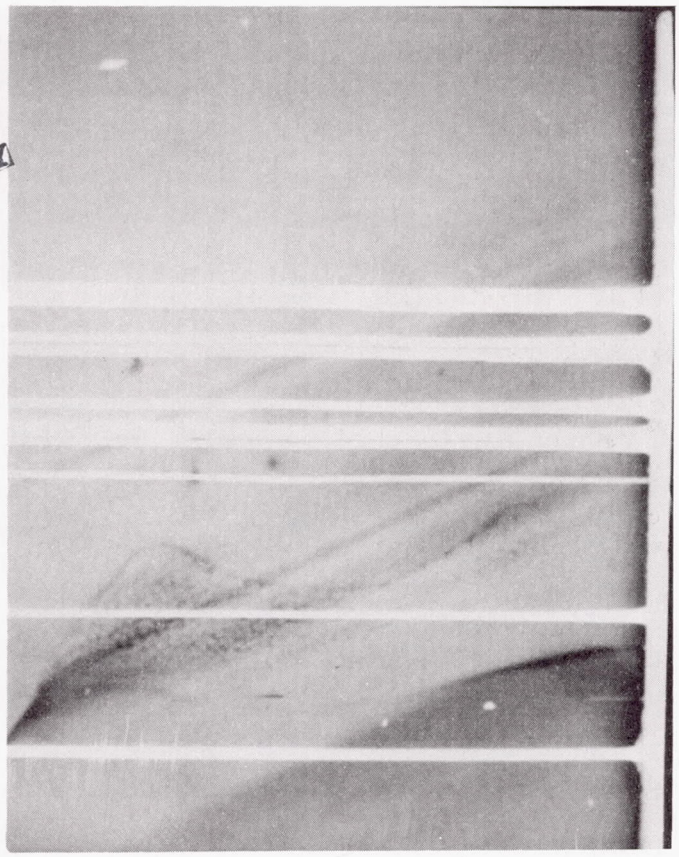

VIDEO MONITOR DISPLAY

Light source	3400	°K
Spectral filter	0.4000	microns
Average well population	50	%
Temperature	25	°C
Data rate	4.0	MHz
Frame time	223	ms

CCD UNIFORMITY OF RESPONSE

Device Number 367-1-5 Device Type 250 x 400

Light source 3400 °K Spectral filter 0.4000 microns

Average well population 50 % Temperature 25 °C

Data rate 4.0 MHz Frame time 223 ms

ORIGINAL PAGE IS
OF POOR QUALITY

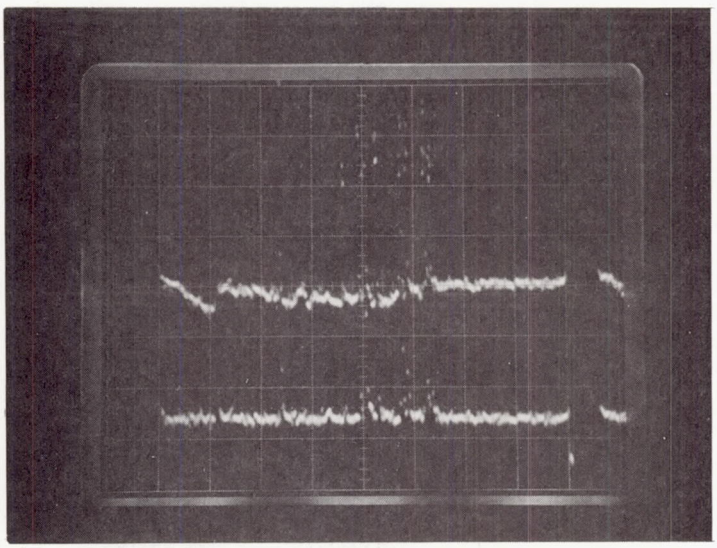

Oscilloscope presentation
Video line number 50

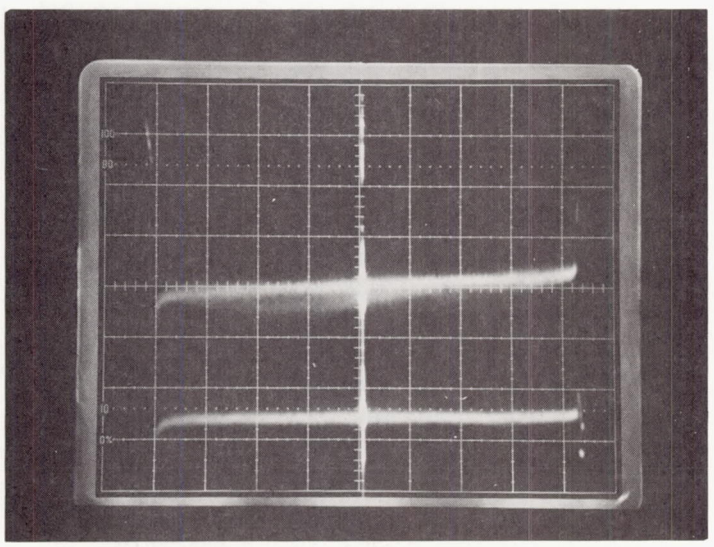

Oscilloscope presentation
Complete video frame

CCD SPECTRAL RESPONSIVITY

Device 367-1-5

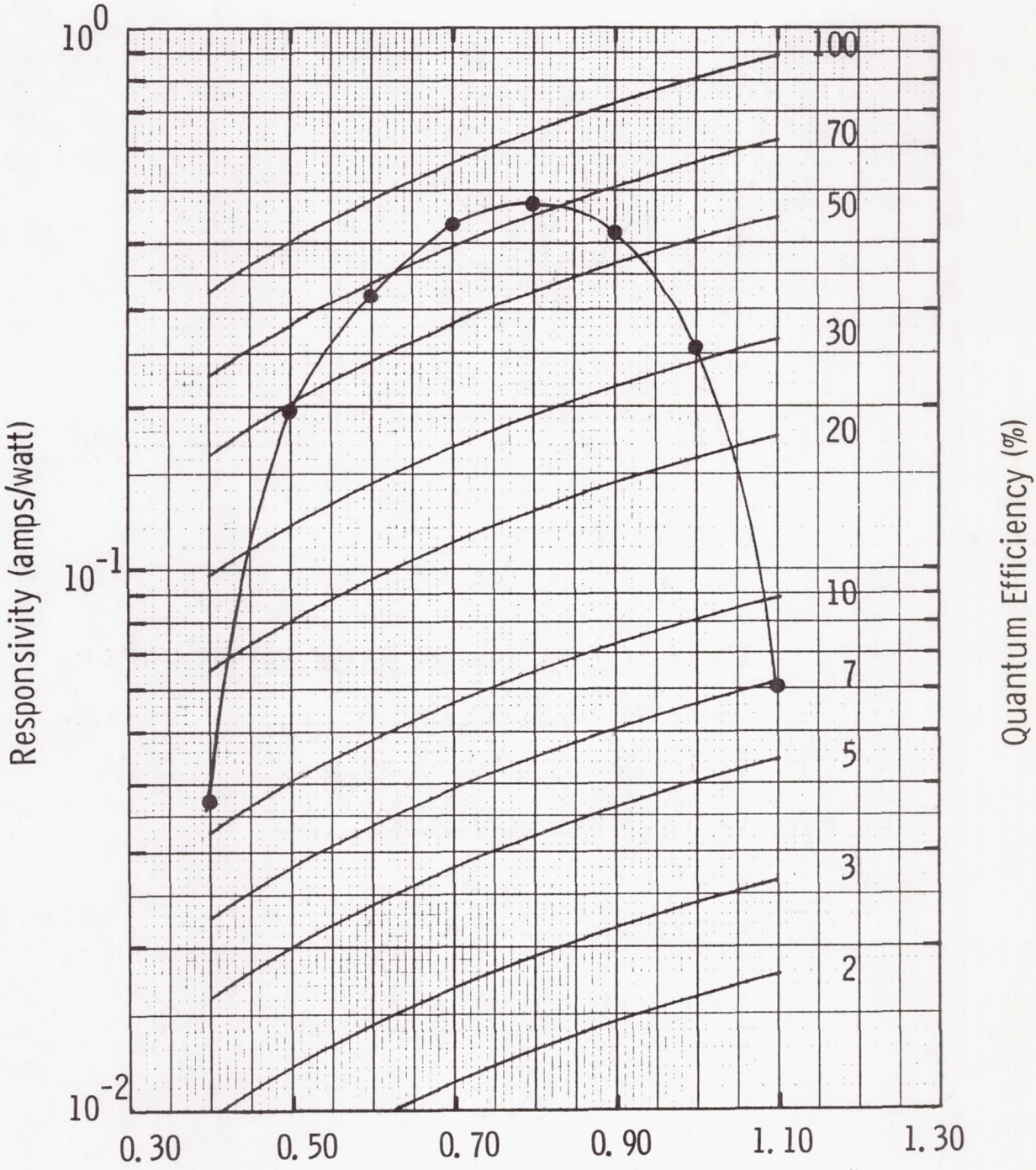

DATA RATE 3.0 MHz

FRAME TIME 50 MS

TEMPERATURE 25 °C

CENTRAL RESEARCH LABORATORIES
CCD Optical and Electrical
Characterization Test Report

for

Customer NASA/GODDARD SPACE FLIGHT CENTER

Contract No. NAS5-22924

Device No. 367-2-6 Tube # 287

Device Type 250 x 400

CCD OPTICAL AND ELECTRICAL CHARACTERIZATION
TEST REPORT

1. CCD DEVICE NUMBER 367-2-6

2. DEVICE TYPE 250 x 400 HEADER TYPE Varo tube header

Active area 0.636 cm^2 , pixel dimensions 1.08 mils x 0.9 mils

3. OPERATING LEVELS in volts

Substrate	-.5	Lower reference	20
Parallel clocks	10	Upper reference	20
Serial clocks	10	Lower drain	28
Input diode	32	Upper drain	28
Output gate	2	Precharge pulse	9

4. AMPLIFIER CONFIGURATION used for the tests in this report:
precharge amplifier with off-chip load

5. SPECTRAL RESPONSE (see accompanying graph)

Quantum efficiency is 9.4 % at 0.4 microns

73.6 % at 0.7 microns

25.9 % at 1.0 microns

6. DARK CURRENT measured by the precharge method

35 nanoamps/cm^2 or 1.4×10^6 electrons/pixel/sec

T = 25 C, data rate 4.0 MHz, frame time 100 ms

7. R.M.S. NOISE ELECTRONS/PIXEL
Dark current shot noise 380 (100ms) electrons added in quadrature to a readout noise of 30 electrons gives a calculated R.M.S. noise of 380 electrons/pixel

8. FULL WELL CHARGE CAPABILITY, determined from the saturation exposure level, is 9.5×10^5 electrons.

9. DYNAMIC RANGE is computed to be 2500 :1.

10. CHARGE TRANSFER EFFICIENCY at 4.0 MHz is 0.99995.

11. COMMENTS

CCD IMAGING PERFORMANCE

Device Number 367-2-6 Device Type 250 x 400

Light Source strobe °K Spectral filter none microns

Temperature 25 °C Data rate 4.0 MHz

Frame time 33 ms

ORIGINAL PAGE IS
OF POOR QUALITY

CCD DARK CURRENT UNIFORMITY

Device Number 367-2-6 Device Type 250 x 400

ORIGINAL PAGE IS
OF POOR QUALITY

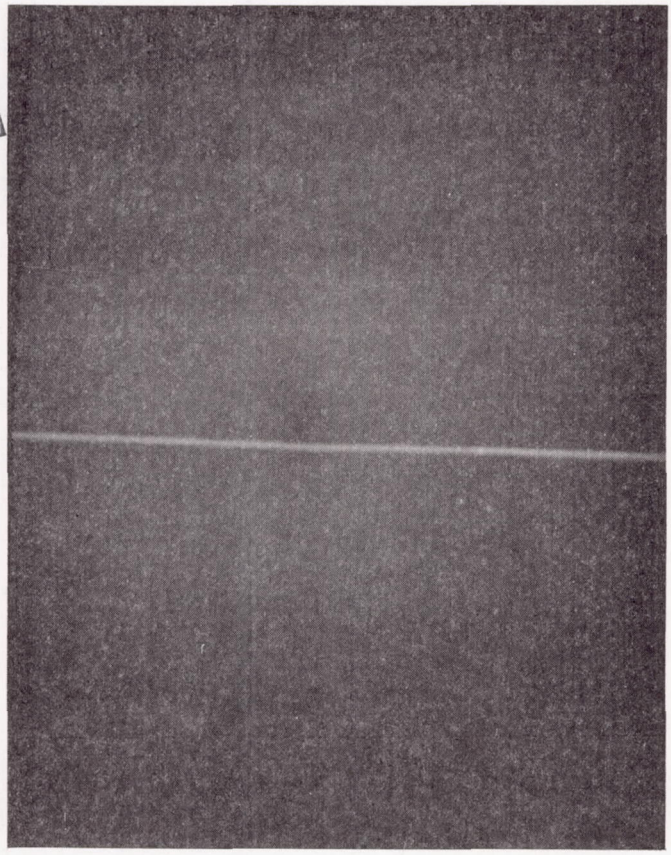

VIDEO MONITOR DISPLAY

Temperature 25 °C

Data rate 4.0 MHz

Frame time 100 ms

CCD DARK CURRENT UNIFORMITY

Device Number 367-2-6 Device Type 250 x 400

Temperature 25 °C Data rate 4.0 MHz

Frame time 100 ms

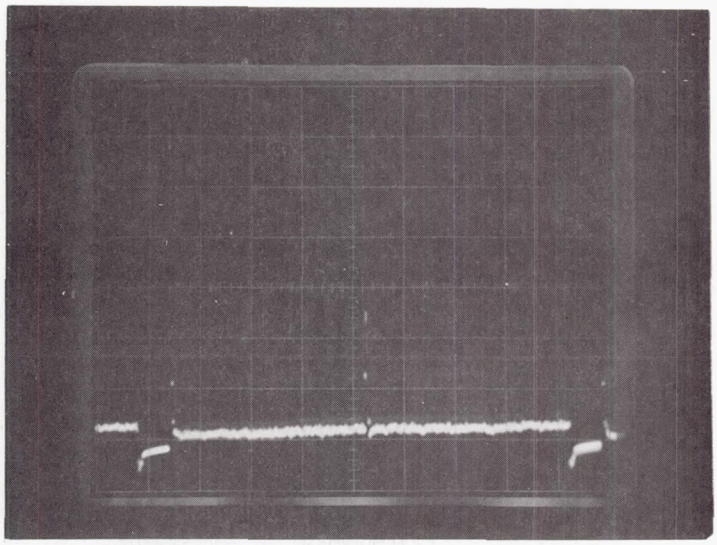

ORIGINAL PAGE IS
OF POOR QUALITY

Oscilloscope presentation

Video line number 50

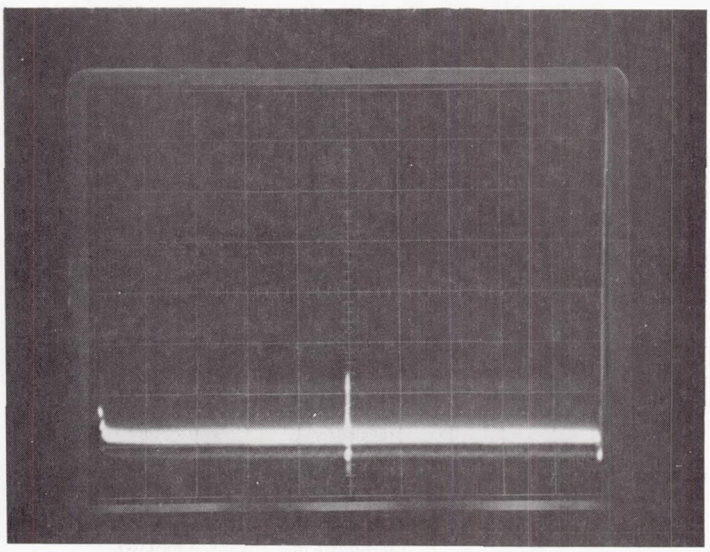

Oscilloscope presentation

Complete video frame

CCD UNIFORMITY OF RESPONSE

Device Number 367-2-6 Device Type 250 x 400

ORIGINAL PAGE IS
OF POOR QUALITY

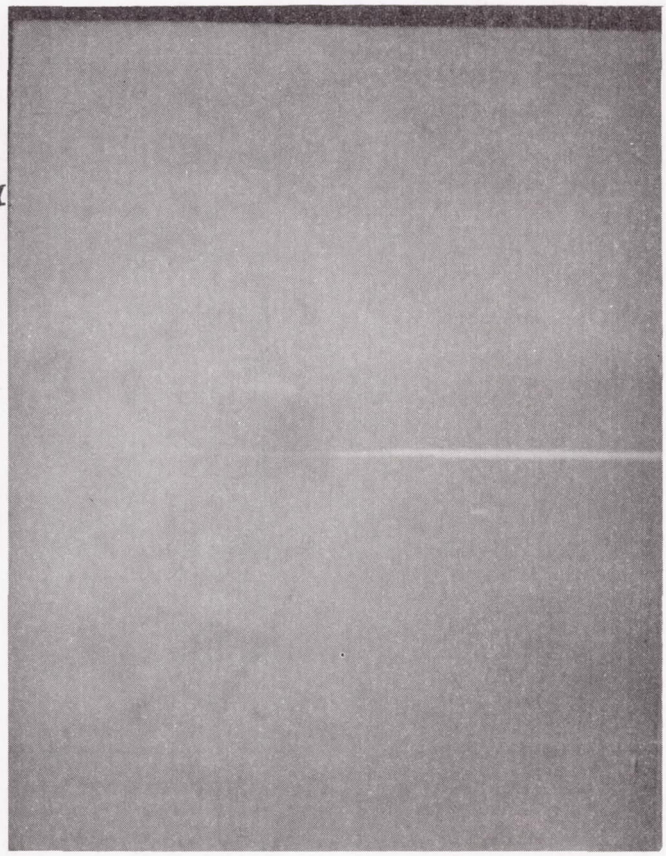

VIDEO MONITOR DISPLAY

Light source	3400	°K
Spectral filter	0.4000	microns
Average well population	50	%
Temperature	25	°C
Data rate	4.0	MHz
Frame time	224	ms

CCD UNIFORMITY OF RESPONSE

Device Number 367-2-6 Device Type 250 x 400

Light source 3400 °K Spectral filter 0,4000 microns

Average well population 50 % Temperature 25 °C

Data rate 4.0 MHz Frame time 224 ms

ORIGINAL PAGE IS
OF POOR QUALITY

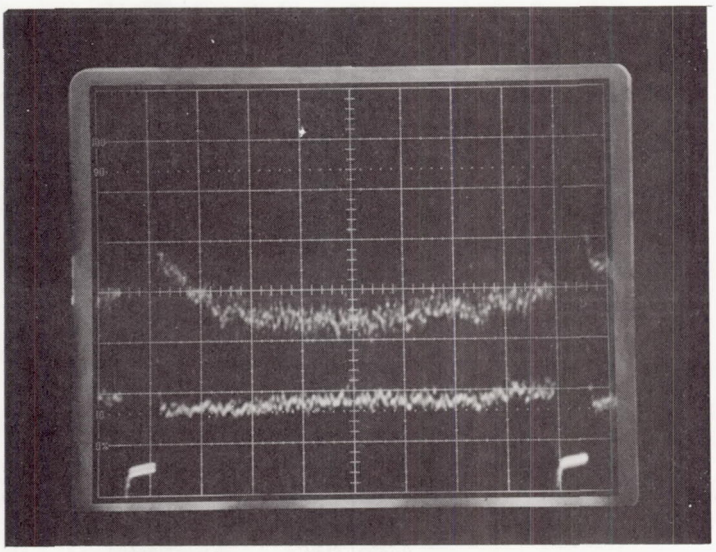

Oscilloscope presentation
Video line number 50

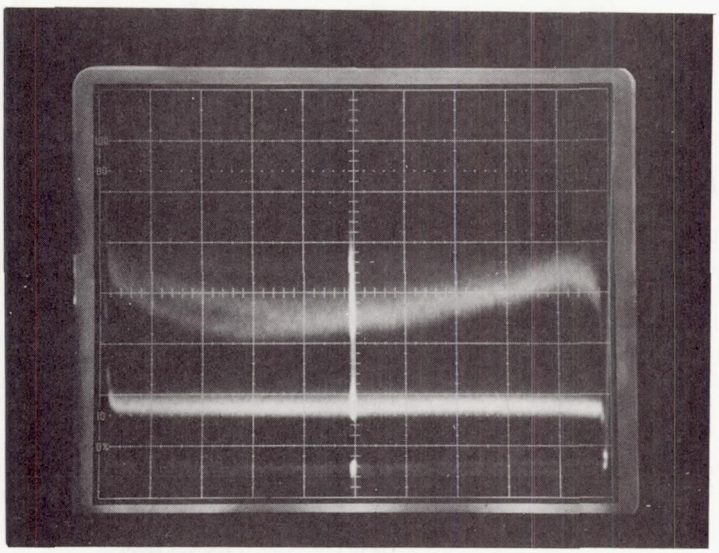

Oscilloscope presentation
Complete video frame

CCD SPECTRAL RESPONSIVITY

Device 367-2-6

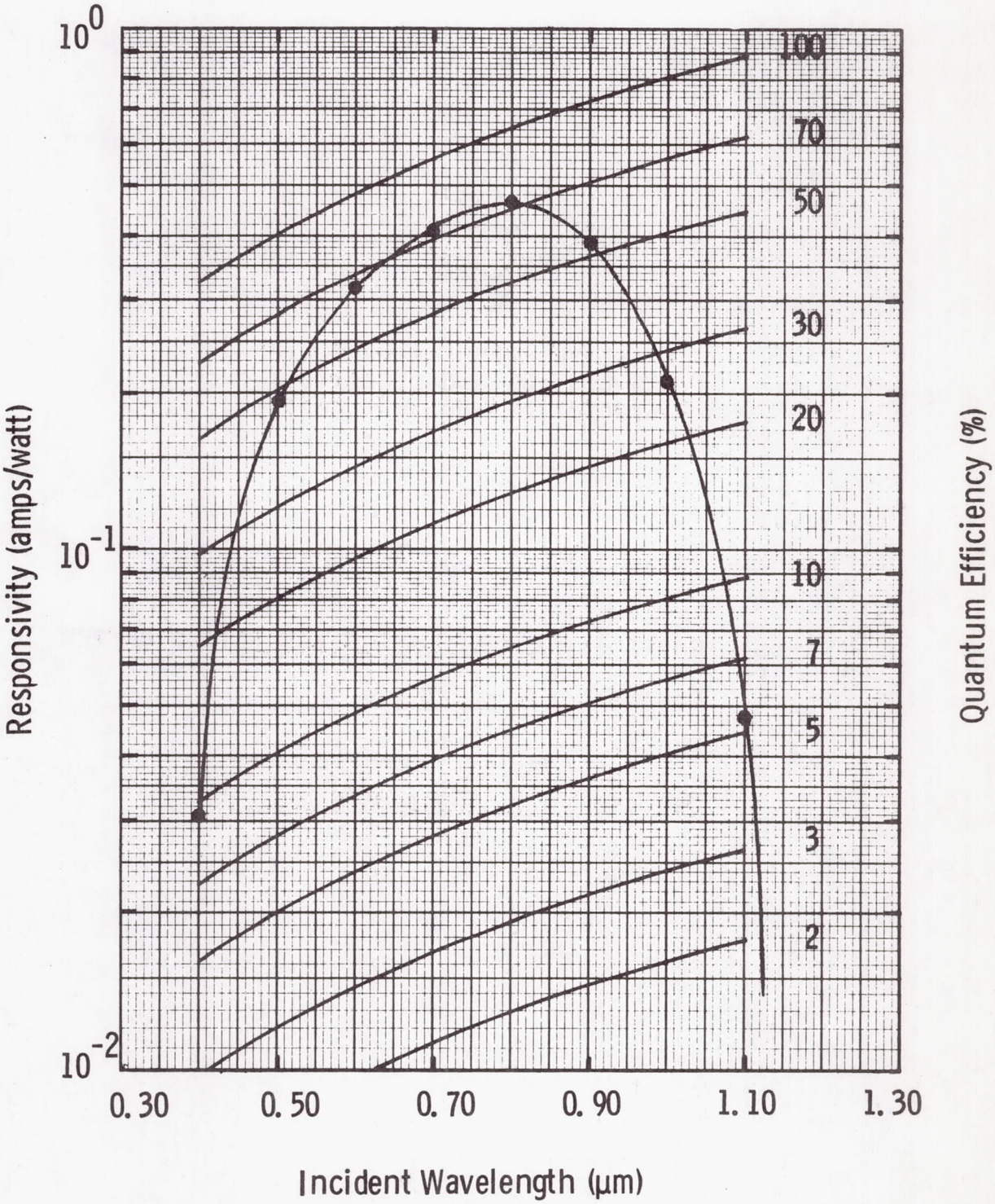

DATA RATE 3.0 MHz

FRAME TIME 50 MS

TEMPERATURE 25 °C

CENTRAL RESEARCH LABORATORIES
CCD Optical and Electrical
Characterization Test Report

for

Customer NASA/GODDARD SPACE FLIGHT CENTER

Contract No. NAS5-22924

Device No. 367-4-4

Device Type 250 x 400

CCD OPTICAL AND ELECTRICAL CHARACTERIZATION
TEST REPORT

1. CCD DEVICE NUMBER 367-4-4

2. DEVICE TYPE 250 x 400 HEADER TYPE Varo tube header

Active area 0.636 cm^2 , pixel dimensions 1.08 mils x 0.9 mils

3. OPERATING LEVELS in volts

Substrate	-.5	Lower reference	20
Parallel clocks	14	Upper reference	20
Serial clocks	15	Lower drain	28
Input diode	32	Upper drain	28
Output gate	2	Precharge pulse	9

4. AMPLIFIER CONFIGURATION used for the tests in this report:
precharge amplifier with off-chip load

5. SPECTRAL RESPONSE (see accompanying graph)

Quantum efficiency is 13.2 % at 0.4 microns

74.6 % at 0.7 microns

27.2 % at 1.0 microns

6. DARK CURRENT measured by the precharge method

5.5 nanoamps/cm^2 or 2.2×10^5 electrons/pixel/sec

T = 25 C, data rate 4.0 MHz, frame time 100 ms

7. R.M.S. NOISE ELECTRONS/PIXEL
Dark current shot noise 148 (100ms) electrons added in quadrature to a readout noise of 30 electrons gives a calculated R.M.S. noise of 150 electrons/pixel

8. FULL WELL CHARGE CAPABILITY, determined from the saturation exposure level, is 1.8×10^6 electrons.

9. DYNAMIC RANGE is computed to be 11900 :1.

10. CHARGE TRANSFER EFFICIENCY at 4.0 MHz is 0.99995.

11. COMMENTS open parallel electrode, reverse operation best

CCD IMAGING PERFORMANCE

Device Number 367-4-4 Device Type 250 x 400

Light Source strobe °K Spectral filter none microns

Temperature 25 °C Data rate 4.0 MHz

Frame time 33 ms

ORIGINAL PAGE IS OF POOR QUALITY

CCD DARK CURRENT UNIFORMITY

Device Number 367-4-4 Device Type 250 x 400

ORIGINAL PAGE IS
OF POOR QUALITY

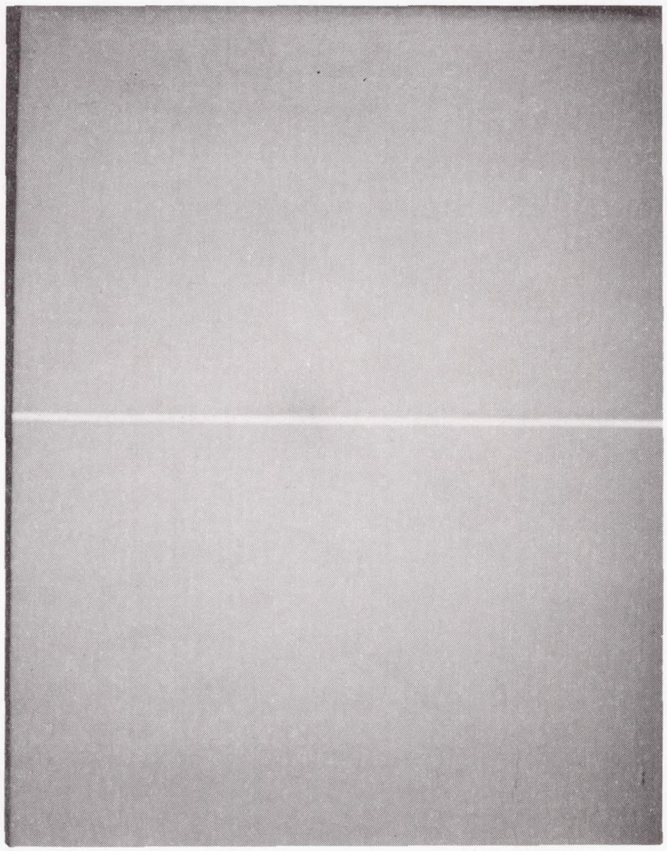

VIDEO MONITOR DISPLAY

Temperature 25 °C

Data rate 4.0 MHz

Frame time 100 ms

CCD DARK CURRENT UNIFORMITY

Device Number 367-4-4 Device Type 250 x 400

Temperature 25 °C Data rate 4.0 MHz

Frame time 100 ms

ORIGINAL PAGE IS
OF POOR QUALITY

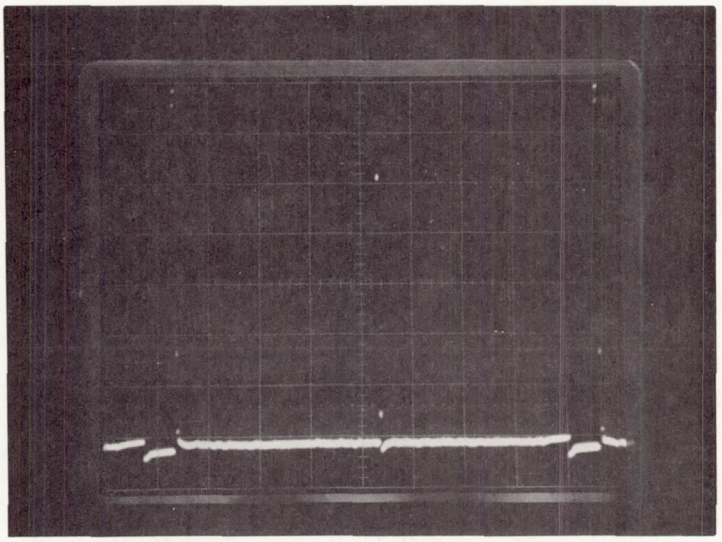

Oscilloscope presentation

Video line number 50

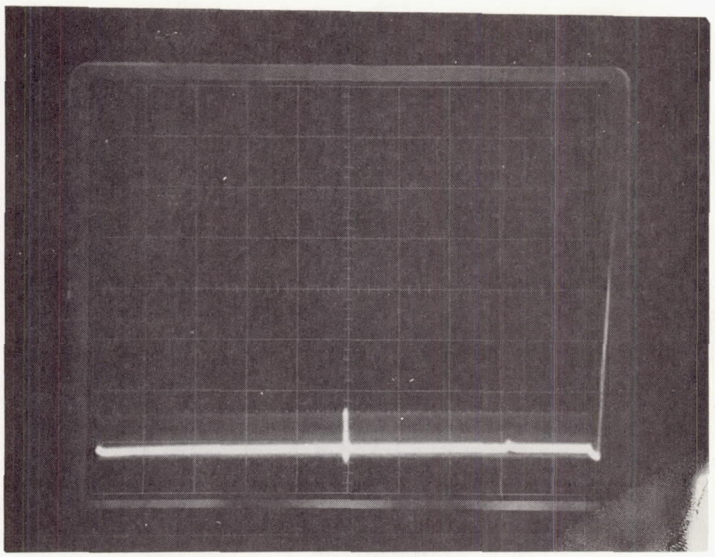

Oscilloscope presentation

Complete video frame

CCD UNIFORMITY OF RESPONSE

Device Number 367-4-4 Device Type 250 x 400

ORIGINAL PAGE IS
OF POOR QUALITY

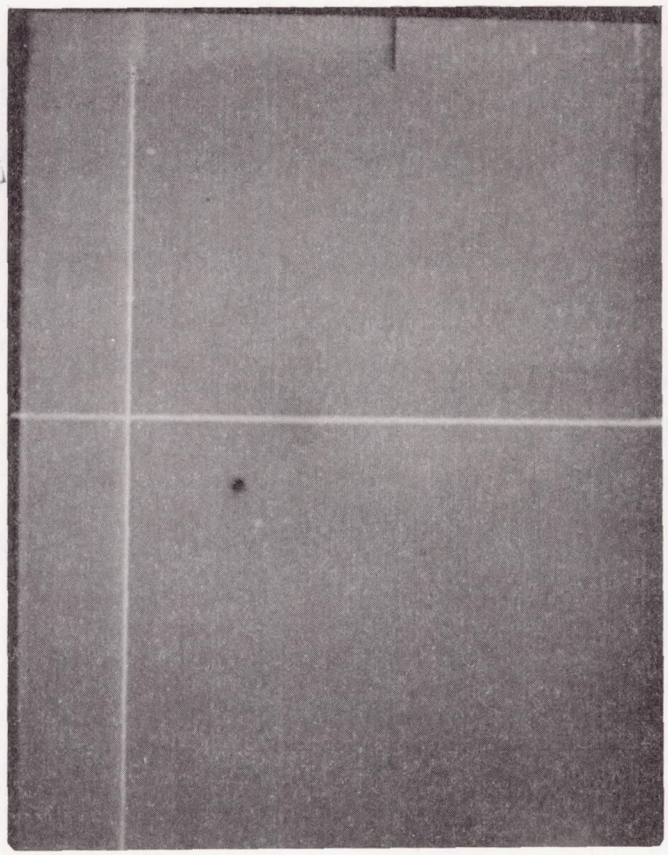

VIDEO MONITOR DISPLAY

Light source	3400	°K
Spectral filter	0.4000	microns
Average well population	50	%
Temperature	25	°C
Data rate	4.0	MHz
Frame time	330	ms

CCD UNIFORMITY OF RESPONSE

Device Number 367-4-4 Device Type 250 x 400

Light source 3400 °K Spectral filter 0,4000 microns

Average well population 50 % Temperature 25 °C

Data rate 4.0 MHz Frame time 330 ms

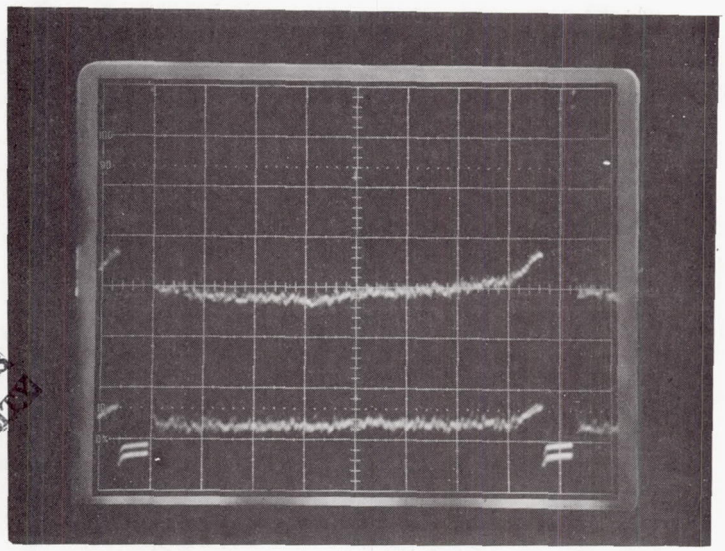

ORIGINAL PAGE IS
OF POOR QUALITY

Oscilloscope presentation
Video line number 50

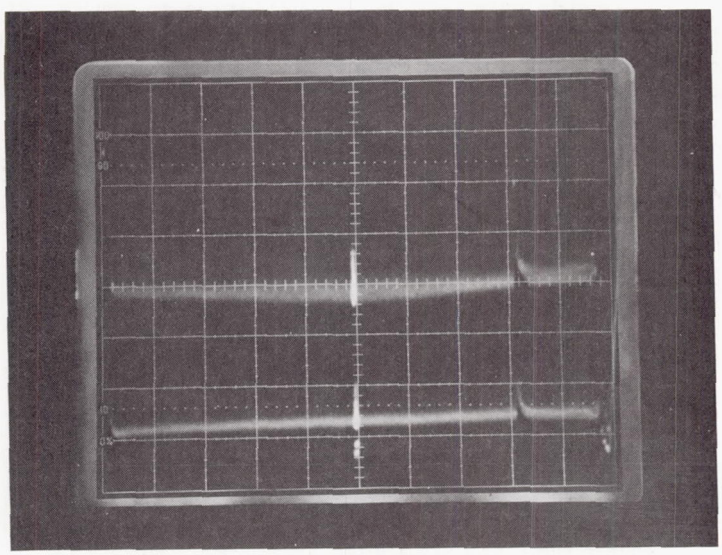

Oscilloscope presentation
Complete video frame

CCD SPECTRAL RESPONSIVITY

Device 367-4-4

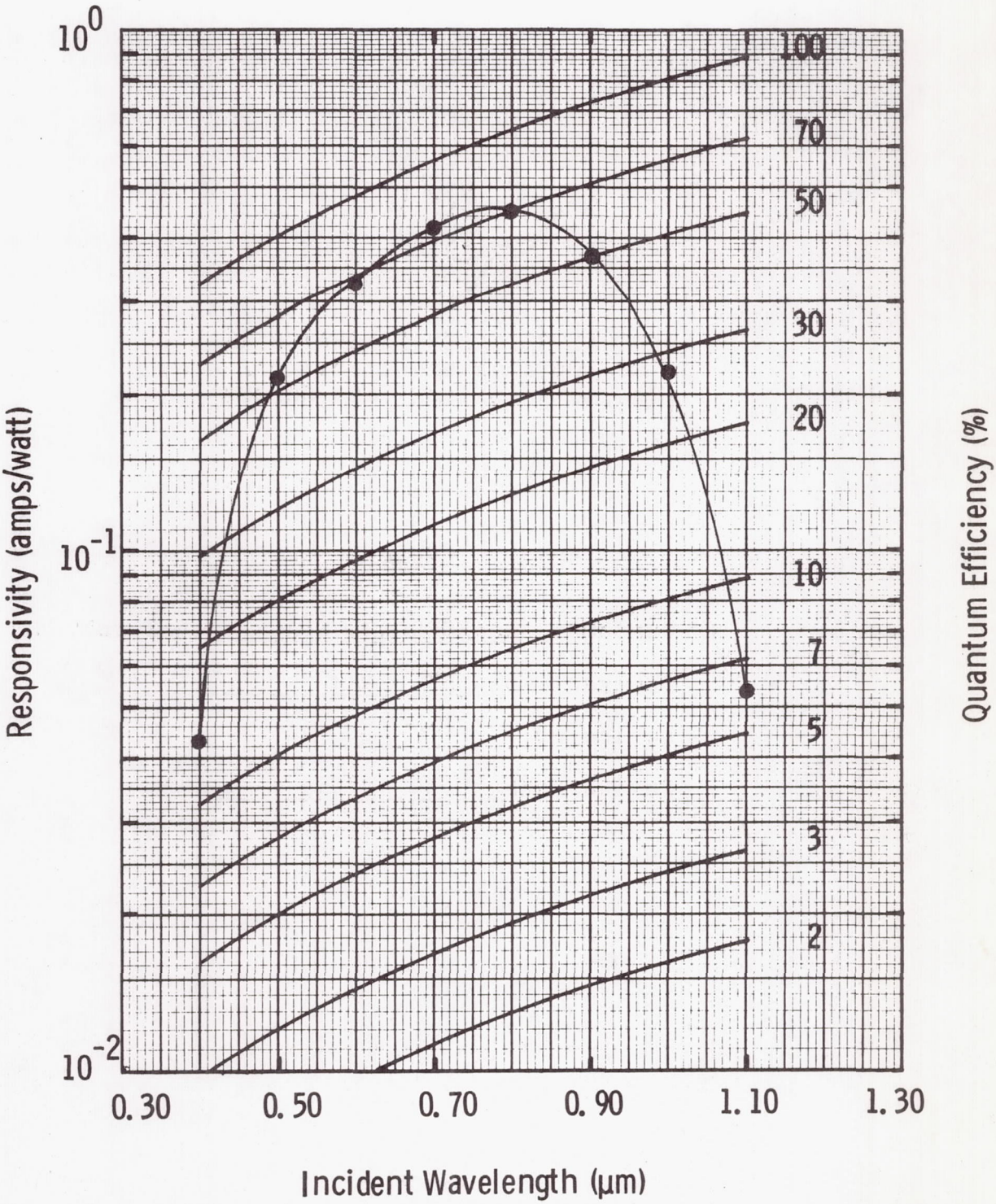

DATA RATE 3.0 MHz

FRAME TIME 50 MS

TEMPERATURE 25 °C

CENTRAL RESEARCH LABORATORIES
CCD Optical and Electrical
Characterization Test Report

for

Customer NASA/GODDARD SPACE FLIGHT CENTER

Contract No. NAS5-22924

Device No. 367-6-5

Device Type 250 x 400

CCD OPTICAL AND ELECTRICAL CHARACTERIZATION
TEST REPORT

1. CCD DEVICE NUMBER 367-6-5

2. DEVICE TYPE 250 x 400 HEADER TYPE ITT tube header

Active area 0.636 cm^2 , pixel dimensions 1.08 mils x 0.9 mils

3. OPERATING LEVELS in volts

Substrate	-.5	Lower reference	20
Parallel clocks	10	Upper reference	20
Serial clocks	15	Lower drain	28
Input diode	32	Upper drain	28
Output gate	2	Precharge pulse	9

4. AMPLIFIER CONFIGURATION used for the tests in this report:
precharge amplifier with off-chip load

5. SPECTRAL RESPONSE (see accompanying graph)

Quantum efficiency is 16 % at 0.4 microns

75 % at 0.7 microns

34 % at 1.0 microns

6. DARK CURRENT measured by the precharge method

10.7 nanoamps/cm^2 or 4.3×10^5 electrons/pixel/sec

T = 25 C, data rate 4.0 MHz, frame time 100 ms

7. R.M.S. NOISE ELECTRONS/PIXEL

Dark current shot noise 207 (100ms) electrons added in quadrature to a readout noise of 30 electrons gives a calculated R.M.S. noise of 210 electrons/pixel

8. FULL WELL CHARGE CAPABILITY, determined from the saturation exposure level, is 1×10^6 electrons.

9. DYNAMIC RANGE is computed to be 4760 :1.

10. CHARGE TRANSFER EFFICIENCY at 4.0 MHz is >.99996.

11. COMMENTS

CCD IMAGING PERFORMANCE

Device Number 367-6-5 Device Type 250 x 400

Light Source strobe °K Spectral filter none microns

Temperature 25 °C Data rate 2.0 MHz

Frame time 54 ms

ORIGINAL PAGE IS
OF POOR QUALITY

CCD UNIFORMITY OF RESPONSE

Device Number 367-6-5 Device Type 250 x 400

ORIGINAL PAGE IS
OF POOR QUALITY

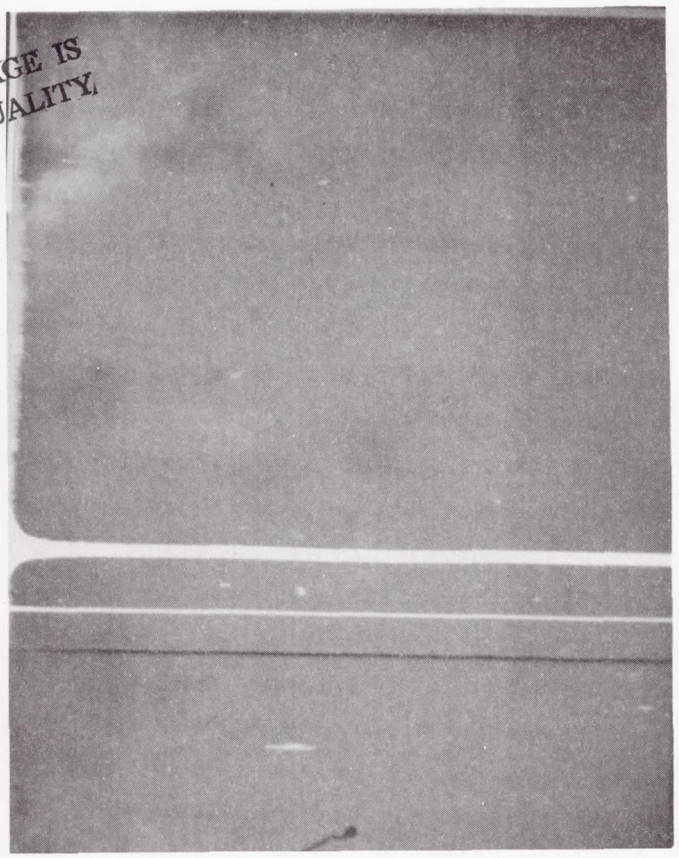

VIDEO MONITOR DISPLAY

Light source	3400	°K
Spectral filter	0.4000	microns
Average well population	50	%
Temperature	25	°C
Data rate	4.0	MHz
Frame time	179	ms

CCD UNIFORMITY OF RESPONSE

Device Number 87-6-5 Device Type 250 x 400

Light source 3400 °K Spectral filter 0.4000 microns

Average well population 50 % Temperature 25 °C

Data rate 2.5 MHz Frame time 179 ms

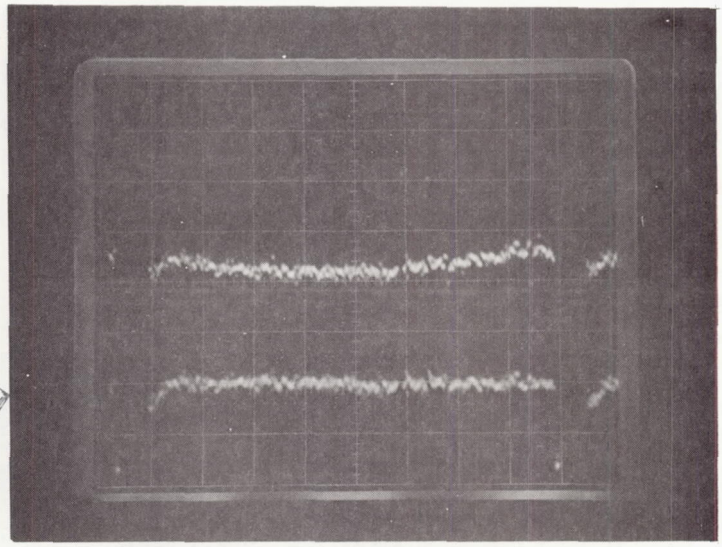

ORIGINAL PAGE IS OF POOR QUALITY

Oscilloscope presentation
Video line number 50

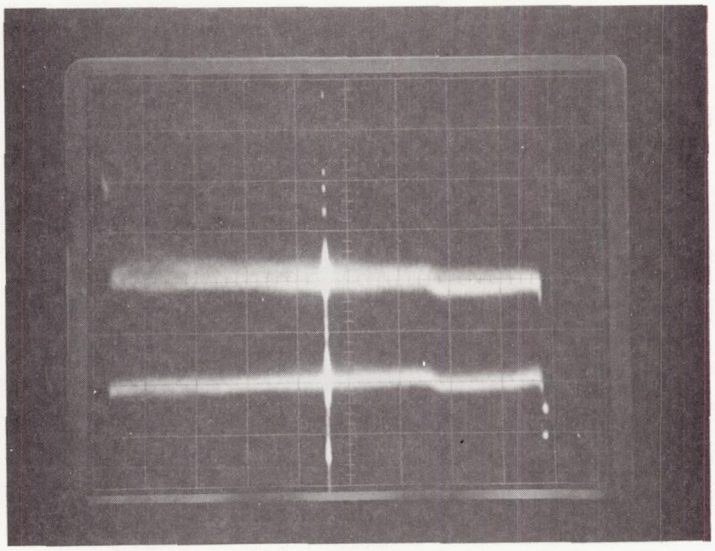

Oscilloscope presentation
Complete video frame

CCD DARK CURRENT UNIFORMITY

Device Number 367-6-5 Device Type 250 x 400

ORIGINAL PAGE IS
OF POOR QUALITY

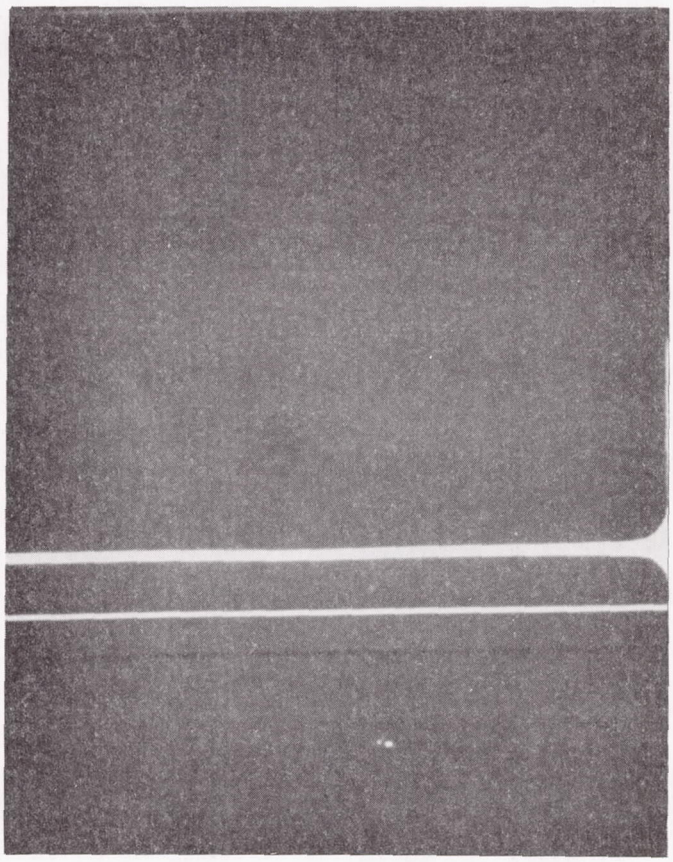

VIDEO MONITOR DISPLAY

Temperature 25 °C

Data rate 2.5 MHz

Frame time 87 ms

CCD DARK CURRENT UNIFORMITY

Device Number 367-6-5 Device Type 250 x 400

Temperature 25 °C Data rate 2.5 MHz

Frame time 87 ms

ORIGINAL PAGE IS
OF POOR QUALITY

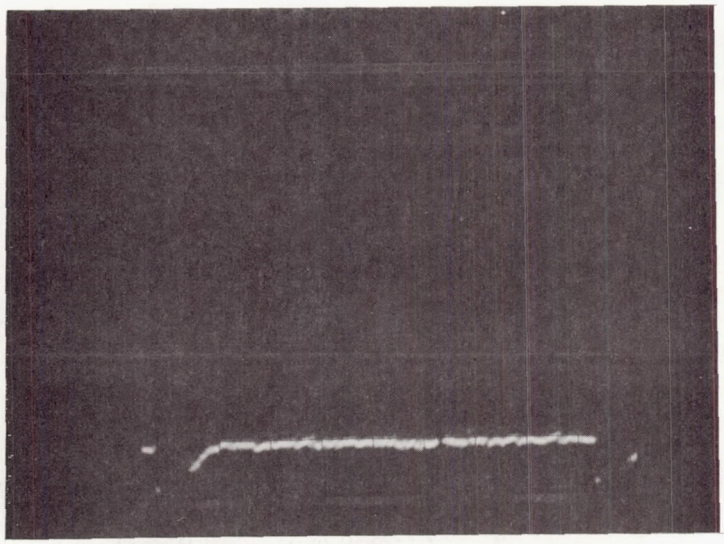

Oscilloscope presentation

Video line number 50

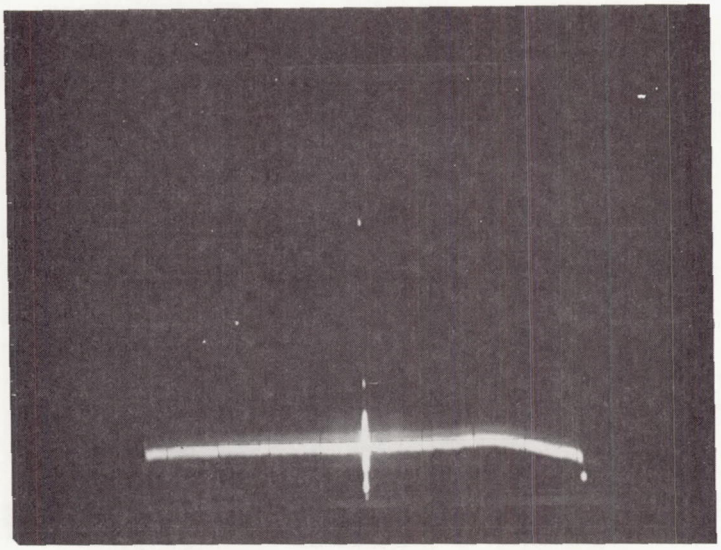

Oscilloscope presentation

Complete video frame

CCD SPECTRAL RESPONSIVITY

Device 367-6-5

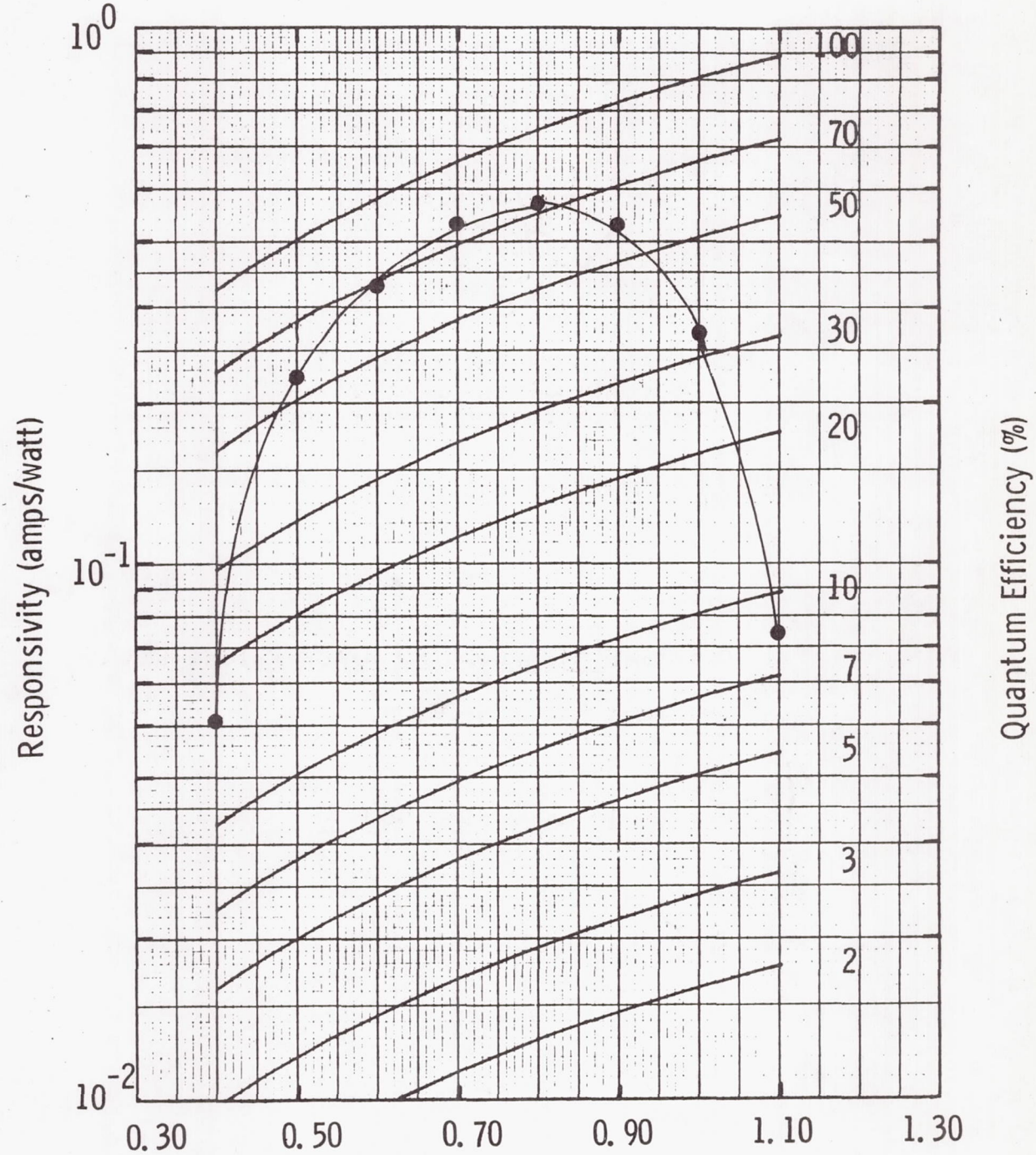

DATA RATE 3.0 MHz

FRAME TIME 50 MS

TEMPERATURE 25 °C

CENTRAL RESEARCH LABORATORIES
CCD Optical and Electrical
Characterization Test Report

for

Customer NASA/GODDARD SPACE FLIGHT CENTER

Contract No. NAS5-22924

Device No. 367-8-6

Device Type 250 x 400

C-3

CCD OPTICAL AND ELECTRICAL CHARACTERIZATION
TEST REPORT

1. CCD DEVICE NUMBER 367-8-6

2. DEVICE TYPE 250 x 400 HEADER TYPE ITT tube header

Active area 0.636 cm^2 , pixel dimensions 1.08 mils x 0.9 mils

3. OPERATING LEVELS in volts

Substrate	-.5	Lower reference	20
Parallel clocks	14	Upper reference	20
Serial clocks	15	Lower drain	28
Input diode	32	Upper drain	28
Output gate	2	Precharge pulse	9

4. AMPLIFIER CONFIGURATION used for the tests in this report:
precharge amplifier with off-chip load

5. SPECTRAL RESPONSE (see accompanying graph)

Quantum efficiency is 7.0% at 0.4 microns

63.4% at 0.7 microns

28.6% at 1.0 microns

6. DARK CURRENT measured by the precharge method

49.5 nanoamps/cm^2 or 2.0×10^6 electrons/pixel/sec

T = 25 C, data rate 4.0 MHz, frame time 100 ms

7. R.M.S. NOISE ELECTRONS/PIXEL
Dark current shot noise 440 (100ms) electrons added in quadrature to a readout noise of 30 electrons gives a calculated R.M.S. noise of 440 electrons/pixel

8. FULL WELL CHARGE CAPABILITY, determined from the saturation exposure level, is 1.6×10^6 electrons.

9. DYNAMIC RANGE is computed to be 3600 :1.

10. CHARGE TRANSFER EFFICIENCY at 4.0 MHz is 0.99995.

11. COMMENTS open parallel electrode

CCD IMAGING PERFORMANCE

Device Number 367-8-6 Device Type 250 x 400

Light Source strobe °K Spectral filter none microns

Temperature 25 °C Data rate 4.0 MHz

Frame time 33 ms

ORIGINAL PAGE IS
OF POOR QUALITY

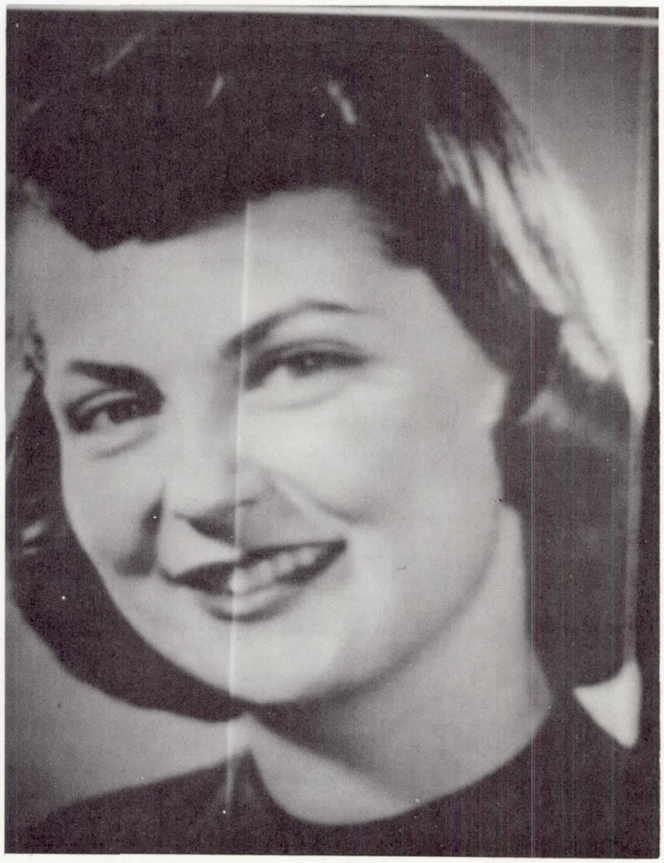

CCD UNIFORMITY OF RESPONSE

Device Number 367-8-6 Device Type 250 x 400

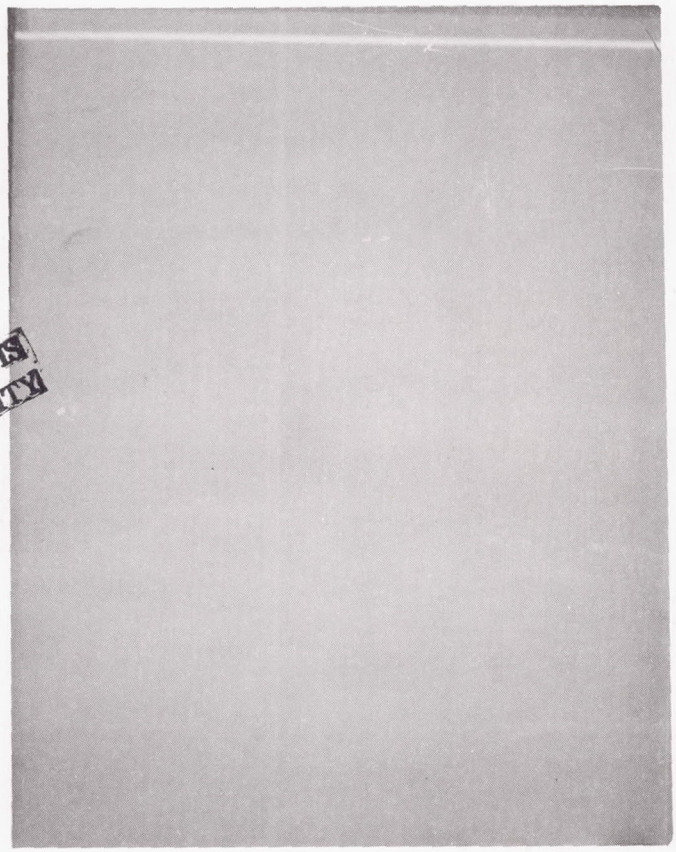

ORIGINAL PAGE IS
OF POOR QUALITY

VIDEO MONITOR DISPLAY

Light source	3400	°K
Spectral filter	0.4000	microns
Average well population	50	%
Temperature	25	°C
Data rate	4.0	MHz
Frame time	159	ms

CCD UNIFORMITY OF RESPONSE

Device Number 367-8-6 Device Type 250 x 400

Light source 3400 °K Spectral filter 0.4000 microns

Average well population 50 % Temperature 25 °C

Data rate 4.0 MHz Frame time 159 ms

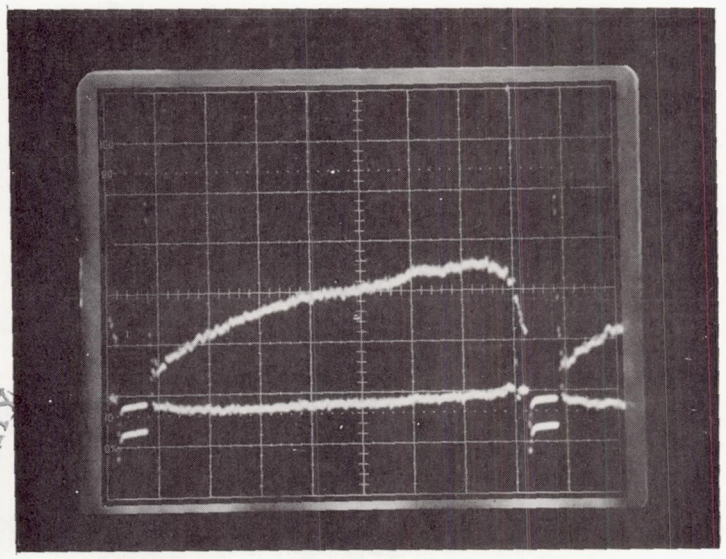

ORIGINAL PAGE IS OF POOR QUALITY

Oscilloscope presentation
Video line number 50

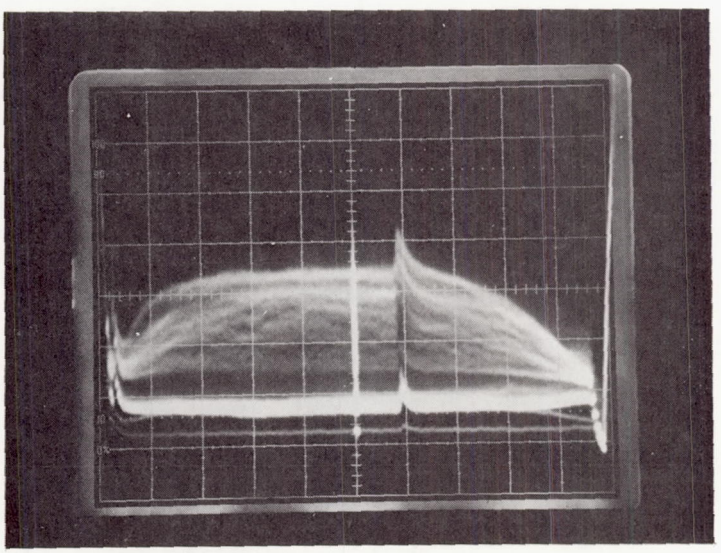

Oscilloscope presentation
Complete video frame

CCD DARK CURRENT UNIFORMITY

Device Number 367-8-6 Device Type 250 x 400

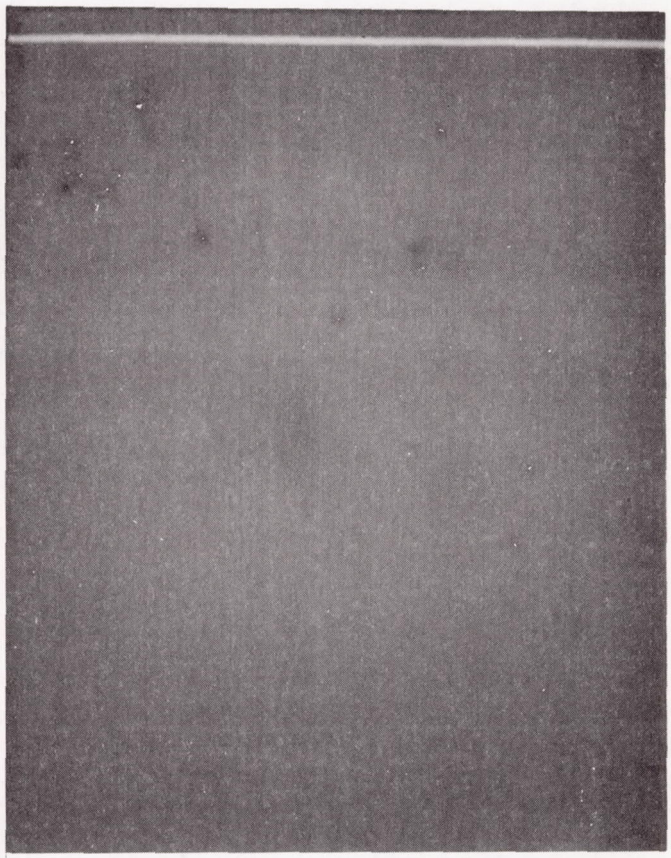

ORIGINAL PAGE IS
OF POOR QUALITY

VIDEO MONITOR DISPLAY

Temperature 25 °C

Data rate 4.0 MHz

Frame time 100 ms

CCD DARK CURRENT UNIFORMITY

Device Number 367-8-6 Device Type 250 x 400

Temperature 25 °C Data rate 4.0 MHz

Frame time 100 ms

PAGE IS OF POOR QUALITY

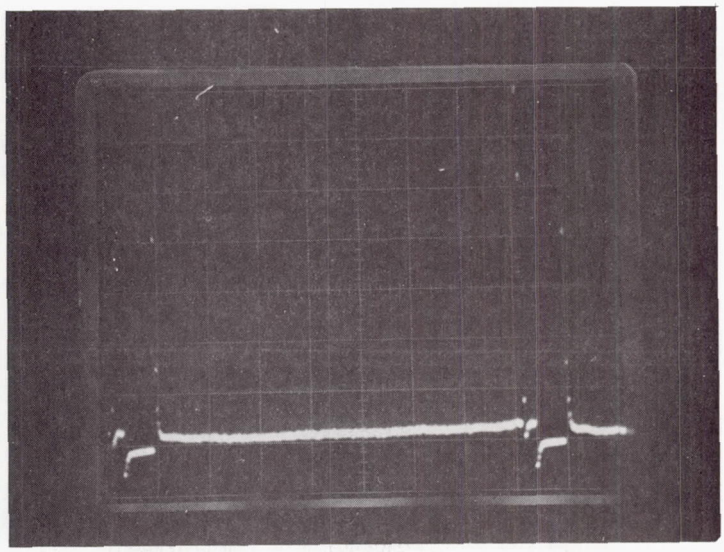

Oscilloscope presentation

Video line number 50

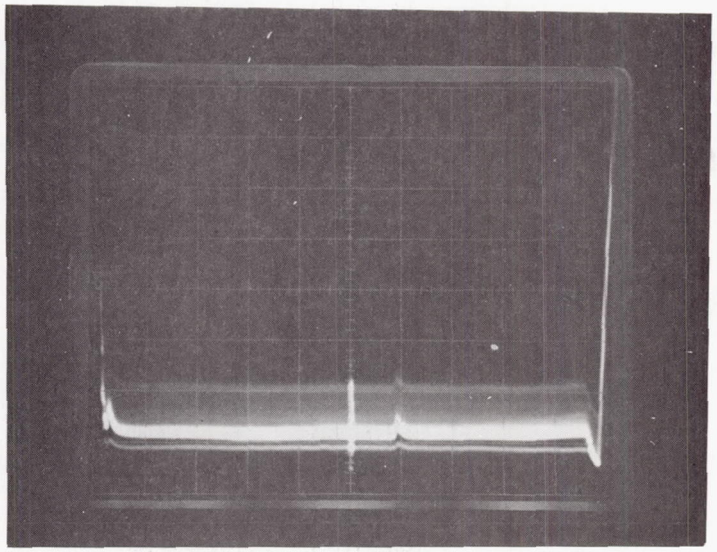

Oscilloscope presentation

Complete video frame

CCD SPECTRAL RESPONSIVITY

Device 367-8-6

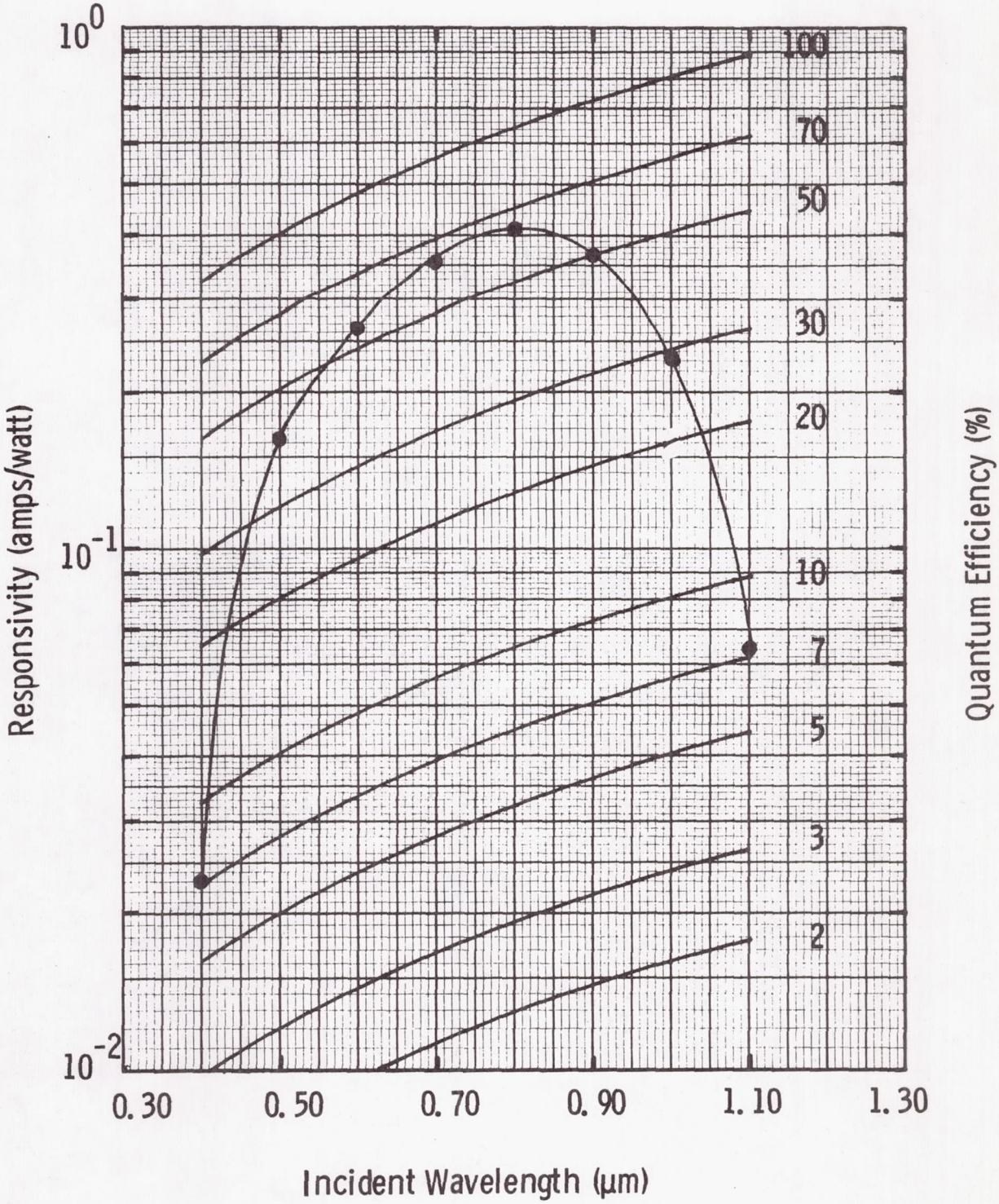

DATA RATE 3.0 MHz

FRAME TIME 50 MS

TEMPERATURE 25 °C

CENTRAL RESEARCH LABORATORIES
CCD Optical and Electrical
Characterization Test Report

for

Customer NASA/GODDARD SPACE FLIGHT CENTER

Contract No. NAS5-22924

Device No. 367-9-2

Device Type 250 x 400

CCD OPTICAL AND ELECTRICAL CHARACTERIZATION
TEST REPORT

1. CCD DEVICE NUMBER 367-9-2

2. DEVICE TYPE 250 x 400 HEADER TYPE ITT tube header

Active area 0.636 cm^2 , pixel dimensions 1.08 mils x 0.9 mils

3. OPERATING LEVELS in volts

Substrate	-.5	Lower reference	20
Parallel clocks	14	Upper reference	20
Serial clocks	15	Lower drain	28
Input diode	32	Upper drain	28
Output gate	2	Precharge pulse	9

4. AMPLIFIER CONFIGURATION used for the tests in this report:
precharge amplifier with off-chip load

5. SPECTRAL RESPONSE (see accompanying graph)

Quantum efficiency is 9.1 % at 0.4 microns

66.1 % at 0.7 microns

30.1 % at 1.0 microns

6. DARK CURRENT measured by the precharge method

40.6 nanoamps/cm^2 or 1.6×10^6 electrons/pixel/sec

T = 25 C, data rate 4.0 MHz, frame time 100 ms

7. R.M.S. NOISE ELECTRONS/PIXEL

Dark current shot noise 400 (100ms) electrons added in quadrature to a readout noise of 30 electrons gives a calculated R.M.S. noise of 401 electrons/pixel

8. FULL WELL CHARGE CAPABILITY, determined from the saturation exposure level, is 1.6×10^6 electrons.

9. DYNAMIC RANGE is computed to be 4000 :1.

10. CHARGE TRANSFER EFFICIENCY at 4.0 MHz is 0.99995.

11. COMMENTS open parallel electrode; reverse operation best

CCD IMAGING PERFORMANCE

Device Number 367-9-2 Device Type 250 x 400

Light Source strobe °K Spectral filter none microns

Temperature 25 °C Data rate 4.0 MHz

Frame time 33 ms

PAGE IS OF POOR QUALITY

CCD DARK CURRENT UNIFORMITY

Device Number 367-9-2 Device Type 250 x 400

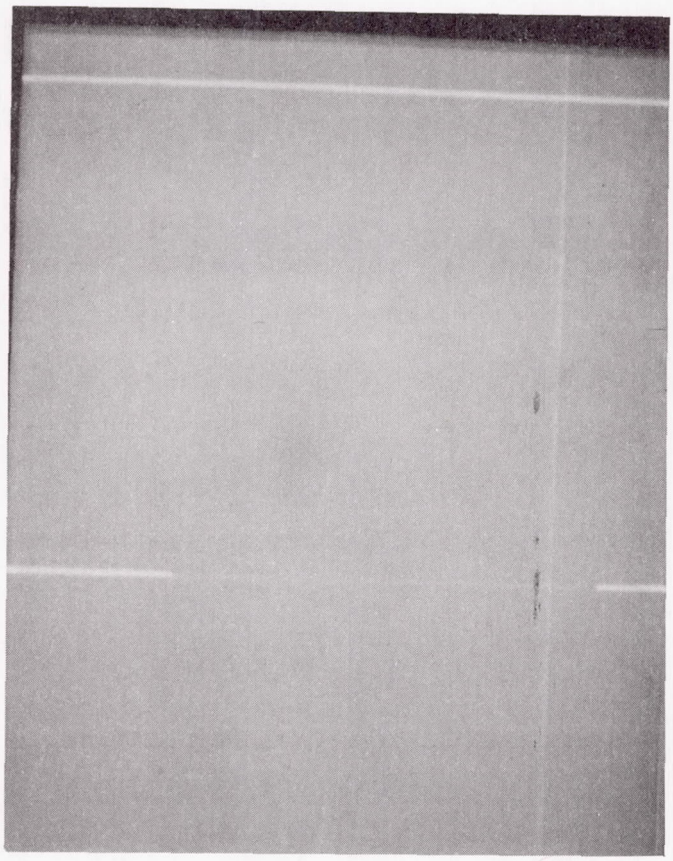

ORIGINAL PAGE IS OF POOR QUALITY

VIDEO MONITOR DISPLAY

Temperature 25 °C

Data rate 4.0 MHz

Frame time 100 ms

CCD DARK CURRENT UNIFORMITY

Device Number 367-9-2 Device Type 250 x 400

Temperature 25 °C Data rate 4.0 MHz

Frame time 100 ms

ORIGINAL PAGE IS
OF POOR QUALITY

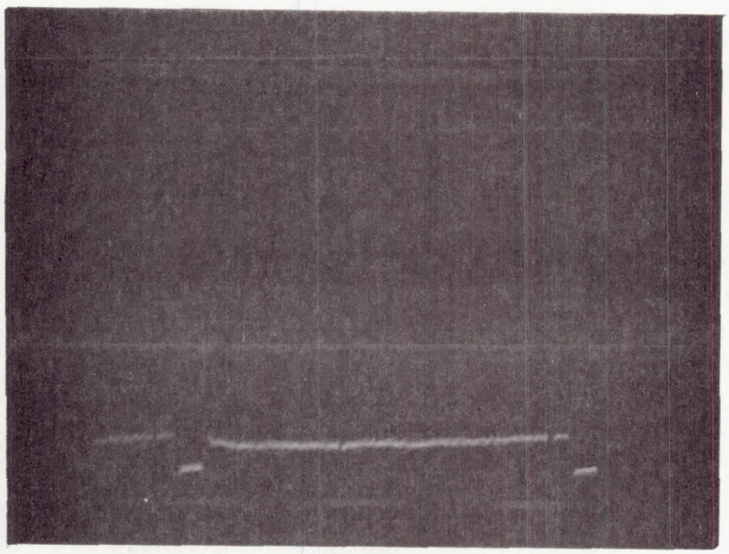

Oscilloscope presentation

Video line number 50

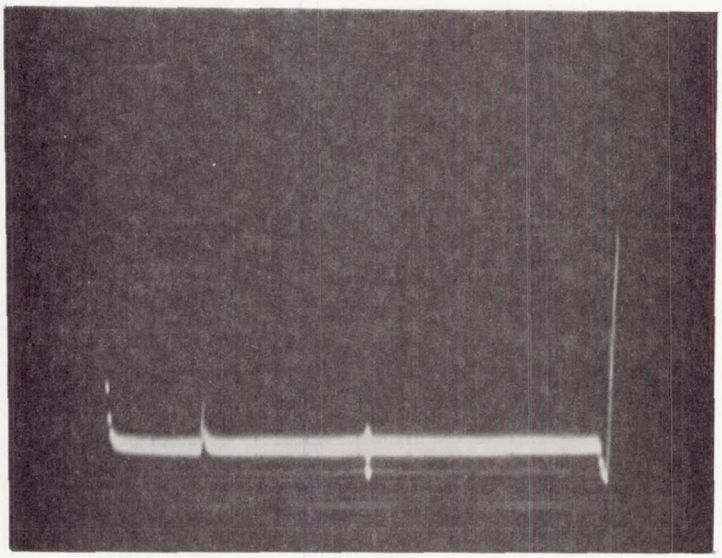

Oscilloscope presentation

Complete video frame

CCD UNIFORMITY OF RESPONSE

Device Number 367-9-2 Device Type 250 x 400

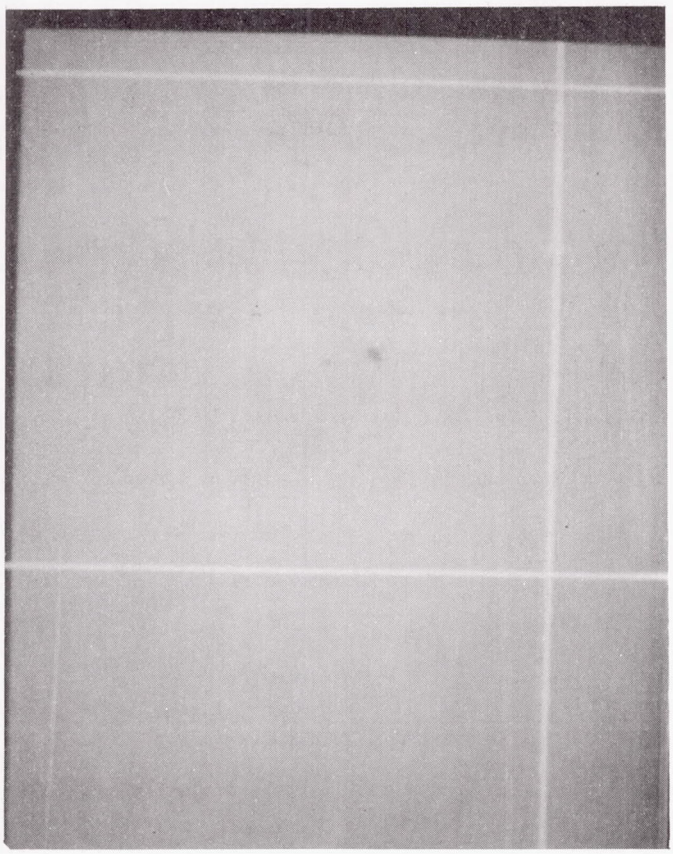

ORIGINAL PAGE IS OF POOR QUALITY

VIDEO MONITOR DISPLAY

Light source	3400	°K
Spectral filter	0.4000	microns
Average well population	50	%
Temperature	25	°C
Data rate	4.0	MHz
Frame time	175	ms

CCD UNIFORMITY OF RESPONSE

Device Number 367-9-2 Device Type 250 x 400

Light source 3400 °K Spectral filter 0.4000 microns

Average well population 50 % Temperature 25 °C

Data rate 4.0 MHz Frame time 175 ms

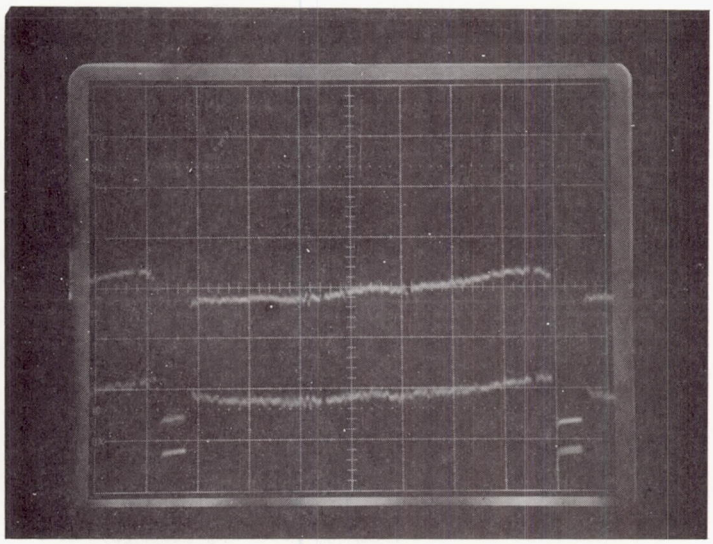

ORIGINAL PAGE IS
OF POOR QUALITY

Oscilloscope presentation
Video line number 50

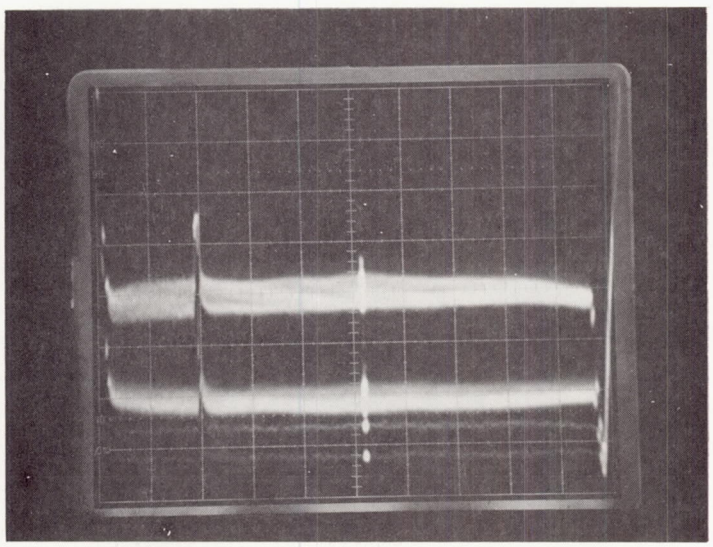

Oscilloscope presentation
Complete video frame

CCD SPECTRAL RESPONSIVITY

Device 367-9-2

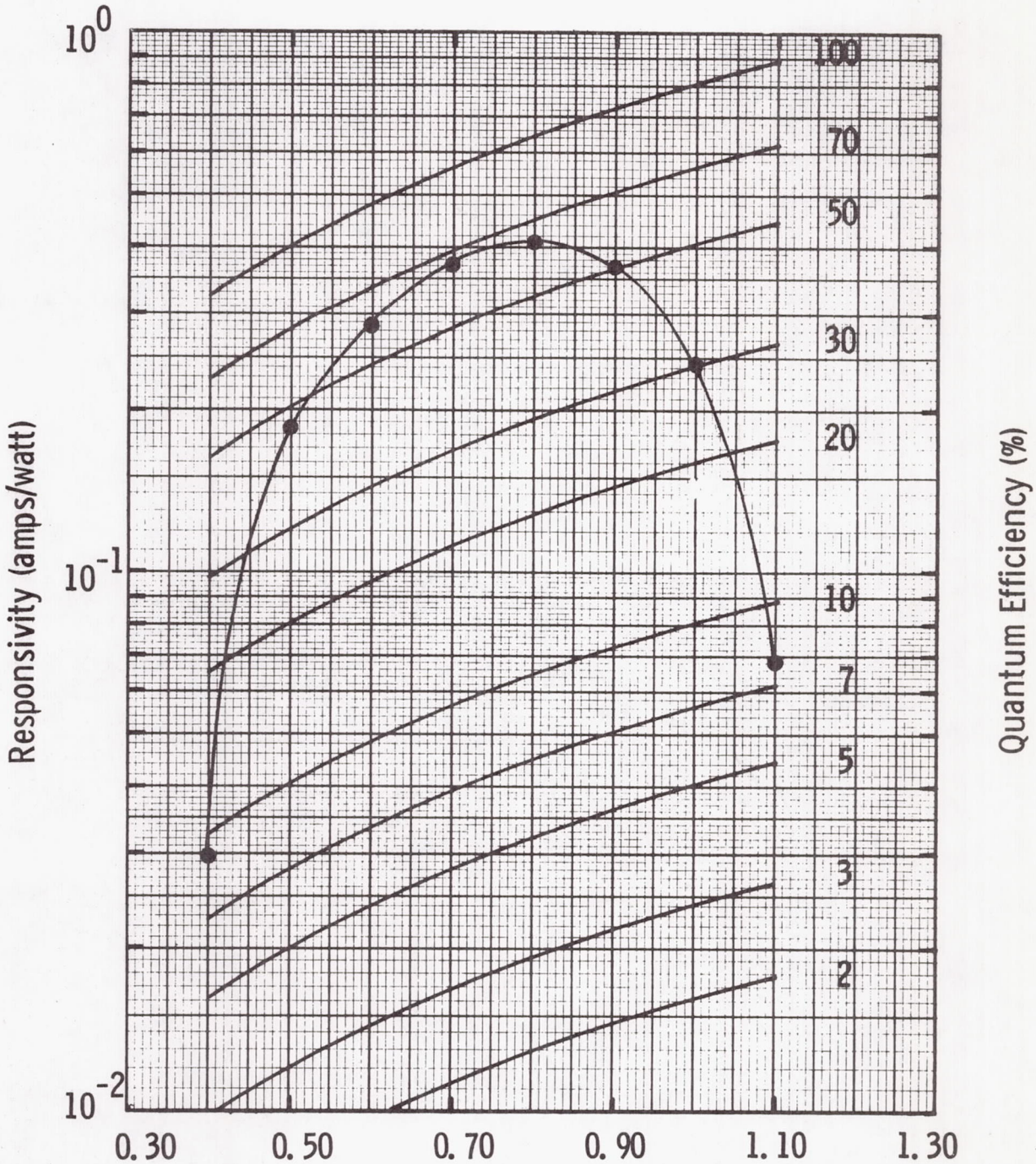

DATA RATE 3.0 MHz

FRAME TIME 50 MS

TEMPERATURE 25 °C

CENTRAL RESEARCH LABORATORIES
CCD Optical and Electrical
Characterization Test Report

for

Customer NASA/GODDARD SPACE FLIGHT CENTER

Contract No. NAS5-22924

Device No. 367-10-2

Device Type 250 x 400

CCD OPTICAL AND ELECTRICAL CHARACTERIZATION
TEST REPORT

1. CCD DEVICE NUMBER 367-10-2

2. DEVICE TYPE 250 x 400 HEADER TYPE ITT tube header

Active area 0.636 cm^2 , pixel dimensions 1.08 mils x 0.9 mils

3. OPERATING LEVELS in volts

Substrate	-.5	Lower reference	20
Parallel clocks	14	Upper reference	20
Serial clocks	15	Lower drain	28
Input diode	32	Upper drain	28
Output gate	2	Precharge pulse	9

4. AMPLIFIER CONFIGURATION used for the tests in this report:
precharge amplifier with off-chip load

5. SPECTRAL RESPONSE (see accompanying graph)

Quantum efficiency is 12.6 % at 0.4 microns

74.8 % at 0.7 microns

27.4 % at 1.0 microns

6. DARK CURRENT measured by the precharge method

20.8 nanoamps/cm^2 or 8.3×10^5 electrons/pixel/sec

T = 25 C, data rate 4.0 MHz, frame time 100 ms

7. R.M.S. NOISE ELECTRONS/PIXEL
Dark current shot noise 288 (100ms) electrons added in quadrature to a readout noise of 30 electrons gives a calculated R.M.S. noise of 290 electrons/pixel

8. FULL WELL CHARGE CAPABILITY, determined from the saturation exposure level, is 1.6×10^6 electrons.

9. DYNAMIC RANGE is computed to be 5500 :1.

10. CHARGE TRANSFER EFFICIENCY at 4.0 MHz is 0.99995.

11. COMMENTS

CCD IMAGING PERFORMANCE

Device Number 367-10-2 Device Type 250 x 400

Light Source strobe °K Spectral filter none microns

Temperature 25 °C Data rate 4.0 MHz

Frame time 33 ms

ORIGINAL PAGE IS
OF POOR QUALITY

CCD DARK CURRENT UNIFORMITY

Device Number 367-10-2 Device Type 250 x 400

ORIGINAL PAGE IS
OF POOR QUALITY

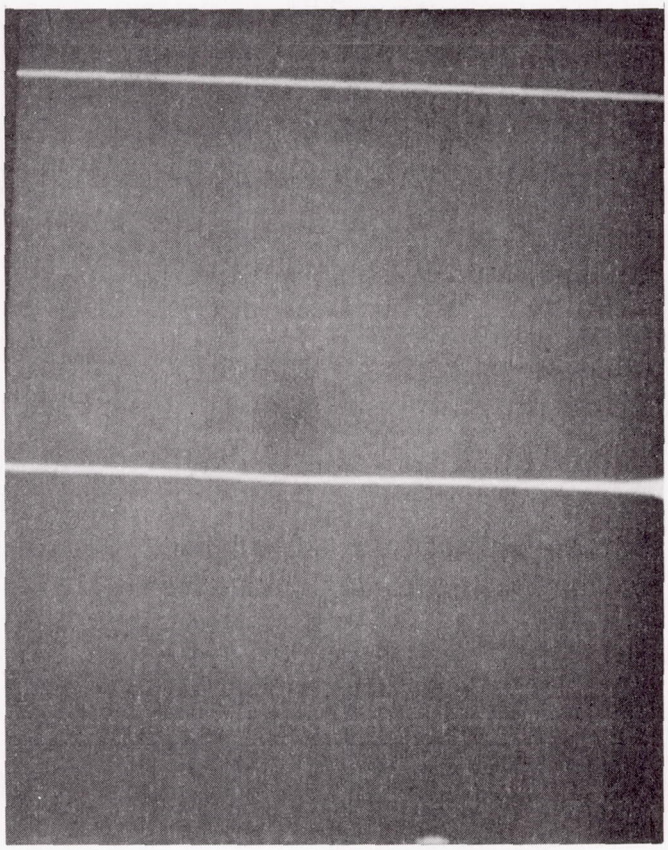

VIDEO MONITOR DISPLAY

Temperature 25 °C

Data rate 4.0 MHz

Frame time 100 ms

CCD DARK CURRENT UNIFORMITY

Device Number 367-10-2 Device Type 250 x 400

Temperature 25 °C Data rate 4.0 MHz

Frame time 100 ms

ORIGINAL PAGE IS
OF POOR QUALITY

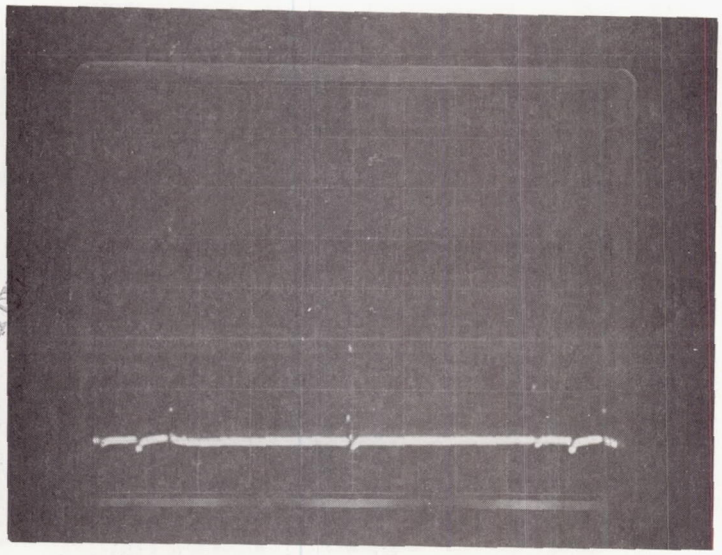

Oscilloscope presentation

Video line number 50

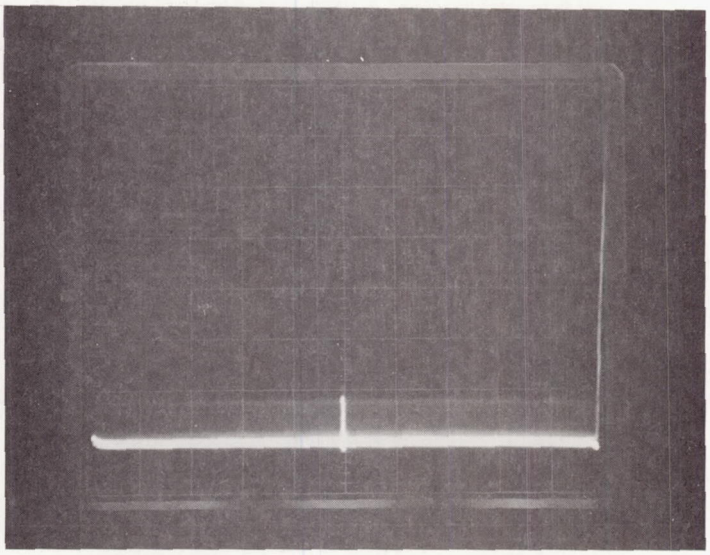

Oscilloscope presentation

Complete video frame

CCD UNIFORMITY OF RESPONSE

Device Number 367-10-2 Device Type 250 x 400

ORIGINAL PAGE IS
OF POOR QUALITY

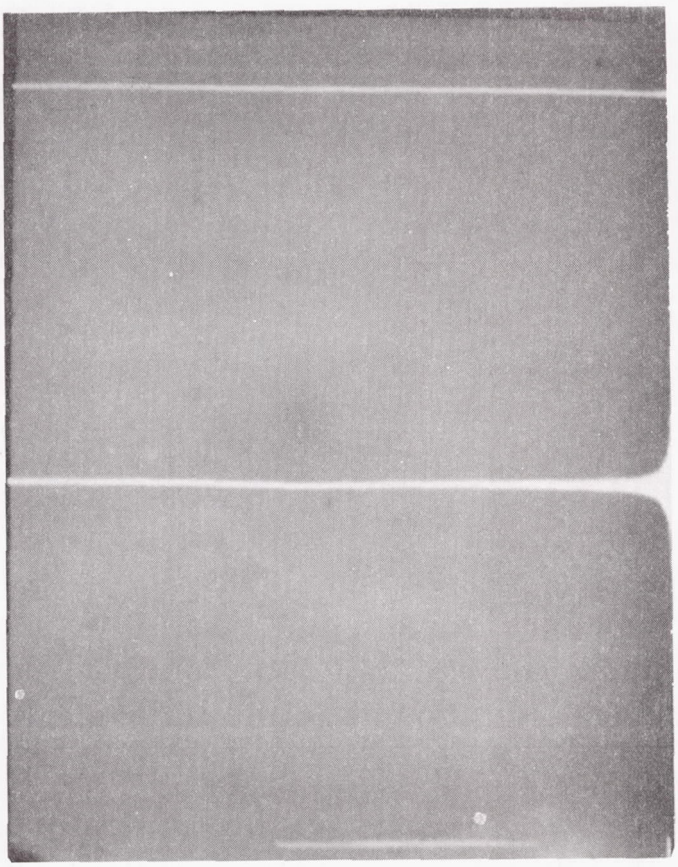

VIDEO MONITOR DISPLAY

Light source	3400	°K
Spectral filter	0.4000	microns
Average well population	50	%
Temperature	25	°C
Data rate	4.0	MHz
Frame time	330	ms

CCD UNIFORMITY OF RESPONSE

Device Number 367-10-2 Device Type 250 x 400

Light source 3400 °K Spectral filter 0,4000 microns

Average well population 50 % Temperature 25 °C

Data rate 4.0 MHz Frame time 330 ms

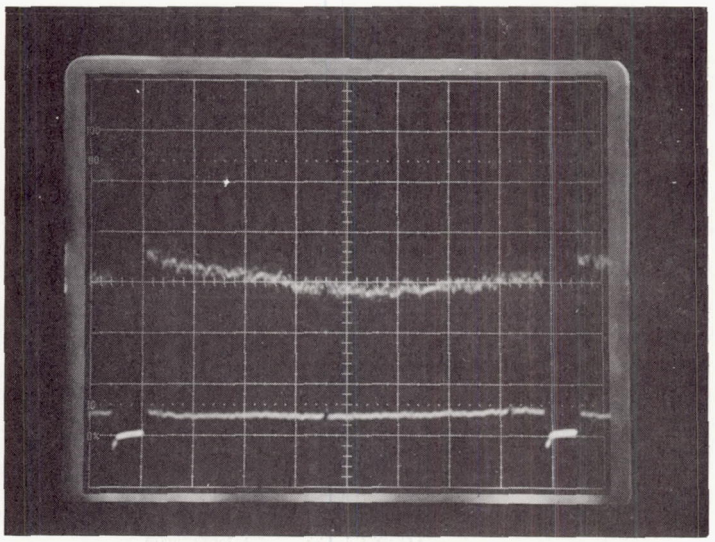

ORIGINAL PAGE IS
OF POOR QUALITY

Oscilloscope presentation
Video line number 50

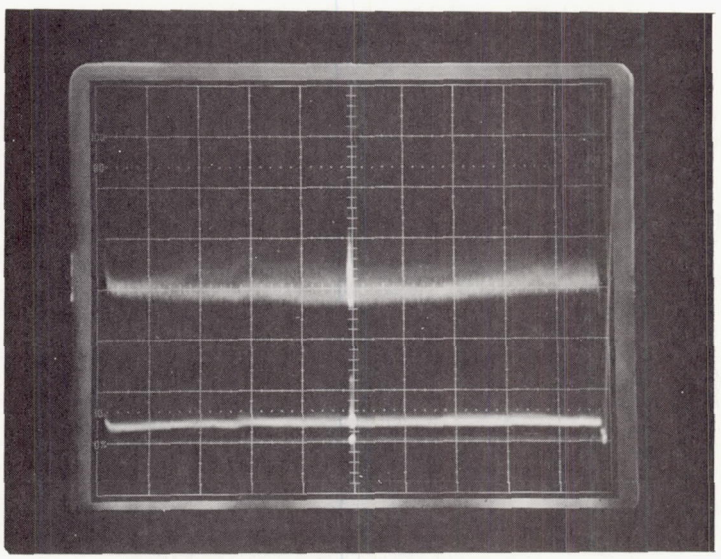

Oscilloscope presentation
Complete video frame

CCD SPECTRAL RESPONSIVITY

Device 367-10-2

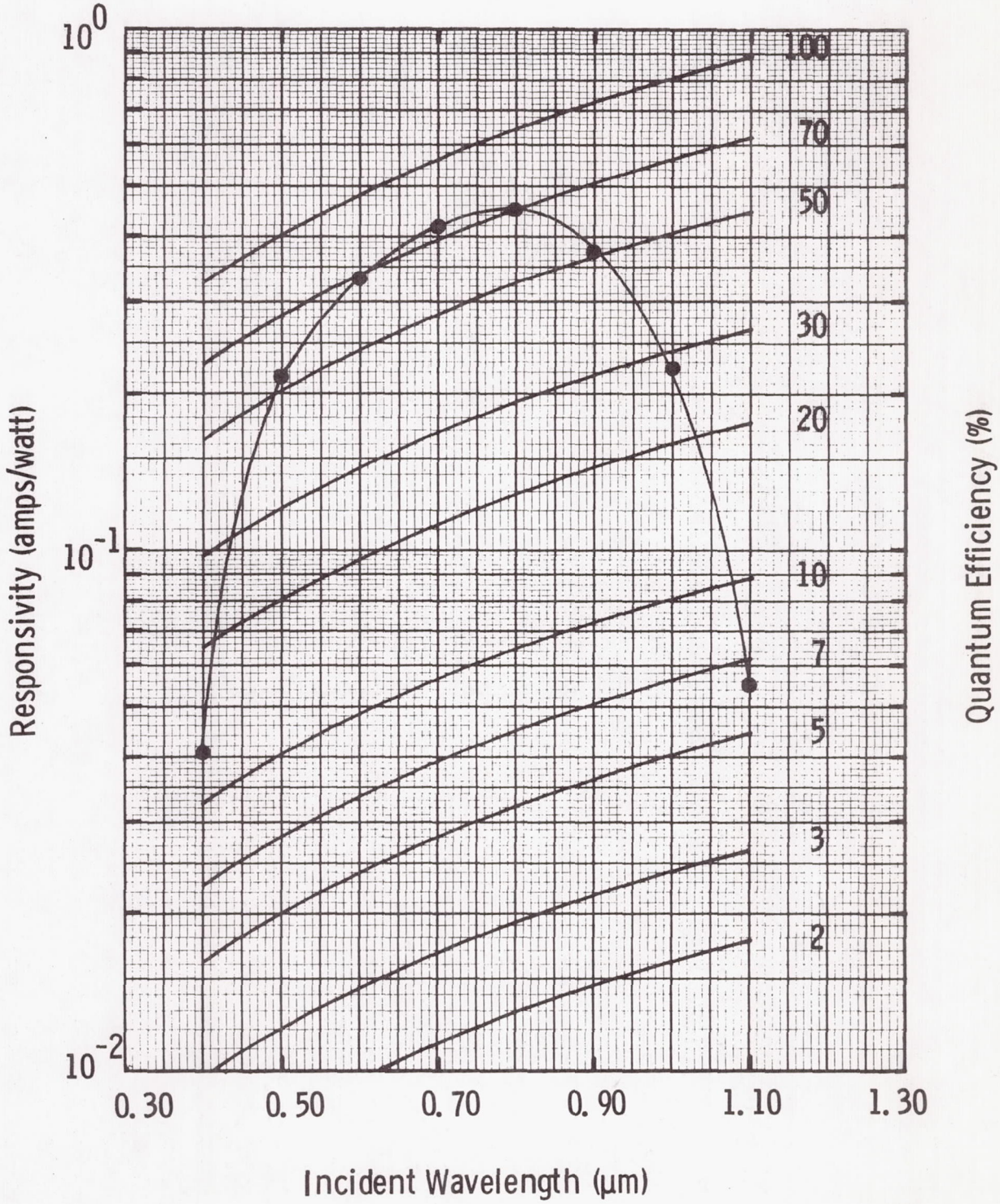

DATA RATE 3.0 MHz

FRAME TIME 50 MS

TEMPERATURE 25 °C

CENTRAL RESEARCH LABORATORIES
CCD Optical and Electrical
Characterization Test Report

for

Customer NASA/GODDARD SPACE FLIGHT CENTER

Contract No. NAS5-22924

Device No. 367-11-2

Device Type 250 x 400

CCD OPTICAL AND ELECTRICAL CHARACTERIZATION
TEST REPORT

1. CCD DEVICE NUMBER 367-11-2

2. DEVICE TYPE 250 x 400 HEADER TYPE ITT tube header

Active area 0.636 cm^2 , pixel dimensions 1.08 mils x 0.9 mils

3. OPERATING LEVELS in volts

Substrate	-.5	Lower reference	20
Parallel clocks	14	Upper reference	20
Serial clocks	15	Lower drain	28
Input diode	32	Upper drain	28
Output gate	2	Precharge pulse	9

4. AMPLIFIER CONFIGURATION used for the tests in this report:
precharge amplifier with off-chip load

5. SPECTRAL RESPONSE (see accompanying graph)

Quantum efficiency is 11.0 % at 0.4 microns

75.5 % at 0.7 microns

26.7 % at 1.0 microns

6. DARK CURRENT measured by the precharge method

17.9 nanoamps/cm^2 or 7.1×10^5 electrons/pixel/sec

T = 25 C, data rate 4.0 MHz, frame time 100 ms

7. R.M.S. NOISE ELECTRONS/PIXEL
Dark current shot noise 267 (100ms) electrons added in quadrature to a readout noise of 30 electrons gives a calculated R.M.S. noise of 269 electrons/pixel

8. FULL WELL CHARGE CAPABILITY, determined from the saturation exposure level, is 1.6×10^6 electrons.

9. DYNAMIC RANGE is computed to be 5950 :1.

10. CHARGE TRANSFER EFFICIENCY at 4.0 MHz is 0.99995.

11. COMMENTS

CCD IMAGING PERFORMANCE

Device Number 367-11-2 Device Type 250 x 400

Light Source strobe °K Spectral filter none microns

Temperature 25 °C Data rate 4.0 MHz

Frame time 33 ms

ORIGINAL PAGE IS OF POOR QUALITY

CCD DARK CURRENT UNIFORMITY

Device Number 367-11-2 Device Type 250 x 400

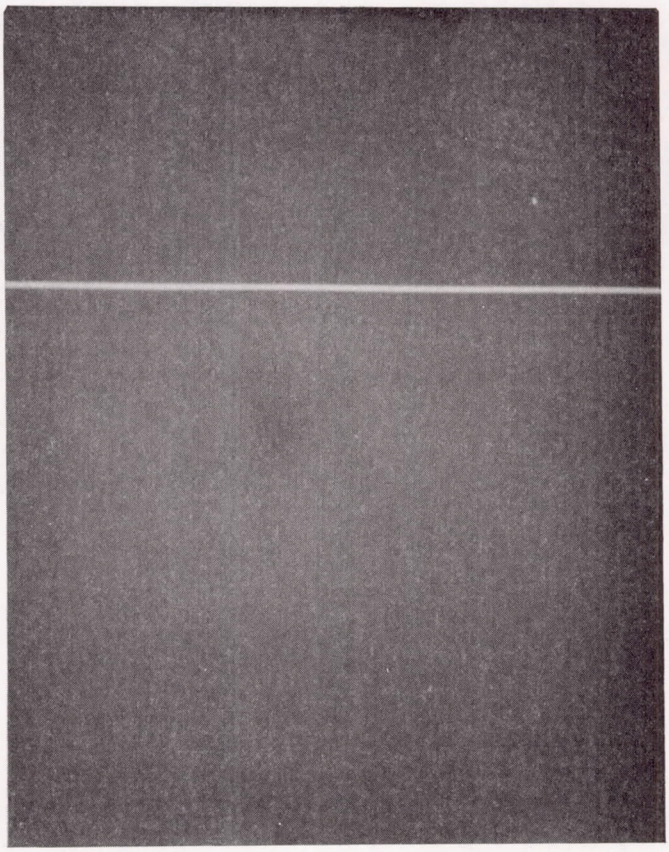

ORIGINAL PAGE IS
OF POOR QUALITY

VIDEO MONITOR DISPLAY

Temperature 25 °C

Data rate 4.0 MHz

Frame time 100 ms

CCD DARK CURRENT UNIFORMITY

Device Number 367-11-2 Device Type 250 x 400

Temperature 25 °C Data rate 4.0 MHz

Frame time 100 ms

ORIGINAL PAGE IS
OF POOR QUALITY

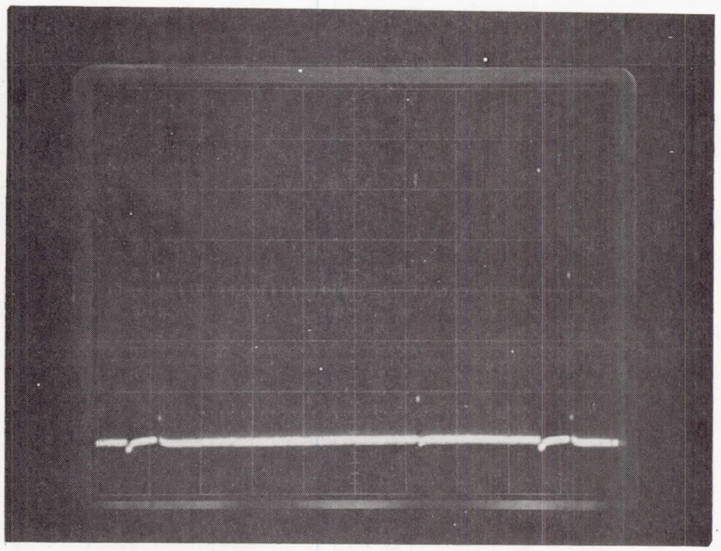

Oscilloscope presentation

Video line number 50

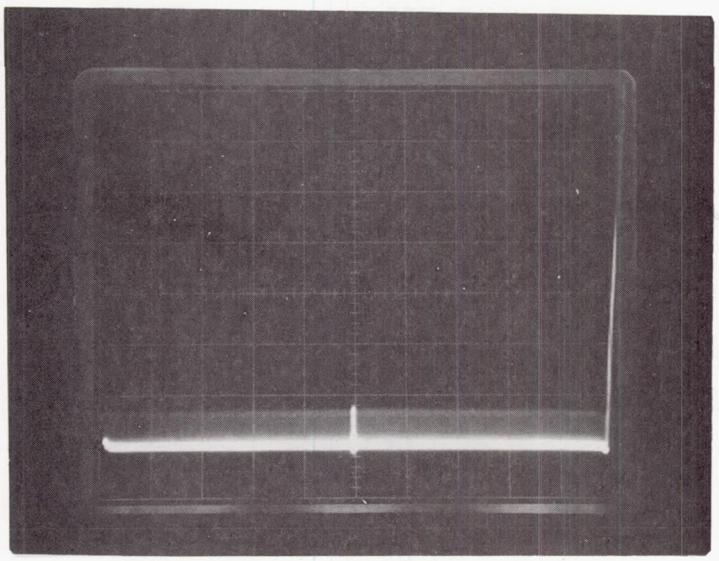

Oscilloscope presentation

Complete video frame

CCD UNIFORMITY OF RESPONSE

Device Number 367-11-2 Device Type 250 x 400

ORIGINAL PAGE IS
OF POOR QUALITY

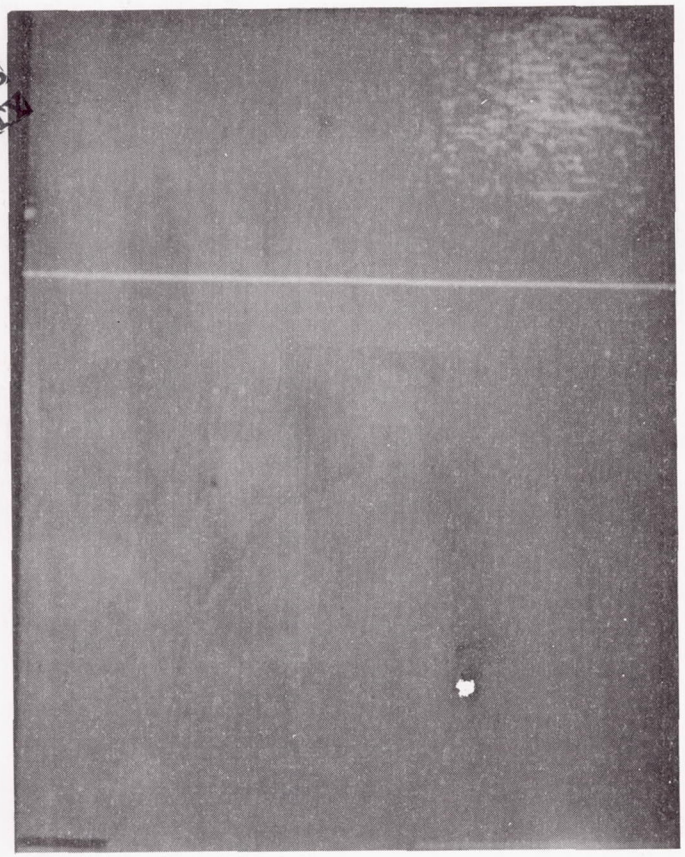

VIDEO MONITOR DISPLAY

Light source	3400	°K
Spectral filter	0.4000	microns
Average well population	50	%
Temperature	25	°C
Data rate	4.0	MHz
Frame time	424	ms

CCD UNIFORMITY OF RESPONSE

Device Number 367-11-2 Device Type 250 x 400

Light source 3400 °K Spectral filter 0.4000 microns

Average well population 50 % Temperature 25 °C

Data rate 4.0 MHz Frame time 424 ms

ORIGINAL PAGE IS
OF POOR QUALITY

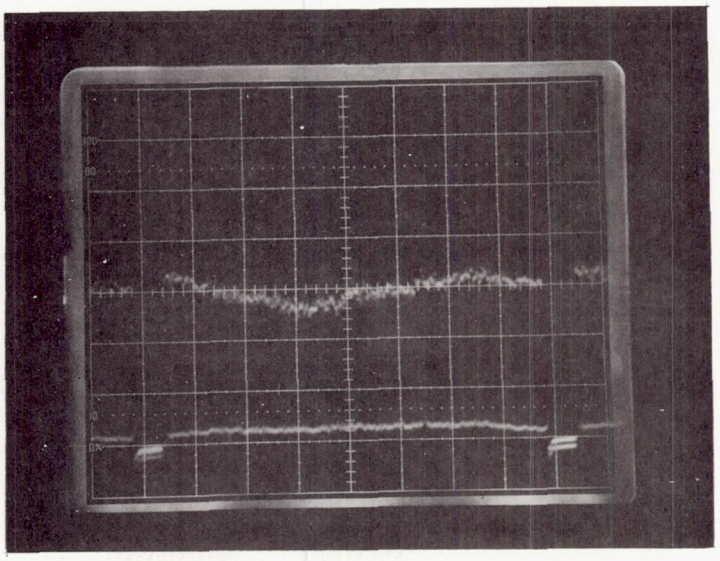

Oscilloscope presentation
Video line number 50

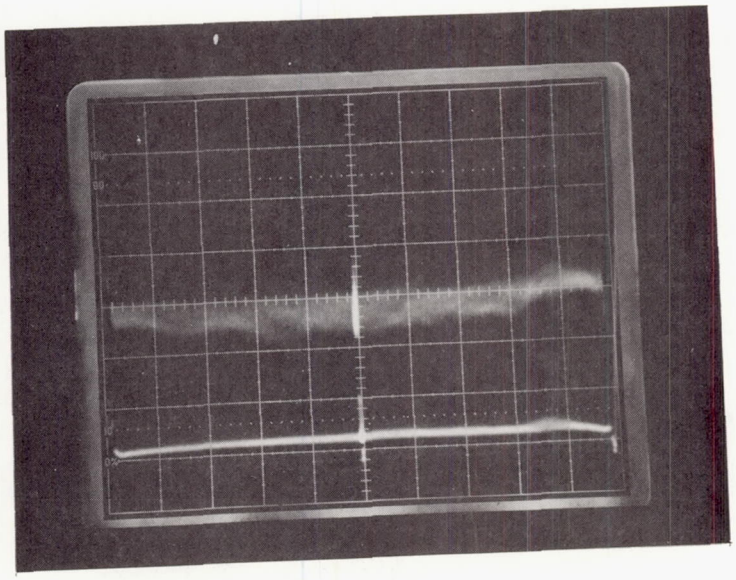

Oscilloscope presentation
Complete video frame

CCD SPECTRAL RESPONSIVITY

Device 367-11-2

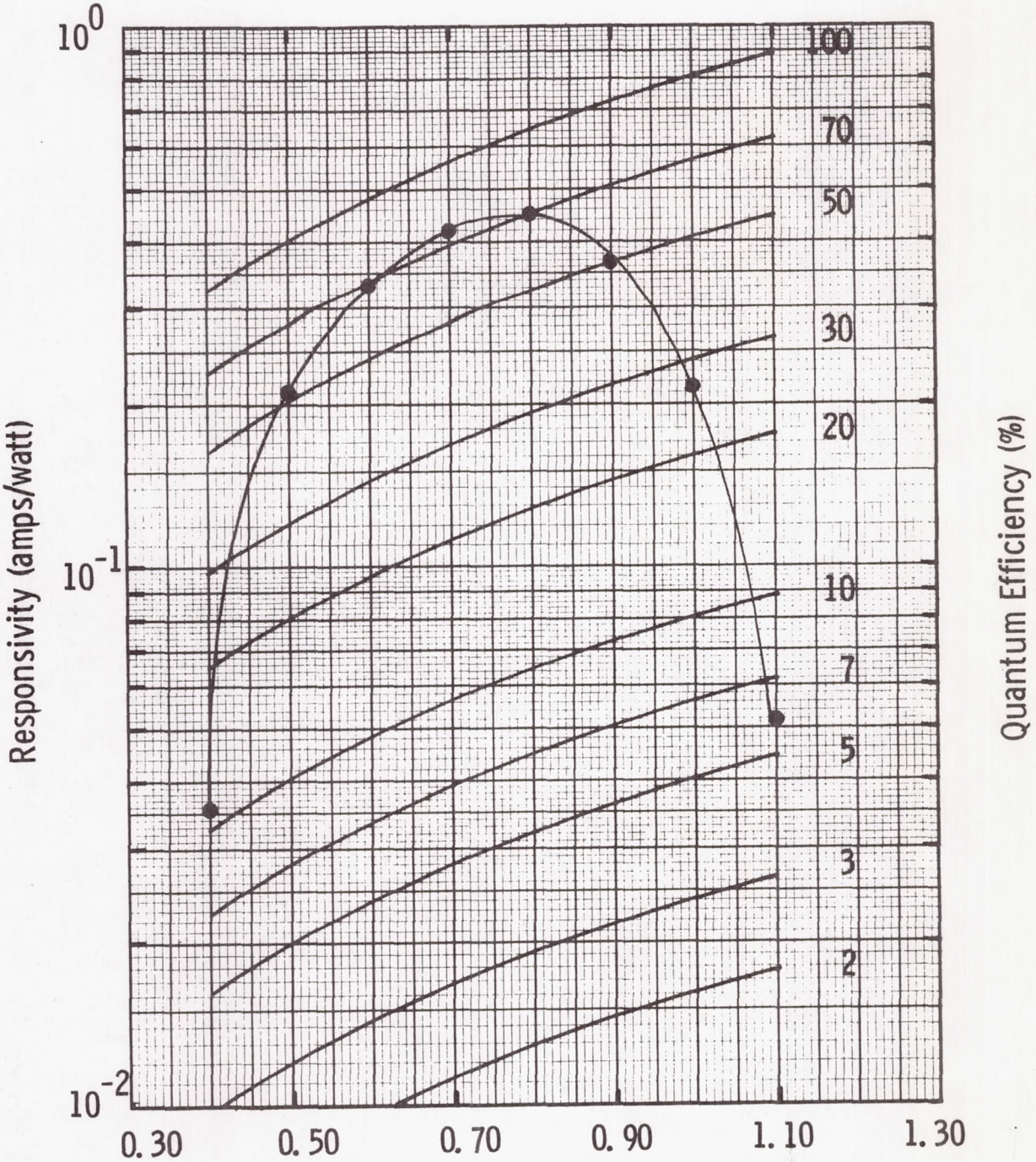

DATA RATE 3.0 MHz

FRAME TIME 50 MS

TEMPERATURE 25 °C

CENTRAL RESEARCH LABORATORIES
CCD Optical and Electrical
Characterization Test Report

for

Customer NASA/GODDARD SPACE FLIGHT CENTER

Contract No. NAS5-22924

Device No. 395-5-2

Device Type 250 x 400

CCD OPTICAL AND ELECTRICAL CHARACTERIZATION
TEST REPORT

1. CCD DEVICE NUMBER 395-5-2

2. DEVICE TYPE 250 x 400 HEADER TYPE ITT tube header

Active area 0.636 cm^2 , pixel dimensions 1.08 mils x 0.9 mils

3. OPERATING LEVELS in volts

Substrate	-.5	Lower reference	20
Parallel clocks	14	Upper reference	20
Serial clocks	15	Lower drain	28
Input diode	32	Upper drain	28
Output gate	2	Precharge pulse	9

4. AMPLIFIER CONFIGURATION used for the tests in this report:
precharge amplifier with off-chip load

5. SPECTRAL RESPONSE (see accompanying graph)

Quantum efficiency is 24.6 % at 0.4 microns

69.1 % at 0.7 microns

20.6 % at 1.0 microns

6. DARK CURRENT measured by the precharge method

66.4 nanoamps/cm^2 or 2.7×10^6 electrons/pixel/sec

T = 25 C, data rate 4.0 MHz, frame time 100 ms

7. R.M.S. NOISE ELECTRONS/PIXEL

Dark current shot noise 520(100ms) electrons added in quadrature to a readout noise of 30 electrons gives a calculated R.M.S. noise of 520 electrons/pixel

8. FULL WELL CHARGE CAPABILITY, determined from the saturation exposure level, is 1.8×10^6 electrons.

9. DYNAMIC RANGE is computed to be 3500 :1.

10. CHARGE TRANSFER EFFICIENCY at 4.0 MHz is >0.99996.

11. COMMENTS open electrode in the lower serial register

CCD IMAGING PERFORMANCE

Device Number 395-5-2 Device Type 250 x 400

Light Source strobe °K Spectral filter none microns

Temperature 25 °C Data rate 4.0 MHz

Frame time 54 ms

ORIGINAL PAGE IS OF POOR QUALITY

CCD DARK CURRENT UNIFORMITY

Device Number 395-5-2 Device Type 250 x 400

ORIGINAL PAGE IS
OF POOR QUALITY

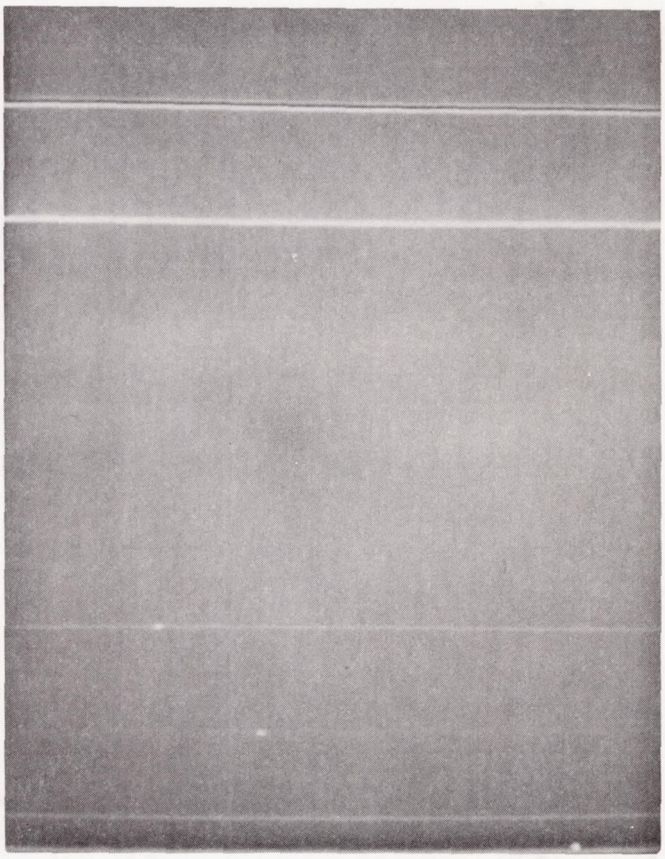

VIDEO MONITOR DISPLAY

Temperature 25 °C

Data rate 4.0 MHz

Frame time 87 ms

CCD DARK CURRENT UNIFORMITY

Device Number 395-5-2 Device Type 250 x 400

Temperature 25 °C Data rate 4.0 MHz

Frame time 87 ms

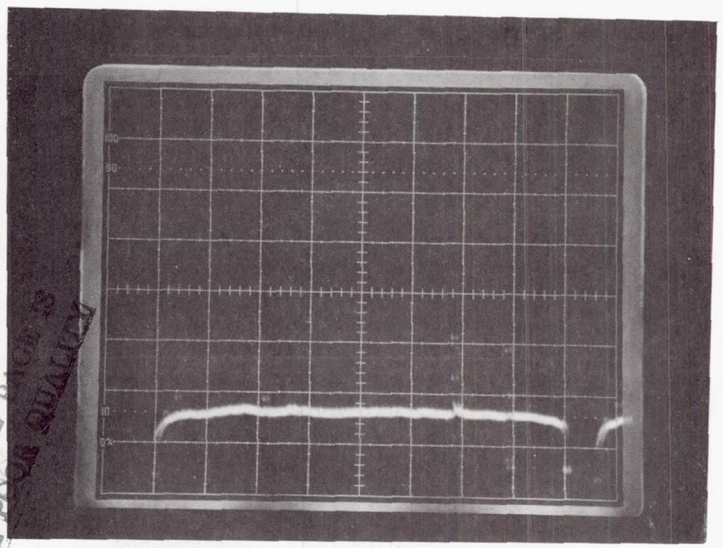

ORIGINAL PAGE IS OF POOR QUALITY

ORIGINAL PAGE IS OF POOR QUALITY

Oscilloscope presentation

Video line number 50

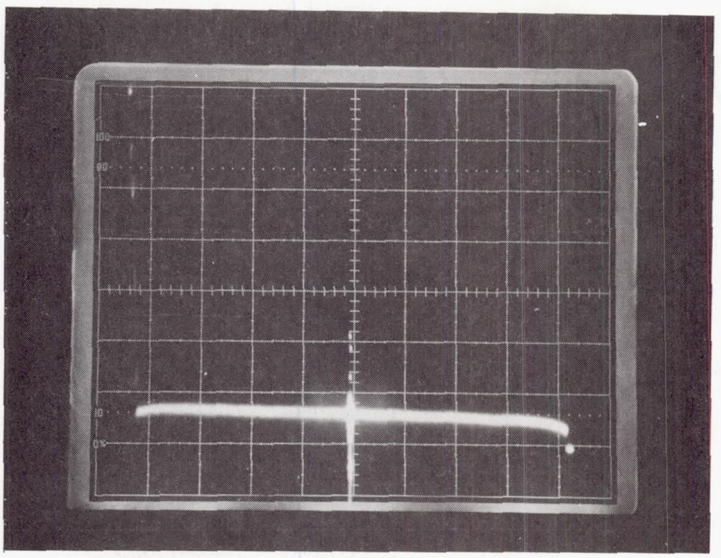

Oscilloscope presentation

Complete video frame

CCD UNIFORMITY OF RESPONSE

Device Number 395-5-2 Device Type 250 x 400

ORIGINAL PAGE IS
OF POOR QUALITY

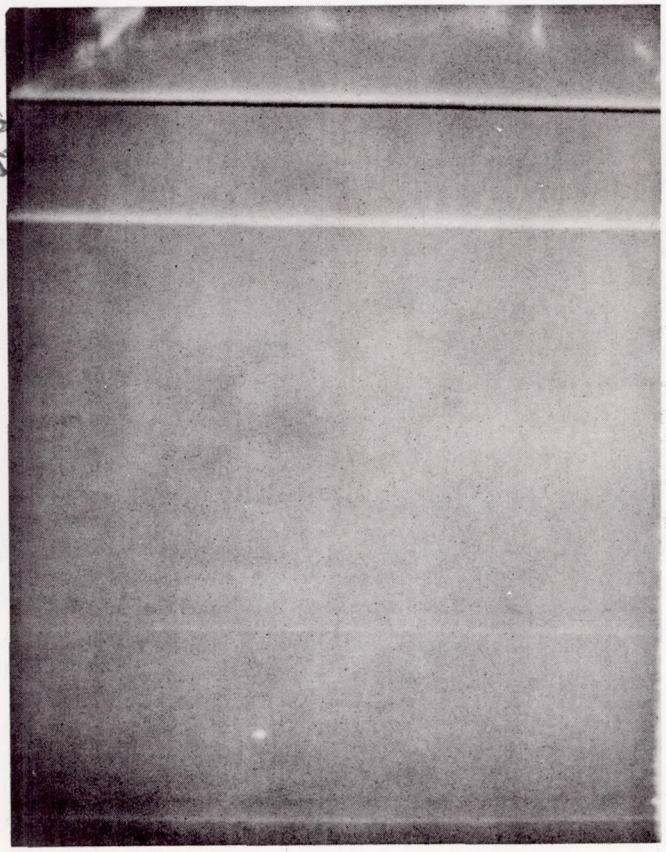

VIDEO MONITOR DISPLAY

Light source	3400	°K
Spectral filter	0.4000	microns
Average well population	50	%
Temperature	25	°C
Data rate	4.0	MHz
Frame time	171	ms

CCD UNIFORMITY OF RESPONSE

Device Number 395-5-2 Device Type 250 x 400

Light source 3400 °K Spectral filter 0,4000 microns

Average well population 50 % Temperature 25 °C

Data rate 4.0 MHz Frame time 171 ms

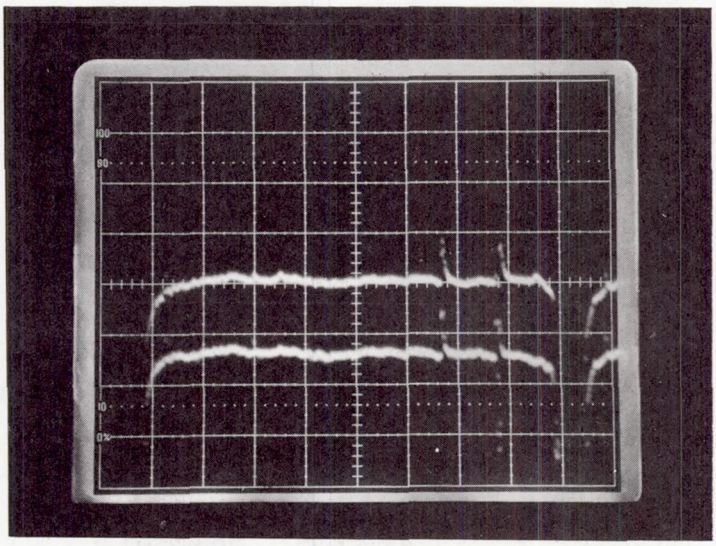

ORIGINAL PAGE IS
OF POOR QUALITY

Oscilloscope presentation
Video line number 50

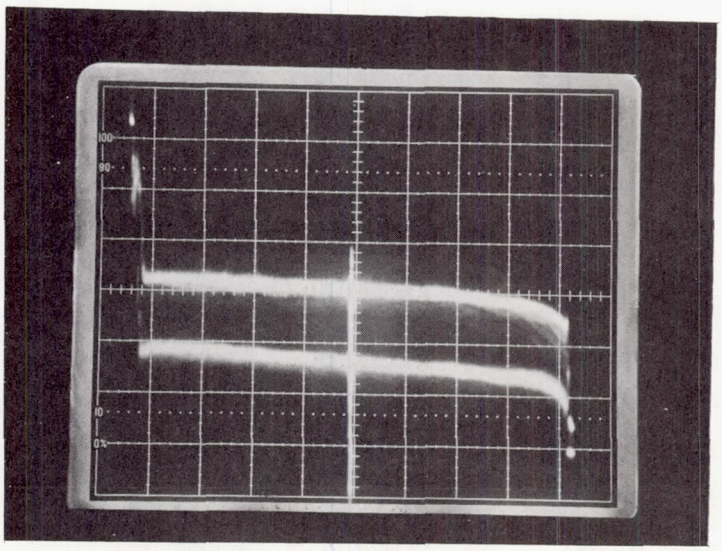

Oscilloscope presentation
Complete video frame

CCD SPECTRAL RESPONSIVITY

Device 395-5-2

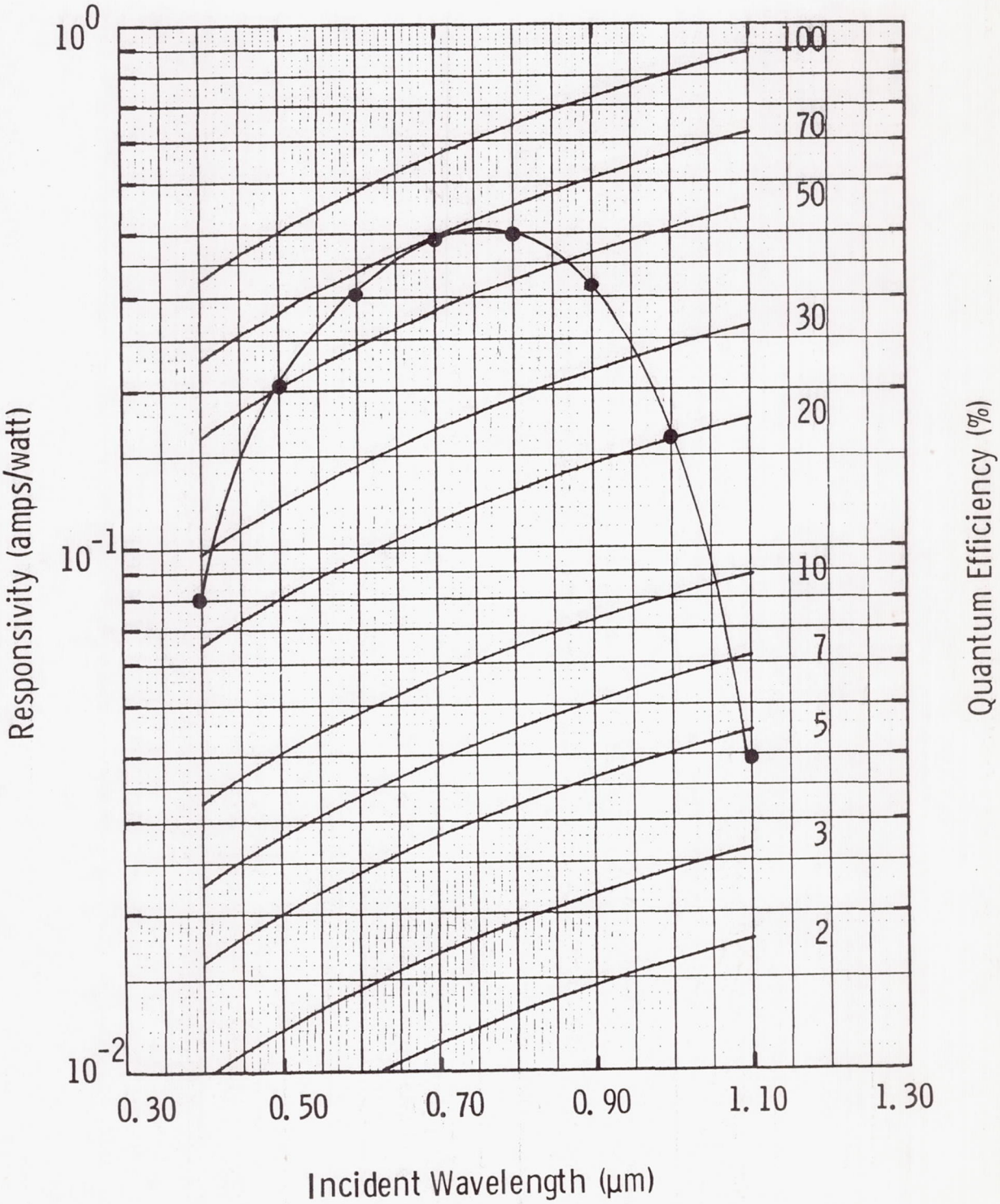

DATA RATE 3.0 MHz

FRAME TIME 50 MS

TEMPERATURE 25 °C

CENTRAL RESEARCH LABORATORIES
CCD Optical and Electrical
Characterization Test Report

for

Customer NASA/GODDARD SPACE FLIGHT CENTER

Contract No. NAS5-22924

Device No. 395-10-3

Device Type 250 x 400

CCD OPTICAL AND ELECTRICAL CHARACTERIZATION
TEST REPORT

1. CCD DEVICE NUMBER 395-10-3

2. DEVICE TYPE 250 x 400 HEADER TYPE ITT tube header

Active area 0.636 cm^2 , pixel dimensions 1.08 mils x 0.9 mils

3. OPERATING LEVELS in volts

Substrate	-.5	Lower reference	20
Parallel clocks	14	Upper reference	20
Serial clocks	15	Lower drain	28
Input diode	32	Upper drain	28
Output gate	2	Precharge pulse	9

4. AMPLIFIER CONFIGURATION used for the tests in this report:
precharge amplifier with off-chip load

5. SPECTRAL RESPONSE (see accompanying graph)

Quantum efficiency is 16.0 % at 0.4 microns

69.1 % at 0.7 microns

21.1 % at 1.0 microns

6. DARK CURRENT measured by the precharge method

61 nanoamps/cm^2 or 2.5×10^6 electrons/pixel/sec

T = 25 C, data rate 4.0 MHz, frame time 100 ms

7. R.M.S. NOISE ELECTRONS/PIXEL
Dark current shot noise 500(100ms) electrons added in quadrature to a readout noise of 30 electrons gives a calculated R.M.S. noise of 500 electrons/pixel

8. FULL WELL CHARGE CAPABILITY, determined from the saturation exposure level, is 2.0×10^6 electrons.

9. DYNAMIC RANGE is computed to be 4000 :1.

10. CHARGE TRANSFER EFFICIENCY at 4.0 MHz is >0.99996.

11. COMMENTS reverse operation best; forward operation gives an inverted image

CCD IMAGING PERFORMANCE

Device Number 395-10-3 Device Type 250 x 400

Light Source strobe °K Spectral filter none microns

Temperature 25 °C Data rate 4.0 MHz

Frame time 54 ms

ORIGINAL PAGE IS OF POOR QUALITY

CCD DARK CURRENT UNIFORMITY

Device Number 395-10-3 Device Type 250 x 400

ORIGINAL PAGE IS
OF POOR QUALITY

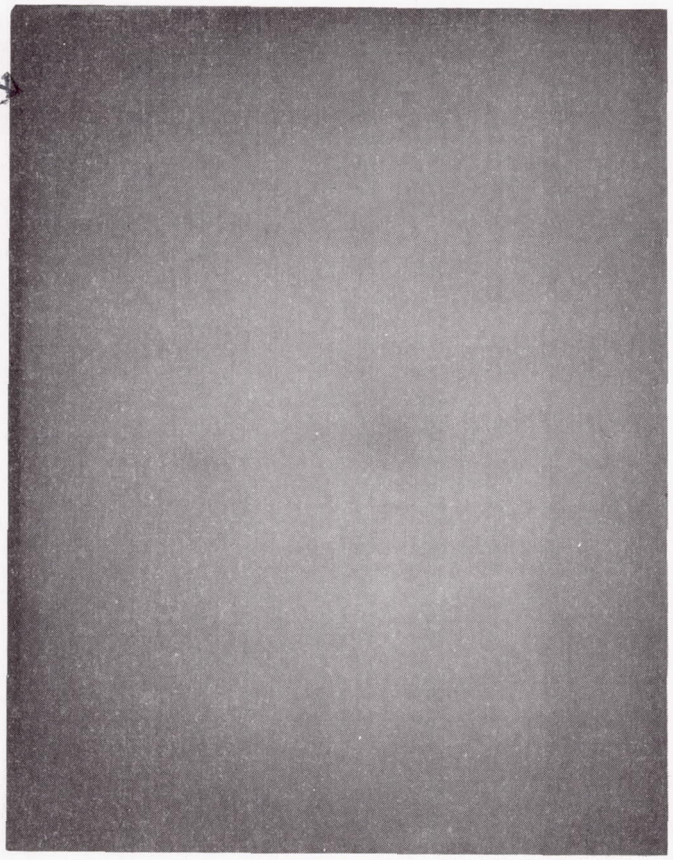

VIDEO MONITOR DISPLAY

Temperature 25 °C

Data rate 4.0 MHz

Frame time 87 ms

CCD DARK CURRENT UNIFORMITY

Device Number 395-10-3 Device Type 250 x 400

Temperature 25 °C Data rate 4.0 MHz

Frame time 87 ms

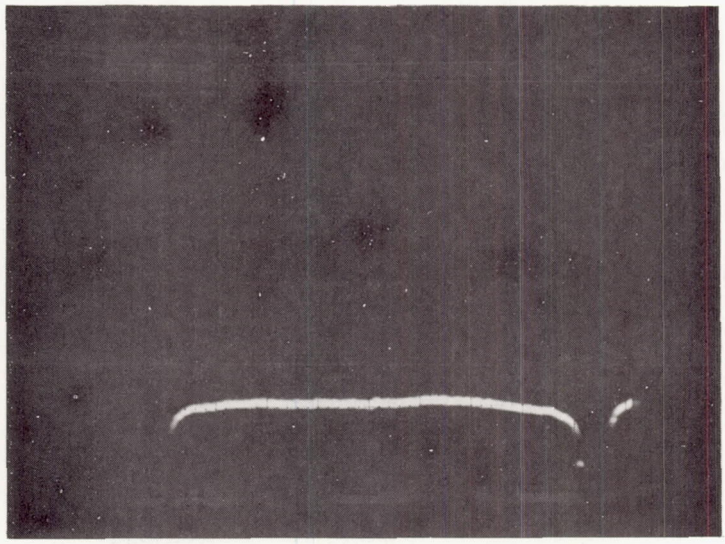

ORIGINAL PAGE IS OF POOR QUALITY

Oscilloscope presentation

Video line number 50

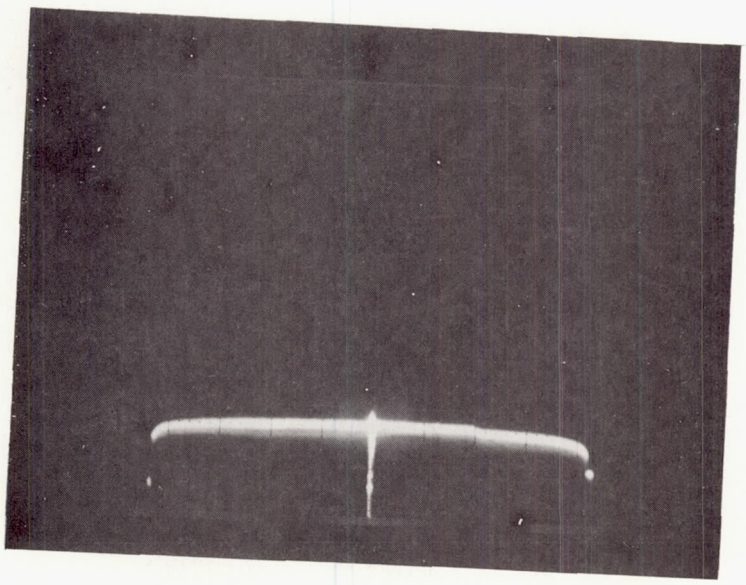

Oscilloscope presentation

Complete video frame

CCD UNIFORMITY OF RESPONSE

Device Number 395-10-3 Device Type 250 x 400

ORIGINAL PAGE IS
OF POOR QUALITY

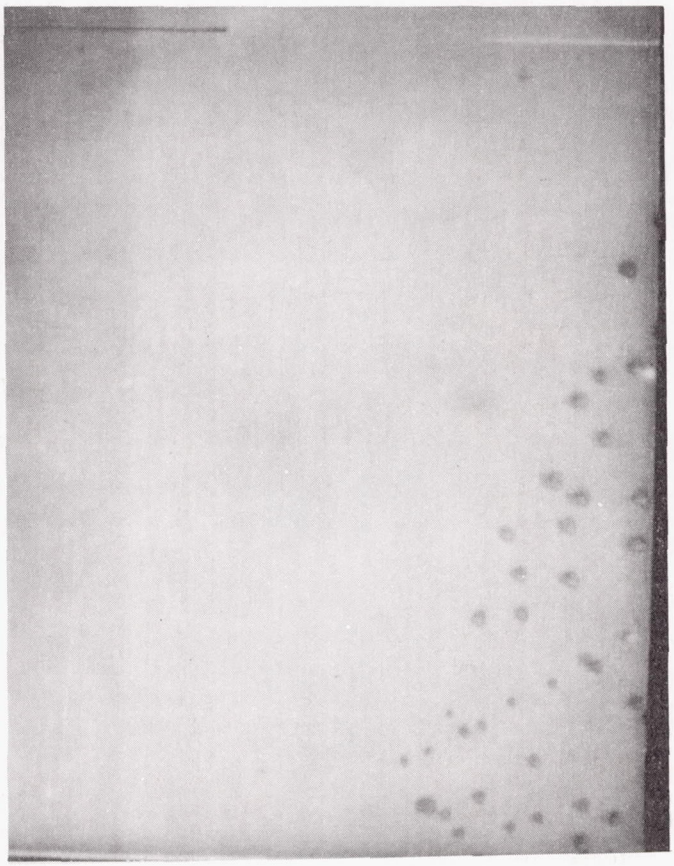

VIDEO MONITOR DISPLAY

Light source	3400	°K
Spectral filter	0.4000	microns
Average well population	50	%
Temperature	25	°C
Data rate	4.0	MHz
Frame time	155	ms

CCD UNIFORMITY OF RESPONSE

Device Number 395-10-3 Device Type 250 x 400

Light source 3400 °K Spectral filter 0,4000 microns

Average well population 50 % Temperature 25 °C

Data rate 4.0 MHz Frame time 155 ms

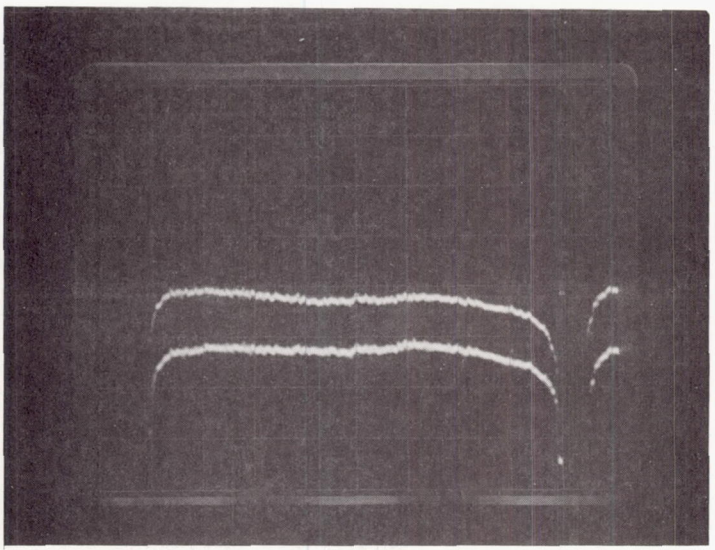

ORIGINAL PAGE IS
OF POOR QUALITY

Oscilloscope presentation
Video line number 50

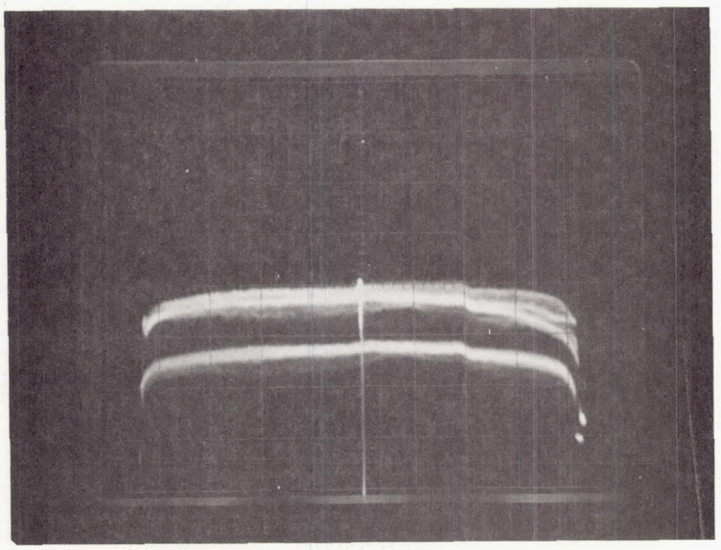

Oscilloscope presentation
Complete video frame

CCD SPECTRAL RESPONSIVITY

Device 395-10-3

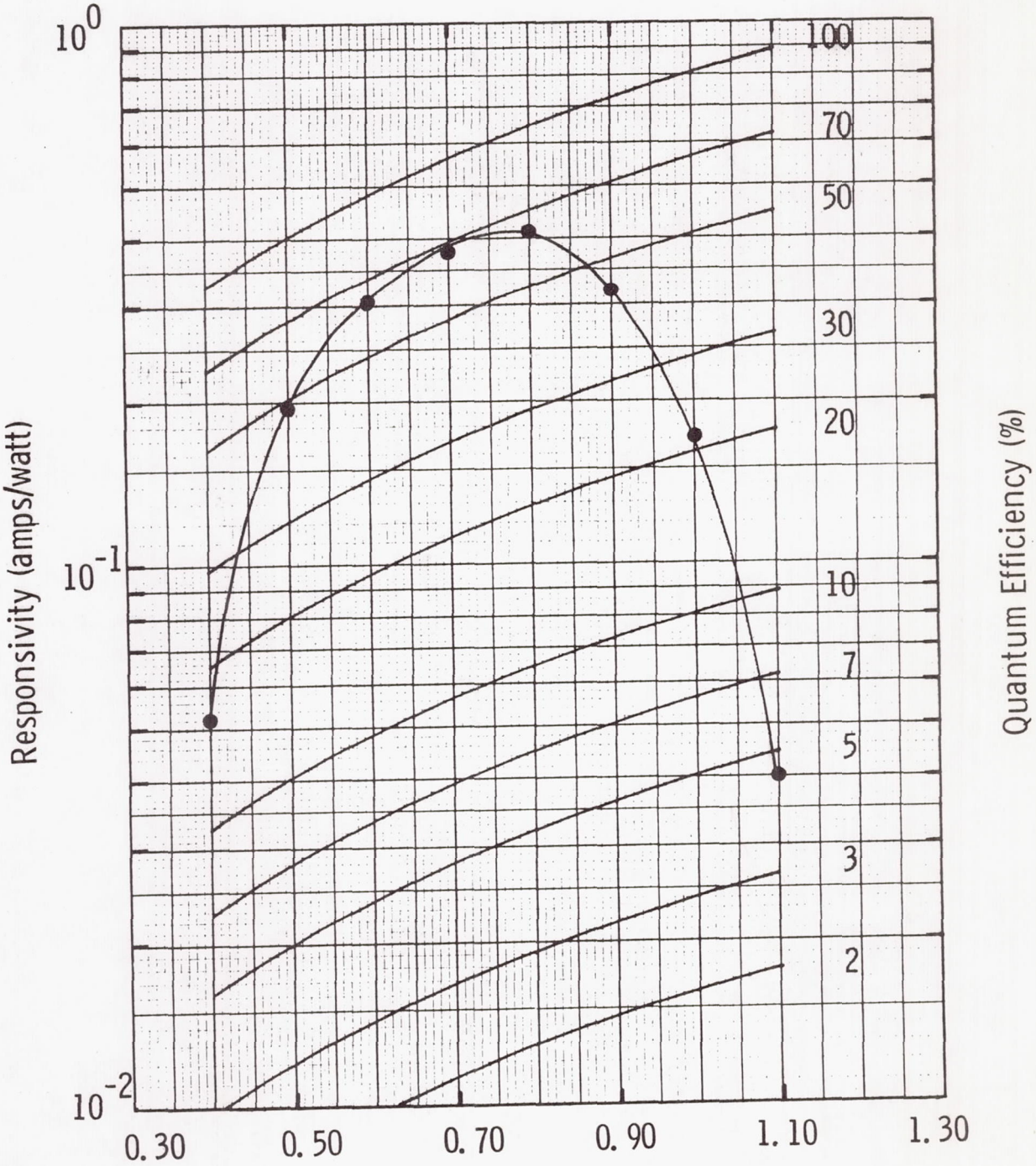

DATA RATE 3.0 MHz

FRAME TIME 50 MS

TEMPERATURE 25 °C

CENTRAL RESEARCH LABORATORIES
CCD Optical and Electrical
Characterization Test Report

for

Customer NASA/GODDARD SPACE FLIGHT CENTER

Contract No. NAS5-22924

Device No. 395-10-5

Device Type 250 x 400

CCD OPTICAL AND ELECTRICAL CHARACTERIZATION
TEST REPORT

1. CCD DEVICE NUMBER 395-10-5

2. DEVICE TYPE 250 x 400 HEADER TYPE ITT tube header

Active area 0.636 cm^2 , pixel dimensions 1.08 mils x 0.9 mils

3. OPERATING LEVELS in volts

Substrate	-.5	Lower reference	20
Parallel clocks	14	Upper reference	20
Serial clocks	15	Lower drain	28
Input diode	32	Upper drain	28
Output gate	2	Precharge pulse	9

4. AMPLIFIER CONFIGURATION used for the tests in this report:
precharge amplifier with off-chip load

5. SPECTRAL RESPONSE (see accompanying graph)

Quantum efficiency is 16.0 % at 0.4 microns

58.2 % at 0.7 microns

19.3 % at 1.0 microns

6. DARK CURRENT measured by the precharge method

60.5 nanoamps/cm^2 or 2.4×10^6 electrons/pixel/sec

T = 25 C, data rate 4.0 MHz, frame time 100 ms

7. R.M.S. NOISE ELECTRONS/PIXEL

Dark current shot noise 490 (100ms) electrons added in quadrature to a readout noise of 30 electrons gives a calculated R.M.S. noise of 490 electrons/pixel

8. FULL WELL CHARGE CAPABILITY, determined from the saturation exposure level, is 1.6×10^6 electrons.

9. DYNAMIC RANGE is computed to be 3200 :1.

10. CHARGE TRANSFER EFFICIENCY at 4.0 MHz is >0.99996.

11. COMMENTS

CCD IMAGING PERFORMANCE

Device Number 395-10-5 Device Type 250 x 400

Light Source strobe °K Spectral filter none microns

Temperature 25 °C Data rate 4.0 MHz

Frame time 54 ms

ORIGINAL PAGE IS OF POOR QUALITY

CCD DARK CURRENT UNIFORMITY

Device Number 395-10-5 Device Type 250 x 400

ORIGINAL PAGE IS
OF POOR QUALITY

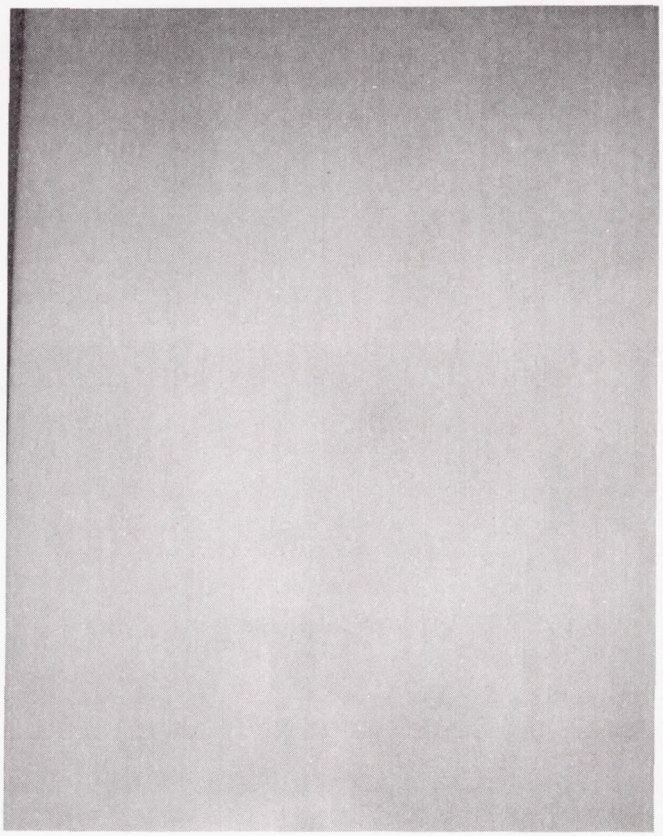

VIDEO MONITOR DISPLAY

Temperature 25 °C

Data rate 4.0 MHz

Frame time 87 ms

CCD DARK CURRENT UNIFORMITY

Device Number 395-10-5 Device Type 250 x 400

Temperature 25 °C Data rate 4.0 MHz

Frame time 87 ms

ORIGINAL PAGE IS OF POOR QUALITY

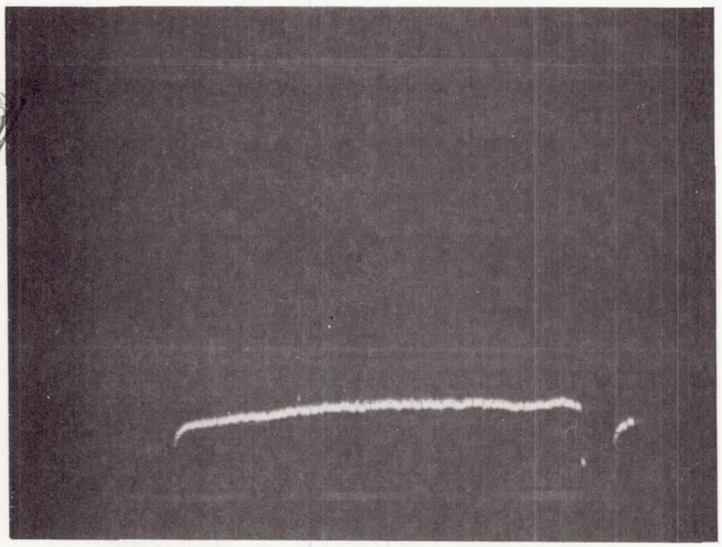

Oscilloscope presentation

Video line number 50

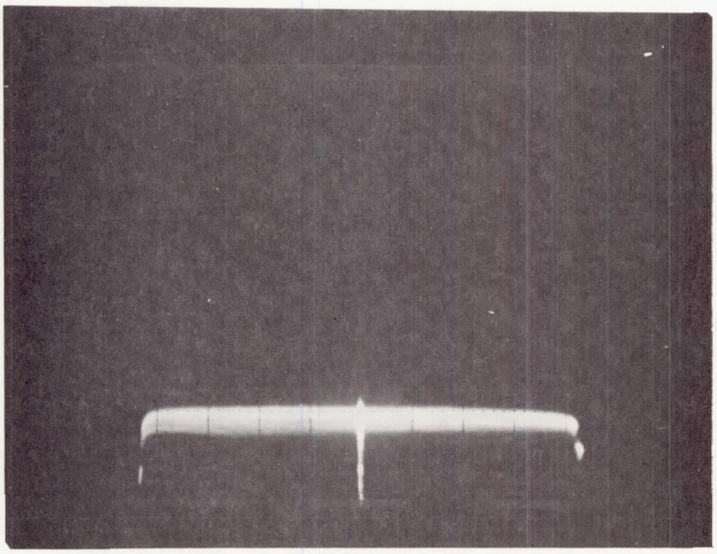

Oscilloscope presentation

Complete video frame

CCD UNIFORMITY OF RESPONSE

Device Number 395-10-5 Device Type 250 x 400

ORIGINAL PAGE IS OF POOR QUALITY

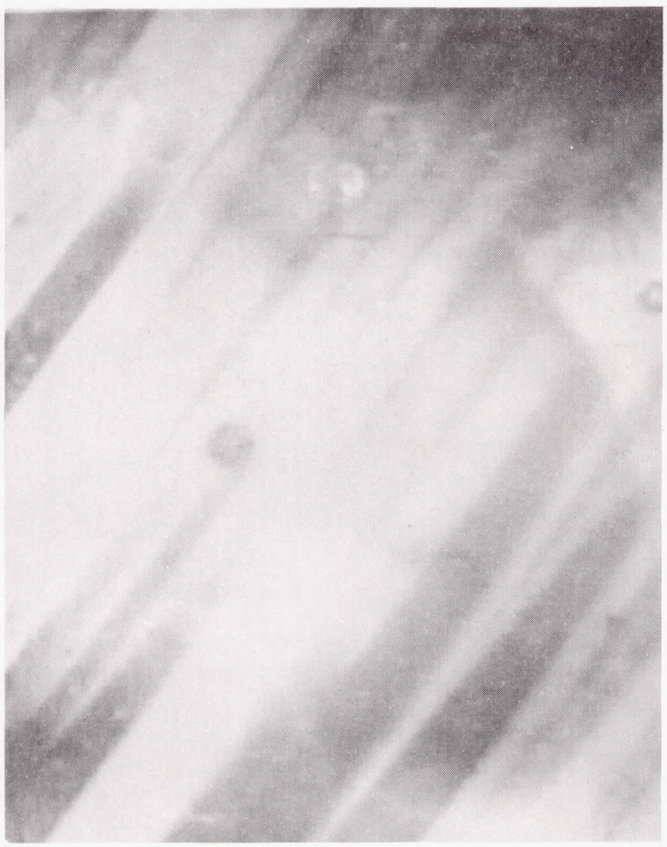

VIDEO MONITOR DISPLAY

Light source	3400	°K
Spectral filter	0.4000	microns
Average well population	50	%
Temperature	25	°C
Data rate	4.0	MHz
Frame time	159	ms

CCD UNIFORMITY OF RESPONSE

Device Number 395-10-5 Device Type 250 x 400

Light source 3400 °K Spectral filter 0.4000 microns

Average well population 50 % Temperature 25 °C

Data rate 4.0 MHz Frame time 159 ms

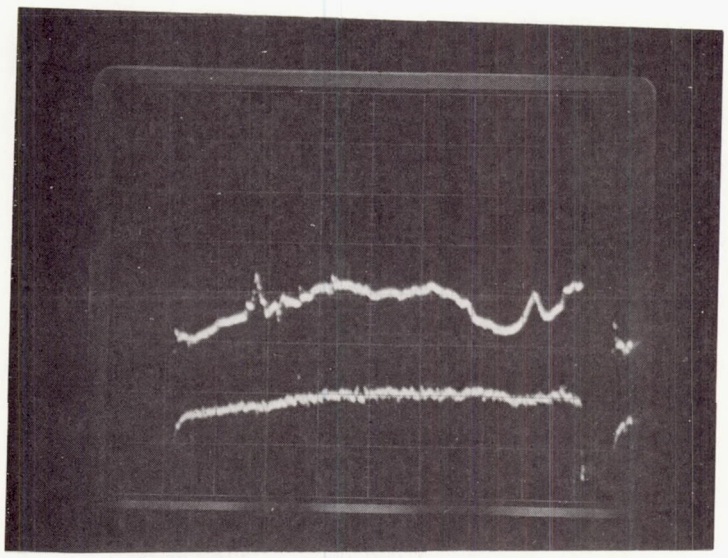

ORIGINAL PAGE IS
OF POOR QUALITY

Oscilloscope presentation
Video line number 50

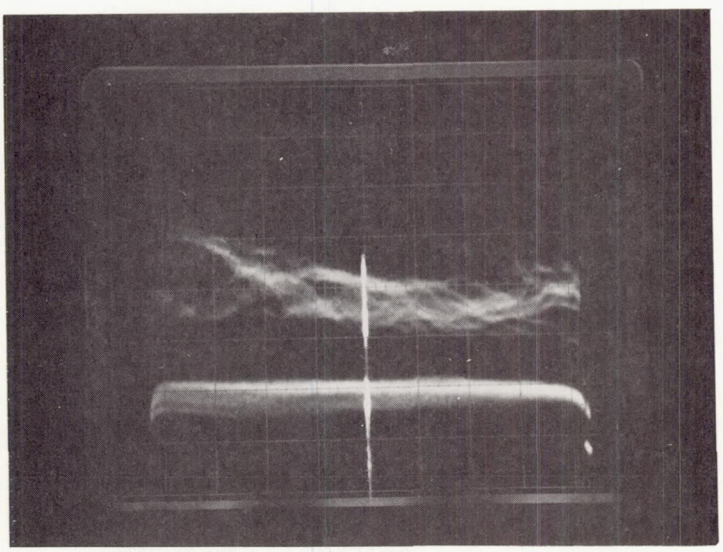

Oscilloscope presentation
Complete video frame

CCD SPECTRAL RESPONSIVITY

Device 395-10-5

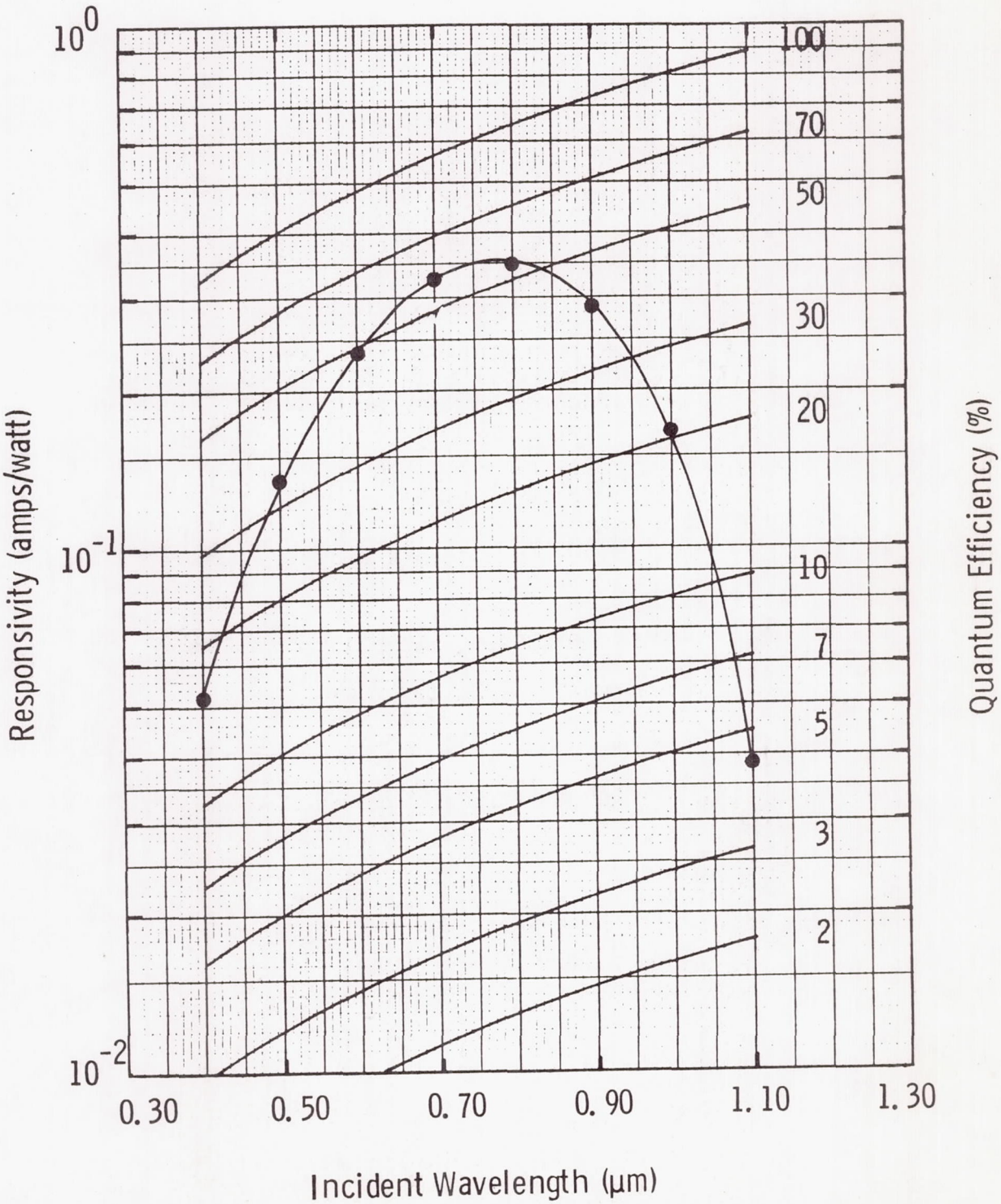

DATA RATE 3.0 MHz

FRAME TIME 50 MS

TEMPERATURE 25 °C

CENTRAL RESEARCH LABORATORIES
CCD Optical and Electrical
Characterization Test Report

for

Customer NASA/GODDARD SPACE FLIGHT CENTER

Contract No. NAS5-22924

Device No. 395-12-3

Device Type 250 x 400

CCD OPTICAL AND ELECTRICAL CHARACTERIZATION
TEST REPORT

1. CCD DEVICE NUMBER 395-12-3

2. DEVICE TYPE 250 x 400 HEADER TYPE ITT tube header

Active area 0.636 cm^2 , pixel dimensions 1.08 mils x 0.9 mils

3. OPERATING LEVELS in volts

Substrate	-.5	Lower reference	20
Parallel clocks	9	Upper reference	20
Serial clocks	15	Lower drain	28
Input diode	32	Upper drain	28
Output gate	2	Precharge pulse	9

4. AMPLIFIER CONFIGURATION used for the tests in this report:
precharge amplifier with off-chip load

5. SPECTRAL RESPONSE (see accompanying graph)

Quantum efficiency is 16.9 % at 0.4 microns

60.5 % at 0.7 microns

20.4 % at 1.0 microns

6. DARK CURRENT measured by the precharge method

28 nanoamps/cm^2 or 1.1×10^6 electrons/pixel/sec

T = 25 C, data rate 4.0 MHz, frame time 100 ms

7. R.M.S. NOISE ELECTRONS/PIXEL

Dark current shot noise 336(100ms) electrons added in quadrature to a readout noise of 30 electrons gives a calculated R.M.S. noise of 338 electrons/pixel

8. FULL WELL CHARGE CAPABILITY, determined from the saturation exposure level, is 9.8×10^5 electrons.

9. DYNAMIC RANGE is computed to be 2900 :1.

10. CHARGE TRANSFER EFFICIENCY at 4.0 MHz is 0.99996.

11. COMMENTS forward operation only

CCD IMAGING PERFORMANCE

Device Number 395-12-3 Device Type 250 x 400

Light Source strobe °K Spectral Filter none microns

Temperature 25 °C Data rate 4.0 MHz

Frame time 54 ms

ORIGINAL PAGE IS OF POOR QUALITY

CCD DARK CURRENT UNIFORMITY

Device Number 395-12-3 Device Type 250 x 400

ORIGINAL PAGE IS
OF POOR QUALITY

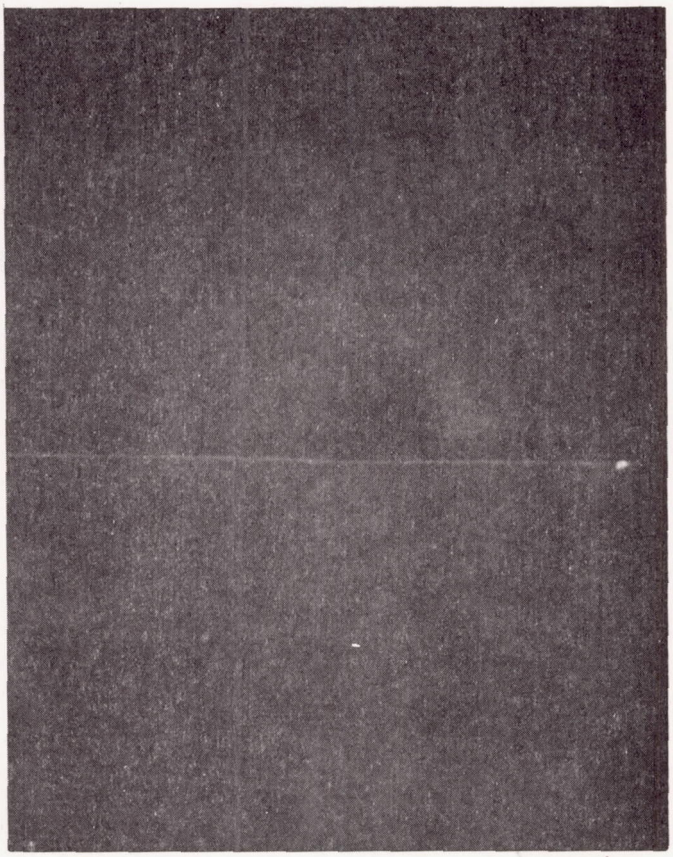

VIDEO MONITOR DISPLAY

Temperature 25 °C

Data rate 4.0 MHz

Frame time 87 ms

CCD DARK CURRENT UNIFORMITY

Device Number 395-12-3 Device Type 250 x 400

Temperature 25 °C Data rate 4.0 MHz

Frame time 87 ms

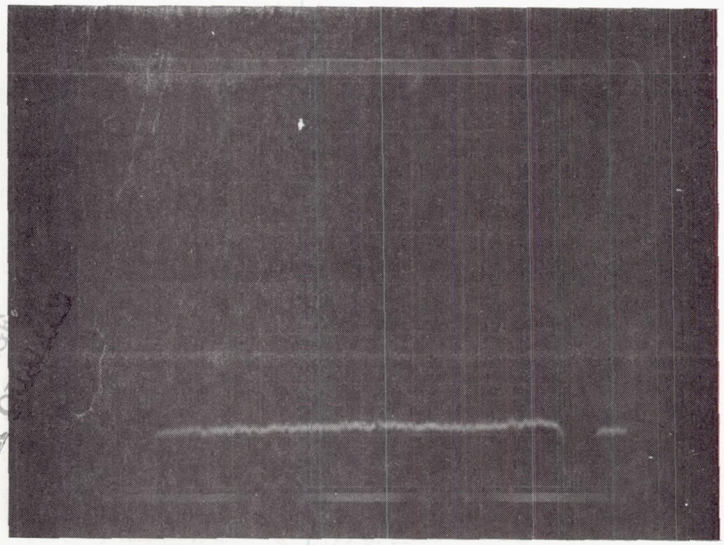

ORIGINAL PAGE IS OF POOR QUALITY

Oscilloscope presentation

Video line number 50

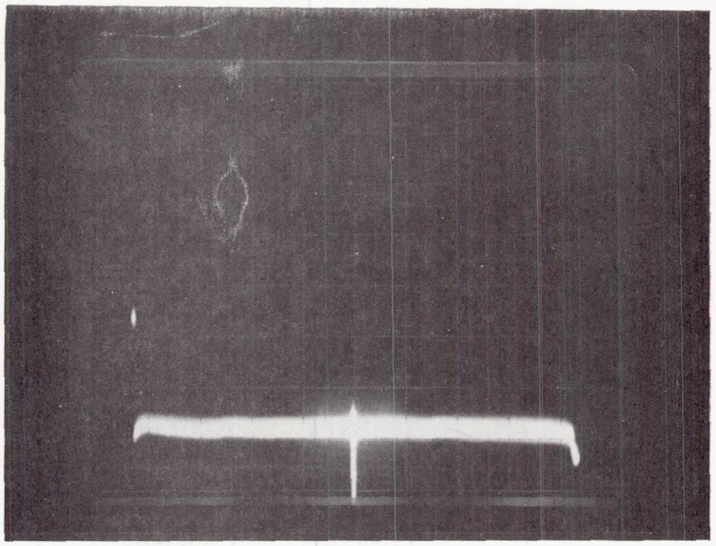

Oscilloscope presentation

Complete video frame

CCD UNIFORMITY OF RESPONSE

Device Number 395-12-3 Device Type 250 x 400

ORIGINAL PAGE IS OF POOR QUALITY

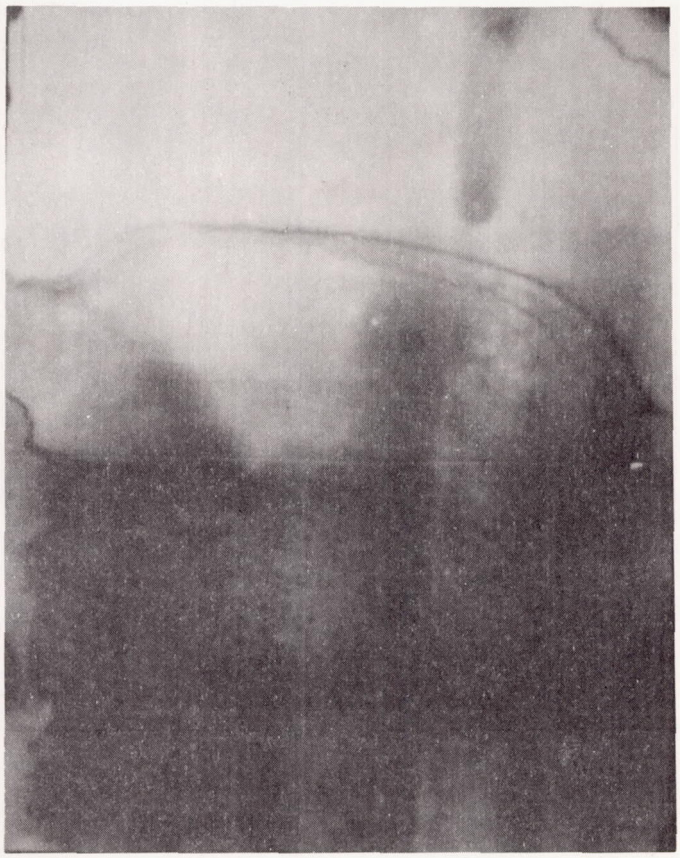

VIDEO MONITOR DISPLAY

Light source	3400	°K
Spectral filter	0.4000	microns
Average well population	50	%
Temperature	25	°C
Data rate	4.0	MHz
Frame time	87	ms

CCD UNIFORMITY OF RESPONSE

Device Number 395-12-3 Device Type 250 x 400

Light source 3400 °K Spectral filter 0.4000 microns

Average well population 50 % Temperature 25 °C

Data rate 4.0 MHz Frame time 87 ms

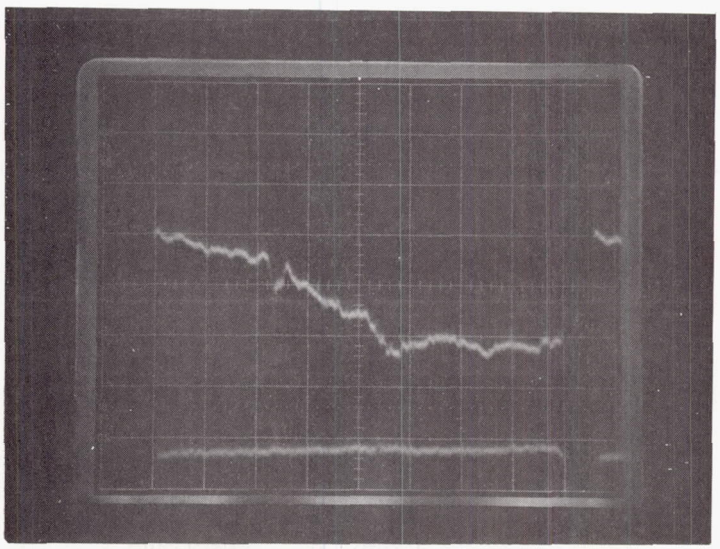

ORIGINAL PAGE IS
OF POOR QUALITY

Oscilloscope presentation
Video line number 50

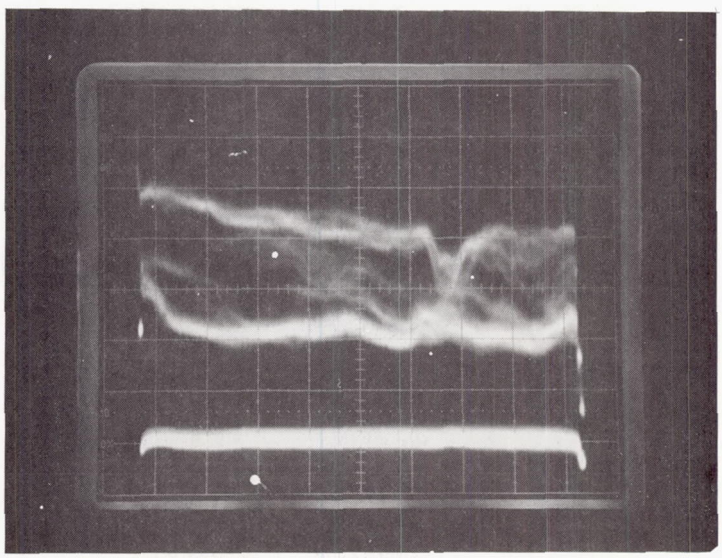

Oscilloscope presentation
Complete video frame

CCD SPECTRAL RESPONSIVITY

Device 395-12-3

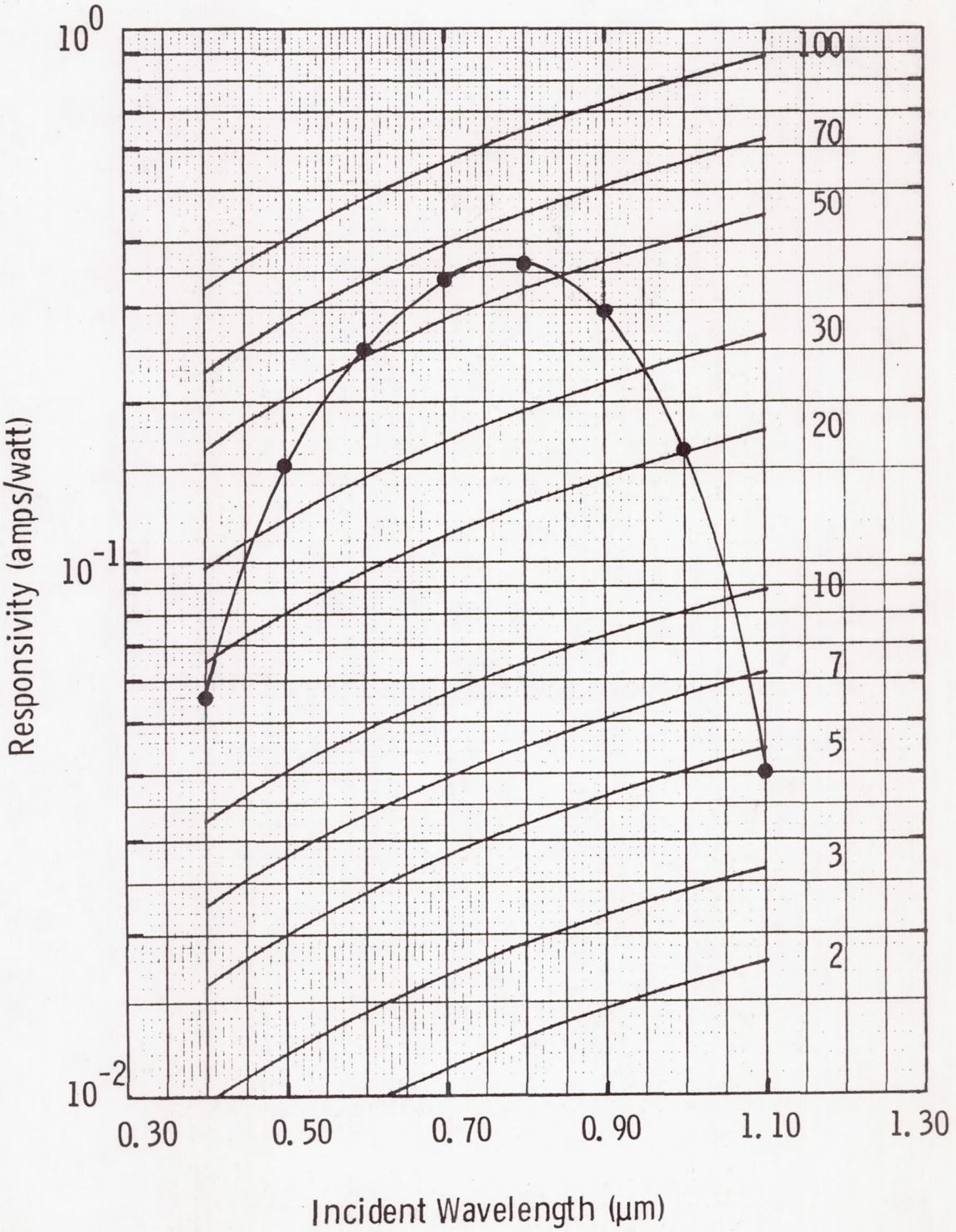

DATA RATE 3.0 MHz

FRAME TIME 50 MS

TEMPERATURE 25 °C

CENTRAL RESEARCH LABORATORIES
CCD Optical and Electrical
Characterization Test Report

for

Customer NASA/GODDARD SPACE FLIGHT CENTER

Contract No. NAS5-22924

Device No. 395-12-6

Device Type 250 x 400

CCD OPTICAL AND ELECTRICAL CHARACTERIZATION
TEST REPORT

1. CCD DEVICE NUMBER 395-12-6

2. DEVICE TYPE 250 x 400 HEADER TYPE ITT tube header

Active area 0.636 cm^2 , pixel dimensions 1.08 mils x 0.9 mils

3. OPERATING LEVELS in volts

Substrate	-.5	Lower reference	20
Parallel clocks	8	Upper reference	20
Serial clocks	8	Lower drain	28
Input diode	32	Upper drain	28
Output gate	2	Precharge pulse	9

4. AMPLIFIER CONFIGURATION used for the tests in this report:
precharge amplifier with off-chip load

5. SPECTRAL RESPONSE (see accompanying graph)

Quantum efficiency is 13.2 % at 0.4 microns

62.3 % at 0.7 microns

21.3 % at 1.0 microns

6. DARK CURRENT measured by the precharge method

33 nanoamps/cm^2 or 1.3×10^6 electrons/pixel/sec

T = 25 C, data rate 4.0 MHz, frame time 100 ms

7. R.M.S. NOISE ELECTRONS/PIXEL
Dark current shot noise 360 (100ms) electrons added in quadrature to a readout noise of 30 electrons gives a calculated R.M.S. noise of 360 electrons/pixel

8. FULL WELL CHARGE CAPABILITY, determined from the saturation exposure level, is 6.0×10^5 electrons.

9. DYNAMIC RANGE is computed to be 1650 :1.

10. CHARGE TRANSFER EFFICIENCY at 4.0 MHz is >0.99996.

11. COMMENTS forward operation only

CCD IMAGING PERFORMANCE

Device Number 395-12-6 Device Type 250 x 400

Light Source strobe °K Spectral filter none microns

Temperature 25 °C Data rate 4.0 MHz

Frame time 54 ms

ORIGINAL PAGE IS OF POOR QUALITY

CCD DARK CURRENT UNIFORMITY

Device Number 395-12-6 Device Type 250 x 400

ORIGINAL PAGE IS OF POOR QUALITY

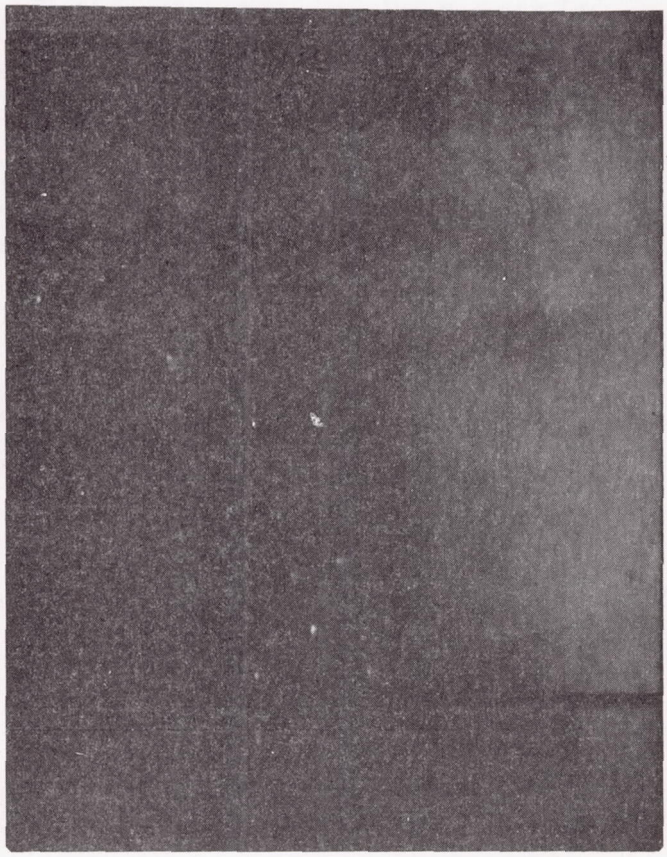

VIDEO MONITOR DISPLAY

Temperature 25 °C

Data rate 4.0 MHz

Frame time 87 ms

CCD DARK CURRENT UNIFORMITY

Device Number 395-12-6 Device Type 250 x 400

Temperature 25 °C Data rate 4.0 MHz

Frame time 87 ms

ORIGINAL PAGE IS
OF POOR QUALITY

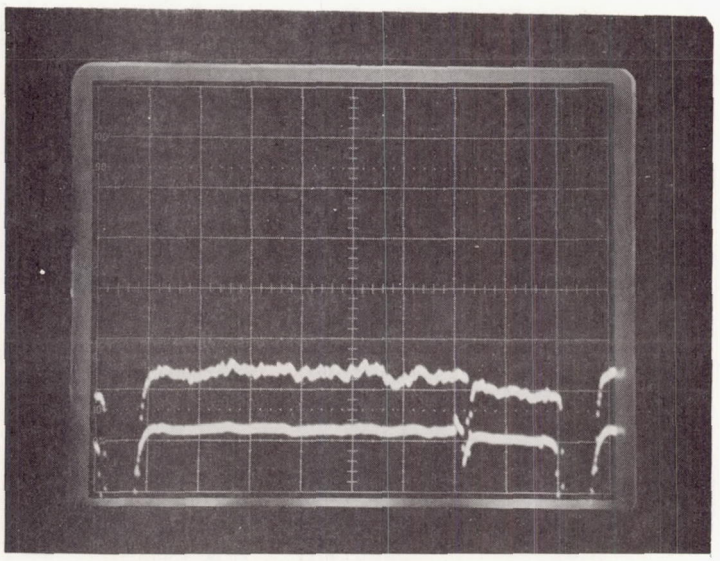

Oscilloscope presentation

Video line number 50

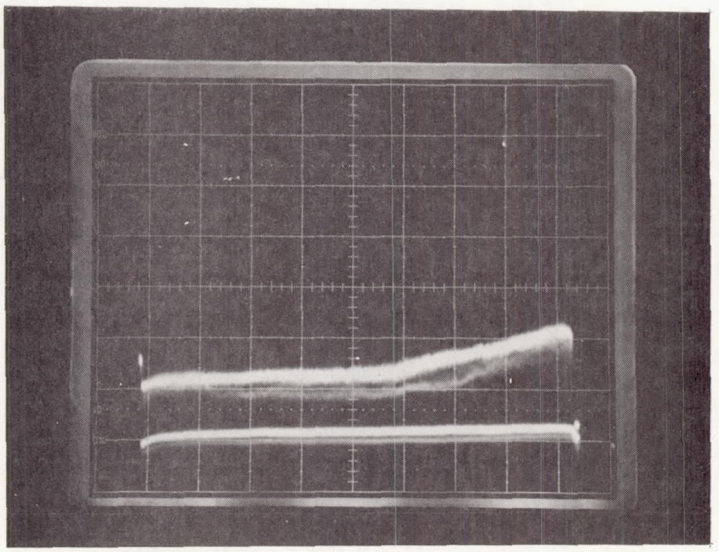

Oscilloscope presentation

Complete video frame

CCD UNIFORMITY OF RESPONSE

Device Number 395-12-6 Device Type 250 x 400

ORIGINAL PAGE IS
OF POOR QUALITY

VIDEO MONITOR DISPLAY

Light source	3400	°K
Spectral filter	0.4000	microns
Average well population	50	%
Temperature	25	°C
Data rate	4.0	MHz
Frame time	87	ms

CCD UNIFORMITY OF RESPONSE

Device Number 395-12-6 Device Type 250 x 400

Light source 3400 °K Spectral filter 0.4000 microns

Average well population 50 % Temperature 25 °C

Data rate 4.0 MHz Frame time 87 ms

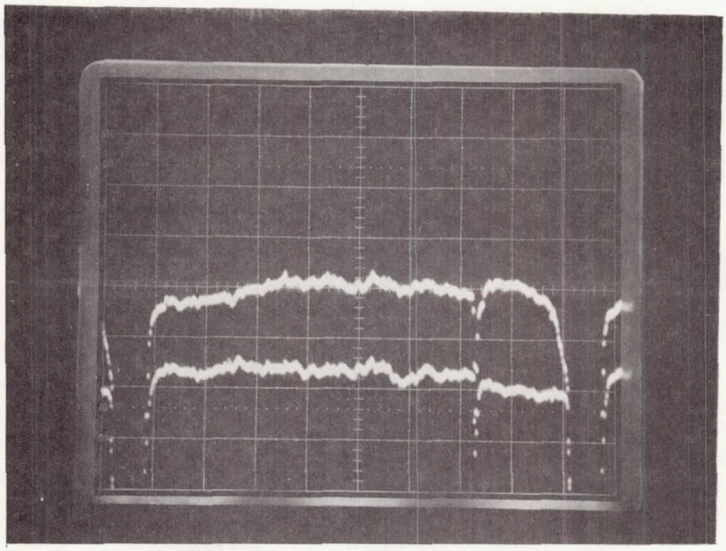

ORIGINAL PAGE IS
OF POOR QUALITY

ORIGINAL PAGE IS
OF POOR QUALITY

Oscilloscope presentation
Video line number 50

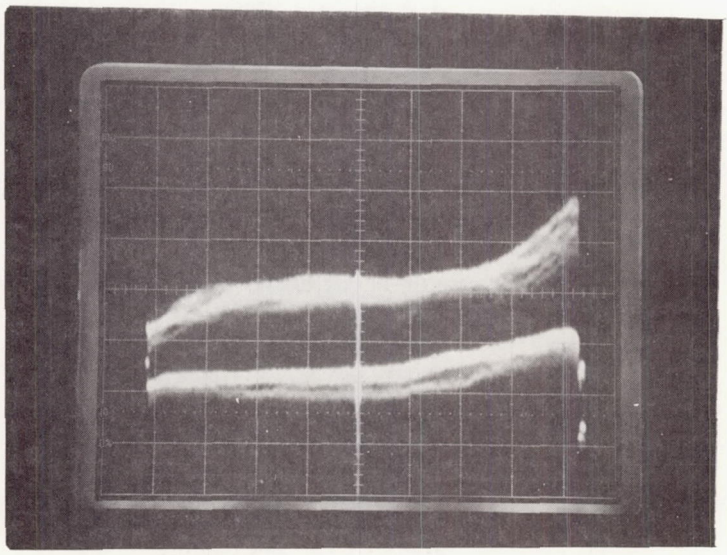

Oscilloscope presentation
Complete video frame

CCD SPECTRAL RESPONSIVITY

Device 395-12-6

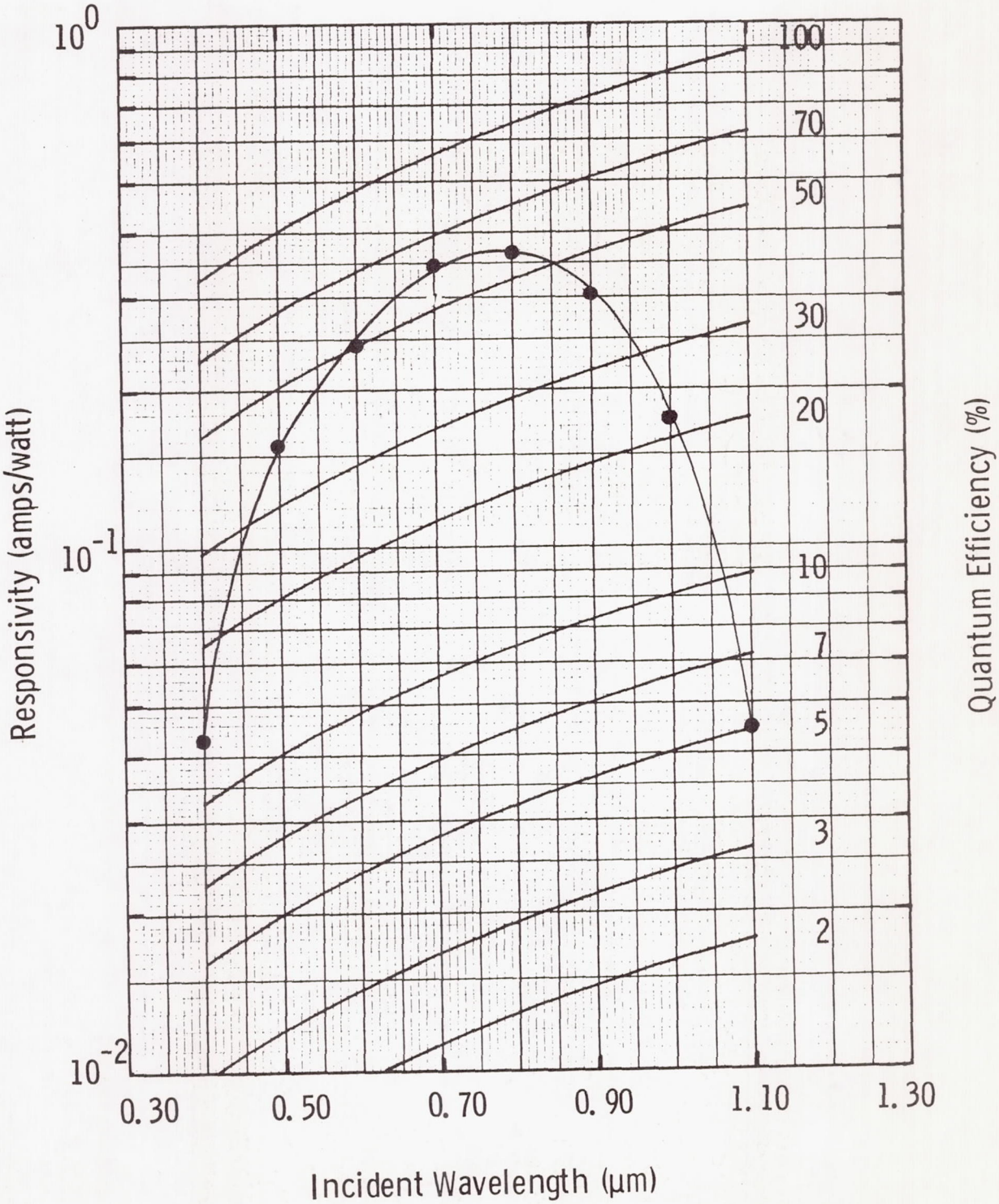

DATA RATE 3.0 MHz

FRAME TIME 50 MS

TEMPERATURE 25 °C

APPENDIX B

BOND PAD PROTECTION DEVELOPMENTS

APPENDIX B

BOND PAD PROTECTION DEVELOPMENTS

A. Bond Pad Protection

1. Bond Strength Degradation

Electrical interconnection is made between the array and the header using gold wire, thermocompression-bonded between the aluminum metallization of the array and the gold metallization of the header. In early work on ICCDs, it was observed that occasionally the gold metallization would separate from the aluminum bond pad after the high temperature (350°C) bake associated with tube processing. This problem was found to be caused by intermetallic formation which led to the introduction of voids in the aluminum-to-gold interface. This effect has been discussed by Philofsky.* According to Philofsky, during the anneal of aluminum-to-gold couples, intermetallic compounds are formed. (Some of these are purple, which leads to the term "purple-plague.") To form these compounds, diffusion of the two metals occurs. In the case of aluminum bond pad, it is possible for enough aluminum to be absorbed by the gold wire to weaken the contact to the array. This can result in bond failure.

Experiments were performed to quantify this effect for typical bonds undergoing a 350°C anneal. To do this, bonding samples were prepared by evaporating the standard thickness of aluminum bond pads (11,000 Å) onto oxidized silicon slices and patterning the metal using the second-level metal mask of the 100 x 160 bar. Gold wire was then thermocompression-bonded from one bond pad to a neighboring pad to form loops of wire. Ten to twenty loops per slice were prepared. Bond strength was determined by pulling on these loops with a calibrated force, increasing this force until either the wire broke or the bond failed. The minimum acceptable pull strength for a bond is generally accepted to be 2 dynes. Measurements on unannealed samples indicated pull strengths ranging from 6 to 14 dynes, all breaks occurring in the wire.

---

* E. Philofsky, Solid State Electronics 13, 1391 (1970).

The initial experiment consisted of isothermal anneals at 350°C. Figure B-1 presents the results of the measurements of pull strength after anneals of two, four, six, and eight hours. Open circles represent wire breaks, Δ's represent bond failure, and dark circles represent the numeric average. The data indicate the following:

(1) There is a gradual degradation in bond pull strength with increasing anneal time; initially, all failures are wire breaks, and finally, all failures are bond separation;

(2) Pull strength degradation seems to saturate with increasing anneal time;

(3) Considerable scatter exists in the data; and

(4) Only one value falls below the 2 dyne limit.

Typical annealing results are illustrated in Figure B-2. Figure B-2(a) shows a bond prior to anneal. Figure B-2(b) shows this same bond after anneal. The dark area surronding the bond is the intermetallic formation. Figure B-2(c) shows a bond pad after pull tests that resulted in bond separation. In the center of the bond area, the aluminum has been completely absorbed, revealing the underlying oxide.

In an attempt to determine causes of the scatter in the data, anneal tests were performed on bonds with varying bond diameters. Small bonds (about twice the wire diameter of 1 mil), medium bonds (about three times the diameter), and large bonds (about four times the diameter) were prepared. The results of the pull tests after anneal were significant. All the small bonds annealed failed the 2 dyne limit, all the large bonds passed the 2 dyne limit, and the medium bonds resulted in a mixture of passes and failures. All bonds displayed visual degradation similar to Figure B-2(b).

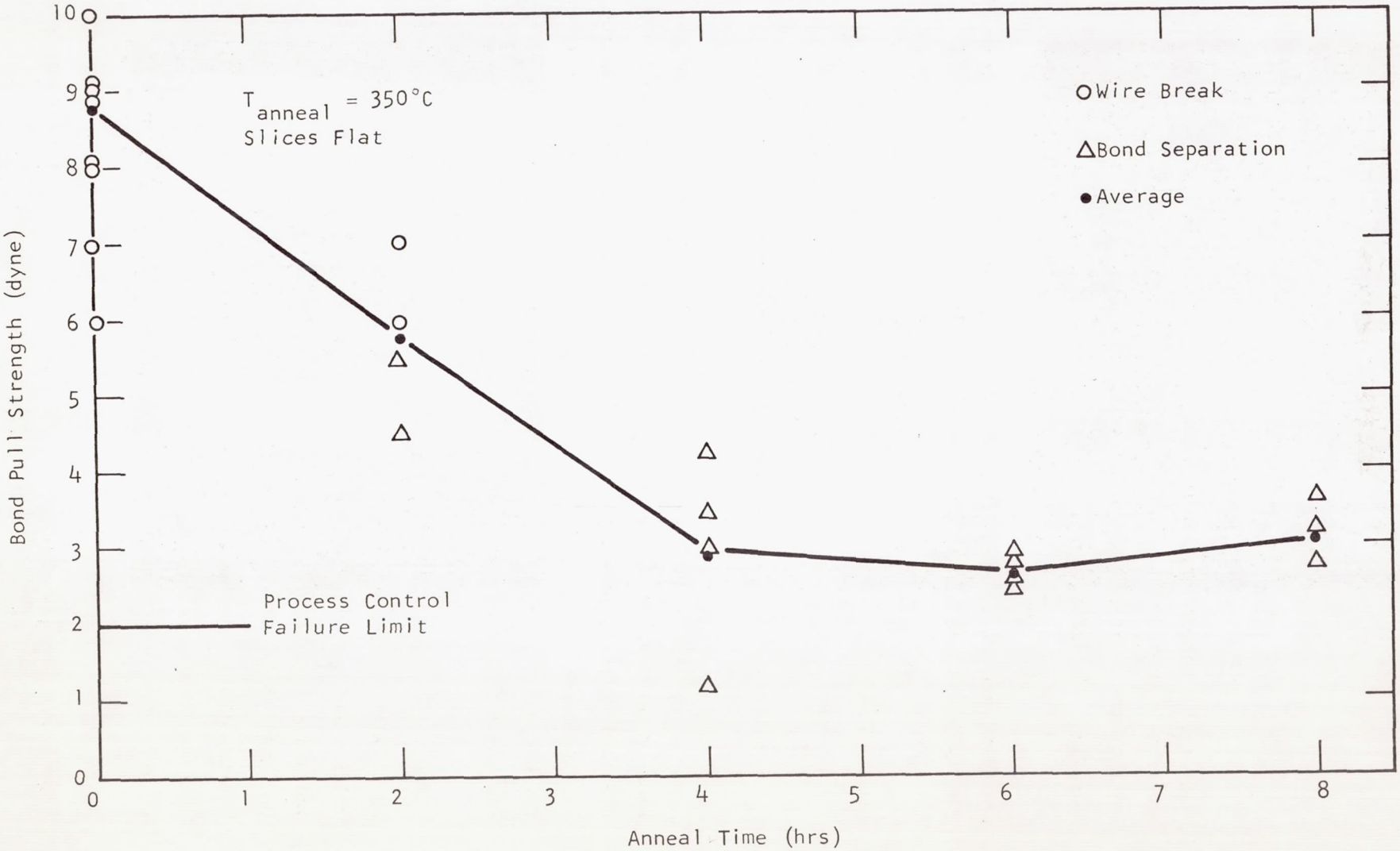

Figure B-1 Bond Strength Degradation at 350°C

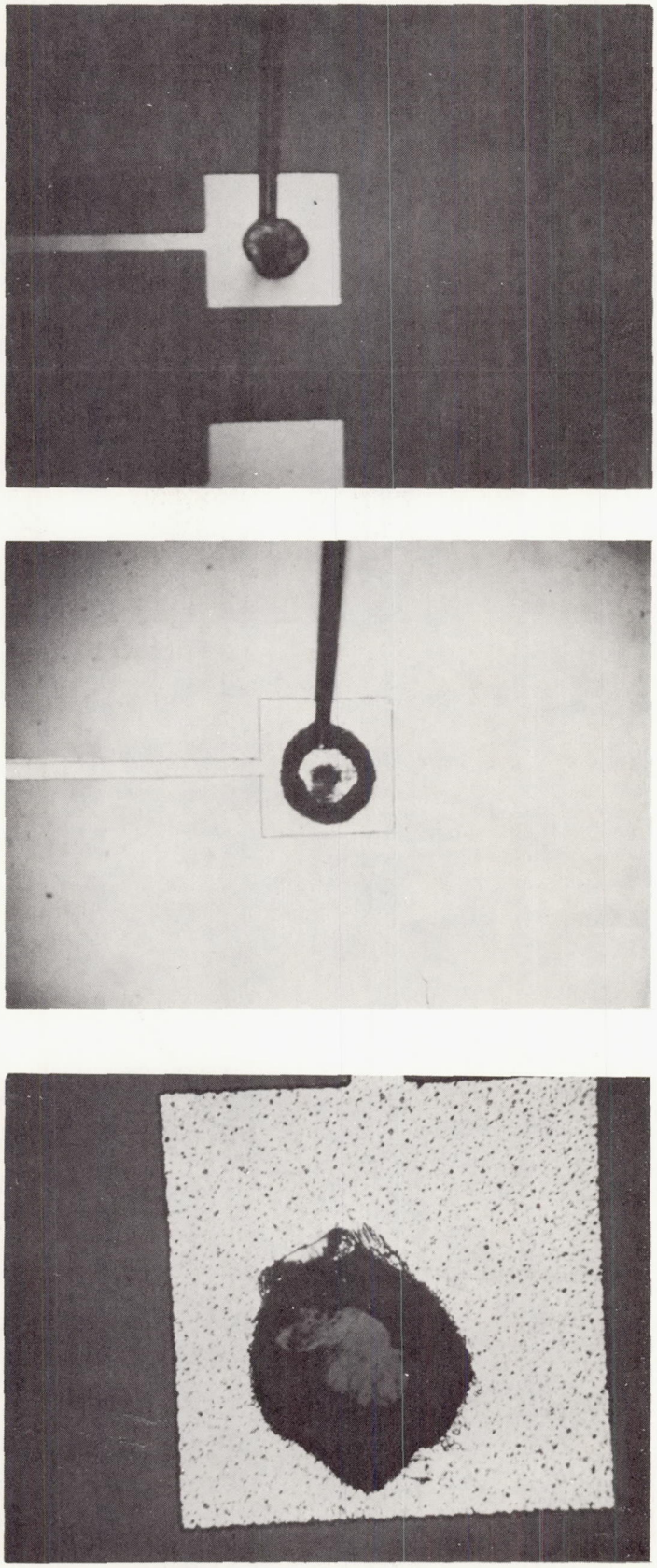

(a)

(b)

(c)

ORIGINAL PAGE IS
OF POOR QUALITY

Figure B-2 (a) Bond Appearance Before Anneal. (b) Bond Appearance After Anneal.
(c) Bond Pad Appearance After Bond Separation.

This result seems to indicate that the pull strength after 350°C anneal is related to the periphery of the gold-aluminum contact area. Since the pull strength degradation is due to the depletion of aluminum, this result can be understood by observing that the supply of aluminum for diffusion parallel to the oxide surface is not limited compared to the aluminum for diffusion perpendicular to the surface. This means that as annealing continues, the aluminum under the central area of the bond is depleted by diffusion into the gold wire, whereas around the edges of the bond, aluminum is replenished by diffusion from the unbonded pad area. In the final state, the bond is attached only around the periphery, and bond strength should be directly proportional to the bond circumference.

Assuming this analysis to be correct, the previously observed bond failures were caused by bonds with circumferences somewhat smaller than the normal. After these results were obtained, bonding procedures were changed to insure that all bonds were made with circumferences large enough to insure bond reliability.

2. Bond Pad Protection Process

In addition to efforts to determine the cause of bond failure and to quantify the effect, the contract also provided for the development of a process to eliminate bond strength degradation. Since the cause of this degradation is the formation of compounds of aluminum and gold, such a process must provide for bonds which provide separation of these two elements. Elimination of one of the elements would be difficult. Aluminum is an integral part of the processing of CCD arrays, and its elimination would require extensive process development, beyond the scope of this contract. Gold is required on the headers for low contact resistance and for lifetime and reliability considerations. Therefore, a process was required which would allow separation of the aluminum bond pads from the gold of the bond wire and header.

Aluminum wire was not considered because it required ultrasonic bonding techniques, which could cause membrane fracture. Similar problems would be expected at the bond of the aluminum wire to the gold header.

The process selected for development called for the insertion of a barrier metal (such as molybdenum, chrome, or titanium) between the aluminum and the gold. This could be done by depositing the barrier metal over the aluminum and patterning both metals at once. However, these metals are generally too hard to allow thermocompression bonding. For this reason, gold must be deposited over the barrier metal to allow bonding. An additional problem is that the barrier metals are deposited in thin layers (1000 Å) to avoid cracking. The possibility exists for the thermocompression bond to penetrate this thin barrier metal during bonding. For this reason, the bonding area must be offset from the original aluminum bond pad.

This requirement for offset bond pads presents the final problem. Since the aluminum is 11,000 Å thick, a step coverage problem exists when the 1000 Å barrier metal is deposited. It would be expected that the metal on top of the pads would be separated from the remainder of the offset pad and electrical continuity would not exist. For this reason, it is necessary to introduce a beveled edge to the aluminum bond pad. A process is used which allows continuous metal films to be produced from the top of the aluminum bond pad to the surrounding oxide. Figure B-3 shows the results of the application of this process to an aluminum bond pad.

The steps in the bond pad protection process are illustrated in Figure B-4. Figure B-4(a) shows an aluminum bond pad after completion of standard processing. The area of the bond pad is reduced and its edges are sloped as shown in Figure B-4(b). The slice is then ready for deposition of the barrier metal and the gold. These two layers are patterned to form an offset bond structure as shown in Figure B-4(c). Thermocompression bonding is performed on

ORIGINAL PAGE IS
OF POOR QUALITY

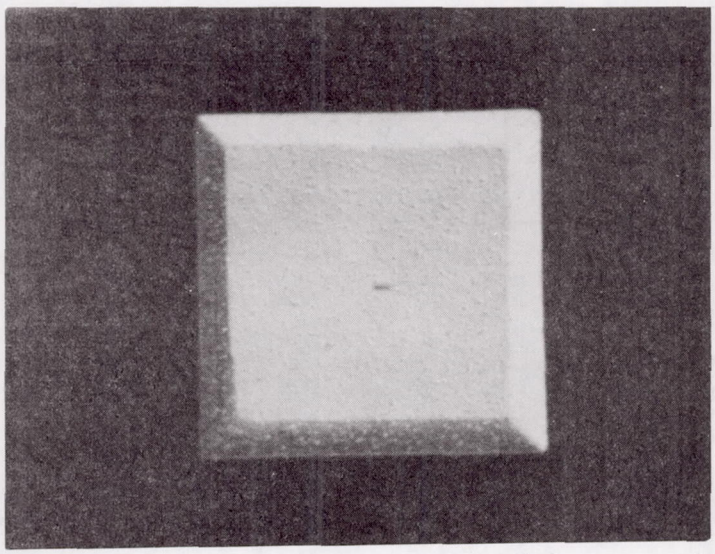

Figure B-3 Aluminum Bond Pad with Sloped Edges

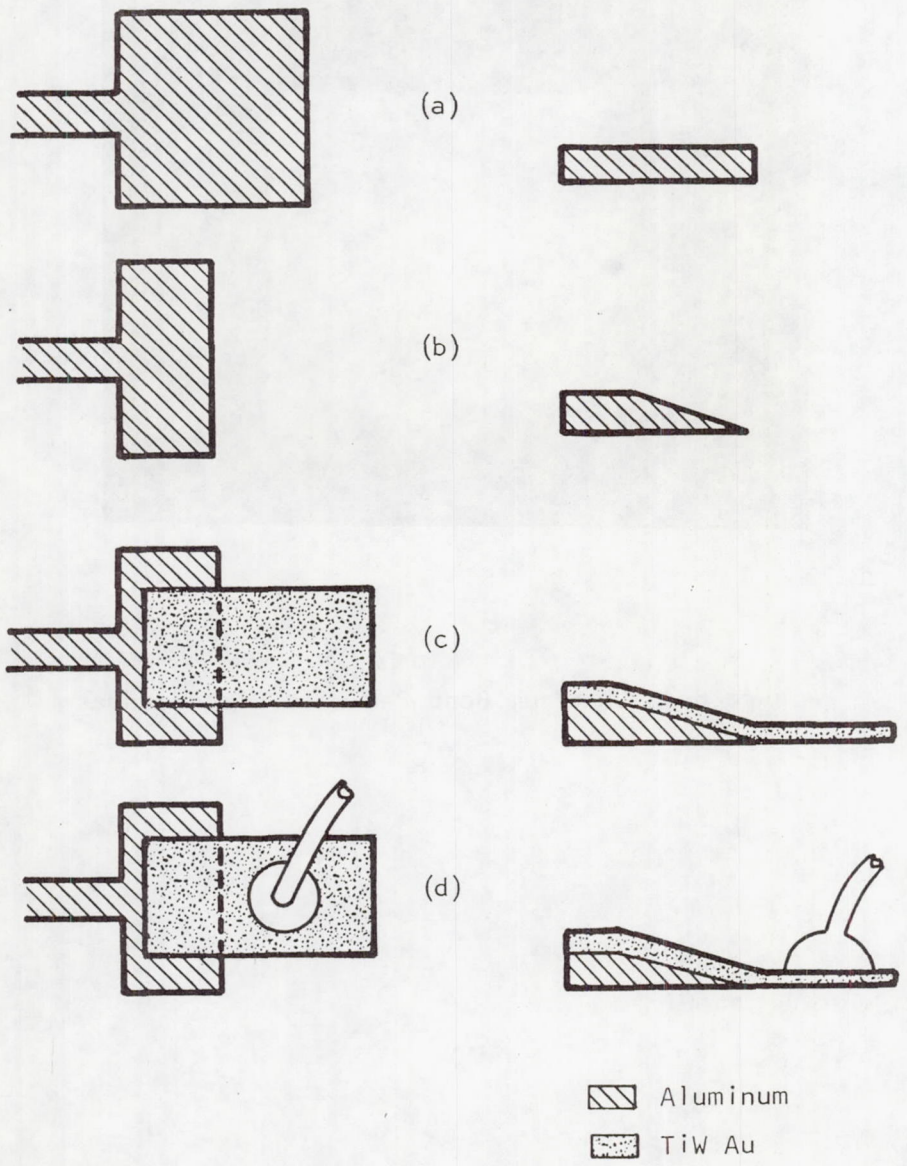

Figure B-4 Bond Pad Protection Processing Steps

the offset area of the pad as shown in Figure B-4(d). This process was successfully implemented on CCD arrays as indicated in Figure B-5. Tests were performed to determine if any electrical continuity problems existed. In no case was an electrical open observed between the offset bond area and the aluminum metallization.

Other potential problems involved with this process were investigated. One possibility is the introduction of metal shorts during the patterning process, and another is an increase in dark current caused by the metal deposition processing. Careful measurements of device yield before and after bond pad protection processing indicated no loss of functional devices due to this processing. Dark current changes were monitored using test diodes. Measurements of the dark current before and after processing indicated an average increase in dark current of 10% of the initial value. This was considered to be acceptable, and no attempt was made to eliminate this increase.

Anneal tests were performed to verify that these new bond pads would eliminate bond degradation during tube processing. Samples of the offset pad structure were prepared and bond loops constructed as shown in Figure B-6. Three barrier metals were tested: chrome, molybdenum, and a mixture of titanium and tungsten. Pull tests were performed after anneals at various times and temperature. Control samples of unprotected aluminum bond pads with uncontrolled bond size were also annealed. Typical results for the case of titanium-tungsten are given in Table B-1. Similar results were obtained for the case of molybdenum and chrome.

As this table indicates, the protected bond pads exhibited no bond strength degradation introduced by annealing. In no case, for any of three barrier metals considered, did a bond separate; all failures occurred in the wire at pull force well above 2 dynes.

ORIGINAL PAGE IS
OF POOR QUALITY

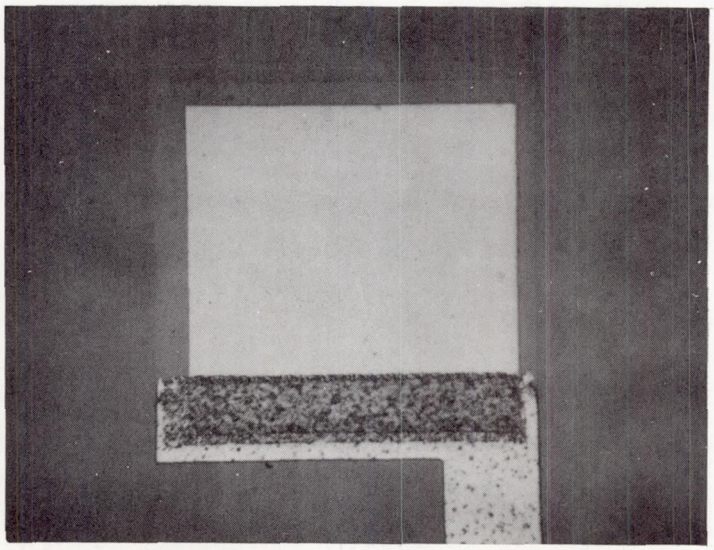

Figure B-5 Bond Pad Protection Structure

ORIGINAL PAGE IS
OF POOR QUALITY

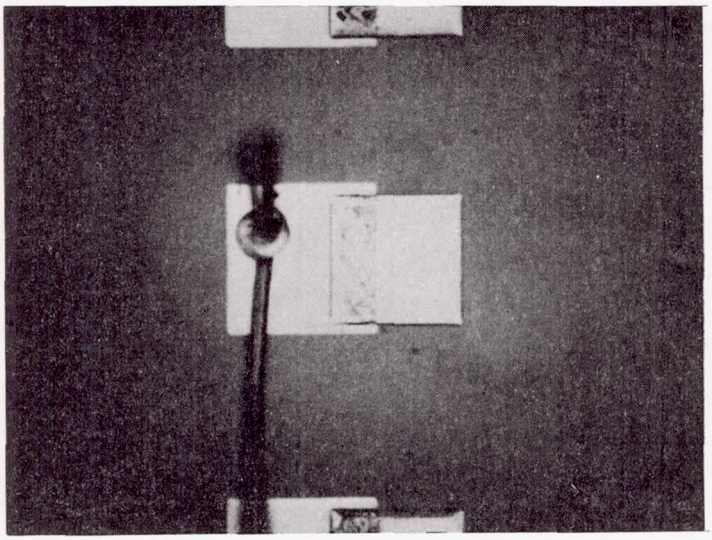

Figure B-6 Offset Bond Pad Structure for Anneal Tests

Table B-1

Anneal Test Results for Titanium-Tungsten-Protected Bond Pads

Anneal Temperature (°C)	Time (hrs)	Unprotected Pads Pull Strength (dynes)	Unprotected Pads Failure Mode	Protected Pads Pull Strength (dynes)	Protected Pads Failure Mode
300	3	7.0	wire	7.5	wire
		5.0	wire	7.0	wire
		6.5	wire	7.0	wire
	6	9.0	bond	7.0	wire
		3.0	wire	6.0	wire
		6.0	wire	8.0	wire
	8.5	7.0	bond	7.5	wire
		0.5	bond	7.0	wire
		8.0	wire	7.0	wire
350	3	7.0	wire	9.0	wire
		5.0	bond	6.5	wire
		9.5	bond	8.0	wire
	6	9.0	wire	6.0	wire
		7.0	bond	7.0	wire
		5.0	bond	9.0	wire
	10	0.0	bond	7.0	wire
		2.0	bond	7.0	wire
		7.0	wire	7.0	wire
400	4	2.0	bond	6.5	wire
		3.5	bond	6.5	wire
		9.0	wire	7.0	wire
	6	0.5	bond	6.0	wire
		3.0	bond	7.0	wire
		5.0	bond	8.0	wire
	9	1.0	bond	7.0	wire
		2.0	bond	7.0	wire
		7.0	wire	7.5	wire
450	3	6.0	bond	8.0	wire
		6.0	wire	7.0	wire
		8.0	wire	9.0	wire
	6	7.0	bond	9.0	wire
		6.0	bond	7.0	wire
		6.5	wire	7.5	wire
	9	7.0	wire	8.0	wire
		8.0	bond	6.0	wire
		6.0	bond	7.0	wire

At higher temperatures, some intermetallic formation was observed. Figure B-7 shows a bond annealed at 450°C for nine hours. In this figure the area of overlap of the aluminum and the gold bond pads is purple. Even in cases like this, failure was observed to occur in the wire rather than at the bond.

These tests indicated that all three barrier metals are acceptable. Titanium-tungsten was chosen for the remaining work since it is employed somewhat more often in semiconductor devices.

At this point in the development, all evaluation had been performed using test structures. The remaining step was to process a functional device through the bond pad protection steps and then through the tube fabrication steps. The first time this was done, the device failed to operate after the 350°C tube bake due to the introduction of metal shorts in the parallel section. Optical inspection of the device revealed discolored regions in the parallel section. Other functional devices with protected bond pads were annealed at 350°C with similar results.

The cause of this problem was traced to the nitride overcoat. Bond pad protection processing for these devices had begun after the nitride had been deposited and patterned. The titanium-tungsten and gold were therefore deposited over the nitride. It was postulated that for some reason related to the nitride, patches of these metals remained after patterning the bond pads. These patches would be isolated from the parallel section metal by the nitride and therefore would not be electrically observable. However, during the anneal, these metals apparently diffused through the nitride, resulting in the observed discolored regions and in electrical shorts in the parallel section. This analysis was verified by taking functional chips, stripping the nitride overcoat (and thereby the residual metal), and annealing. No failures were observed with these chips, and successful tube processing resulted.

ORIGINAL PAGE IS
OF POOR QUALITY

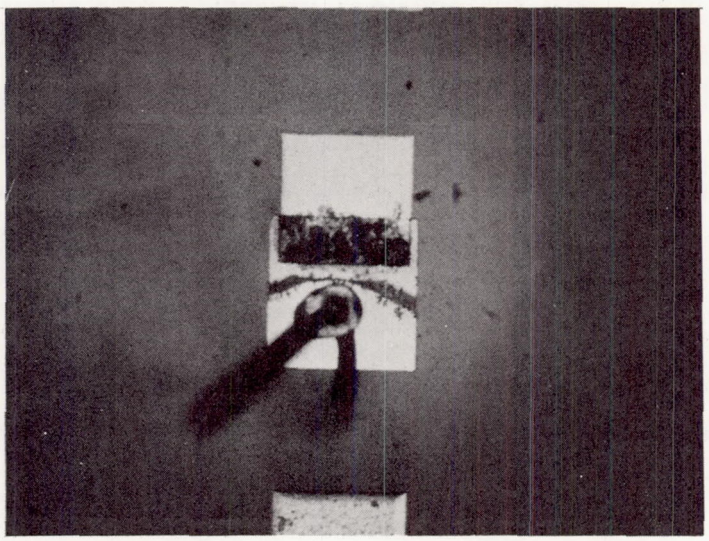

Figure B-7 Intermetallic Formation at 450°C

The problem was eliminated from existing chips by stripping the nitride. In future processing, the nitride overcoat will be applied after the bond pad protection process has been completed. The last two devices delivered under this contract had protected bond pads.

3. Conclusions

At the beginning of this contract, there was serious concern about the reliability of the bonding scheme for ICCDs. As a result of the work described here, two solutions have been obtained. One results from the observation that, despite some degradation, bond strength can be conserved in the aluminum-gold system by using bonds with sufficiently large circumferences. This procedure was implemented during the development of the bond pad protection process. Approximately 30 ICCDs have since been fabricated using these bonds, with no indication of bond failure. The second solution completely eliminates bond degradation by inserting a barrier metal between the gold and aluminum. ICCDs have been fabricated with protected bond pads with no significant change in the CCD characteristics.

In view of the equal success of these two solutions, it is recommended that the standard ICCD processing continue to be the gold-aluminum system due to the increased processing time and cost associated with the barrier metal process. However, the development of this barrier metal process could have great significance in the future development of backside-illuminated CCD imagers. It is a relatively simple matter to take the process as it now exists and extend it to allow the plating of gold on the bond pads to sufficient thickness for the construction of beam leads. Beam leads would allow the bonding of devices frontside down, greatly simplifying the header design required. In addition, beam leads could provide a method of relieving the strain currently introduced by the different thermal expansion coefficients of the silicon and the molybdenum alloy stage.

REFERENCES

1. S. Sobieski, Proc. SPIE 78, 78 (1976).

2. G. A. Hartsell and A. R. Kmetz, 1974 IEDM, Digest of Technical Papers, p. 59 (1974).

3. S. R. Shortes, W. W. Chan, W. C. Rhines, J. B. Barton, and D. R. Collins, Appl. Phys. Lett. 24, 565 (1974).

4. G. A. Antcliffe, "Development of CCD Imaging Sensors For Space Applications," Final Technical Report - Phase I, JPL Contract No. 953788, Texas Instruments Incorporated, 1975.

5. T. M. Buck, H. C. Casey, Jr., J. V. Dalton, and M. Yavin, "Influence of Bulk and Surface Properties on Image Sensing Silicon Diode Arrays," Bell Syst. Tech. J. 47, 1827 (1968).

6. A. S. Grove, Physics and Technology of Semiconductor Devices (John Wiley and Sons, Inc., New York, 1967), pp. 298-302.